U.S. Department
of Commerce

Volume 119
Number 1
January 2021

Fishery Bulletin

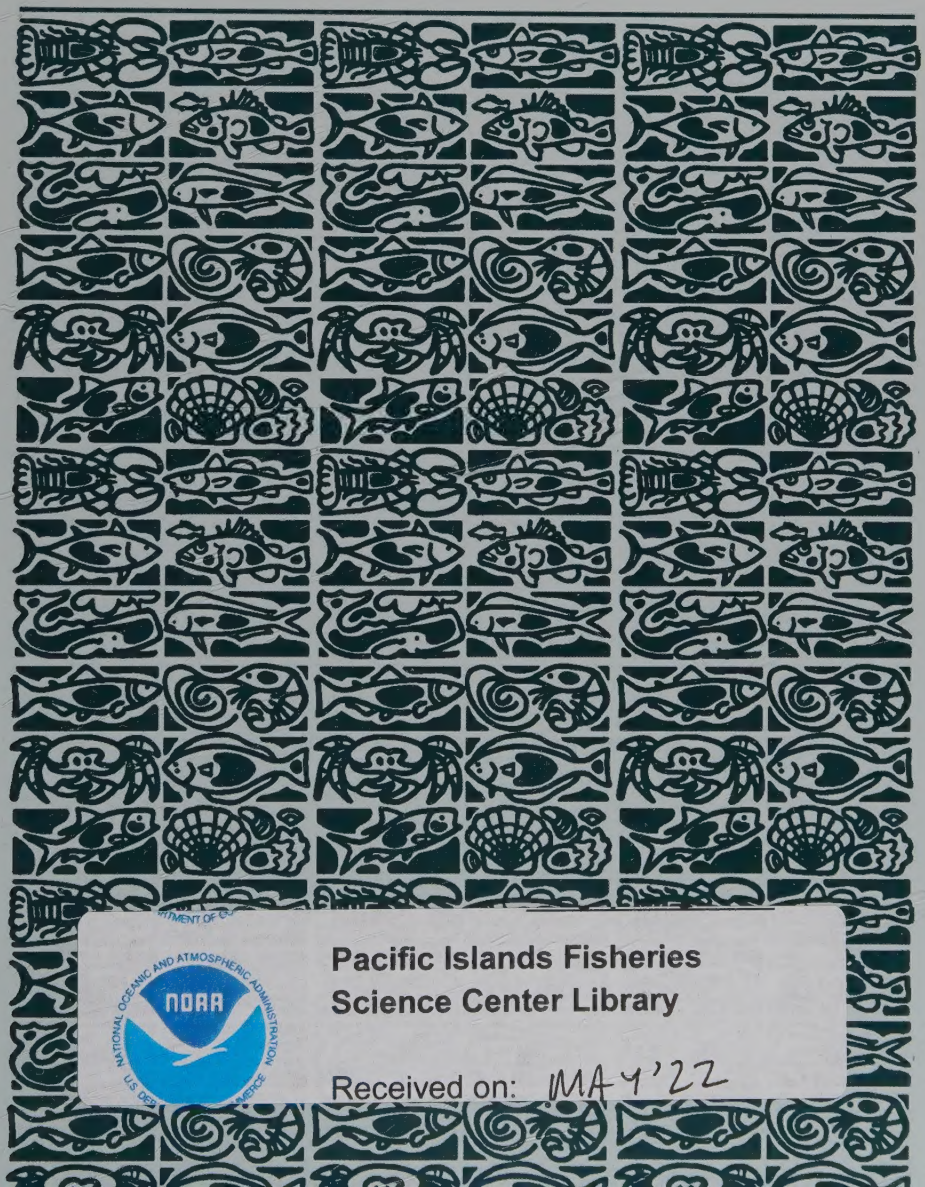

Pacific Islands Fisheries
Science Center Library

Received on: MAY '22

U.S. Department of Commerce

Gina M. Raimondo
Secretary

National Oceanic and Atmospheric Administration

Richard W. Spinrad
Administrator

National Marine Fisheries Service

Janet Coit
Assistant Administrator
for Fisheries

Fishery Bulletin (ISSN 0090-0656) is published quarterly by the Scientific Publications Office, National Marine Fisheries Service, NOAA, 7600 Sand Point Way NE, Seattle, WA 98115-0070.

Although the contents of this publication have not been copyrighted and may be reprinted entirely, reference to source is appreciated.

The Secretary of Commerce has determined that the publication of this periodical is necessary according to law for the transaction of public business of this Department. Use of funds for printing of this periodical has been approved by the Director of the Office of Management and Budget.

For Sale by the Superintendent of Documents, U.S. Government Publishing Office, Washington, DC 20401. Subscription price per year: $32.00 domestic and $44.80 foreign. Cost per single issue: $19.00 domestic and $26.60 foreign. **See back for order form.**

Fishery Bulletin

Scientific Editor
José I. Castro
National Marine Fisheries Service, NOAA
263 13th Avenue South
Saint Petersburg, Florida 33701

Managing Editor
Kathryn Dennis
Scientific Publications Office
National Marine Fisheries Service, NOAA
1845 Wasp Boulevard, Building 176
Honolulu, Hawaii 96818

Associate Editor
Cara Mayo
Scientific Publications Office
National Marine Fisheries Service, NOAA
7600 Sand Point Way NE
Seattle, Washington 98115-0070

Editorial Board

Henry L. Bart Jr.	Tulane University, New Orleans, Louisiana
Matthew D. Campbell	National Marine Fisheries Service, Pascagoula, Mississippi
Shannon L. Cass-Calay	National Marine Fisheries Service, Miami, Florida
William B. Driggers III	National Marine Fisheries Service, Pascagoula, Mississippi
Gretchen L. Grammer	South Australian Research and Development Institute, Adelaide, Australia
Richard Langton	National Marine Fisheries Service, Walpole, Maine (retired)
Richard S. McBride	National Marine Fisheries Service, Woods Hole, Massachusetts
Richard L. Merrick	National Marine Fisheries Service, Falmouth, Massachusetts (retired)
Richard D. Methot	National Marine Fisheries Service, Seattle, Washington
Lisa J. Natanson	National Marine Fisheries Service, Narragansett, Rhode Island
Mark S. Peterson	University of Southern Mississippi, Ocean Springs, Mississippi
André E. Punt	University of Washington, Seattle, Washington
Joseph M. Quattro	University of South Carolina, Columbia, South Carolina
John F. Walter III	National Marine Fisheries Service, Miami, Florida
Bruce Wright	Aleutian Pribilof Island Association, Anchorage, Alaska

***Fishery Bulletin* website: https://spo.nmfs.noaa.gov/fb.htm**

Fishery Bulletin carries original research reports on investigations in fishery science, engineering, and economics. It began as the Bulletin of the United States Fish Commission in 1881; it became the Bulletin of the Bureau of Fisheries in 1904 and the *Fishery Bulletin* of the U.S. Fish and Wildlife Service in 1941. Separates were issued as documents through volume 46; the last document was no. 1103. Beginning with volume 47 in 1931 and continuing through volume 62 in 1963, each separate appeared as a numbered bulletin. A new system began in 1963, with volume 63, in which papers are bound together in a single issue. Beginning with volume 70, number 1, January 1972, *Fishery Bulletin* became a periodical, issued quarterly. In this form, it is available by subscription from the Superintendent of Documents, U.S. Government Publishing Office, Washington, DC 20401. It is also available free in limited numbers to libraries, research institutions, and state and federal agencies and in exchange for other scientific publications.

U.S. Department of Commerce
Seattle, Washington

Volume 119
Number 1
January 2021

Fishery Bulletin

Contents

Perspective essay

1–2 **James A. Bohnsack, Laura Jay W. Grove, and Joseph E. Serafy**

Use of the term *harvest* when referring to wild stock exploitation

Note

3–9 **Cristopher G. Avalos Castillo and Omar Santana Morales**

Characterization of the artisanal elasmobranch fisheries off the Pacific coast of Guatemala

Articles

10–20 **Luis D. Carrillo-Colín, J. Fernando Márquez-Farías, Raúl E. Lara-Mendoza, and Oscar G. Zamora-García**

Bayesian estimation of the age and growth of the golden cownose ray (*Rhinoptera steindachneri*) in the southern Gulf of California in Mexico

21–32 **Amy M. Schueller, Amanda Rezek, Raymond M. Mroch III, Eric Fitzpatrick, and Alicia Cheripka**

Comparison of ages determined by using an Eberbach projector and a microscope to read scales from Atlantic menhaden (*Brevoortia tyrannus*) and Gulf menhaden (*B. patronus*)

33–40 **Ilya Gordeev, Kristina Zhukova, and Svetlana Frenkel**

The first data on the diet and reproduction of Fedorov's lumpsucker (*Eumicrotremus fedorovi*)

The National Marine Fisheries Service (NMFS) does not approve, recommend, or endorse any proprietary product or proprietary material mentioned in this publication. No reference shall be made to NMFS, or to this publication furnished by NMFS, in any advertising or sales promotion that would indicate or imply that NMFS approves, recommends, or endorses any proprietary product or proprietary material mentioned herein or that has as its purpose an intent to cause directly or indirectly the advertised product to be used or purchased because of this NMFS publication.

The NMFS Scientific Publications Office is not responsible for the contents of the articles.

41–49 **Kelsey C. James, Lisa J. Natanson, Christopher Flight, Cindy Tribuzio, John Hoey, and Camilla McCandless**

Validation of the use of vertebrae and dorsal-fin spines for age determination of spiny dogfish (*Squalus acanthias*) in the western North Atlantic Ocean

50–65 **Encarnación García-Rodríguez, Miguel Vivas, José M. Bellido, Antonio Esteban, and María Ángeles Torres**

Ontogenetic shifts and feeding strategies of 7 key species of Gadiformes in the western Mediterranean Sea

66–76 **Shannon L. Meseck, Renee Mercaldo-Allen, Paul Clark, Catherine Kuropat, Dylan Redman, David Veilleux, and Lisa Milke**

Effects of ocean acidification on larval Atlantic surfclam (*Spisula solidissima*) from Long Island Sound in Connecticut

77–92 **Kenneth A. Erickson and Marc O. Nadon**

An extension of the stepwise stochastic simulation approach for estimating distributions of missing life history parameter values for sharks, groupers, and other taxa

93–96 **Guidelines for authors**

National Marine Fisheries Service
NOAA

Fishery Bulletin
established in 1881

Spencer F. Baird
First U.S. Commissioner of Fisheries and founder of *Fishery Bulletin*

Abstract—We contend that *harvest* is a misleading term when referring to wild organisms removed from natural systems and suggest that fishery professionals reserve the word for aquaculture products. When referring to wild stock extraction, replacing the word *harvest* with *catch* removes the implication of extractor entitlement, better indicates the fishery product source, and does not distract from the issue of bycatch.

Use of the term *harvest* when referring to wild stock exploitation

James A. Bohnsack
Laura Jay W. Grove
Joseph E. Serafy (contact author)

Email address for contact author: joe.serafy@noaa.gov

Southeast Fisheries Science Center
National Marine Fisheries Service, NOAA
75 Virginia Beach Drive
Miami, Florida 33149

Manuscript submitted 24 August 2020.
Manuscript accepted 9 December 2020.
Fish. Bull. 119:1–2 (2021).
Online publication date: 28 December 2020.
doi: 10.7755/FB.119.1.1

The views and opinions expressed or implied in this article are those of the author (or authors) and do not necessarily reflect the position of the National Marine Fisheries Service, NOAA.

> The fish harvest is not a harvest produced by human labour. It is Nature's gift—some would say God's gift—to humanity (Archer, 1944).

Words matter in all walks of life, including in fishery science. As professionals, we strive to communicate information clearly with many audiences, especially the public. Since at least the early 19th century (according to a search for the use of *fish harvest* during 1800–2019 in the Google Books Ngram Viewer, available from website, accessed August 2020; Michel et al., 2011), *harvest* has been used somewhat interchangeably with *catch* and *landings*. Likewise, *harvesting* has been a synonym for *fishing* or *collecting* biota from natural waters. The glossary of fishery terms published by our own organization, the National Marine Fisheries Service, is replete with the word *harvest* when referring to removal of wild fish (NMFS, 2006). Certainly, dictionary definitions allow for the use of *harvest* (in noun and verb form) to apply to a given biomass extracted from a natural system, and to the act of gathering that biomass. However, primary dictionary definitions of *harvest* (Merriam-Webster[1]) and *harvesting* (Merriam-Webster[2]) typically evoke agriculture, and we feel such definitions transmit several connotations that are subtlety misleading, particularly to non-practitioners. Here, we suggest that fishery professionals reserve the word *harvest* for reference to fish, invertebrates, and algae produced through aquaculture, and we explain why its usage makes us wince a little when it is applied to wild catches.

In fisheries, catch constitutes all organisms permanently or temporarily extracted from natural ecological communities, and landings are the portion of catch retained. Wild fish populations are not *crops* that were *sowed* and nurtured by people, for people. Therefore, labelling wild catches as *harvests* attaches undue human entitlement to the donor populations and the natural ecosystems of which they are a part. Typically, what is extracted comes from populations that have existed for millennia, before human extraction began, and that would likely thrive well into the future were they not depleted by fishing or anthropogenic modification of their habitats. They persist in spite of humans, not because of humans, with most modern examples of successful

[1] Merriam-Webster. 2020. Harvest. Merriam-Webster.com. [Available from website, accessed August 2020.]

[2] Merriam-Webster. 2020. Harvesting. Merriam-Webster.com. [Available from website, accessed August 2020.]

fishery management ensuing from measures taken to stem serious damage previously done.

We suggest that fisheries terms should reflect the fundamental differences between wild and cultured stocks. To use terrestrial analogies, hunters hunt and kill game, and to say they *harvest* them has been criticized as inaccurate and euphemistic (McWilliams, 2011). Likewise, fishermen hunt and catch fish, they do not harvest them. Farmers harvest cultured crops: vegetables, grains, and fruits from the fields or orchards that they planted and eggs and meat from the domesticated animals that they raised. When fish farmers garner the fish, invertebrates, or algae they have raised, we do not call that act *fishing* nor do we call their yield a *catch*. We feel *harvest* and *harvesting* are appropriate for aquaculture products. In aquaculture operations, substantial resources are devoted to selection, health, and nutrition of broodstock. In contrast, wild stock management typically focuses on controlling total fishing mortality on a given population to avoid overfishing, especially over-removal of the largest, oldest, most fecund individuals that sustain fisheries. In other words, fishery managers protect wild stocks mostly from humans, not from other natural predators, disease, starvation, and weather extremes. Cultured organisms stocked in, and subsequently retrieved from, natural systems occupy a gray area with the term *harvest* being less appropriate the longer they are at liberty and become integrated components of the ecosystem.

Differentiating terminology between wild caught and aquaculture fish species can have broader implications by tracing seafood to its source. The how, where, and when fish are removed, processed, transported, and managed prior to purchase are unclear, particularly in comparison with those aspects of other food sectors. In recent years, consumers have become more concerned with the path food takes to their plate. Traceable terminology helps to distinguish a product's source, allowing consumers to make informed decisions related to their health, conservation values, or desire to support their local economy. Moreover, for fishery professionals, distinct terminology simplifies sorting data for management and easily identifies contributions to the global fish market. In some ways, this identification of sources reinforces an implicit decision by the Food and Agriculture Organization to use the terms *capture fisheries* and *aquaculture* for the most part keeping *harvest* out of their fishing terminology.

Fishermen engage in fishing for many purposes, including consumption and recreation in addition to commerce. Although fishermen invest heavily in their fishing vessels, gear, fuel, licenses, etc., and fishery professionals invest in stock assessment and management plans, they do not directly invest, at least not to the degree a farmer does, in the ecosystem from which biomass is extracted. Fishery managers aim to maximize economic benefit accrued from exploitation of targeted species, but for most untargeted species, often no care per se is provided (i.e., no regulations). We acknowledge that fishermen are compelled, sometimes at substantial cost, by fishery management measures (or their own ethical codes) to modify how, when, how much, and what they land from the ecosystems (e.g., through bag, minimum size, gear, season, and area limitations). However, we disagree that taking on these conservation burdens justifies use of the term *harvest* for what was hunted and removed from a natural system. In addition, when *harvest* is applied to wild stocks, it diverts attention from the issue of bycatch in many fisheries. The benign term *harvest* narrows the focus on the landed (or hooked) biomass of target species as opposed to the biomass and diversity actually affected (i.e., untargeted species or size classes killed or injured), which can be significant and even exceed landings in some fisheries.

Likely guided by the National Marine Fisheries Service glossary (NMFS, 2006), nongovernmental organizations, policy makers, and the U.S. legal system (Auslander and Tipple, 2020) similarly apply *harvest* to wild fish extraction. Indeed, the Southeast Fisheries Science Center, our own part of the National Marine Fisheries Service, has a unit labelled *Harvesting Systems*, when in fact, much of its research emphasis has been on minimizing bycatch without reducing target catch rates. *Fishing Systems* would be a more appropriate label. More examples of *harvest* and *harvesting* being applied to catches or fishing, with suggested replacement text, include the following: *harvest season is open* (i.e., *fishing season is open*) and *Anglers can harvest 2 red snapper per day* (i.e., *Anglers can land, retain, or possess 2 red snapper per day*).

For us, simple substitution of the word *catch* for *harvest* and of *fishing* for *harvesting* when referring to wild stocks is a step toward accuracy, better indicates the source of a fishery product, and removes any implication that a natural population's production is due to, or owed to, those exploiting it. As fishery professionals, we have a duty and obligation to communicate with accuracy and clarity, particularly to the public. In that regard, using *harvesting* as a euphemism for fishing is not helpful. Among our colleagues, we doubt *harvest control rules* will become *catch control rules* or that *harvest recommendations* will become *catch recommendations* any time soon. But we wish they would.

Literature cited

Archer, J. K.
1944. Address in reply. New Zealand Parliamentary Debates 264:416–418. [Available from website.]

Auslander, J. M., and K. A. Tipple.
2020. Fifth circuit finds National Marine Fisheries Service has no authority to regulate aquaculture. National Law Review, 12 August 2020. [Available from website.]

McWilliams, J. E.
2011. Hunting for euphemisms: how we trick ourselves to excuse killing. Atlantic, 21 December 2011. [Available from website.]

Michel, J.-B., Y. K. Shen, A. P. Aiden, A. Veres, M. K. Gray, W. Brockman, The Google Books Team, J. P. Pickett, D. Hoiberg, D. Clancy et al.
2011. Quantitative analysis of culture using millions of digitized books. Science 331:176–182.

NMFS (National Marine Fisheries Service).
2006. NOAA Fisheries glossary, rev. ed. NOAA Tech. Memo. NMFS-F/SPO-69, 61 p.

National Marine Fisheries Service
NOAA

Fishery Bulletin
established in 1881

Spencer F. Baird
First U.S. Commissioner of Fisheries and founder of *Fishery Bulletin*

Characterization of the artisanal elasmobranch fisheries off the Pacific coast of Guatemala

Cristopher G. Avalos Castillo (contact author)[1,2]
Omar Santana Morales[3,4]

Email address for contact author: criss.ac.13@gmail.com

[1] Fundación Mundo Azul
Carretera a Villa Canales
km 21-22 Finca Moran
01069 Villa Canales, Guatemala

[2] Centro de Estudios del Mar y Acuicultura
Universidad de San Carlos de Guatemala
Ciudad Universitaria Zona 12
Edificio M14
01012 Guatemala City, Guatemala

[3] Facultad de Ciencias Marinas
Universidad Autónoma de Baja California
Carretera Ensenada-Tijuana 3917
Fraccionamiento Playitas
22860 Ensenada, Baja California, Mexico

[4] ECOCIMATI A.C.
Avenida del Puerto 2270
Colonia Hidalgo
22880 Ensenada, Baja California, Mexico

Abstract—The landings of the artisanal elasmobranch fisheries of 3 communities located along the Pacific coast of Guatemala from May 2017 through March 2020 were evaluated. Twenty-one elasmobranch species were identified in this study. Bottom longlines used for multispecific fishing captured ray species and represented 59% of the fishing effort. Gill nets captured small shark species and represented 41% of the fishing effort. The most frequently caught species were the longtail stingray (*Hypanus longus*), scalloped hammerhead (*Sphyrna lewini*), and Pacific sharpnose shark (*Rhizoprionodon longurio*), accounting for 47.88%, 33.26%, and 7.97% of landings during the monitoring period, respectively. The landings were mainly neonates and juveniles. Our findings indicate the presence of nursery areas on the continental shelf off Guatemala. This study included the first survey of commercial exploitation of ray species in the artisanal fisheries off the Pacific coast of Guatemala. It is imperative to protect shark nursery areas and to develop management strategies for ray species that are important to artisanal fisheries.

Manuscript submitted 9 July 2020.
Manuscript accepted 19 January 2021.
Fish. Bull. 119:3–9 (2021).
Online publication date: 2 March 2021.
doi: 10.7755/FB.119.1.2

The views and opinions expressed or implied in this article are those of the author (or authors) and do not necessarily reflect the position of the National Marine Fisheries Service, NOAA.

Despite the widespread consumption and commercialization of elasmobranch catches in Latin America, there are no consistent statistical records and few studies of the catches of elasmobranch species in Guatemala or of products made from captured individuals. Nonetheless, Hacohen-Domené et al. (2020) described an artisanal elasmobranch fishery on the Caribbean coast of Guatemala and evaluated biological data from 688 Chondrichthyan species (24 shark, 6 ray, and 1 chimaera species) landed from January 2015 through July 2017. They concluded that a high proportion of the specimens of shark species for which data were recorded were juveniles. Ruíz Alvarado and Mijangos López (1999) first described the shark fisheries that operate off the Pacific coast of Guatemala and recorded 15 landed species. The most recent study about sharks species, which included a monitoring program of 5 communities along the Pacific coast, was carried out during 2006–2007 by Ixquiac Cabrera et al.[1], who found that the most captured species were the silky shark (*Carcharhinus falciformis*), scalloped hammerhead (*Sphyrna lewini*), and whitenose shark (*Nasolamia velox*). Lastly, in the most recent study about ray species in 2006, Ixquiac Cabrera et al.[2] determined that the main species of Guatemala's continental shelf are the golden cownose ray (*Rhinoptera steindachneri*), longtail stingray (*Hypanus longus*), and blotched stingray (*Urotrygon chilensis*).

The aim of this study was to continuously monitor the landings of artisanal fisheries of 3 Pacific coast communities in Guatemala from May 2017 through

[1] Ixquiac Cabrera, J., I. Franco Arenales, C. A. Tejeda Velásquez, M. R. Sánchez Rodas, and J. A. Sikahall Prado. 2009. Áreas de crianza de tiburones en la plataforma continental del Pacífico de Guatemala: Herramienta para el manejo y aprovechamiento sostenido del recurso tiburón. Proyecto Fodecyt 13-2006, 48 p. Cent. Estud. Mar Acuic., Univ. San Carlos Guatemala, Guatemala City, Guatemala. [In Spanish.] [Available from website.]

[2] Ixquiac Cabrera, M., I. Franco, J. Lemus, S. Méndez, and A. López-Roulet. 2010. Identificación, abundancia, distribución espacial de batoideos (rayas) en el Pacífico guatemalteco. Proyecto Fodecyt 34-2006, 41 p. Fondo Nac. Cienc. Tecnol., Cent. Estud. Mar Acuic., Organ. Conserv. el Medio Ambiente, Guatemala. [In Spanish.] [Available from website.]

March 2020 and ultimately to provide the first characterization of the ray species captured by the artisanal fleet and the shark species present in landings. The information from this study will contribute to the identification of elasmobranch nursery areas in Guatemala and facilitate the design of conservation strategies. Our results highlight the need to establish rays as important fishery species in this region.

Materials and methods

Study area

Approximately 1.8 million people live in the communities along the Pacific coast of Guatemala (14% of the national population), and the main sources of income for these people are related to fishing activities (SEGEPLAN and DOT[3]). The continental platform of Guatemala (14,009 km^2) is narrow, extends ~50 km offshore, and contains the economic exclusive zone of the country. Along the 250-km coastline where Guatemala meets the Pacific Ocean, about 45 communities have artisanal fisheries, in which elasmobranch species are incidentally captured and landed. Three of the largest fishing communities were selected for this study: Las Lisas, Buena Vista, and Sipacate (Fig. 1). These communities were selected for their importance and because their fishing efforts were greater than those of the other communities in the region. The community of Buena Vista was not monitored in the study until January 2019.

Landings

Biological and morphometric data were collected from elasmobranchs sampled from landings between May 2017 and March 2020, in addition to information on fishing effort and gear. Over the study period, sampling was undertaken during 83 visits to the 3 fishing communities: 34 visits in Las Lisas, 35 visits in Sipacate, and 14 visits in Buena Vista. Most individuals were landed whole and were identified to the species level by using identification guides and specialized books (Mejía-Falla et al., 2011; Ebert et al., 2013; Last et al., 2016). The sources for the nomenclature of ray, shark, and shrimp species were Last et al. (2016), Ebert et al. (2013), and Holthuis (1980), respectively. The presence or absence of male claspers was used to determine the sex of each specimen. Maturity was determined by the degree of clasper calcification (males) and the presence of reproductive scars or embryos (females). Size at first maturity was obtained from the literature (Mejía-Salazar, 2007; Navia et al., 2009; Zanella et al., 2009; López-Garro and Zanella, 2015; Pollom et al., 2020). Measurements to the nearest 0.5 cm were recorded for landed individuals in a natural position. For sharks, total length was measured by using the natural extension of the caudal fin (Compagno, 2001), and fork length was recorded. For rays, disc width and disc length were recorded. Total length was also recorded for small rays.

Given that the vessels in the artisanal fisheries used a variable and unquantifiable quantity of fishhooks or nets, the landings per unit of effort (LPUE) was calculated for each species by using fishing nights as the unit of effort. To ensure that calculations were as accurate as possible, an attempt was made to count the total number of elasmobranchs per fishing trip (every shark and ray landed by every boat that arrived at the dock on monitoring days), even if it was not possible to measure all individuals. For species in which the number of sampled individuals (n) was greater than 15, size histograms were generated and compared with information on sexual maturity from the literature.

In Las Lisas, a trawl fishery directed at the whiteleg shrimp (*Litopenaeus vannamei*) and seabob (*Xiphopenaeus kroyeri*) is also present. Data on incidentally caught

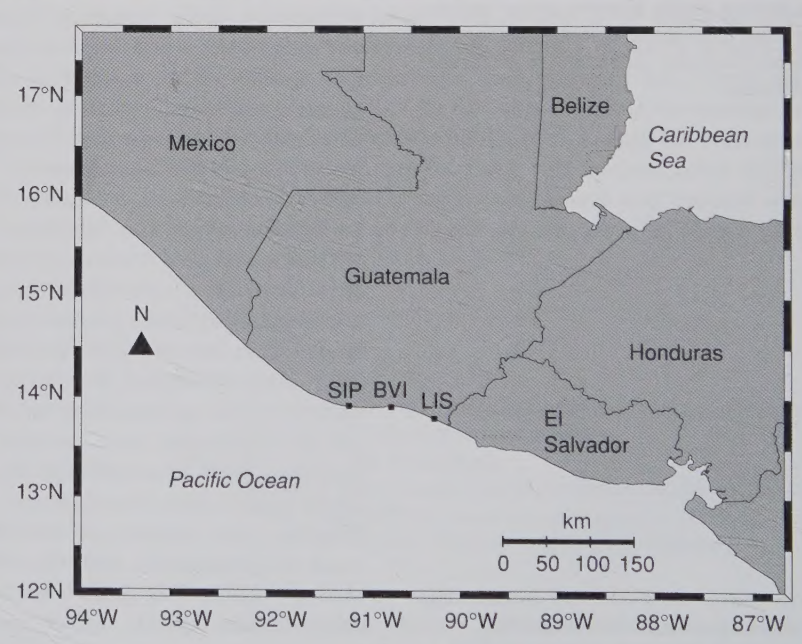

Figure 1

A map of the locations of the 3 communities where landings of ray and shark species in artisanal fisheries were monitored between May 2017 and March 2020. These communities along the Pacific coast of Guatemala are Las Lisas (LIS) in the Santa Rosa Department and Buena Vista (BVI) and Sipacate (SIP) in the Escuintla Department. Landings at Buena Vista were not monitored until January 2019.

[3] SEGEPLAN (Secretaría de Planificación y Programación de la Presidencia) and DOT (Dirección de Ordenamiento Territorial). 2011. Plan de desarrollo integral del litoral del Pacífico, 190 p. SEGEPLAN and DOT, Guatemala City, Guatemala. [In Spanish.] [Available from website.]

elasmobranchs were collected from the landings of the trawl boats in this fishery. Data recorded includes size, sex, and maturity. For this fishery, it was not possible to calculate LPUE.

Results and discussion

Fishing activity

The fishing activities of the communities in this study are carried out year-round, and there are no restrictions or seasonal closures. Fishermen do not engage in other economic activities. The fishermen from Las Lisas worked independently from one another, owned their own boats, and went fishing 5–6 d per week; the durations of their fishing trips were 1–2 nights. The fishermen from Sipacate and Buena Vista were hired by boat owners to work as part of fishing fleets (1–10 boats), and the durations of their fishing trips were generally 2 nights. Two types of fishing gears were identified: bottom and mid-water gill nets made of monofilament (mesh: 4–6 cm; length: 300–700 m; height: 5–7 m) and bottom longlines with small J hooks or Eagle Claw[4] half circle hooks (Wright and McGill Co., Denver, CO; height: 3–6 cm). The gill nets were linked together (maximum of 5 connected nets), remained in the water for 5–6 h, and were used 3–5 times per trip. Although gill nets were set to catch bony fish species, small sharks and rays were incidentally caught as species of moderate-to-high commercial value. The bottom longlines spanned 2–6 km, contained 300–700 hooks, remained in the water for 3–4 h, and were changed 2–4 times per trip. The bottom longlines targeted demersal bony fish and ray species, and some shark species were incidentally caught.

The artisanal fisheries of the communities of Las Lisas, Sipacate, and Buena Vista are classified as commercial demersal and small pelagic fisheries, according to the General Law of Fisheries and Aquaculture of Guatemala (MAGA, 2002), and do not include the capture of elasmobranch species as target species. A notable problem is that artisanal fishing activities are carried out without permits from the Fisheries and Aquaculture Regulations Department of Guatemala because of a lack of resources.

Landings

In Las Lisas, 131 fishing trips were recorded, of which 70 trips (53%) used gill nets and 61 trips (47%) used bottom longlines. In addition, landings of 3 shrimp trawl boats with incidentally caught elasmobranchs were evaluated. Data on 669 elasmobranchs were recorded. In total, 48% (n=321) and 41% (n=274) of the sampled individuals were caught in gill nets and bottom longlines, respectively. Finally, shrimp trawl nets were responsible for only 11% (n=74) of the incidentally caught individuals. In this location, 6 species were identified (3 shark and 3 ray species; Table 1). Only 6% (n=37) of the recorded individuals were mature (Fig. 2).

In Sipacate, fishing vessels use longlines and gill nets simultaneously. During 282 fishing trips (64%), 103 fishing trips (23%), and 57 fishing trips (13%), elasmobranch species were caught with both gears, longlines only, and gill nets only, respectively. In total, 2603 elasmobranchs were recorded, of which 1608 individuals (62%) were captured with bottom longlines and 991 individuals (38%) were captured with gill nets. A total of 16 species were identified (9 shark and 7 ray species; Table 1). Only 7% (n=179) of the specimens were mature (Fig. 2).

In Buena Vista, fishing vessels used longlines and gill nets simultaneously. In 50 fishing trips (57%), 21 fishing trips (24%), and 17 fishing trips (19%), both gears, bottom longlines only, and gill nets only were used, respectively. Information was obtained on 526 elasmobranchs, of which 271 individuals (52%) were captured with bottom longlines and 255 individuals (48%) were captured with gill nets. A total of 17 species were identified in this location (8 shark and 9 ray species; Table 1). Only 4% (n=24) of the specimens were mature (Fig. 2). The statistics for rarely landed species (n<15) in all 3 communities are presented in Table 2.

The LPUE varied over the course of the study, and periods of high LPUE values were determined for each species. The shark species that appeared most in the landings was the scalloped hammerhead (70% of landings), and the longtail stingray was the most common ray (91% of landings). For the longtail stingray, most of the landings occurred during the first months of the year. An increase in landings during the rainy season was observed for the scalloped hammerhead (May–September).

The scalloped hammerhead was 1 of 5 shark species that dominated the landings in Guatemala during 1997–1999 (Ruíz Alvarado et al.[5]), and during 2006–2007, the scalloped hammerhead was the second-most-caught shark species along the Pacific coast of Guatemala. Abundance of scalloped hammerhead has also been observed to be higher during the rainy season in Costa Rica (Zanella et al., 2009) and Mexico (Alejo-Plata et al., 2007) than during other seasons; during the rainy season, waters in coastal areas have higher concentrations of nutrients than during other periods. The fishing areas of the communities of Las Lisas and Sipacate evaluated in our study correspond to 2 of the 3 nursery areas used by scalloped hammerhead that were identified by Ixquiac Cabrera et al.[1], areas in which 88% of the landed individuals were classified as either neonates or juveniles. Ten years later, the results of our study indicate a continued presence of neonates and juveniles in these areas. According to this information and to the 3 criteria

[4] Mention of trade names or commercial companies is for identification purposes only and does not imply endorsement by the National Marine Fisheries Service, NOAA.

[5] Ruíz Alvarado, C., M. Ixquiac Cabrera, C. Baldetti Herrera, and J. Martínez. 2000. Evaluación del potencial de explotación del recurso tiburón en las costas del Pacífico de Guatemala, 56 p. Fondo Nac. Cienc. Tecnol., Cent. Estud. Mar Acuic., Unidad Manejo Pesca Acuic., Guatemala. [In Spanish.] [Available from website.]

Table 1

Statistics for elasmobranch species landed from May 2017 through March 2020 in artisanal fisheries that operate from 3 communities off the Pacific coast of Guatemala: Las Lisas, Sipacate, and Buena Vista. The number of documented individuals (n), percentage of the landing records, landings per unit of effort (LPUE) with fishing nights used as unit of effort, and fishing gear used to capture individuals are provided for each species by community. The LPUE is not presented for vermiculate electric rays (*Narcine vermiculata*) landed in Las Lisas because they were captured by shrimp trawl boats.

	Las Lisas			Sipacate			Buena Vista			
Species	*n*	%	LPUE	*n*	%	LPUE	*n*	%	LPUE	Fishing gear
Hypanus longus	258	39	1.73	1328	51	1.60	239	44	1.39	Bottom longline
Sphyrna lewini	348	52	2.33	716	28	0.86	204	38	1.18	Gill net
Rhizoprionodon longurio				289	11	0.35	15	3	0.08	Gill net
Mustelus lunulatus				170	7	0.20	5	1	0.02	Bottom longline
Carcharhinus limbatus	1	<1	0.01	32	1	0.03	2	<1	0.01	Gill net
Narcine vermiculata	57	9	–	30	1	0.03	4	1	0.02	Gill net
Aetobatus laticeps	4	1	0.02	8	<1	0.01	7	1	0.04	Bottom longline
Pseudobatos leucorhynchus				7	<1	0.01	17	3	0.09	Gill net
Galeocerdo cuvier	1	<1	0.01	7	<1	0.01				Gill net
Narcine entemedor				4	<1	0.01				Bottom longline
Styracura pacifica				3	<1	0.01				Bottom longline
Nasolamia velox				2	<1	<0.01	1	<1	0.01	Gill net
Carcharhinus falciformis				2	<1	<0.01	11	2	0.06	Gill net
Rhinoptera steindachneri				2	<1	<0.01	2	<1	0.01	Bottom longline
Carcharhinus leucas				2	<1	<0.01	1	<1	0.01	Bottom longline
Sphyrna mokarran				1	<1	<0.01				Bottom longline
Mobula thurstoni							25	5	0.14	Gill net
Mobula munkiana							3	1	0.01	Gill net
Urotrygon aspidura							2	<1	0.01	Gill net
Urotrygon chilensis							1	<1	0.01	Gill net
Alopias pelagicus							1	<1	0.01	Bottom longline
Total	669	100		2603	100		540	100		

that were established by Heupel et al. (2007) for the definition of a shark nursery area, it is highly probable that these sites are important nursery areas for the scalloped hammerhead in the eastern central Pacific Ocean.

The 3 criteria of Heupel et al. (2007) used to define a nursery area for shark species are as follows: 1) sharks of a species are most commonly found in a particular area instead of in other areas (for example, the density in some areas is higher than in other areas), 2) neonate and young-of-the-year sharks tend to remain or return for extended periods of time (weeks or months) in an area, and 3) an area or habitat is used repeatedly over the years while other sites are not.

Other shark species also had high incidences of capture during specific times of the year. For example, 75% of the landings of the Pacific sharpnose shark (*Rhizoprionodon longurio*) occurred during November 2018, and blacktip sharks (*C. limbatus*) were caught only from February through May in 2018 and 2019. Seasonality has also been observed for landings of the Pacific sharpnose shark off the Pacific coast of Mexico, with a high proportion of the total catch occurring from November through April (Márquez-Farias, 2005). Interestingly, the Pacific sharpnose shark has not been reported in previous studies of fisheries in Guatemala despite being a common species in the eastern central Pacific Ocean (Márquez-Farias, 2005). Although Ixquiac Cabrera et al.[1] reported that the silky shark was the most abundant shark species in landings recorded in Guatemala during 2006–2007, only a few individuals were observed in our study. The difference in abundance for this species may be a result of the inclusion of offshore longline fisheries in previous studies and the focus of our study on only coastal fisheries.

The results of our study provide the first characterization of ray exploitation in the artisanal fisheries of Guatemala. In total, 11 ray species were identified, with the longtail stingray having the most records (n=1825). It is important to mention that not all ray species are locally exploited, as is the longtail stingray, given that some do not reach large sizes. According to the information obtained in this study, the meat of longtail stingrays was mainly used locally in fillet form. As such, it has become a target species for the multispecies bottom longline fishery in Sipacate and to lesser extents for the fisheries in Las Lisas and Buena Vista. The remaining ray species that reached large sizes and that were occasionally reported were the Pacific eagle ray (*Aetobatus laticeps*), Pacific chupare (*Styracura pacifica*), and golden cownose ray, all of which are consumed

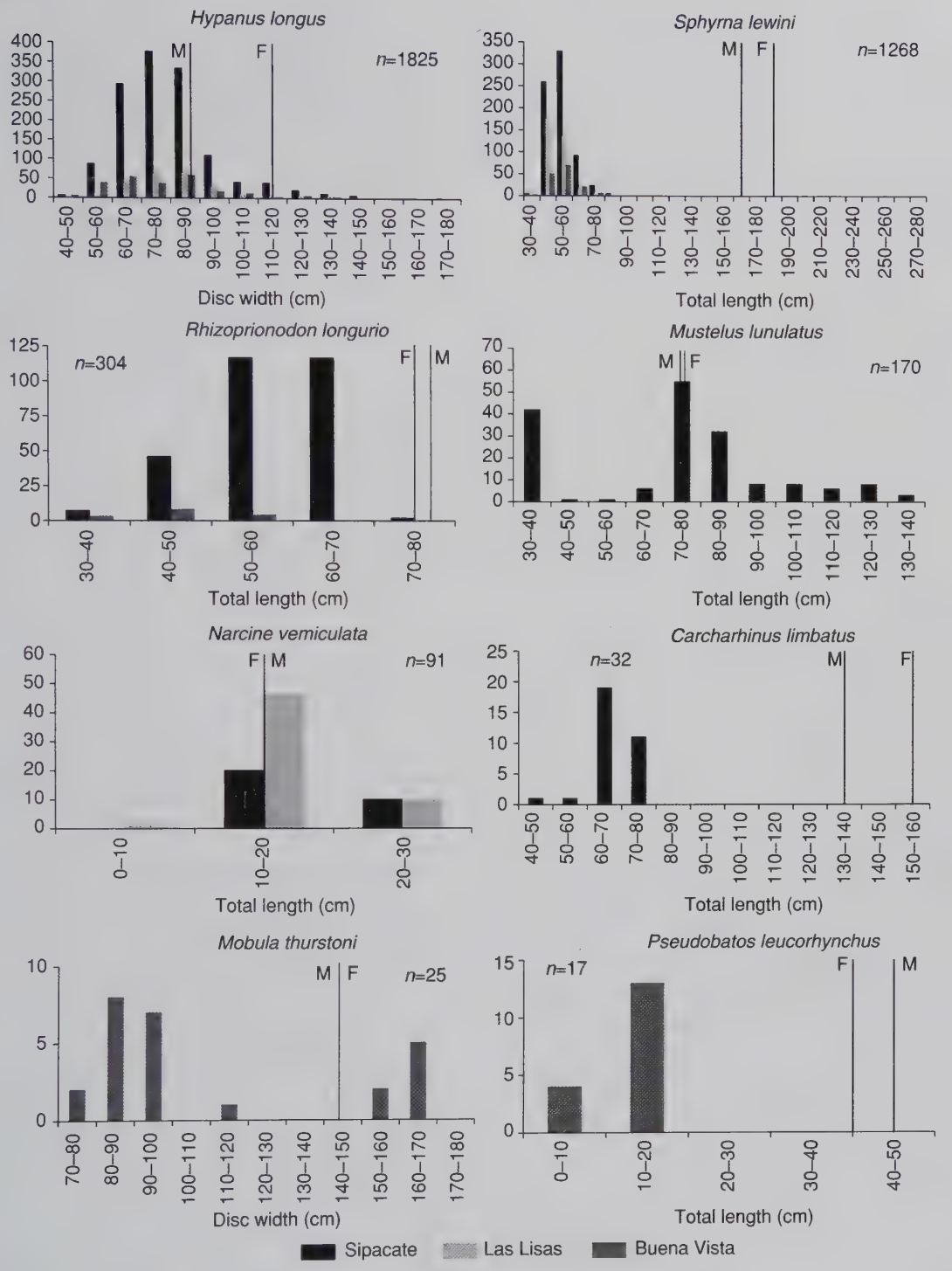

Figure 2

Pooled size-frequency distribution of the elasmobranch species in landings sampled between May 2017 and March 2020 from artisanal fisheries that operate from 3 communities along the Pacific coast of Guatemala: Las Lisas (light gray bars), Buena Vista (medium gray bars), and Sipacate (black bars). Species include the longtail stingray (*Hypanus longus*), scalloped hammerhead (*Sphyrna lewini*), Pacific sharpnose shark (*Rhizoprionodon longurio*), sicklefin smoothhound (*Mustelus lunulatus*), vermiculate electric ray (*Narcine vermiculata*), blacktip shark (*Carcharhinus limbatus*), smoothtail mobula (*Mobula thurstoni*), and whitesnout guitarfish (*Pseudobatos leucorhynchus*). The histograms are based on the number of sampled individuals (*n*) and not necessarily on the total number of individuals captured. The black vertical lines indicate the size at first maturity for males (M) and females (F).

Table 2

Statistics for elasmobranch species rarely landed from May 2017 through March 2020 in artisanal fisheries that operate from 3 communities along the Pacific coast of Guatemala: Las Lisas, Sipacate, and Buena Vista. The number of documented individuals (n), mean size (total length or disc width, depending on the species), and standard error of the mean (SE) are presented for each species by community. The interdorsal lengths of pelagic threshers (*Alopias pelagicus*) were recorded because they were landed without heads or caudal fins. Species are considered rarely landed if $n<15$.

	Las Lisas			Sipacate			Buena vista		
Species	n	Mean size (cm)	SE	n	Mean size (cm)	SE	n	Mean size (cm)	SE
Aetobatus laticeps	4	79.75	5.09	8	81.81	2.45	7	87.21	10.36
Carcharhinus falciformis				2	92.00	1.00	11	86.45	3.53
Galeocerdo cuvier	1	90.50	–	7	89.29	0.71			
Pseudobatos leucorhynchus				7	32.71	4.43			
Mustelus lunulatus							5	60.01	5.33
Narcine entemedor				4	49.25	10.94			
Rhinoptera steindachneri				2	74.50	9.50	2	77.50	0.50
Narcine vermiculata							4	20.75	1.03
Nasolamia velox				2	59.50	1.50	1	68.00	–
Mobula munkiana							3	101.33	0.33
Styracura pacifica				3	77.33	5.90			
Carcharhinus leucas				2	109.00	11.00	1	262.00	–
Carcharhinus limbatus									
Urotrygon aspidura							2	10.75	0.25
Sphyrna mokarran				1	122.00	–			
Alopias pelagicus							1	16.00	
Urotrygon chilensis							1	10.50	–

locally. Fishermen indicated that the vermiculate electric ray (*Narcine vermiculata*) is used as bait in the bottom longline fisheries. Dulvy et al. (2000) highlighted that batoid species in general are arguably the most vulnerable species in marine fisheries. Clarke et al. (2018) conducted a productivity susceptibility analysis for elasmobranch species in bottom fisheries and revealed that the longtail stingray is one of the most vulnerable species in Costa Rica, mainly because of its low reproductive potential and distribution, which overlaps greatly with shallow-water fishing grounds.

Conservation and management

Although elasmobranch species are not recognized as target species in artisanal fisheries in Guatemala, they are captured in high volumes during several months of the year and, therefore, account for a high percentage of the income of fishermen. There are currently no regulations for the management and conservation of elasmobranch species off the Pacific coast of Guatemala, and most artisanal fleets operate without permits or official records. Although all shark species can be exploited in artisanal, large-scale, or industrial fisheries (MAGA, 2002), ray species are not included as target species for any coastal fishery. Currently, the nongovernmental organization Fundación Mundo Azul and the Fisheries and Aquaculture Regulations Department of Guatemala have created a technical group to supervise and update the management plan for the conservation of Chondrichthyan species in Guatemala (this plan is in the final stages of approval and publication). However, Guatemala has not yet imposed national fishing regulations for any elasmobranch species, as other countries in Latin America, such as Mexico, have done (Saldaña-Ruiz et al., 2019). Off the Pacific coast of Mexico, shark nursery areas have been considered priority areas for elasmobranch conservation, and legislation has banned fishing activities inside those areas (Saldaña-Ruiz et al., 2019).

In Guatemala, it is also necessary to protect elasmobranch nursery areas, particularly for the scalloped hammerhead, which is listed as critically endangered in the IUCN Red List of Threatened Species and uses areas along the coasts of Guatemala during the early stages of its life cycle (Rigby et al., 2019). In addition, it is important to develop adequate management strategies because rays are highly vulnerable to coastal fisheries because of their very low productivity potential (Clarke et al., 2018). Therefore, it is important to support conservation actions and continuous monitoring efforts to improve the management of elasmobranch species in the eastern central Pacific Ocean.

Acknowledgments

This study was supported by the Fundación Mundo Azul, the Rufford Foundation (grant no. 22366-1), the PADI Foundation (grant no. 32809), the Waitt Foundation (grant no. 44306), and the Shark Conservation Fund. We thank the National Council of Protected Areas of Guatemala for issuing the research license (license no. I-DRSO-001-2018) and J. Ortíz and the Center for Marine Studies and Aquaculture of the University of San Carlos of Guatemala for their support. We recognize A. Hacohen Domené for her support of the master thesis of the senior author. We are especially grateful for the support in the field provided by F. Polanco, A. Paz, and the fishermen we worked with and for the contributions of D. Cartamil.

Literature cited

Alejo-Plata, C., J. L. Gómez-Márquez, S. Ramos, and E. Herrera.
2007. Presencia de neonatos y juveniles del tiburón martillo *Sphyrna lewini* (Griffith and Smithe, 1834) y del tiburón sedoso *Carcharhinus falciformis* (Müller and Henle, 1839) en la costa de Oaxaca, México. Rev. Biol. Mar. Oceanogr. 42:403–413. [In Spanish.]

Pollom, R., J. Bizzarro, M. I. Burgos-Vázquez, C. Avalos, M. Espinoza, A. González, J. C. Pérez Jiménez, and O. Sosa-Nishizaki.
2020. *Narcine vermiculatus.* The IUCN Red List of Threatened Species 2009:e.T161423A124482181. [Available from website, accessed June 2020.]

Clarke, T. M., M. Espinoza, R. R. Chaves, and I. S. Wehrtmann.
2018. Assessing the vulnerability of demersal elasmobranchs to a data-poor shrimp trawl fishery in Costa Rica, Eastern Tropical Pacific. Biol. Conserv. 217:321–328.

Compagno, L. V. J.
2001. Sharks of the world. An annotated and illustrated catalogue of shark species known to date. Vol. 2. Bullhead, mackerel and carpet sharks (Heterodontiformes, Lamniformes and Orectolobiformes). FAO species catalogue for fishery purposes 1, 269 p. FAO, Rome.

Dulvy, N. K., J. D. Metcalfe, J. Glanville, M. G. Pawsan, and J. D. Reynolds.
2000. Fishery stability, local extinctions, and shifts in community structure in skates. Conserv. Biol. 14:283–293.

Ebert, D. A., S. Fowler, and L. Compagno.
2013. Sharks of the world: a fully illustrated guide, 528 p. Wild Nat. Press, Plymouth, UK.

Hacohen-Domené, A., F. Polanco-Vásquez, C. Estupiñan-Montaño, and R. T. Graham.
2020. Description and characterization of the artisanal elasmobranch fishery on Guatemala's Caribbean coast. PloS ONE 15(1):e0227797.

Heupel, M. R., J. K. Carlson, and C. A. Simpfendorfer.
2007. Shark nursery areas: concepts, definition, characterization and assumptions. Mar. Ecol. Prog. Ser. 337:287–297.

Holthuis, L. B.
1980. FAO species catalogue. Vol. 1. Shrimps and prawns of the world. An annotated catalogue of species of interest to fisheries. FAO Fish. Synop. 125, 271 p. FAO, Rome.

Last, P. R., W. T. White, M. R. de Carvalho, B. Séret, M. F. W. Stehmann, and G. J. P. Naylor (eds.).
2016. Rays of the world, 832 p. Cornell Univ. Press, Ithaca, NY.

López-Garro, A., and I. Zanella.
2015. Capturas de la raya *Dasyatis longa* (Myliobatiformes: Dasyatidae) en las pesquerías artesanales de Golfo Dulce, Costa Rica. Rev. Biol. Trop. 63(Suppl. 1):319–327. [In Spanish.]

MAGA (Ministerio de Agricultura, Ganadería y Alimentación).
2002. Ley general de pesca y acuitultura. Decreto no. 80-2002. Congreso de la Republica de Guatemala, Guatemala City, Guatemala. [In Spanish.] [Available from website.]

Márquez-Farias, J. F.
2005. Gillnet mesh selectivity for the shovelnose guitarfish (*Rhinobatos productus*) from fishery-dependent data in the artisanal ray fishery of the Gulf of California, Mexico. J. Northwest Atl. Fish. Sci. 35:443–452.

Mejía-Falla, P. A., A. F. Navia, and V. Puentes (eds.).
2011. Guía para la identificación de especies de tiburones, rayas y quimeras de Colombia, 338 p. Ministerio de Ambiente y Desarrollo Sostenible; Corporación para el Desarrollo Sostenible del Archipiélago de San Andrés, Providencia y Santa Catalina—CORALINA; Gobernación de San Andrés, Providencia y Santa Catalina; Fundación SQUALUS. Bogotá, Colombia. [In Spanish.] [Available from website.]

Mejía-Salazar, L.
2007. Biología reproductiva del cazón bironche, *Rhizoprionodon longurio* (Jordan and Gilbert, 1882) en el Pacífico Mexicano. M.S. thesis, 67 p. Cent. Interdiscip. Cienc. Mar., Inst. Politéc. Nac., La Paz, Mexico. [Available from website.]

Navia, A. F., P. A. Mejía-Falla, L. A. Zapata, S. Bessudo, G. Soler, and E. A. Rubio.
2009. Estado del conocimiento de tiburones y rayas del Pacífico colombiano. *In* Avances en el conocimiento de tiburones, rayas y quimeras de Colombia (V. Puentes, A. F. Navia, P. A. Mejía-Falla, J. P. Caldas, M. C. Diazgranados, and L. A. Zapáta, eds.), p. 133–194. Fundación SQUALUS, Ministerio de Ambiente, Vivienda y Desarrollo Territorial, Instituto Colombiano Agropecuario, COLCIENCIAS, Conservación Internacional, WWF, Colombia.

Rigby, C. L., N. K. Dulvy, R. Barreto, J. Carlson, D. Fernando, S. Fordham, M. P. Francis, K. Herman, R. W. Jabado, K. M. Liu et al.
2019. *Sphyrna lewini.* The IUCN Red List of Threatened Species. 2019:e.T39385A2918526. [Available from website, accessed May 2020.]

Ruíz Alvarado, C. L., and N. Mijangos López.
1999. Estudio sobre la pesquería del tiburón en Guatemala. *In* Case studies of the management of elasmobranch fisheries (R. Shotton, ed.), p. 174–198. FAO Fish. Tech. Pap. 378, part 1. FAO, Rome. [In Spanish.] [Available from website.]

Saldaña-Ruiz, L. E., E. García-Rodríguez, J. C. Pérez-Jiménez, J. Tovar-Ávila, and E. Rivera-Téllez.
2019. Chapter 2—biodiversity and conservation of sharks in Pacific Mexico. Adv. Mar. Sci. 83:11–60.

Zanella, I., A. López, and R. Arauz.
2009. Characterization of the fishing of the hammer shark, *Sphyrna lewini*, in the external part of the Gulf of Nicoya, Costa Rica. J. Mar. Coast. Sci. 1:175–195. [In Spanish.]

National Marine
Fisheries Service
NOAA

Fishery Bulletin
established in 1881

Spencer F. Baird
First U.S. Commissioner
of Fisheries and founder
of *Fishery Bulletin*

Bayesian estimation of the age and growth of the golden cownose ray (*Rhinoptera steindachneri*) in the southern Gulf of California in Mexico

Luis D. Carrillo-Colín[1]
J. Fernando Márquez-Farías (contact author)[2]
Raúl E. Lara-Mendoza[3]
Oscar G. Zamora-García[4]

Email address for contact author: fmarquez@uas.edu.mx

[1] Posgrado en Ciencias del Mar y Limnología
Universidad Nacional Autónoma
de Mexico
Avenida Ciudad Universitaria 3000
04510 Coyoacán, Mexico City,
Mexico

[2] Facultad de Ciencias del Mar
Universidad Autónoma de Sinaloa
Paseo Claussen s/n
82000 Mazatlán, Sinaloa, Mexico

[3] Dirección General Adjunta de Investigación
Pesquera en el Atlántico
Instituto Nacional de Pesca y Acuacultura
Secretaría de Agricultura y Desarrollo Rural
Avenida Mexico 190
Colonia del Carmen
04100 Coyoacán, Mexico City, Mexico

[4] Servicios Integrales de Recursos Biológicos,
Acuáticos y Ambientales
Calle Genaro Estrada 406 Centro
82000 Mazatlán, Sinaloa, Mexico

Abstract—The aim of this study was to use a Bayesian approach to estimate age and growth parameters for the golden cownose ray (*Rhinoptera steindachneri*) in the southern Gulf of California in Mexico. Age estimates were obtained through analysis of vertebrae of 249 individuals. The von Bertalanffy growth function (VBGF) and Gompertz growth model (GM) were fit to length-at-age data by using a Markov chain Monte Carlo algorithm for parameter estimation. Prior distributions of parameters were included for an informative prior for disc width at birth (DW_0) and uninformative priors for the theoretical maximum disc width (DW_∞) and growth coefficients (k and g, for the VBGF and GM, respectively). Our results indicate that the golden cownose ray lives up to 13 years. The GM for combined sexes was selected as the best model by using the Watanabe–Akaike information criterion for model selection suitable for Bayesian estimation. The mean values of the GM parameters were as follows: DW_∞=101.10 cm (95% credible interval [CI]: 94.19–110.43), g=0.15 year^{-1} (CI: 0.12–0.18), and DW_0=40.00 cm (CI: 39.29–40.71). This study of the golden cownose ray contributes to the information available to develop better management and conservation strategies for this species.

Manuscript submitted 30 June 2020.
Manuscript accepted 3 March 2021.
Fish. Bull. 119:10–20 (2021).
Online publication date: 22 March 2021.
doi: 10.7755/FB.119.1.3

The views and opinions expressed or implied in this article are those of the author (or authors) and do not necessarily reflect the position of the National Marine Fisheries Service, NOAA.

The golden cownose ray (*Rhinoptera steindachneri*) ranges from the Gulf of California (GOC) to Peru, including the Galapagos Islands. Abundant in the GOC in summer, this species inhabits coastal waters and migrates seasonally (McEachran and Notarbartolo-di-Sciara, 1995). Bizzarro et al. (2007) investigated the biology of the golden cownose ray in the GOC and reported a maximum length of 104 cm disc width (DW) and a median length at maturity of around 70 cm DW. This species produces a single embryo at a size of 38–45 cm DW after 12 months of gestation. Low fecundity, typical of chondrichthyan species, is recognized as a limiting factor for the sustainability of the fisheries that target them and leads to the rapid overexploitation of populations.

The GOC supports the largest artisanal and multi-specific ray fishery in Mexico, and the golden cownose ray is among the most commonly captured species (Bizzarro et al., 2007). Its dorsoventrally flattened and broad body makes it susceptible to being caught in gill-net fisheries and as bycatch by the trawlers licensed to catch shrimp and operate in the GOC (Márquez-Farías, 2002). Despite the importance of the golden cownose ray in the artisanal ray fishery of the GOC, detailed information on the life history of this species and age estimates are scarce. Aging is necessary to determine age-specific survival and reproduction rates, which are useful for assessing species productivity (Cortés, 1998). However, determining age in chondrichthyans is challenging because of the logistical problems of collecting samples that result from their seasonal migrations and because of the difficulty of identifying growth bands in hard parts (Cailliet, 2015). Growth is a fundamental component of life history, and the ability to model it is imperative for practical fishery assessments (Smart et al., 2016).

The von Bertalanffy growth function (VBGF) has been used conventionally to describe growth in elasmobranchs (Cailliet et al., 2006) and involves the assumption that variation in growth rate is determined by an individual's metabolic state, diet, and reproduction and by environmental factors (Pitcher and Hart, 1982). However, the VBGF does not always reflect the growth of elasmobranchs. Therefore, it is necessary to explore alternative models (Smart et al., 2016). Neer and Thompson (2005) evaluated various models for estimating the growth of the cownose ray (*R. bonasus*) in the Gulf of Mexico, and they found that the Gompertz model (GM) described its growth convincingly.

In our study, we estimated age by using counts of growth bands on vertebrae of golden cownose rays collected in the artisanal ray fishery of the GOC. We evaluated the ability of 2 models (VBGF and GM) to describe growth. We used a Bayesian approach to estimate the posterior probability of the growth parameters (marginal posteriors). The availability of marginal posteriors of growth parameters allows the explicit incorporation of the uncertainty of parameters into further demographic or stock assessment studies to obtain more realistic estimates.

Materials and methods

Samples of golden cownose rays were collected in 2008–2014 from landings of the artisanal fishery and from bycatch of the commercial shrimp trawl fishery in the southern GOC (Fig. 1). We recorded the sex of each sampled ray and measured the DW (in centimeters), avoiding the curvature of the body. A section of 8–10 cervical vertebrae was extracted from each specimen (Natanson et al., 2018). Excess tissue and neural arches were excised from the vertebral segments, and vertebrae were exposed to sodium hypochlorite (5%) to remove the remaining fascial tissue (Anislado-Tolentino et al., 2008).

A single vertebra was removed from each section by using a blade to expose the surface of the centrum and

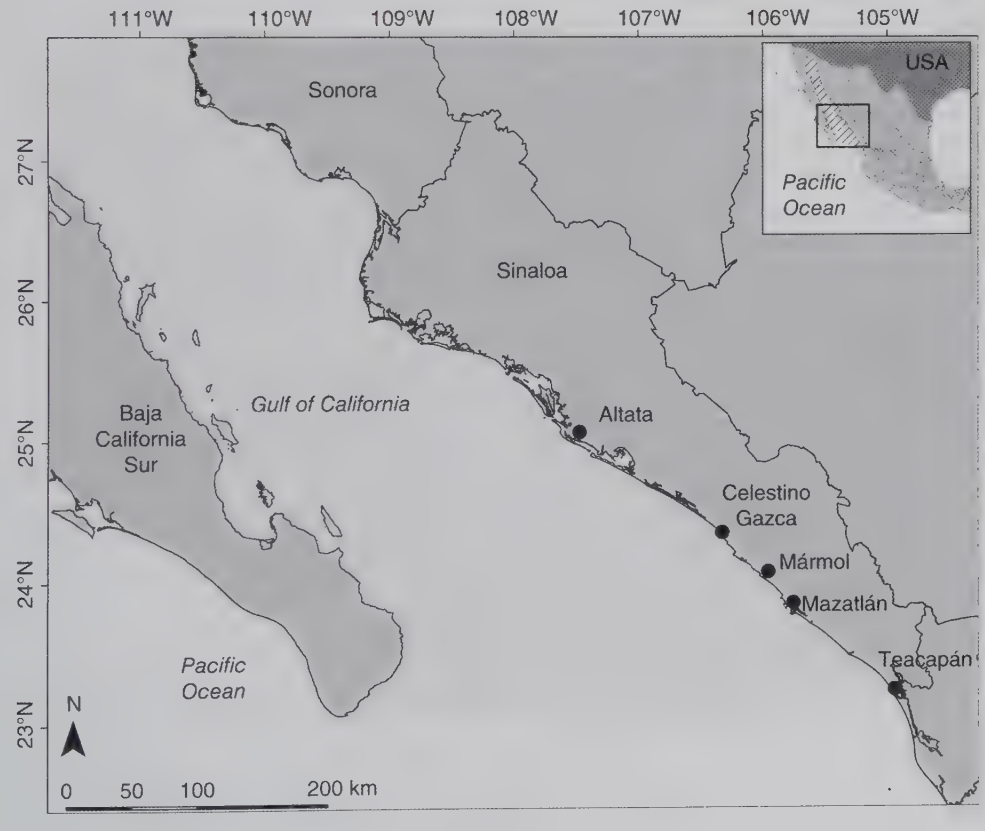

Figure 1

Map showing the primary locations (black circles) where golden cownose rays (*Rhinoptera steindachneri*) were sampled from landings of the artisanal fishery and from bycatch of the shrimp trawl fishery in the southern Gulf of California in Mexico between 2008 and 2014. The area with the diagonal lines indicates the Gulf of California.

was fixed to a flat piece of wood with synthetic resin. Each vertebral centrum was sectioned in a sagittal plane through the focus with an IsoMet Low Speed Saw[1] (Buehler Ltd., Lake Bluff, IL) that had double blades separated by 0.24 mm. Each section was mounted on a slide and photographed with transmitted light on an Olympus SZ61 stereomicroscope (Olympus Corp., Tokyo, Japan) equipped with an OptixCam S7N digital camera (Microscope LLC, Roanoke, VA). We created a database of section images for the interpretation and counting of growth bands.

Age estimation

Opaque and translucent bands form annually, and under transmitted light, these bands appear dark and light, respectively (Beamish, 1979). Age estimates were made by counting these band pairs (one dark and one light band) along the corpus calcareum after identifying the birthmark, the first distinct band after the focus (Cailliet et al., 2006). The distance from the focus to the edge of a vertebra and the thickness of each band were recorded by using Image-Pro Plus image analysis software (vers. 6.0, Media Cybernetics Inc., Rockville, MD). Images were projected onto a screen for the identification of growth bands. We used several vertebrae for defining reading criteria, and 3 independent readers counted the growth bands along the corpus calcareum on each vertebral section. We considered only age estimates with which at least 2 readers coincided. Otherwise, readings were discarded. We used a Bayesian *t*-test by using reference (uninformative) priors for the mean (μ) and standard deviation (σ) of DW (Suppl. Table 1) (online only) to determine the support for the difference in mean DW between sexes, as previously described by Doll and Jacquemin (2018). We fit a Bayesian linear regression with reference priors (Suppl. Table 1) (online only) to assess the proportionality of growth between vertebral diameter (VD) and DW.

The agreement of growth band counts was evaluated by using a bias plot (Campana et al., 1995). Reproducibility and precision of growth band counts were assessed by using the index of average percent error (IAPE), the coefficient of variation (CV), and the precision index (*D*) for readings of all 3 readers together and between readers (Beamish and Fournier, 1981; Chang, 1982; Goldman and Musick, 2006):

$$IAPE = 100\left[\frac{1}{N}\sum_{j=1}^{N}\left(\frac{1}{R}\sum_{i=1}^{R}\frac{\left|x_{ij}-\bar{x}_j\right|}{\tilde{x}_j}\right)\right]; \quad (1)$$

$$CV = 100\left[\frac{1}{N}\left(\sqrt{\sum_{i=1}^{R}\frac{(x_{ij}-\bar{x}_j)^2}{R}}\right)\right]; \text{ and} \quad (2)$$

$$D = \left[100\left(\frac{A}{B}\right)\right], \quad (3)$$

where N = the number of vertebrae;
R = the number of readers;
x_{ij} = the age i determined for individual j;
$\tilde{x}_j$ = the mean age calculated for individual j;
A = the numbers of agreements; and
B = the number of readings done.

Periodicity of band formation

We performed and compared 2 methods to infer the period of band formation: edge percentage analysis and relative marginal increment (MI) analysis following Cailliet (2015). We categorized the edge type of each section of a vertebra as *opaque* or *translucent*, and the relative frequency of each edge type was tabulated in bimesters (2-month intervals).

The MI analysis was conducted over bimesters by using vertebrae from rays at the ages of 1–3 years (number of rays=94) to reduce bias that can be caused by the inclusion of older individuals with many bands (Lessa et al., 2006). Bimesters with mean MI values close to 1 were interpreted to be the time of year when the growth cycle is about to be completed (Cailliet et al., 2006):

$$MI = \left(\frac{VR - r_n}{r_n - r_{n-1}}\right), \quad (4)$$

where MI = the marginal increment;
VR = the vertebral radius;
r_n = the distance from the focus to the last band pair; and
r_{n-1} = the distance from the focus to the penultimate band pair.

To evaluate differences in the MI values among bimesters, we used a Bayesian one-way analysis of variance (Gerrodette, 2011). First, we estimated the posteriors of the mean MI for each bimester (μ_i), using reference priors to nullify their influence on posterior distribution of mean MI. Then, we estimated the difference between bimesters (d) by subtracting the entire posterior mean MI of one bimester from another (i.e., μ_1–μ_2, μ_1–μ_3 . . . , μ_5–μ_6). We used the odds of difference, $P(d<0)/P(d>0)$, as an informative statistic of the effect of mean MI (Suppl. Table 1) (online only).

Growth models

Two models were fit to the observed age–length data. The first was the VBGF (von Bertalanffy, 1938), described as follows:

$$DW_t = DW_\infty - (DW_\infty - DW_0)e^{-kt}, \quad (5)$$

where DW_t = the estimated disc width (in centimeters) at a given age t (in years);
DW_∞ = the theoretical maximum disc width (in centimeters);
DW_0 = disc width at birth (in centimeters); and
k = the growth coefficient (year^{-1}).

[1] Mention of trade names or commercial companies is for identification purposes only and does not imply endorsement by the National Marine Fisheries Service, NOAA.

The second model was a modified version of the GM (Ricker, 1975), described as follows:

$$DW_t = DW_0 e^{-\log(\frac{DW_0}{DW_\infty})(1-e^{-gt})}, \quad (6)$$

where g = the completion growth parameter (Smart and Grammer, 2021).

Model fitting was done by using the software JAGS (vers. 4.3.0; Plummer, 2003). An additive error was assumed, indicating that, for individual i at given age t, DW_i follows a normal distribution expressed by a mean of zero, and its precision (τ), which is the inverse of its variance, is expressed as $\tau=1/\sigma^2$ (Doll and Jacquemin, 2018).

It is necessary to specify a prior distribution for the parameters to fit the growth models by using Bayesian methods. The priors for the parameters DW_∞, k, and g were chosen to be relatively uninformative, expressed as a uniform distribution (UD) based on growth estimates and information about maximum size in waters of Mexico (Villavicencio-Garáyzar, 1996; Gámez-Moedano et al., 2006): UD(80,200) and UD(0,1), respectively. The prior for size at birth DW_0 was informative and normally distributed (ND): ND(41.5,1.0) based on the reported range of DW_0 (38–45 cm; Bizzarro et al., 2007; Burgos-Vázquez et al., 2018). The prior for σ^2 was UD(0,100). The posterior distribution for the parameters of the 2 growth models (Equations 5 and 6) was computed by using Bayes formula (Smart and Grammer, 2021):

$$P(\theta \mid d) = \left(\frac{P(d \mid \theta)P(\theta)}{\int_1^n P(d \mid \theta)P(\theta)\partial\theta} \right). \quad (7)$$

Given the complexity of this multiparameter equation, the evaluation of the denominator requires numerical methods. The posterior probability distribution is summarized by drawing random samples from the vector of all parameters with the Markov chain Monte Carlo algorithm (Robert and Casella, 2004). A total of 1 million runs were completed after an initial burn-in of 20,000 runs. Every tenth iteration was saved to test convergence (Gerrodette and Eguchi, 2011).

The growth models (VBGF and GM) were fit to data and then compared by using the Watanabe–Akaike information criterion (WAIC). The WAIC is considered a better version of the deviance information criterion, which is commonly used to assess Bayesian models because it uses the entire posterior distribution to make an inference (Coll et al., 2019). The best model was chosen by considering a difference of at least 2 units in WAIC as is typically done for the Akaike information criterion (Burnham and Anderson, 2002). Once the best model was selected, we compared 2 versions of the best model, with and without sex variation, and the WAIC was used to choose the best model. All statistical analyses were performed by using Microsoft Excel 2015 (Microsoft Corp., Redmond, WA) and R, vers. 3.6.1. (R Core Team, 2019).

Results

Age estimation

A total of 256 specimens of golden cownose rays (129 females and 127 males) were analyzed. Seven vertebrae were discarded because the band pairs were unreadable. The size range for females was 29.4–96.9 cm DW (mean: 49.20 cm DW [standard deviation (SD) 14.62]), and males ranged in size from 21.5 to 92.9 cm DW (mean: 49.69 cm DW [SD 15.71]). A higher proportion of organisms were observed in the 10-cm-DW interval of 35–45 cm DW (Fig. 2). The difference in mean size between sexes was 0.49 cm DW, and the mean difference in DW between sexes was –0.15 cm (SD 1.93), with a 95% credible interval (95% CI) of –1.49–1.27 cm. This difference in mean DW is considered irrelevant because the probabilities of males being larger (P=0.53) or smaller (P=0.47) than females are almost equal (odds=1.13).

We found strong evidence of a linear relationship between VD and DW, given that the 95% CI of 12.49–13.52 for the marginal posterior of the slope did not include zero. The equation that describes the relationship is as follows: DW=1.98+12.98(VD). The bias plot shows 13 growth bands identified by the 3 readers, indicating that variability increases with the number of growth bands. For the readings of the 3 readers, the overall IAPE was 12.11%, the CV was 15.73%, and the precision index was 67.47%. The precision of readings between each pair of readers is shown in Figure 3.

Results of the MI analysis indicate that deposition of growth bands on examined vertebrae was close to

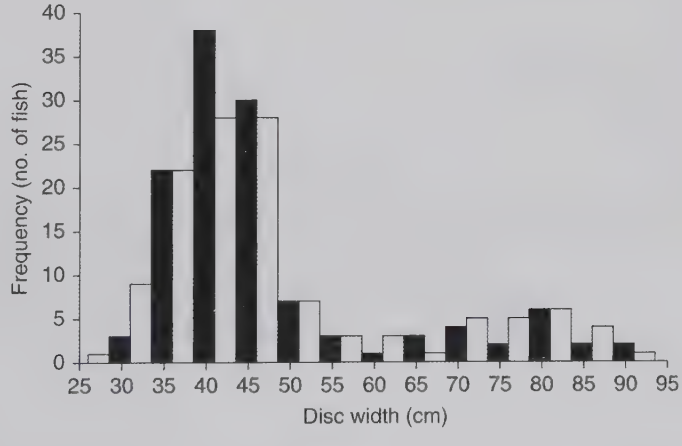

Figure 2

Length–frequency distributions for female (black bars) and male (white bars) golden cownose rays (*Rhinoptera steindachneri*) sampled during 2008–2014 in the southern Gulf of California in Mexico (number of rays=256).

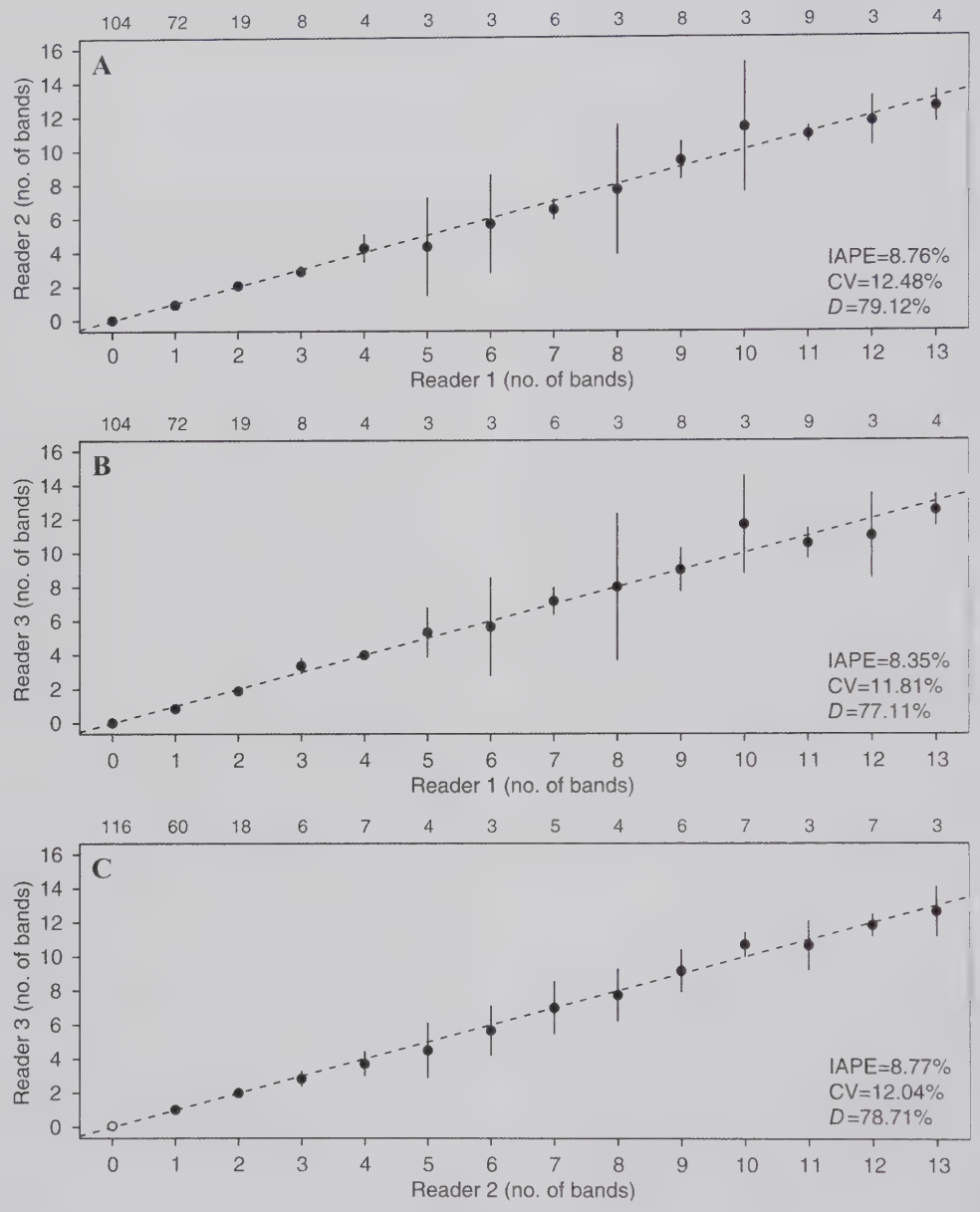
104 72 19 8 4 3 3 6 3 8 3 9 3 4
A
Reader 2 (no. of bands)
IAPE=8.76%
CV=12.48%
D=79.12%
Reader 1 (no. of bands)
104 72 19 8 4 3 3 6 3 8 3 9 3 4
B
Reader 3 (no. of bands)
IAPE=8.35%
CV=11.81%
D=77.11%
Reader 1 (no. of bands)
116 60 18 6 7 4 3 5 4 6 7 3 7 3
C
Reader 3 (no. of bands)
IAPE=8.77%
CV=12.04%
D=78.71%
Reader 2 (no. of bands)

Figure 3

Age-bias plots of counts of growth bands on vertebrae of golden cownose rays (*Rhinoptera steindachneri*) sampled between 2008 and 2014 in the southern Gulf of California in Mexico. Black circles represent mean counts (**A**) of reader 2 relative to reader 1, (**B**) of reader 3 relative to reader 1, and (**C**) of reader 3 relative to reader 2. Error bars represent the 95% confidence intervals for the mean number of band counts assigned by readers. The dashed line indicates 1:1 equivalence. Numerals on the superior axis represent the number of counts for each number of bands. Reproducibility and precision of age estimates were assessed by using the index of average percent error (IAPE), coefficient of variation (CV), and precision index (*D*).

completion in September–October when the highest mean MI value was reached (Fig. 4A). We found strong evidence for a difference in posterior mean MI between bimester 2 (March–April) and bimester 5 (September–October), a difference that could serve as support for the annual pattern of growth-band formation (Suppl. Table 2) (online only). Results of the edge analysis indicate that opaque growth bands form during March–August (spring–summer) and translucent bands form during September–February (autumn–winter), as expected for annual formation of growth bands (Fig. 4B). Therefore, the age structure of the golden cownose rays sampled in the study area

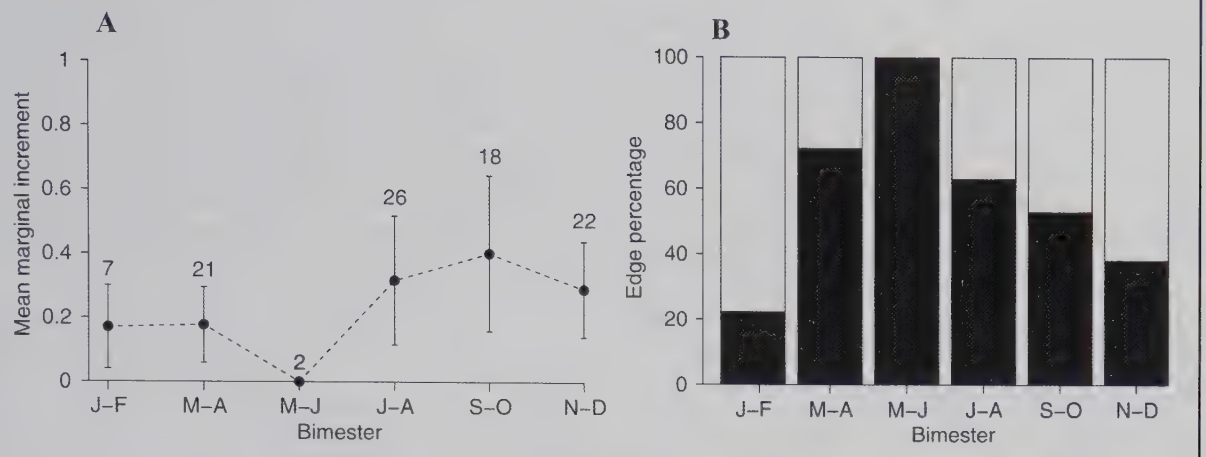

Figure 4

The periodicity of band formation was assessed by using (**A**) relative marginal increment analysis and (**B**) edge percentage analysis for golden cownose rays (*Rhinoptera steindachneri*) sampled during 2008–2014 in the southern Gulf of California in Mexico. In panel A, the black circles represent the mean marginal increments, the error bars indicate the 95% credible intervals, and the numerals above the error bars indicate sample sizes by bimester. In panel B, the black and white bars represent percentages of edges that were opaque and translucent, respectively. Results of analyses are shown for 2-month periods or bimesters: January–February, March–April, May–June, July–August, September–October, and November–December.

ranged from 0 to 13 years for both sexes combined, with 69.1% of individuals assigned ages of 0–1 years (Fig. 5). The oldest individuals were 13 years old for both females (92.9 cm DW) and males (96.6 cm DW).

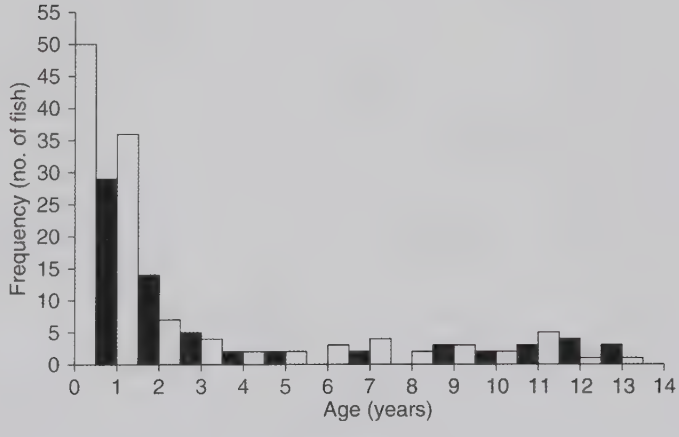

Figure 5

Age–frequency distributions indicating the estimated age structure of female (black bars) and male (white bars) golden cownose rays (*Rhinoptera steindachneri*) sampled during 2008–2014 in the southern Gulf of California in Mexico (number of rays=249).

Growth estimation

The results of the process in which the WAIC was used for model selection indicate that the GM was better at explaining the growth of golden cownose rays, given the reduction of 2.44 units of WAIC from the WAIC of the VBGF (Table 1). Similarly, there was no gain in the model fitting from the inclusion of sex variation in the GM. When sex was included in the GM, the WAIC increased by 7.85 units (from 1459.82 to 1467.67). Therefore, we selected the model for both sexes combined.

Results from use of the GM indicate that the golden cownose ray grows rapidly during its first 4 years of life, and its growth rate decreases after age 4 as it approaches its asymptotic size at the age of 13 years (Fig. 6). After the burn-in period, the simulations generated the marginal posterior probability distributions of the GM (Fig. 7, A–C). The predicted mean values of growth parameters of the GM were more realistic than those predicted with the VBGF (Table 1), which were considerably higher than the actual maximum lengths observed for the golden cownose ray and seemed to be overestimated.

Discussion

Our results indicate that the golden cownose ray lives up to 13 years, an age that is similar to the ages reported for the cownose ray (*R. bonasus*) in the Chesapeake Bay (13 years for females and 8 years for males; Smith and Merriner, 1987). However, the maximum reported age for the

Table 1

Comparison of the Gompertz and von Bertalanffy growth models fit to length-at-age data for golden cownose rays (*Rhinoptera steindachneri*) sampled between 2008 and 2014 in the southern Gulf of California in Mexico. Posterior values and 95% credible intervals (lower quartile: 2.5%; upper quartile: 97.5%) are provided from the fit of the growth models with a Markov chain Monte Carlo algorithm to data pooled for both sexes of golden cownose rays. The model parameters are disc width (DW) at birth (DW_0, in centimeters), theoretical maximum length (DW_∞, in centimeters), the completion growth parameter (g, year^{-1}), and the growth coefficient (k, year^{-1}). The standard deviations (SDs) and median values are given in addition to mean values. The Watanabe–Akaike information criterion (WAIC) was used in model selection.

Model	Parameter	Mean	SD	2.5%	Median	97.5%	WAIC
Gompertz							1459.82
	DW_0	40.00	0.36	39.29	40.00	40.71	
	$DW\infty$	101.10	4.15	94.19	100.67	110.43	
	g	0.15	0.01	0.12	0.15	0.18	
	SD	4.5	0.2	4.12	4.49	4.92	
von Bertalanffy							1462.26
	DW_0	39.93	0.37	39.20	39.93	40.65	
	$DW\infty$	118.78	9.35	104.06	117.41	140.85	
	k	0.08	0.01	0.05	0.08	0.10	
	SD	4.52	0.21	4.15	4.51	4.95	

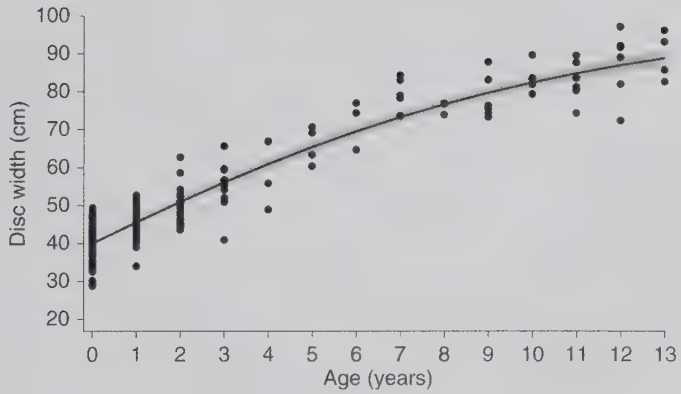

Figure 6

Estimated growth curve for golden cownose rays (*Rhinoptera steindachneri*) in the southern Gulf of California in Mexico, from use of the Gompertz growth model for sexes combined. The black circles represent observed lengths at age for rays sampled during 2008–2014, and the gray shaded area indicates 95% credible intervals of estimates.

cownose ray is 21 years (Fisher et al., 2013). Vertebrae are considered a valid structure for aging the golden cownose ray, as indicated by the proportional growth of the vertebrae to body size observed in our study. Also, values of IAPE and CV for band counts among readers were within the standard threshold for age determination in elasmobranchs (Campana, 2001).

The assumption of an annual pair of bands in the vertebrae is supported by the results of MI and edge percentage analyses and has been validated for the golden cownose ray by using biomarkers (Osuna-Soto, 2016). In addition, the same pattern of band formation has been observed for other species of the same genus (Neer and Thompson, 2005; Fisher et al., 2013). An annual pattern of band pairs has also been described for other batoids in the tropical and subtropical Pacific Ocean (Davis et al., 2007; Hale and Lowe, 2008; Mejía-Falla et al., 2014). Although there are more precise methods for validation of periodicity of band formation for aquatic organisms (e.g., biomarkers and mark and recapture), MI and edge percentage analyses provide the advantage of producing cost-effective and comparable results (Campana, 2001).

We found that the GM best described the growth of the golden cownose ray in the GOC for sexes combined, as indicated by the WAIC. Such a model includes an inflection point that represents a change in growth rate (Joung et al., 2011); this change in growth rate is assumed to be associated with a difference in ontogenetic feeding patterns between juveniles and adults. The GM may be a better option when the volume of an organism greatly expands with age, as has been observed for myliobatiform rays (Cailliet and Goldman, 2004; Neer and Thompson, 2005) and for elasmobranchs that have a change in growth rate after age 0 (Smart et al., 2016).

Results of several studies indicate that the conventional VBGF does not always satisfactorily describe the growth of chondrichthyans (Cailliet et al., 2006), and the authors of some studies have emphasized the need to explore different nonlinear models to describe growth (Bishop et al., 2006; Natanson et al., 2007). In our study, an exhaustive

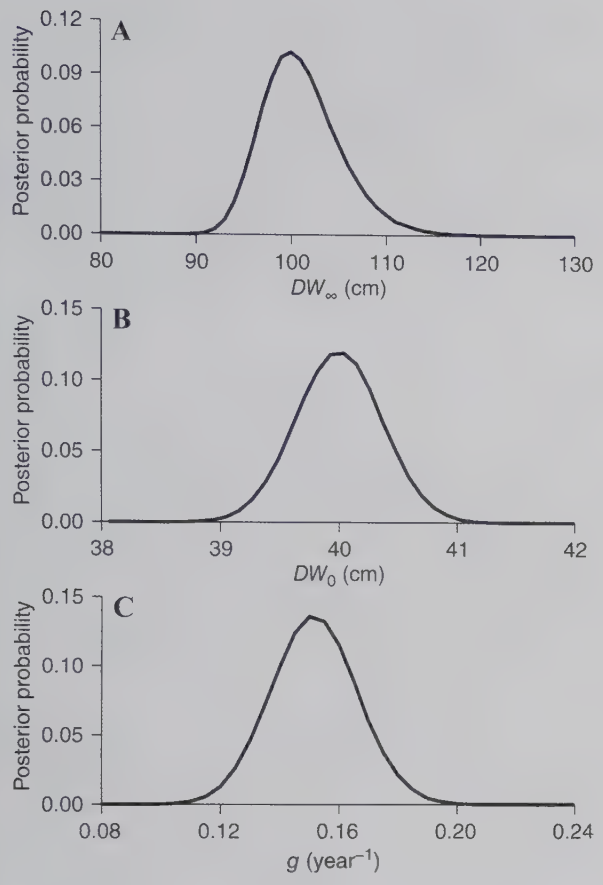

Figure 7

The posterior probability distribution of (**A**) theoretical maximum length (DW_∞), (**B**) length or disc width (DW) at birth (DW_0), and (**C**) the completion growth parameter (g) predicted with the Gompertz growth model for golden cownose rays (*Rhinoptera steindachneri*) in the southern Gulf of California in Mexico. The model was fit to length-at-age data pooled for both sexes of golden cownose rays sampled during 2008–2014.

test of other growth models was not done because the versions of both models tested (VBGF and GM) conveniently include length at birth, an appropriate inclusion for viviparous species (Cailliet et al., 2006).

The multi-model approach to estimation of growth parameters allows selection of the model that best fits the data (Katsanevakis, 2006). Although growth models with multiple parameters may be useful for estimating growth of elasmobranchs (Richards, 1959; Chapman, 1961; Schnute, 1981), the multi-model approach suffers from testing models with more parameters, some of which might have no biological meaning as is the case with the theoretical age when length is zero in the VBGF (Cailliet and Goldman, 2004). In addition, researchers may eventually be conditioned to ignore factors that potentially bias the selection of data collected from a fishery when fitting models to that data.

Use of fishery-dependent data can potentially lead to a distorted growth curve through sampling bias due to gear selectivity and migration (Ricker, 1979; Moulton et al., 1992). Such biases can potentially straighten the growth curve and change the magnitude of parameters because of their autocorrelation (Gallucci and Quinn, 1979). Such an effect, known as the *phenomenon of apparent change in growth rate*, is common in studies of age and growth of chondrichthyans (Lee, 1912; Walker et al., 1998). The occurrence of the phenomenon of apparent change in growth rate in our study may have been caused by the susceptibility of fish of certain sizes to be caught by the fishing gears used during our sampling campaign (Moulton et al., 1992).

Distorted growth curves are common for shark species in fisheries that use highly size-selective fishing gear and high fishing intensity (Walker, 1998). In the samples of golden cownose ray taken from the artisanal fishery, small individuals (<55 cm DW) predominated. Individuals older than 4 years could escape from fishing gears because of their large size (>59 cm DW). Their shape means they avoid the proper length selectivity of gill nets and, therefore, are easily captured or entangled. In contrast, length selectivity of fishing gear is more likely to work for thinner guitarfish species with a more pointed shape (Márquez-Farías, 2005). However, the inclusion of golden cownose rays caught incidentally in the shrimp trawl fishery in the GOC allowed an increase in size ranges because it has been reported that trawl nets do not allow their escape (Garcés-García et al., 2020). Another explanation for size classes being misrepresented in our sample could be size-dependent migration, and it should be investigated in the future. We believe bias was minimal in our sample because we included individuals in all classes within the known size range for the golden cownose ray and combined the DW for both sexes.

The Bayesian approach applied in our study was particularly useful for exploring the effect of uncertainty in modeling life history characteristics (Cortés et al., 2015; Doño et al., 2015) and is likely to be useful for examining life history traits of other data-deficient batoid species. For instance, Rolim et al. (2020) implemented a Bayesian approach to assess estimates of life history characteristics derived from a growth model. This approach included more realism in the process of fitting the model to data and accounting for uncertainty in the other growth parameters.

The convergence of the growth parameters DW_∞, g, and DW_0 was satisfactorily achieved, considering the well-defined posterior distribution profile of each parameter. The informative prior distribution for DW_0 favored model fitting because it helped select realistic birth size values and because it represents the y-axis intercept (Rolim et al., 2020). The size at birth of elasmobranchs is often well-defined and known; therefore, it is easy to judge whether the DW_0 from the fitted model is a reasonable value (Cailliet et al., 2006). However, using prior values and uncertainty seems to be a better alternative than using fixed values for the length at birth and solving only for g and DW_∞ (Smart et al., 2016).

Low availability of data is a common problem in studies of elasmobranch growth because most of the data on species of low value in fisheries usually come from instances of bycatch; therefore, it becomes difficult to determine the real asymptotic size for such species (White et al., 2014). Nevertheless, our results were similar to those of other studies in which the GM was a better fit to data and yielded more realistic estimates of growth parameters (Mollet and Cailliet, 2002; Carlson and Baremore, 2003; Neer and Thompson, 2005).

Information on the age structure and growth parameters provided from our study is valuable input for further demographic studies. The data are useful for estimating the trajectory of stock productivity and the resilience to fishing of the golden cownose ray.

Acknowledgments

We express our gratitude to A. Grant for English editing and I. Martínez for help in early language revision. We thank the anonymous reviewers for their careful reading of our manuscript and their insightful comments and suggestions. We also thank R. Bonfil for his comments on the manuscript. We dedicate this article to the life and work of J. Musick. This research was funded by Universidad Autónoma de Sinaloa, through the project PROFAPI-UAS (99-2013).

Literature cited

Anislado-Tolentino, V., M. Gallardo-Cabello, F. Amezcua-Linares, and C. Robinson-Mendoza.
2008. Age and growth of the scalloped hammerhead shark, *Sphyrna lewini* (Griffith & Smith, 1834) from the southern coast of Sinaloa, Mexico. Hidrobiológica 18:31–40.

Beamish, R. J.
1979. Differences in the age of Pacific hake (*Merluccius productus*) using whole otoliths and sections of otoliths. J. Fish. Res. Board Can. 36:141–151.

Beamish, R. J., and D. A. Fournier.
1981. A method for comparing the precision of a set of age determinations. Can. J. Fish. Aquat. Sci. 38:982–983.

Bishop, S. D. H., M. P. Francis, C. Duffy, and J. C. Montgomery.
2006. Age, growth, maturity, longevity and natural mortality of the shortfin mako shark (*Isurus oxyrinchus*) in New Zealand waters. Mar. Freshw. Res. 57:143–154.

Bizzarro, J. J., W. D. Smith, J. F. Márquez-Farías, and R. E. Hueter.
2007. Artisanal fisheries and reproductive biology of the golden cownose ray, *Rhinoptera steindachneri* Evermann and Jenkins, 1891, in the northern Mexican Pacific. Fish. Res. 84:137–146.

Burgos-Vázquez, M. I., V. E. Chávez-García, V. H. Cruz-Escalona, A. F. Navia, and P. A. Mejía-Falla.
2018. Reproductive strategy of the Pacific cownose ray *Rhinoptera steindachneri* in the southern Gulf of California. Mar. Freshw. Res. 70:93–106.

Burnham, K. P., and D. R. Anderson.
2002. Model selection and multimodel inference: a practical information-theoretic approach, 2nd ed., 488 p. Springer Science, New York.

Cailliet, G. M.
2015. Perspectives on elasmobranch life-history studies: a focus on age validation and relevance to fishery management. J. Fish Biol. 87:1271–1292.

Cailliet, G. M., and K. J. Goldman.
2004. Age determination and validation in chondrichthyan fishes. *In* Biology of sharks and their relatives (J. C. Carrier, J. A. Musick, and M. R. Heithaus, eds.), p. 399–447. CRC Press, Boca Raton, FL.

Cailliet, G. M., W. D. Smith, H. F. Mollet, and K. J. Goldman.
2006. Age and growth studies of chondrichthyan fishes: the need for consistency in terminology, verification, validation, and growth function fitting. Environ. Biol. Fishes 77:211–228.

Campana, S. E.
2001. Accuracy, precision and quality control in age determination, including a review of the use and abuse of age validation methods. J. Fish Biol. 59:197–242.

Campana, S. E., M. C. Annand, and J. I. McMillan.
1995. Graphical and statistical methods for determining the consistency of age determinations. Trans. Am. Fish. Soc. 124:131–138.

Carlson, J. K., and I. E. Baremore.
2003. Changes in biological parameters of Atlantic sharpnose shark *Rhizoprionodon terraenovae* in the Gulf of Mexico: evidence for density-dependent growth and maturity? Mar. Freshw. Res. 54:227–234.

Chang, W. Y. B.
1982. A statistical method for evaluating the reproducibility of age determination. Can. J. Fish. Aquat. Sci. 39:1208–1210.

Chapman, D. G.
1961. Statistical problems in dynamics of exploited fisheries population. *In* Proceedings of the fourth Berkeley symposium on mathematical statistics and probability. Volume 4: contributions to biology and problems of medicine; Berkeley, 20 June–30 July 1960 (J. Neyman, ed.), p. 153–168. Univ. Calif. Press, Berkeley, CA.

Coll, M., M. G. Pennino., J. Steenbeek., J. Sole., and J. M. Bellido.
2019. Predicting marine species distributions: complementarity of food-web and Bayesian hierarchical modelling approaches. Ecol. Model. 405:86–101.

Cortés, E.
1998. Demographic analysis as an aid in shark stock assessment and management. Fish. Res. 39:199–208.

Cortés, E., E. N. Brooks, and K. W. Shertzer.
2015. Risk assessment of cartilaginous fish populations. ICES J. Mar. Sci. 72:1057–1068.

Davis, C. D., G. M. Cailliet, and D. A. Ebert.
2007. Age and growth of the roughtail skate *Bathyraja trachura* (Gilbert 1892) from the eastern North Pacific. Environ. Biol. Fishes 80:325.

Doll, J. C., and S. J. Jacquemin.
2018. Introduction to Bayesian modeling and inference for fisheries scientists. Fisheries 43:152–161.

Doño, F., S. Montealegre-Quijano, A. Domingo, and P. G. Kinas.
2015. Bayesian age and growth analysis of the shortfin mako shark *Isurus oxyrinchus* in the western South Atlantic Ocean using a flexible model. Environ. Biol. Fishes 98:517–533.

Fisher, R. A., G. C. Call, and R. D. Grubbs.
2013. Age, growth, and reproductive biology of cownose rays in Chesapeake Bay. Mar. Coast. Fish. 5:224–235.

Gallucci, V. F., and T. J. Quinn II.
1979. Reparameterizing, fitting, and testing a simple growth model. Trans. Am. Fish. Soc. 108:14–25.

Gámez-Moedano, L. G., V. Anislado-Tolentino, and D. C. Espinosa.
2006. Estudio preeliminar de la historia de vida del gavilán negro, *Rhinoptera steindachneri* (Everman y Jenkins, 1982) en el estado de Sinaloa, México. *In* Memorias del 3ro foro científico de pesca ribereña; Jalisco, 3–5 October (E. E. Bar, M. Águila, and M. Gómez, eds.), p. 23–24. Secr. Agric. Ganaderia Desarro. Rural Pesca Aliment, Mexico City, Mexico. [In Spanish.] [Available from website.]

Garcés-García, K. C., J. Tovar-Ávila, B. Vargas-Trejo, D. A. Chávez-Arrequín, T. I. Walker, and R. W. Day.
2020. Elasmobranch bycatch by prawn trawls in the Gulf of California: first comprehensive analysis and the effect of fish escape devices. Fish. Res. 230:105639.

Gerrodette, T.
2011. Inference without significance: measuring support for hypotheses rather than rejecting them. Mar. Ecol. 32:404–418.

Gerrodette, T., and T. Eguchi.
2011. Precautionary design of a marine protected area based on a habitat model. Endanger. Species Res. 15:159–166.

Goldman, K. J., and J. A. Musick.
2006. Growth and maturity of salmon sharks (*Lamna ditropis*) in the eastern and western North Pacific, and comments on back-calculation methods. Fish. Bull. 104:278–292.

Hale, L. F., and C. G. Lowe.
2008. Age and growth of the round stingray *Urobatis halleri* at Seal Beach, California. J. Fish Biol. 73:510–523.

Joung, S.-J., P.-H. Lee, K.-M. Liu, and Y.-Y. Liao.
2011. Estimates of life history parameters of the sharpspine skate, *Okamejei acutispina*, in the northeastern waters of Taiwan. Fish. Res. 108:258–267.

Katsanevakis, S.
2006. Modelling fish growth: model selection, multi-model inference and model selection uncertainty. Fish. Res. 81:229–235.

Lee, R. M.
1912. An investigation into the methods of growth determination in fishes by means of scales. ICES J. Mar. Sci. S1(63):3–34.

Lessa, R., F. M. Santana, and P. Duarte-Neto.
2006. A critical appraisal of marginal increment analysis for assessing temporal periodicity in band formation among tropical sharks. Environ. Biol. Fishes 77:309–315.

Márquez-Farías, J. F.
2002. The artisanal ray fishery in the Gulf of California: development, fisheries research and management issues. Shark News 14, March.
2005. Gillnet mesh selectivity for the shovelnose guitarfish (*Rhinobatos productus*) from fishery-dependent data in the artisanal ray fishery of the Gulf of California, Mexico. J. Northwest Atl. Fish. Sci. 35:443–452.

McEachran, J. D., and G. Notarbartolo-di-Sciara.
1995. Peces batoideos. *In* Guía FAO para identificación de especies para los fines de la pesca. Pacifico centro oriental. Vol. 2. Vertebrados, parte 1 (W. Fischer, F. Krupp, W. Schneider, C. Sommer, K. E. Carpenter, and V. H. Niem, eds.), p. 745–792. FAO, Rome. [In Spanish.]

Mejía-Falla, P. A., E. Cortés, A. F. Navia, and F. A. Zapata.
2014. Age and growth of the round stingray *Urotrygon rogersi*, a particularly fast-growing and short-lived elasmobranch. PLoS ONE 9(4):e96077.

Mollet, H. F., and G. M. Cailliet.
2002. Comparative population demography of elasmobranch using life history tables, Leslie matrices and stage-based matrix models. Mar. Freshw. Res. 53:503–516.

Moulton, P. L., T. I. Walker, and S. R. Saddlier.
1992. Age and growth studies of gummy shark, *Mustelus antarcticus* Günther, and school shark, *Galeorhinus galeus* (Linnaeus), from southern Australian waters. Aust. J. Mar. Freshw. Res. 43:1241–1267.

Natanson, L. J., J. A. Sulikowski, J. R. Kneebone, and P. C. Tsang.
2007. Age and growth estimates for the smooth skate, *Malacoraja senta*, in the Gulf of Maine. Environ. Biol. Fishes 80:293–308.

Natanson, L. J., G. B. Skomal, S. L. Hoffmann, M. E. Porter, K. J. Goldman, and D. Serra.
2018. Age and growth of sharks: do vertebral band pairs record age? Mar. Freshw. Res. 69:1440–1452.

Neer, J. A., and B. A. Thompson.
2005. Life history of the cownose ray, *Rhinoptera bonasus*, in the northern Gulf of Mexico, with comments on geographic variability in life history traits. Environ. Biol. Fishes 73:321–331.

Osuna-Soto, J. E.
2016. Validación de la edad de la raya tecolote *Rhinoptera steindachneri* Evermann y Jenkins, 1891 utilizando oxitetraciclina como biomarcador. Bachelor's thesis, 60 p. Univ. Autonoma Sinaloa, Sinaloa, Mexico. [In Spanish.]

Pitcher, T. J., and P. J. B. Hart.
1982. Fisheries ecology, 414 p. Kluwer Acad. Publ., Dordrecht, Netherlands.

Plummer, M.
2003. JAGS: a program for analysis of Bayesian graphical models using Gibbs sampling. *In* Proceedings of the 3rd international workshop on distributed statistical computing (DSC 2003); Vienna, 20–22 March (K. Hornik, F. Leisch, and A. Zeileis, eds.), 10 p. [Available from website.]

R Core Team.
2019. R: a language and environment for statistical computing. R Foundation for Statistical Computing, Vienna, Austria. [Available from website, accessed December 2019.]

Richards, F. J.
1959. A flexible growth function for empirical use. J. Exp. Bot. 10:290–301.

Ricker, W. E.
1975. Computation and interpretation of biological statistics of fish populations. Bull. Fish. Res. Board Can. 191, 382 p.
1979. Growth rates and models. *In* Fish physiology, vol. 8 (W. S. Hoar, D. J. Randall, and J. R. Brett, eds.), p. 677–743. Academic Press, New York.

Robert, C. P., and G. Casella.
2004. Monte Carlo statistical methods, 2nd ed., 649 p. Springer, New York.

Rolim, F. A., Z. A. Siders, F. P. Caltabellota, M. M. Rotundo, and T. Vaske-Júnior.
2020. Growth and derived life-history characteristics of the Brazilian electric ray *Narcine brasiliensis*. J. Fish Biol. 97:396–408.

Schnute, J.
1981. A versatile growth model with statistically stable parameters. Can. J. Fish. Aquat. Sci. 38:1128–1140.

Smart, J. J., and G. L. Grammer.
2021. Modernising fish and shark growth curves with Bayesian length-at-age models. PLoS ONE 16(2):e0246734.

Smart, J. J., A. Chill, A. J. Tobin, and C. A. Simpfendorfer.
2016. Multimodel approaches in shark and ray growth studies: strengths, weaknesses and the future. Fish Fish. 17:955–971.

Smith, J. W., and J. V. Merriner.
1987. Age and growth, movements and distribution of the cownose ray, *Rhinoptera bonasus*, in Chesapeake Bay. Estuaries 10:153–164.

Villavicencio-Garáyzar, C. J.
1996. Reproductive biology of the Pacific cownose, *Rhinoptera steindachneri*, in Baja California, México. Presentation at the 12th annual meeting of the American Elasmobranch Society; New Orleans, 13–19 June (S. A. Moss, ed.). Am. Elasmobranch Soc. [Abstract.] [Available from website.]

von Bertalanffy, L.
1938. A quantitative theory of organic growth (Inquiries on growth laws. II). Hum. Biol. 10:181–213.

Walker, T. I.
1998. Can shark resources be harvested sustainably? A question revisited with a review of shark fisheries. Mar. Freshw. Res. 49:553–572.

Walker, T. I., B. L. Taylor, R. J. Hudson, and J. P. Cottier.
1998. The phenomenon of apparent change of growth rate in gummy shark (*Mustelus antarcticus*) harvested off southern Australia. Fish. Res. 39:139–163.

White, J., C. A. Simpfendorfer, A. J. Tobin, and M. R. Heupel.
2014. Age and growth parameters of shark-like batoids. J. Fish Biol. 84:1340–1353.

National Marine
Fisheries Service
NOAA

Fishery Bulletin
established in 1881

Spencer F. Baird
First U.S. Commissioner
of Fisheries and founder
of *Fishery Bulletin*

Comparison of ages determined by using an Eberbach projector and a microscope to read scales from Atlantic menhaden (*Brevoortia tyrannus*) and Gulf menhaden (*B. patronus*)

Amy M. Schueller (contact author)
Amanda Rezek
Raymond M. Mroch III
Eric Fitzpatrick
Alicia Cheripka

Email address for contact author: amy.schueller@noaa.gov

Beaufort Laboratory
Southeast Fisheries Science Center
National Marine Fisheries Service
101 Pivers Island Road
Beaufort, North Carolina 28516

Abstract—Age determination is important for estimating productivity and status in fisheries stock assessments. Aging methods must balance advances in technology with continuity of data for long-term sampling programs. The long-term sampling program for Atlantic menhaden (*Brevoortia tyrannus*) and Gulf menhaden (*B. patronus*) has resulted in a database of ages that were determined by using an Eberbach projector, a now outdated technology. The objective of this study was to compare ages determined with an Eberbach projector to those determined with a more recent technology, the stereo microscope. Scales from Atlantic (total number of fish [N]=1317) and Gulf menhaden (N=1569) were aged by using both an Eberbach projector and a stereo microscope, and results were compared by using percent agreement, average percent error, Chang's average coefficient of variation, bias tests, and simultaneous multinomial confidence intervals. The results from these measures for comparing age estimates were generally within standard, expected levels. Some bias was detected between estimates from the use of the 2 devices but was likely due to the use of poorly preserved scales or images of low quality on the Eberbach projector. Our results indicate that the use of a microscope will help maintain continuity in age estimates over time for long-term monitoring and for stock assessments.

Manuscript submitted 2 July 2020.
Manuscript accepted 8 March 2021.
Fish. Bull. 119:21–32 (2021).
Online publication date: 5 April 2021.
doi: 10.7755/FB.119.1.4

The views and opinions expressed or implied in this article are those of the author (or authors) and do not necessarily reflect the position of the National Marine Fisheries Service, NOAA.

Determining the health of fish populations is of the utmost importance to ensure that fishery yields are sustainable over time. Knowledge of the life histories of species is integral to understanding the population dynamics and factors that may influence the sustainability of a fishery. Several life history statistics, including size estimates for fishable year classes, can be determined by knowing the age of individuals caught (June and Roithmayr, 1960; Campana, 2001). Collecting these age data can be done by grouping fish by length frequencies or by counting annuli on otoliths or scales (Secor et al., 1995; Campana and Thorrold, 2001). Determining age through the use of otoliths can sometimes be impractical because of the time and effort required to extract, prepare, and age the structure. The use of scale samples can yield age data, and the collection and preparation time required is significantly less for using scales than for using otoliths (Nicholson and Schaaf, 1978; VanderKooy[1]). Aging with scales also does not require sacrificing the fish (Khan and Khan, 2009; Vilizzi, 2018).

Age data from collected scales and otoliths are used to calculate statistics such as productivity of a population, growth rate, and mortality rate (June and Roithmayr, 1960; Campana, 2001). These calculated variables form the basis of stock assessments, which provide information essential to the management of fisheries. Specifically, age data include catch composition and the age classes represented by survey data and can be used to track cohorts through the population over time and to estimate life history characteristics, such as growth rate, natural mortality, and fecundity (Beamish and McFarlane, 1995; Morison et al., 1998). All of these data are used to estimate parameters in stock assessments; therefore, the process of aging fish is critically important.

Atlantic menhaden (*Brevoortia tyrannus*) and Gulf menhaden (*B. patronus*)

[1] VanderKooy, S. (ed.). 2009. Gulf menhaden *Brevoortia patronus*. *In* A practical handbook for determining the ages of Gulf of Mexico fishes, 2nd ed., p. 5-70–5-73. Gulf States Mar. Fish. Comm., Publ. 167. Gulf States Mar. Fish. Comm., Ocean Springs, MS. [Available from website.]

are 2 commercially important species in the United States for which the stocks are routinely assessed (SEDAR, 2015, 2018). Both species are schooling clupeids pursued by a large, commercial purse seine fishery, called the *reduction fishery*. Additionally, a smaller bait fishery pursues Atlantic menhaden and captures about a quarter of the coastwide catch in U.S. waters of the Atlantic Ocean (SEDAR, 2015). Atlantic menhaden are caught along the Atlantic coast of the United States, mainly from Virginia to New Jersey. Gulf menhaden are taken in the Gulf of Mexico with most of the catch coming from the waters of Louisiana and Mississippi. These 2 fisheries are the largest by volume on their respective coasts and together compose the second-largest fishery by volume in the United States (NMFS[2]). Both species are important forage species and are eaten by other popular game fish species. The stock assessments for each species are reliant on the age data that have been provided from the Beaufort Laboratory of the NOAA Southeast Fisheries Science Center since 1955 for Atlantic menhaden and since 1964 for Gulf menhaden.

Aging of fish must evolve with time and technology, while continuity of data for long-term sampling programs is maintained. Traditionally, for both menhaden species, readings of scales to estimate ages were done at the Beaufort Laboratory by using an Eberbach[3] projector (Eberbach Corp., Ann Arbor, MI) that was built in the 1930s. However, the projector and its components are now obsolete, and replacement components are difficult to find. Given the challenges and risks of failure that arise from the use of obsolete equipment, alternative aging methods needed to be established. The objective of this study was to determine if ages for Atlantic and Gulf menhaden estimated by using a stereo microscope would be similar to those determined by using the Eberbach projector, with particular emphasis on precision or repeatability and on bias in age estimates between devices and methods. The aim of this study was to provide an alternative, more accessible method for aging menhaden in the future, a method that will decrease the likelihood of system failure as well as allow digital storage of sample images and information.

Materials and methods

Scales for this study were obtained from a long-term monitoring program that regularly samples landings of both the reduction and bait fisheries, in a 2-stage cluster design at various processing plants and dock locations along the Atlantic and Gulf coasts, geographically and temporally covering the entirety of the combined fishery (SEDAR, 2015, 2018). Samples used for this study were collected in 2013 and 2017 for Atlantic menhaden and in 2005 and 2017 for Gulf menhaden. Port agents retrieved a bucket of fish from the top of a randomly selected vessel's fish-hold dockside to characterize the fish caught in the final set of the trip. The agent verified catch data and then selected 10 fish at random from the bucket and recorded fork length (in millimeters) and weight (in grams). From the 10 fish, scales were removed from an area centered in line with the foremost part of the dorsal fin along the lateral line. For each individual fish, 6–10 scales were cleaned and mounted between 2 glass microscope slides. Each scale sample was labeled by processing plant (if from the reduction fishery) or state (if from the bait fishery) and by year and was assigned a scale number or ID code. All scale samples were then used to estimate fish ages with an Eberbach projector and with a stereo microscope (Olympus SZX16, Olympus Corp., Tokyo, Japan).

Age was determined by counting the number of continuous annuli between the focus and edge of the scale and by considering marginal growth as well as size, capture date, and each species' conventional birth date, a standard practice in some systems for the estimation of ages of fish sampled from commercial catches over a series of years (*production aging*) and in the Beaufort Laboratory's menhaden program since the 1960s (June and Roithmayr, 1960; Nicholson and Schaaf, 1978; Morison et al., 1998; VanderKooy[1]). The additional information was important to help place fish in the proper cohort (O'Sullivan[4]), given the protracted spawning seasons of these species, and to provide better, more timely age estimates (Campana, 2001).

For age estimation done with the Eberbach projector, mounted scale samples were placed under the projector's objective (40× magnification), and the best scale was chosen for aging. Ages were recorded on a data sheet. If all scales were unreadable or if data were missing for a fish, the sample for that fish was excluded.

The same scale samples used in aging with the Eberbach projecter were observed by using a stereo microscope (7.5–16.0× magnification). An image of the best scale on each slide was taken by using image analysis software (cellSens, vers. 1.17, Olympus Corp.). Time between readings with the Eberbach projector and with the microscope for the primary reader (reader 1) varied from a few weeks to 3 years. Time between readings was the result of equipment and reader availability, sample selection intervals, and elapsed time between first readings during standard production aging for the long-term sampling program and the second readings for this study.

All scale samples were read on both instruments, and some were read by 2 readers. For Atlantic menhaden, samples were from fish caught in 2013 and 2017 and from the reference collection for this species at the Beaufort Laboratory. For Gulf menhaden, samples were from fish caught in 2005 and 2017 and from the reference collection for this species. These reference collections are sets of quality scale

[2] NMFS (National Marine Fisheries Service). 2018. Fisheries of the United States, 2017. NOAA, Natl. Mar. Fish. Serv., Curr. Fish. Stat. 2017, 142 p. [Available from website.]

[3] Mention of trade names or commercial companies is for identification purposes only and does not imply endorsement by the National Marine Fisheries Service, NOAA.

[4] O'Sullivan, S. 2007. Fisheries long term monitoring program—fish age estimation review, 22 p. Dep. Prim. Ind. Fish., Brisbane, Australia. [Available from website.]

samples with agreed upon ages from experienced readers, ages that are representative of all ages and the monthly seasonality typical in the fishery. The reference collections are used to assess aging consistency between readers and among estimates from a reader over time. The second reader (reader 2) estimated ages with scales on the Eberbach projector but only for Atlantic menhaden sampled in 2013, for Gulf menhaden sampled in 2005, and for both reference collections (SEFSC[5]). From 1969 through 2015, the same reader (reader 2) estimated ages of menhaden by using scales, and those estimates from the database at the Beaufort Laboratory (SEFSC[5]) compose the historical record of ages that was used in this study. Comparisons of ages determined with an Eberbach projector were made between reader 1 and reader 2 for each species for the sample years that could be compared.

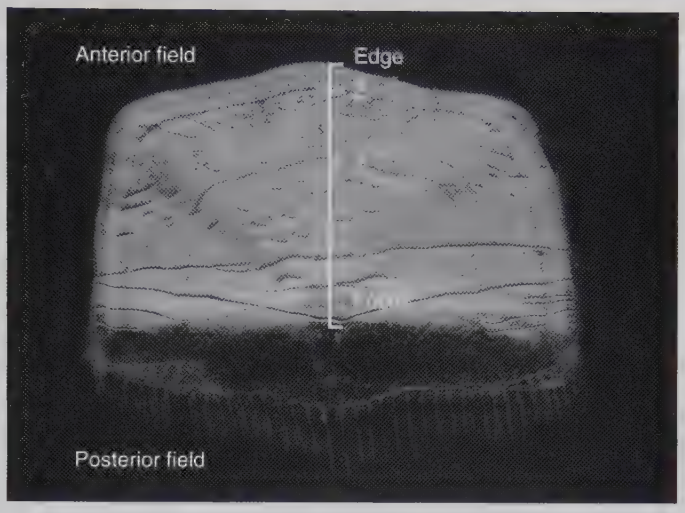

Figure 1

Image of a scale from an Atlantic menhaden (*Brevoortia tyrannus*), collected in 2019 off the Atlantic coast of the United States, showing 2 annuli in the anterior field. Scale measurements were taken for all subsamples and taken from the focus to each successive annulus and to the edge.

A subsample of 200 scales each from the full set of scale samples from Atlantic and Gulf menhaden was used to estimate ages a second time by reader 1 with both the Eberbach projector and the microscope. The best scale for each sample was selected, and its position on the slide was recorded so that the same scale could be used for aging on both devices. Subsampling provided 2 age readings on each device for each scale, allowing comparison of aging errors for each instrument and between them. This subsampling allowed errors to be classified as random reading errors versus errors due to the effect of the device used. On average, for reader 1, 10–19 months separated the first and second readings for scale samples from Atlantic and Gulf menhaden on the Eberbach projector and 6 months separated readings with the microscope.

Measurements of scales were taken for all subsamples (Fig. 1). A sonic digitizer pen fitted on the Eberbach projector was used for measuring distance from the focus of the scale to each annulus and to the edge margin. Measurements were recorded in Eberbach units and later converted to millimeters. The same distances were measured in millimeters on the calibrated image taken with the microscope, by using the image analysis software. On each image, an origin was placed on the scale's focus. The point tool was used to mark each annulus from the point of origin up to and including the edge. A new embedded image was created that included the scale image and the recorded measurements, and measurements were exported for analysis to Microsoft Excel 2016 (Microsoft Corp., Redmond, WA). In addition, while the Eberbach projector was being used for aging, a ruled blue card was placed on top of the projector's screen to manually measure each annulus and edge measurement of a scale image, as was done during the early years of data collection by the Beaufort Laboratory. A comparison of measurements for each scale was used to verify if the same annuli were counted on each device. This process allowed comparison of measurements taken by hand, with a sonic digitizer pen, and with image analysis software, temporally across the age data from the Beaufort Laboratory for both species of menhaden.

Both the full sample and the subsample of scales were chosen to reflect the seasonality of the fishery by month and the spatial spread of the fishery by location of the processing plants. In addition, samples were selected so that the length distribution of fish from which the samples were taken reflected the length distribution of all fish sampled from landings during a given year. Samples were chosen such that an adequate number of fish with younger and older ages were selected and such that the age composition matched that of the fishery samples taken in a given year.

Some scale samples were more than a decade old, and the quality of scales was inconsistent because of storage conditions. Although some scales remained in a quality good enough to age, others had debris or had degraded with time. Scales that were deemed unreadable by reader 1 on either of the instruments or that were missing or lost were excluded before analysis. First, we compared the number of excluded scales between readers and between devices. Second, we compared age readings for those scales that were legible. Finally, we compared successive annulus measurements between the Eberbach projector and the microscope.

Basic plots of ages by reader and device were created for each of the comparisons listed in the previous paragraph

[5] SEFSC (Southeast Fisheries Science Center). 2018. Unpubl. data. Menhaden Biostatistical Database. Beaufort Lab., Southeast Fish. Sci. Cent., Natl. Mar. Fish. Serv., NOAA, 101 Pivers Island Rd., Beaufort, NC 28516.

for both the full sample and subsamples. Plots of mean age with 95% confidence intervals were created, with each plot containing a 1:1 line, and are commonly used to examine age bias (Campana, 2001). We also produced plots of sample sizes by age. We explored the data to determine if the location of the processing plant, area, or month affected differences in aging for Atlantic and Gulf menhaden by comparing the distribution of the samples used in this study to the distribution of samples used in production aging of the long-term sampling program for processing plant, area, and month.

Several statistical tests were used to determine if the age estimates were significantly different between the 2 devices, between readers, and within readings of the same device and reader. The significance level (α) of 0.05 was used. Multiple approaches were needed to assess error, agreement, bias, precision, and symmetry (Campana et al., 1995); therefore, multiple tests are described and justified here.

Average percent error (APE; Beamish and Fournier, 1981; Campana et al., 1995), Chang's average coefficient of variation (ACV; Chang, 1982), and percent agreement (PA) were calculated to determine precision and agreement within the age data (Campana, 2001). All of these statistics are commonly used to compare age estimates. The APE and ACV can be artificially inflated by bias (Campana, 2001) and are related. In general use, APEs <5% are acceptable, as are ACVs of <5%; Campana (2001) calculated an average APE of 5.5% and an average ACV of 7.6% across studies. Values higher than those averages may indicate that structures are difficult to interpret or that readers lack training (Morison et al., 1998).

Three tests were used to determine symmetry within the paired age estimates between readers, by the same reader on the same device, and by the same reader on different devices: Bowker's (Bowker, 1948; Hoenig et al., 1995), Evans and Hoenig's (Evans and Hoenig, 1998), and McNemar's (McNemar, 1947; Hettmansperger and Mckean, 1973) tests. These tests were fairly robust in simulation testing (McBride, 2015), but Evans and Hoenig's test performed best. Bowker's test can detect bias with low APE and is unpooled, but results from this test have a higher incidence of type II errors (McBride, 2015). Evans and Hoenig's test can detect bias at higher APEs and is pooled on the diagonal (McBride, 2015). Evans and Hoenig (1998) found that their test was more powerful than Bowker's test and more general than McNemar's test. Finally, McNemar's test is a pooled test sensitive to small differences on one side of the diagonal (McBride, 2015). Each of these tests provide different information on precision and are not meant to corroborate results of the other tests.

Simultaneous multinomial confidence intervals were estimated to determine if the multinomial distributions differed significantly between age readings from the different instruments (Sison and Glaz, 1995; Zar, 1999). The intent of the use of these intervals was to determine if the age estimates and other information that would be provided to a stock assessment would be similar between the devices used for aging. Ultimately, the end products to which the age estimates contribute are the stock assessments for Atlantic and Gulf menhaden. Therefore, if the overall age compositions produced for those assessments do not differ by the instrument used, either device could be used to successfully provide age compositions. The multinomial confidence intervals were calculated by using the MultinomialCI package (vers. 1.1; Villacorta, 2019) in R (vers. 3.5.3; R Core Team, 2019), and 95% confidence intervals were provided for each age.

Measurements of distances on scales made with the 3 methods (microscope, Eberbach projector, and blue cards) for subsamples were examined separately for the Atlantic and Gulf menhaden for each distance (e.g., focus to first annulus), excluding the final measurement from the focus to the edge of the scale. Box plots were generated to compare across measurement types. A repeated measures analysis of variance was used to determine if the distance measurements among the 3 methods for each increment were significantly different, given an α of 0.05.

Results

Total sample sizes for Atlantic and Gulf menhaden collected from landings were 1317 and 1569, respectively (Table 1). After exclusion of samples, 1119 and 1307 samples remained for Atlantic and Gulf menhaden, respectively. Atlantic menhaden samples were from sampling in 2013 (n=605) and 2017 (n=418) and from a reference collection (n=96). Gulf menhaden samples were from sampling in 2005 (n=759) and 2017 (n=499) and from a reference collection (n=49). Samples were excluded at a greater rate when examined with the Eberbach projector than with the microscope (Table 1). Scales of Atlantic menhaden were excluded 14% of the time when observed with the Eberbach projector and 8% of the time when examined with the microscope. Scales of Gulf menhaden were excluded 12% of the time when observed with the Eberbach projector and 10% of the time when examined with the microscope. A higher percentage of scale subsamples (n=200) were excluded when they were examined with the Eberbach projector than with the microscope (Table 2). For both Atlantic and Gulf menhaden, neither location of processing plant nor area nor month were more indicative of differences in age than the other variables, with an even distribution of differences across those variables; therefore, we do not provide those specific results here.

Both the APE and ACV for age data from the full sample sets for each species were below the level considered a benchmark for aging of fish (5%; Morison et al., 1998). The APEs of the age estimates for all of the samples of Atlantic menhaden and Gulf menhaden were 2.7% and 3.5%, respectively (Table 1). The APEs for age estimates for samples in the reference collections were as low as 0.8% for Atlantic menhaden and as 0.0% for Gulf menhaden. The APEs for age data on Atlantic menhaden were 3.5% for samples taken in 2013 and 1.8% for samples collected in 2017. The APEs for age data on Gulf menhaden

Table 1

Precision and agreement statistics for ages estimated by examining scales on an Eberbach projector and a stereo microscope for Atlantic menhaden (*Brevoortia tyrannus*) and Gulf menhaden (*B. patronus*) sampled from landings along the Atlantic and Gulf coasts of the United States. Scales were from Atlantic menhaden collected in 2013 and 2017, Gulf menhaden collected in 2005 and 2017, and reference collections for each species. The statistical tests used to determine precision and agreement of age estimates included average percent error (APE), average coefficient of variation (ACV), and percent agreement. Total number of fish for which scales were used to determine ages (N), sample size used for analysis after exclusion of scales (n), and percentage of scale samples that were excluded are presented for each data set.

Data set	N	n	Samples excluded (%)		APE	ACV	Percent agreement
			Projector	Microscope			
Atlantic menhaden							
All	1317	1119	14%	8%	2.7%	3.8%	88.9%
2013	730	605	16%	8%	3.5%	5.0%	86.3%
2017	490	418	12%	9%	1.8%	2.6%	91.2%
Reference	100	96	4%	4%	0.8%	1.2%	95.8%
Gulf menhaden							
All	1569	1307	12%	10%	3.5%	5.0%	89.7%
2005	920	759	12%	9%	4.4%	6.2%	86.2%
2017	600	499	12%	11%	2.5%	3.6%	94.0%
Reference	49	49	0%	0%	0.0%	0.0%	100.0%

Table 2

Precision and agreement statistics for ages estimated by examining scale subsamples on an Eberbach projector and a stereo microscope for Atlantic menhaden (*Brevoortia tyrannus*) and Gulf menhaden (*B. patronus*) collected from landings in 2013 and 2017 along the Atlantic coast of the United States and in 2005 and 2017 along the Gulf coast, respectively. The statistical tests used to determine precision and agreement of age estimates included average percent error (APE), average coefficient of variation (ACV), and percent agreement. Reading 1 is the first reading of the sample set on both the projector and microscope, and reading 2 is the second reading on both instruments. Values in the "Projector" and "Microscope" rows are from comparisons of the 2 readings of the scale subsamples on the same device. n=sample size used for analysis.

Data set	n	APE	ACV	Percent agreement
Atlantic menhaden				
Reading 1	186	2.9%	4.2%	89.3%
Reading 2	185	3.1%	4.4%	89.2%
Projector	176	3.1%	4.4%	88.6%
Microscope	176	3.7%	5.2%	86.4%
Gulf menhaden				
Reading 1	177	9.7%	13.8%	83.6%
Reading 2	173	0.7%	1.0%	97.1%
Projector	157	8.7%	12.3%	84.7%
Microscope	157	4.1%	5.8%	92.4%

were 4.4% for samples taken in 2005 and 2.5% for samples collected in 2017. The ACV for age estimates for all of the samples of Atlantic menhaden was 3.8%, and the ACV for age estimates for all of the samples of Gulf menhaden was 5.0% (Table 1). The ACVs for age estimates for samples in the reference collections were as low as 1.2% for Atlantic menhaden and 0.0% for Gulf menhaden. The ACVs for age data on Atlantic menhaden were 5.0% for samples taken in 2013 and 2.6% for the samples collected in 2017. The ACVs for age data on Gulf menhaden were 6.2% for samples taken in 2005 and 3.6% for samples collected in 2017. Age estimates for the more recent samples, those taken in 2017, for each species had better APE and ACV than the age estimates for the older samples from 2013 and 2005 (Table 1).

Average percent errors for the subsamples were below 5% for all comparisons of age data except for 2 comparisons of estimates for Gulf menhaden (Table 2). Specifically, when the first readings of a scale sample were compared between devices, the APE was 9.7%, and when the first and second readings with the Eberbach projector were compared, the APE was 8.7%. The ACVs of age estimates for the subsamples followed the same patterns as the APEs, given that the ACV is a fixed proportion larger than APE when comparisons are between 2 measurements.

Percent agreement was 88.9% for readings of scales from Atlantic menhaden overall and 89.7% for readings of scales from Gulf menhaden overall (Table 1). Percent agreement varied by year of sampling with the readings of

scales from the reference collections having the best agreement with 95.8% for Atlantic menhaden and 100.0% for Gulf menhaden. The readings for more recent samples, those taken in 2017, had better PA than the readings of the older samples from 2013 and 2005. Percent agreement in the age estimates for scale subsamples ranged from 83.6% to 97.1% (Table 2). For age data on subsamples of Atlantic menhaden, PA was consistently >88%. For age data on subsamples of the Gulf menhaden, PA was more variable, with comparisons of the second readings done with the Eberbach projector and microscope and comparisons of the first and second readings done with the microscope having PA above 90%.

For all scale samples examined in our study, the proportion of scales for each of the determined ages reflected the proportion of samples for each observed age in the long-term sampling program for the Atlantic and Gulf menhaden fisheries (Fig. 2; for age compositions used in the respective stock assessments, see SEDAR, 2018, 2020 and Supplementary Figures 1–6 [online only]), and the age bias plots indicate that 95% confidence intervals for mean ages were small (Suppl. Figs. 7–14) (online only). Differences in aging were greatest at the older ages (>3 years) and at age 0; however, sample sizes for these ages were smaller than those for the ages of 1 year and 2 years. Patterns in the number of samples for each of the ages determined for subsamples of Atlantic and Gulf menhaden on the same device are similar to patterns for the full sample, with small numbers of deviations in age that are both above and below the 1:1 line in age bias plots, except for the ages of 3 and 4 years estimated with the Eberbach projector for Atlantic menhaden (Suppl. Fig. 15) (online only).

For samples from the reference collections and samples taken in 2017 for both Atlantic and Gulf menhaden, no bias in age estimates was found in comparisons between the 2 pieces of equipment—across all of the tests of symmetry (Table 3). For the samples of Gulf menhaden from 2005, however, the results of all 3 tests of symmetry indicate significant bias. A significant bias in age estimates for samples of Atlantic menhaden from 2013 is indicated only in results from the Bowker's test. For all samples of Atlantic menhaden in total, results of the Bowker's test indicate some bias, likely influenced heavily by the data set for samples from 2013, and the results of the other tests do not indicate significant bias in age data between the Eberbach projector and microscope. For all samples of Gulf menhaden in total, results of all 3 tests of symmetry indicate significant bias in age estimates, influenced heavily by the data set for samples from 2005. For the subsamples, results from all tests for both species indicate significant bias in ages estimated with the Eberbach projector; results of these tests for both species indicate that bias was not significant for ages determined with the microscope. In comparisons of ages for the subsamples between estimates made with the Eberbach projector and those made with the microscope, results of some tests indicate significant bias, but results from other tests do not, outcomes that are likely influenced by the bias in ages determined with the Eberbach projector.

Overall simultaneous multinomial confidence intervals were slightly different for the ages of 1 year and 2 years

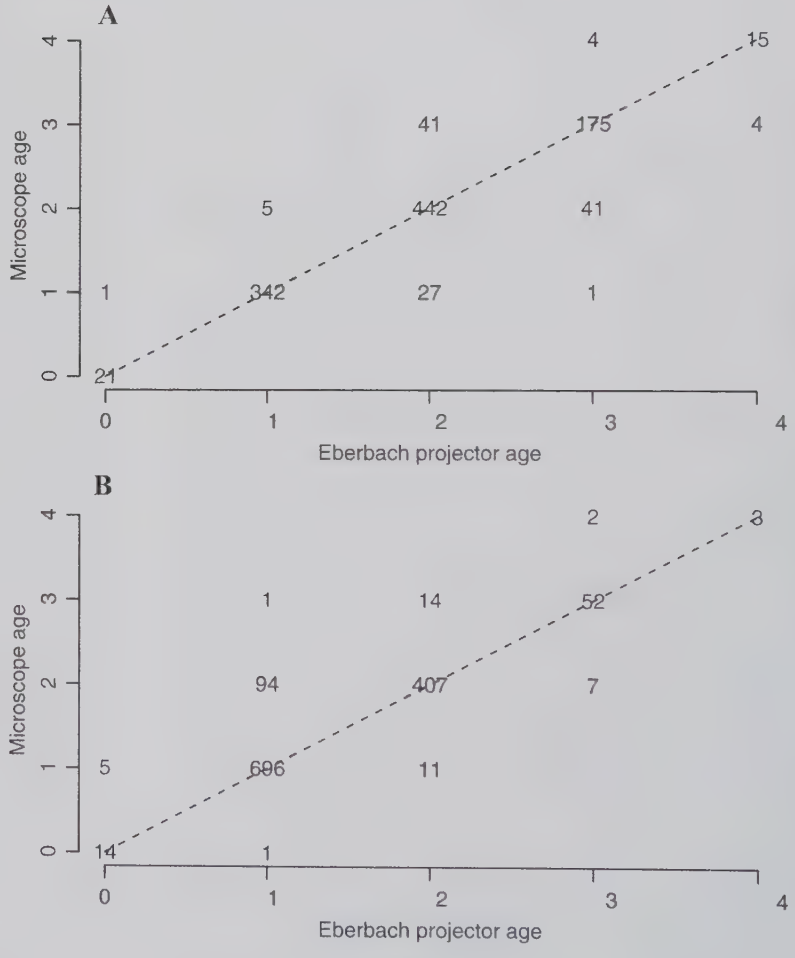

Figure 2

Age bias plots showing the number of samples for each age estimated with an Eberbach projector and stereo microscope for all (**A**) Atlantic menhaden (*Brevoortia tyrannus*) and (**B**) Gulf menhaden (*B. patronus*) collected from landings along the Atlantic and Gulf coasts of the United States. Samples included Atlantic menhaden collected in 2013 and 2017, Gulf menhaden collected in 2005 and 2017, and reference collections for each species. The 1:1 line represents agreement between the age estimates from use of the 2 devices.

Table 3

Results from tests of symmetry in ages estimated by examining scales on an Eberbach projector and a stereo microscope for Atlantic menhaden (*Brevoortia tyrannus*) and Gulf menhaden (*B. patronus*) sampled along the Atlantic and Gulf coasts of the United States. Scales were from Atlantic menhaden collected in 2013 and 2017, Gulf menhaden collected in 2005 and 2017, and reference collections for each species. Reading 1 is the first reading of the sample set on both the projector and microscope, and reading 2 is the second reading on both instruments. Values are from comparisons of the 2 readings of scales in full samples and in subsamples on both devices and from comparisons of ages for subsamples determined on the same instrument. *P*-values for test results are provided in parentheses. *n*=sample size used for analysis. NA=not applicable.

Data set	*n*	Bowker's	Evans and Hoenig's	McNemar's
Atlantic menhaden				
All	1119	17.1 (<0.01)	4.6 (0.10)	3.9 (0.05)
2013	605	17.8 (<0.01)	2.8 (0.25)	2.0 (0.15)
2017	418	2.3 (0.51)	1.3 (0.25)	1.3 (0.25)
Reference	96	1.0 (0.32)	1.0 (0.32)	1.0 (0.32)
Subsample: reading 1	186	3.2 (0.68)	1.5 (0.48)	0.2 (0.65)
Subsample: reading 2	185	16.8 (<0.01)	16.2 (<0.01)	16.2 (<0.01)
Subsample: projector	176	10.3 (0.07)	9.9 (0.01)	7.2 (0.01)
Subsample: microscope	176	4.5 (0.60)	1.6 (0.44)	1.5 (0.22)
Gulf menhaden				
All	1307	73.7 (<0.01)	69.8 (<0.01)	69.7 (<0.01)
2005	759	74.4 (<0.01)	72.1 (<0.01)	72.1 (<0.01)
2017	499	4.4 (0.22)	3.3 (0.07)	3.3 (0.07)
Reference	49	0.0 (1.00)	0.0 (1.00)	NA (NA)
Subsample: reading 1	177	19.8 (0.01)	12.6 (< 0.01)	12.5 (<0.01)
Subsample: reading 2	173	5.0 (0.08)	5.0 (0.03)	5.0 (0.03)
Subsample: projector	157	11.5 (0.02)	6.0 (0.01)	6.0 (0.01)
Subsample: microscope	157	5.7 (0.13)	1.3 (0.25)	1.3 (0.25)

but not for the other ages for both the Atlantic and Gulf menhaden (Fig. 3). The mean ages for samples taken in 2017 and for samples from the reference collections were within the 95% confidence intervals for both species (Suppl. Figs. 16 and 17) (online only). However, the mean ages for older samples that were collected in 2005 and 2013 were significantly different.

Mean annuli distances for Atlantic and Gulf menhaden increased as counts of annuli increased (Suppl. Table 1) (online only). Scale distances measured at each annulus with a blue card were longer than those measured with the Eberbach projector and those measured with the microscope (Suppl. Fig. 18) (online only). Values were significantly different between the methods used, for the measurements from the focus to the second annulus and from the focus to the third annulus for Atlantic menhaden and for the measurement from the focus to the second annulus for Gulf menhaden (Suppl. Table 1) (online only).

Readers 1 and 2 generally agreed on ages determined for samples from both reference collections (Suppl. Table 2) (online only), and APEs and ACVs were low for their age estimates. Average percent error was less than 5% for all comparisons, except for the comparison of ages for the samples of Gulf menhaden taken in 2005, for which the APE was 12.0%. The PA for ages estimated for samples of Gulf menhaden taken in 2005, at 64.5%, was lower than the PAs for age data for the other samples, between 82.2% and 100.0%.

Discussion

Quality assurance (QA) and quality control (QC) are required for integrity of data collected or calculated as part of long-term monitoring programs and for the provision of age estimates for fish sampled from commercial catches over a sequence of years (i.e., data from production aging) to be used in stock assessments. Quality assurance and QC are addressed differently in what is called *research aging*, which is geared toward a validation method and typically uses smaller sample sizes within a shorter time interval in comparison with production aging (Morison et al., 1998). Because it spans long time periods and large numbers of samples, production aging requires QC to ensure consistency among readings of each reader and between readers and methods for checking bias and minimizing errors to be

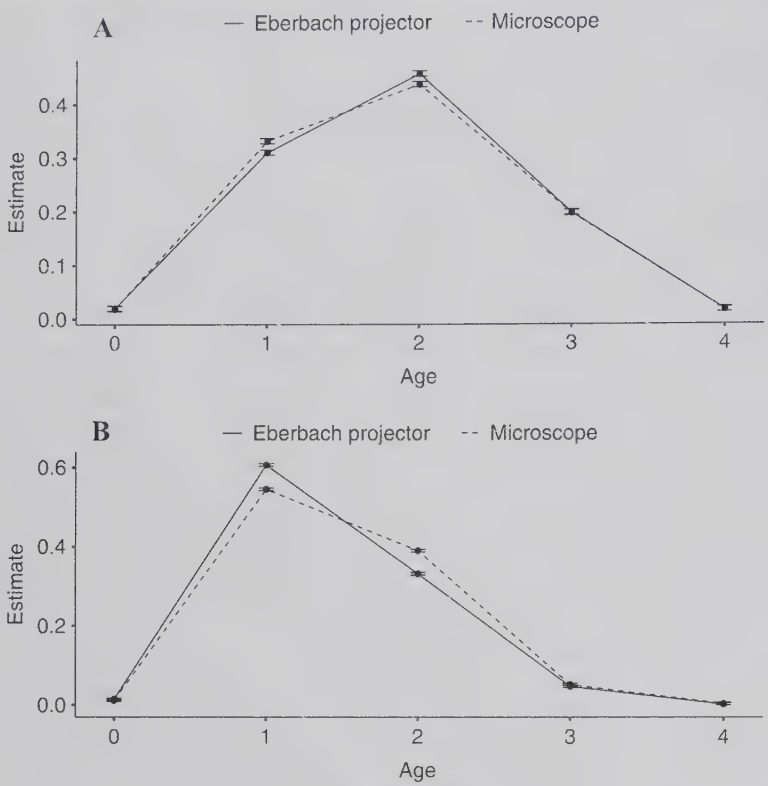

Figure 3

Simultaneous multinomial confidence intervals of age estimates, by method of aging, for all samples of (**A**) Atlantic menhaden (*Brevoortia tyrannus*) and (**B**) Gulf menhaden (*B. patronus*) collected along the Atlantic and Gulf coasts of the United States. Samples included Atlantic menhaden collected in 2013 and 2017, Gulf menhaden collected in 2005 and 2017, and reference collections for each species. Aging methods included the use of either an Eberbach projector or a stereo microscope. The solid line represents estimates of the proportion of samples at each age determined with the projector, and the dashed line represents estimates of the proportion of samples at each age determined with a microscope. Error bars indicate 95% confidence intervals.

appropriate and applied in a timely manner. Quality assurance and QC help to determine whether perceived changes in age estimates are from variation in aging precision or from real changes in fish populations (Morison et al., 1998). Although this study served as QA and QC for the Beaufort Laboratory's menhaden program, its main purpose was to assess the level of continuity in the data if age readings were done on a microscope rather than with the Eberbach projector.

The menhaden program of the Beaufort Laboratory has been run without appreciable change for more than half a century, and well over a million samples have been amassed with a remarkable continuity in collection methods and output. Because of the shift in aging methods that was necessitated by critical program updates, we needed to determine whether outputs from the use of the new method would be consistent with those from the use of the previous method. Results from our study indicate that, although there was some bias in the age estimates for Gulf menhaden and in estimates between readings made by using the Eberbach projector, the precision of age estimates made with the microscope, in comparison with those made with the Eberbach projector, is sufficient to allow the menhaden program to update the technology used for aging these 2 menhaden species. Continued aging for stock assessments should yield the same quality of data throughout the time series.

Sample sizes in our study were larger for each species than in many other studies that have considered aging precision. Experts have suggested a sample size of 200 fish, 100 from a reference collection and 100 from recent production samples, is sufficient to identify significant differences when testing for aging errors or inconsistencies (Campana, 2001). The large sample size in this study could have influenced the results of the bias tests and measures of aging consistency. McBride (2015) used a sample size of 5 fish to produce 5 age estimates per age class, a sample size that like those in most studies is much smaller than the sample sizes used in our study. For example, other studies have used sample sizes of 85–180 per species when comparing aging structures (Khan and Khan, 2009; Khan et al., 2015; Baudouin et al., 2016; Kumbar and Lad, 2016), 14–390 per species when comparing ages between readers (Wakefield et al., 2017; Khan et al., 2019), and 30–182 per species when comparing both aging methods and ages between readers (Gürsoy et al., 2005; Goldman and Musick, 2006; Herbst and Marsden, 2011). Given these smaller sample sizes, comparing age estimates from our study to those from the other studies has been difficult.

How large should sample sizes be to determine if bias occurs? If we consider only data from the reference collections of each species, the conclusions would be different than those from consideration of data from the full sample. For example, the PA is much higher for estimates based on the reference collections alone than for those based on the full sample, and the APE and ACV are much lower. The ages from the reference collections do not indicate significant bias for either species. Because of the smaller sample sizes, use of the reference collection for each species led to different conclusions than those from the use of the full sample; however, the sample sizes of the reference collections are similar to the sample sizes that have been used in other aging studies.

Percent agreement values were all above 86% among age estimates for samples overall between the microscope and Eberbach projector and were all above 83% between first and second readings within an instrument. Our results are similar to those from McBride (2015), who reported PA of around 80% with no bias and low variability. Values of PA were high for reference collections of Atlantic and Gulf menhaden (95.8% and 100.0%, respectively). A workshop on aging Atlantic menhaden that used the same reference collection calculated PA values of 58.2–86.7% for comparisons of microfiche with an Eberbach projector between 10 state laboratories and of 91.8% for comparisons on the Eberbach projector between reader 2 and another reader (ASMFC[6]). These values are similar to the PA of 91.7% between reader 1 and reader 2 in this study. An exchange of 100 fishery-independent scales between reader 1 and an aging technician at the University of Southern Mississippi, aged on the same Eberbach projector, yielded a PA of 79.0% (Leaf[7]). The PA values from our study were also similar to or higher than those from studies for other species, with PA values of 39.8–100.0% when precision of estimates for multiple aging structures were compared (Khan and Khan, 2009; Khan et al., 2015; Kumbar and Lad, 2016) and of 68.1–92.4% when estimated precision was compared between readers (Goldman and Musick, 2006; Khan et al., 2019).

Overall, comparisons of age estimates made with the microscope and the Eberbach projector resulted in APEs under 4.4%, which is similar to or less than published APEs of about 8.0% (Campana, 2001; McBride, 2015), including the mean APEs for estimates from a simulation by McBride (2015) that indicated no bias and that decreased with increasing precision. Average percent errors from other studies have ranged from 0.7% to 16.1% when age estimates were compared among multiple aging structures or between readers (Gürsoy et al., 2005; Khan and Khan, 2009; Khan et al., 2015; Khan et al., 2019). Average percent errors in age readings were best for the reference collections, which had better quality, more legible scales than the scales taken from fish sampled for this study. An APE of 8.2% was calculated at a workshop during which aging was done for a reference collection of Gulf menhaden (n=30) and during which microscope-based age estimates from a group of 6 state laboratories were compared with ages estimated with the Eberbach projector provided by reader 1 (VanderKooy[8]). Age estimates for scale subsamples from Gulf menhaden in our study had APEs of 9.7% when compared across devices and of 8.7% when compared among readings by a reader on the Eberbach projector, values that are higher than the benchmark identified in Campana (2001).

High APEs may indicate difficulty in maintaining consistency in the ages determined for Gulf menhaden with the Eberbach projector because of sample readability and quality. One third of the subsamples from Gulf menhaden were from 2005, a year in which scales had reduced quality due to improper storage. Although the use of both pieces of equipment yielded similar numbers of unreadable scales for reader 1, 55% of samples aged on the Eberbach projector, versus 35% of samples aged on the microscope, were noted to be fuzzy, dirty, or unreadable. Comparisons of subsamples of scales from Atlantic menhaden may have been affected by samples from the bait fishery (20% of the samples were from the bait fishery); samples from the bait fishery can be harder to read because of differences in fishing and sampling practices. Specifically, handling time on the vessel and in storage is greater for samples from the bait fishery than for samples from the reduction fishery, and fish are caught at different times of the year. Also, staff members that mount scales from fish sampled from the bait fishery typically have less experience.

The increase in APE values when comparing between the first and second readings for reader 1 could be due to greater experience. In 2017, when the first reading was done, reader 1 had been estimating ages of menhaden for 2 years, long enough to become proficient but still early enough that another year's experience would likely result in some level of improvement at the time of the second reading in 2018. However, although the APEs for the first readings were higher, they are on par with values of around 10% that have been observed for harder to read samples and for new readers in other studies (Potts[9]; McBride, 2015).

Values of ACV in this study were comparable to or less than values in simulation analyses (McBride, 2015), a workshop for aging Atlantic menhaden (ASMFC[6]), and studies on other species. The highest ACV value in this study was for the samples of Gulf menhaden taken in 2005 (6.2%), and this value is within the range of values reported in McBride (2015) on the basis of simulating age data with no bias across multiple precision levels but is higher than the value of 5% found to be accepted across data from several laboratories reviewed by Campana (2001). Analysis during a workshop on aging Atlantic menhaden resulted in ACVs that are generally above 5% among data from several laboratories but that do not exceed 15% (ASMFC[6]). The workshop participants computed an ACV of 2.1% (ASMFC[6]), a value that is similar to the ACV of 2.2% computed in this study for the same reference collection. Values of ACV for age data for both Atlantic and Gulf menhaden across all comparisons are similar to the values of 1.0–22.8% from other studies across aging structures and between readers (Khan and Khan, 2009; Herbst and Marsden, 2011; Khan et al., 2015; Khan et al., 2019). Values of ACV from this study indicate that the use of the microscope and the use of the Eberbach

[6] ASMFC (Atlantic States Marine Fisheries Commission). 2015. 2015 Atlantic menhaden ageing workshop report, 47 p. Atl. States Mar. Fish. Comm., Washington, D.C. [Available from website.]

[7] Leaf, R. 2018. Personal commun. Univ. South. Miss. 703 East Beach Dr., Ocean Springs, MS 39564.

[8] VanderKooy, S. 2019. Personal comm. Gulf States Mar. Fish. Comm. 2404 Government St., Ocean Springs, MS 39564.

[9] Potts, J. 2014. Personal commun. Natl. Mar. Fish. Serv. 101 Pivers Isl. Rd., Beaufort, NC 28516.

projector are comparable in providing ages for Atlantic and Gulf menhaden.

Our study used 3 bias tests to determine consistency in age readings, which were not consistent across all tests for Atlantic and Gulf menhaden. Bias in age estimates in our study is higher for some years than for others and higher for older samples than for more recent samples. For Atlantic menhaden, the only significant bias test was the Bowker's test, which can be sensitive to one pair of age estimates with a large difference (McBride, 2015). Bias in the age estimates for scale subsamples indicates that use of the Eberbach projector results in less consistency in age readings, and the lack of bias in the readings of subsamples done with the microscope indicates that the use of the microscope lends well to consistency. During a workshop on aging Atlantic menhaden conducted in 2015, comparisons of ages between reader 2 and 10 laboratories yielded inter-laboratory and intra-laboratory *P*-values of 0–1 depending upon the test (ASMFC[6]).

Tests of symmetry for age data are often variable, with not all tests providing the same indication of bias or lack thereof. Results of some studies indicate no bias across tests (Goldman and Musick, 2006; Harry et al., 2011), but other studies have variable results pertaining to bias depending upon the test, reader, or age structure used (Harry et al., 2013; Baudouin et al., 2016; Stewart and Ogle, 2016). McBride (2015) used 100 samples across 20 ages with 5 samples per age and found that bias was subject to varying rates of type I and type II errors depending upon the underlying simulations. Given the sample size used by McBride (2015), the question becomes how sample size might affect those results. Campana et al. (1995) suggested that bias could be ignored when bias was low. Given the low numbers of age-4 fish and the expectation that the bias may have primarily crept in through ages estimated with the Eberbach projector, results of this study indicate that using the microscope for age estimation of menhaden species has a lower chance of introducing bias to the age estimates than using the Eberbach projector. Also, the main use of the age data from the long-term sampling program is to provide age compositions to stock assessments, and the simultaneous multinomial confidence intervals indicate that the composition data will not be affected by a switch to aging on the microscope.

Scale distance measurements changed a small degree as the menhaden program of the Beaufort Laboratory switched from blue cards to the sonic digitizer pen to the microscope; many of the differences were not significant. With each update of the method, measurements may have become more precise. For example, for the method that includes the use of blue cards, the cards are lined up with the scale's focus on a slanted screen below waist height, and annuli are ticked off with a pencil. Consistently placing the blue card ruler slightly below the focus that would have been selected with the sonic digitizer pen could lead to consistent, slightly larger measurements. Updating to the sonic digitizer pen decades ago allowed pen-point precision for measurement selection. Further updating of the method to the use of a microscope has allowed a clearer and full view of the scale at eye level, use of a straight guideline for annulus selection, more precise selection of measurement points, and use of imaging software to view the measurements. The scale distance measurements indicate that similar structures are being measured to indicate true annuli. These data are not used in stock assessments. If these data are used for future research projects, the decreases in annulus measurements with changes in method should be taken into account.

In general, age estimates for Gulf menhaden had lower agreement, and the scale samples of this species were more difficult to read than those of Atlantic menhaden. Several factors, including scale size, consistency in sampler over time, and environmental conditions, could have contributed to these differences. First, individual Atlantic menhaden and their scales tend to be larger in size than Gulf menhaden and their scales. Larger sizes could make it easier for the port sampler to take samples from the proper location on the fish, where scales are more regular in shape and, therefore, more readable. Larger scales could result in more contrast and distance between perceived annuli, making them easier to read. Second, the same full-time employee has been the sampler of Atlantic menhaden since 1992. In the Gulf of Mexico, budgetary constraints have resulted in regular turnover of contract personnel that are selected, hired, and trained on an annual basis. Personnel differences would result in a consistently higher level of expertise in sampling at the port for the fishery in the Atlantic Ocean than that for the fishery in the Gulf of Mexico. Third, Atlantic menhaden caught in the fishery are exposed to environmental conditions that are more seasonally variable than those to which Gulf menhaden are exposed, given the differences in latitude included in their habitat range. Such differences in the habitats of other species have been reported to result in more contrast between rapid- and slow-growth periods (Hoxmeier et al., 2001; Green et al., 2009). The environmental differences could result in relatively higher-contrast scale circuli in Atlantic menhaden than the circuli of Gulf menhaden, therefore making them easier to age.

Overall, on the basis of the results of this study, we have determined that the use of scales on a microscope is an acceptable method for aging menhaden. Age estimates from use of the Eberbach projector were repeatable on the microscope, allowing continuity in the age data that have been maintained by the Beaufort Laboratory for decades. The microscope has many advantages. First, stage, light, and magnification options offer multiple ways to view samples more clearly while allowing for ergonomic considerations. Second, image analysis software used with a microscope allows more accurate straight-line measurements in units of the International System of Units. Third, because most laboratories have microscopes, samples can be viewed in a more uniform manner across facilities, making collaborations and comparisons easier. Fourth, data are more accessible and analysis of data is quicker because the data are no

longer stored in an outdated format. Finally, notes can be added to data entries in the database, along with sample information, and digital images of scales can be captured for easy reference and for training purposes within and across laboratories.

Moving forward, reference collections will be a primary QA and QC tool for training and maintaining aging standards (Eltink et al.[10]; Campana, 2001; Morison et al., 2005). New digital reference collections for Atlantic and Gulf menhaden will be composed of average quality scales with an annotated version to be shared with other aging laboratories for training purposes. A digital collection has longevity and ensures that all aging scales are prepared by the same method (Campana, 2001). Samples for the digital reference collection should represent multiple years and have 10 samples, with varying edge margins, from each of the age classes for each month of landings sampled (Eltink et al.[10]). Campana (2001) suggests that a reference collection composed of 200–500 samples be used for quality control, although a training set of 100 samples is sufficient. For exchanges, a reference collection of 400 samples has been suggested, with possibly 150–200 subsamples sent at a time (Eltink et al.[10]; Campana, 2001). A subsample of the samples used in this study could be assembled as a control collection because they are of unknown ages and are true representatives of the catch. A subsample of this collection should be aged again yearly by the current reader to reassess consistency, precision, and bias of age estimates and could be used to train another reader (Eltink et al.[10]; Campana, 2001). Collections should be updated at regular intervals.

Finally, the standards for determining continuity in age determination and for comparing between methods need further investigation. Sample sizes used in many studies are smaller than those in our study, and work to identify the sample size that is sufficient to answer questions of such examinations is greatly needed. McBride (2015), through simulation, tested PA, APE, ACV, and bias of age estimates by using different types of bias and sample sizes of 5 samples per age class with 20 ages. The behavior of these tests with differences in sample sizes across ages, meaning a more natural sample size distribution given common sampling protocols, would help to elucidate whether ages are consistent across methods.

Acknowledgments

We thank J. Potts, G. Nesslage, and the anonymous reviewers for helpful comments and suggestions on earlier drafts. This project was funded through the Improve a Stock Assessment Program of the Office of Science and Technology, National Marine Fisheries Service.

[10] Eltink, A. T. G. W., A. W. Newton, C. Morgado, M. T. G. Santamaria, and J. Modin. 2000. Guidelines and tools for age reading (PDF document version 1.0 October 2000). Eur. Fish Ageing Netw., EFAN Rep. 3-2000, 54 p. Eur. Fish Ageing Netw., Arendal, Norway.

Literature cited

Baudouin, M., M. Marengo, A. Pere, J.-M. Culioli, M.-C. Santoni, B. Marchand, and E. D. H. Durieux.
2016. Comparison of otolith and scale readings for age and growth estimation of common dentex *Dentex dentex*. J. Fish Biol. 88:760–766.

Beamish, R. J., and D. A. Fournier.
1981. A method for comparing the precision of a set of age determinations. Can. J. Fish. Aquat. Sci. 38:982–983.

Beamish, R. J., and G. A. McFarlane.
1995. A discussion of the importance of aging errors, and an application to walleye pollock: the world's largest fishery. *In* Recent developments in fish otolith research (D. H. Secor, J. M. Dean, and S. E. Campana, eds.), p. 545–565. Univ. South Carolina Press, Columbia, SC.

Bowker, A. H.
1948. A test for symmetry in contingency tables. J. Am. Stat. Assoc. 43:572–574.

Campana, S. E.
2001. Accuracy, precision and quality control in age determination, including a review of the use and abuse of age validation methods. J. Fish Biol. 59:197–242.

Campana, S. E., and S. R. Thorrold.
2001. Otoliths, increments, and elements: keys to a comprehensive understanding of fish populations? Can. J. Fish. Aquat. Sci. 58:30–38.

Campana, S. E., M. C. Annand, and J. I. McMillan.
1995. Graphical and statistical methods for determining the consistency of age determinations. Trans. Am. Fish. Soc. 124:131–138.

Chang, W. Y. B.
1982. A statistical method for evaluating the reproducibility of age determination. Can. J. Fish. Aquat. Sci. 39:1208–1210.

Evans, G. T., and J. M. Hoenig.
1998. Testing and viewing symmetry in contingency tables, with application to readers of fish ages. Biometrics 54:620–629.

Goldman, K. J., and J. A. Musick.
2006. Growth and maturity of salmon sharks (*Lamna ditropis*) in the eastern and western North Pacific, and comments on back-calculation methods. Fish. Bull. 104:278–292.

Green, B. S., B. D. Mapstone, G. Carlos, and G. A. Begg (eds.).
2009. Tropical fish otoliths: information for assessment, management and ecology, 313 p. Springer, Dordrecht, Netherlands.

Gürsoy, C., A. S. Tarkan, Ö. Gaygusuz, and H. Acıpınar.
2005. A comparison of ageing techniques to improve precision of age estimation from fish scales. Ege J. Fish. Aquat. Sci. 22:423–425.

Harry, A. V., W. G. Macbeth, A. N. Gutteridge, and C. A. Simpfendorfer.
2011. The life histories of endangered hammerhead sharks (Carcharhiniformes, Sphyrnidae) from the east coast of Australia. J. Fish Biol. 78:2026–2051.

Harry, A. V., A. J. Tobin, and C. A. Simpfendorfer.
2013. Age, growth and reproductive biology of the spot-tail shark, *Carcharhinus sorrah*, and the Australian blacktip shark, *C. tilstoni*, from the Great Barrier Reef World Heritage Area, north-eastern Australia. Mar. Freshw. Res. 64:277–293.

Herbst, S. J., and J. E. Marsden.
2011. Comparison of precision and bias of scale, fin ray, and otolith age estimates for lake whitefish (*Coregonus clupeaformis*) in Lake Champlain. J. Gt. Lakes Res. 37:386–389.

Hettmansperger, T. P., and J. W. Mckean.
1973. On testing for significant change in cxc tables. Commun. Stat. 2:551–560.
Hoenig, J. M., M. J. Morgan, and C. A. Brown.
1995. Analysing differences between two age determination methods by tests of symmetry. Can. J. Fish. Aquat. Sci. 52:364–368.
Hoxmeier, R. J. H., D. D. Aday, and D. H. Wahl.
2001. Factors influencing precision of age estimation from scales and otoliths of bluegills in Illinois reservoirs. North Am. J. Fish. Manage. 21:374–380.
June, F. C., and C. M. Roithmayr.
1960. Determining age of Atlantic menhaden from their scales. Fish. Bull. 171:323–342.
Khan, M. A., and S. Khan.
2009. Comparison of age estimates from scale, opercular bone, otolith, vertebrae and dorsal fin ray in *Labeo rohita* (Hamilton), *Catla catla* (Hamilton), and *Channa marulius* (Hamilton). Fish. Res. 100:255–259.
Khan, S., M. A. Khan, K. Miyan, and F. A. Lone.
2015. Precision of age estimates from different ageing structures in selected freshwater teleosts. J. Environ. Biol. 36:507–512.
Khan, M. A., S. Khan, Ankita, I. Ahmed, and M. Nadeem.
2019. Age and growth of spotted snakehead, *Channa punctata* from the Ganga River. J. Ichthyol. 59:197–204.
Kumbar, S. M., and S. B. Lad.
2016. Estimation of age and longevity of freshwater fish *Salmophasia balookee* from otoliths, scales and vertebrae. J. Environ. Biol. 37:943–947.
McBride, R. S.
2015. Diagnosis of paired age agreement: a simulation of accuracy and precision effects. ICES J. Mar. Sci. 72:2149–2167.
McNemar, Q.
1947. Note on sampling error of the difference between correlated proportions or percentages. Psychometrika 12:153–157.
Morison, A. K., S. G. Robertson, and D. C. Smith.
1998. An integrated system for production fish ageing: image analysis and quality assurance. North Am. J. Fish. Manage. 18:587–598.
Morison, A. K., J. Burnett, W. J. McCurdy, and E. Moksness.
2005. Quality issues in the use of otoliths for fish age estimation. Mar. Freshw. Res. 56:773–782.
Nicholson, W. R., and W. E. Schaaf.
1978. Aging of Gulf menhaden, *Brevoortia patronus*. Fish. Bull. 76:315–322.
R Core Team.
2019. R: a language and environment for statistical computing. R Foundation for Statistical Computing, Vienna, Austria. [Available from website, accessed May 2019.]
Secor, D. H., T. M. Trice, and H. T. Hornick.
1995. Validation of otolith-based ageing and a comparison of otolith and scale-based ageing in mark-recaptured Chesapeake Bay striped bass, *Morone saxatilis*. Fish. Bull. 93:186–190.
SEDAR (Southeast Data Assessment and Review).
2015. SEDAR 40—Atlantic menhaden stock assessment report, 643 p. SEDAR, North Charleston, SC. [Available from website.]
2018. SEDAR 63—Gulf menhaden stock assessment report, 352 p. SEDAR, North Charleston, SC. [Available from website.]
2020. SEDAR 69—Atlantic menhaden benchmark stock assessment report, 691 p. SEDAR, North Charleston, SC. [Available from website.]
Sison, C. P., and J. Glaz.
1995. Simultaneous confidence intervals and sample size determination for multinomial proportions. J. Am. Stat. Assoc. 90:366–369.
Stewart, T. R., and D. H. Ogle.
2016. Age, growth, and size of Lake Superior pygmy whitefish (*Prosopium coulterii*). Am. Midl. Nat. 175:24–36.
Vilizzi, L.
2018. Age determination in common carp *Cyprinus carpio*: history, relative utility of ageing structures, precision and accuracy. Rev. Fish Biol. Fish. 28:461–484.
Villacorta, P. J.
2019. MultinomialCI: simultaneous confidence intervals for multinomial proportions according to the method by Sison and Glaz. R package, vers. 1.1. [Available from website, accessed January 2020.]
Wakefield, C. B., J. M. O'Malley, A. J. Williams, B. M. Taylor, R. S. Nichols, T. Halafihi, R. L. Humphreys Jr., J. Kaltavara, S. J. Nichol, and S. J. Newman.
2017. Ageing bias and precision for deep-water snappers: evaluating nascent otolith preparation methods using novel multivariate comparisons among readers and growth parameter estimates. ICES J. Mar. Sci. 74:193–203.
Zar, J. H.
1999. Biostatistical analysis, 4th ed., 663 p. Prentice Hall, Upper Saddle River, NJ.

National Marine Fisheries Service
NOAA

Fishery Bulletin
established in 1881

Spencer F. Baird
First U.S. Commissioner of Fisheries and founder of *Fishery Bulletin*

The first data on the diet and reproduction of Fedorov's lumpsucker (*Eumicrotremus fedorovi*)

Ilya Gordeev (contact author)[1,2]
Kristina Zhukova[1]
Svetlana Frenkel[1]

Email address for contact author: gordeev_ilya@bk.ru

[1] Russian Federal Research Institute of Fisheries and Oceanography
17 V. Kransnoselskaya Street
Moscow 107140, Russia

[2] Lomonosov Moscow State University
GSP-1 Leninskije Gory
Moscow 119991, Russia

Abstract—A total of 69 specimens of Fedorov's lumpsucker (*Eumicrotremus fedorovi*) caught on the continental shelf and slope of Simushir Island in the northwest Pacific Ocean were dissected and studied for stomach contents. The Fedorov's lumpsucker was found to feed mainly on the young of fish species, including the walleye pollock (*Gadus chalcogrammus*), northern lampfish (*Stenobrachius leucopsarus*), and northern smoothtongue (*Leuroglossus schmidti*), crustaceans, such as *Themisto pacifica*, *Primno macropa*, calanoids, gammarids, mysids, and caprellids, and squid. Histological analyses of ovaries revealed iteroparity, determinate fecundity, group-synchronous ovarian development, and total spawning. Testes were of an unrestricted lobular type. Chorion and thick zona radiata of Fedorov's lumpsucker correspond to the condition of eggs in specimens of other fish species that release demersal eggs. Absolute fecundity values of Fedorov's lumpsucker in our study were significantly less than those that have been reported for other species of Cyclopteridae. The results of this study provide the first data on this little known species of this family.

Manuscript submitted 12 August 2020.
Manuscript accepted 11 March 2021.
Fish. Bull. 119:33–40 (2021).
Online publication date: 8 April 2021.
doi: 10.7755/FB.119.1.5

The views and opinions expressed or implied in this article are those of the author (or authors) and do not necessarily reflect the position of the National Marine Fisheries Service, NOAA.

The genus *Eumicrotremus*, 1 of 6 genera of Cyclopteridae (Scorpaeniformes: Cottoidei), includes 18 valid species (Froese and Pauly, 2020). This genus is distributed mostly in the northern Pacific Ocean. Four species inhabit subarctic and Arctic areas: pimpled lumpsucker (*E. andriashevi*), leatherfin lumpsucker (*E. derjugini*), Atlantic spiny lumpsucker (*E. spinosus*), and Newfoundland spiny lumpsucker (*E. terraenovae*). The Fedorov's lumpsucker (*E. fedorovi*) inhabits the waters of the northern Kuril Islands off the eastern coast of Russia (Mecklenburg and Sheiko, 2003) and has been rarely recorded as bycatch in the area of the Kuril Islands. Lumpsucker species spend most of their lives away from the shore. They can be found 100 km from shore in the open waters of the Pacific Ocean, before they return to shallow waters (200–300 m) to reproduce (Orlov, 1994; Chuchukalo, 2006).

No information on the diet of Fedorov's lumpsucker was available prior to this study. According to existing records on the diet of other *Eumicrotremus* species (Tabunkov and Chernysheva, 1985; Orlov, 1994; Melnikov, 1995; Kuznetsova, 1997; Chuchukalo et al., 1999; Roshchin, 2006; Antonenko et al., 2009; Berge and Nahrgang, 2013), lumpsucker species feed on various crustaceans, juveniles of squid species, pteropods, juveniles of fish species, and polychaetes. Lumpsucker species feed intensively throughout most of the year and have been reported to make diurnal vertical migrations in the water column to follow their main food item (hyperiids), and this movement pattern explains their regular presence in open water (Chuchukalo, 2006; Antonenko et al., 2009).

The reproductive biology of Cyclopteridae has been previously examined in studies of the lumpfish (*Cyclopterus lumpus*) and smooth lumpsucker (*Aptocyclus ventricosus*) (Cox and Anderson, 1922; Davenport, 1985; Kennedy, 2018; Zhukova et al., 2018). Information on the reproductive processes of other members of Cyclopteridae is scarce and fragmented. Lumpsucker species produce clusters of demersal adhesive eggs and spawn in coastal waters (at depths down to 300 m). After spawning, males guard the fertilized eggs (Mecklenburg and Sheiko, 2003; Panchenko and Balanov, 2020). Female Pacific spiny lumpsucker (*E. orbis*) and spinous lumpfish (*E. soldatovi*) have been reported to have died after a single

spawning, and males have been observed to guard egg clutches and then die when the eggs they were guarding complete development or hatch (Orlov, 1994). It is difficult, therefore, to determine if lumpsucker species feed during their entire life cycles. However, other representatives of Cyclopteridae, the Atlantic spiny lumpsucker, smooth lumpsucker, and lumpfish, can spawn several times during their life cycles (Cox and Anderson, 1922; Berge and Nahrgang, 2013; Zhukova et al., 2018).

In this paper, we provide the first comprehensive data on the stomach contents, gonadal development, and fecundity of Fedorov's lumpsucker and describe the biology and reproductive processes of this little known species.

Materials and methods

A total of 69 adult specimens of the Fedorov's lumpsucker were caught on the shelf and slope of Simushir Island, located near the center of the Kuril Islands in the Sea of Okhotsk in the northwest Pacific Ocean, from 19 March through 25 March 2017 during tows of the bottom trawl of the FV *Anatoly Torchinov* that targeted greenlings (*Pleurogrammus* spp.) at depths of 150–230 m. Specimens were caught near Simushir Island within the area bounded by the following coordinates: 46°46′N and 151°56′E, 46°40′N and 151°52′E, and 46°44′N and 151°46′E (Fig. 1). All 69 specimens were frozen at −20°C immediately after capture and then transported to the laboratory at the Russian Federal Research Institute of Fisheries and Oceanography in Moscow. The Fedorov's lumpsucker examined in this study ranged in total length (TL) from 64 to 103 mm and weighed from 12.4 to 64.0 g. The 59 females caught were 64–103 mm TL (mean: 81.3 mm TL [standard deviation (SD) 1.23]) and 12.4–64.0 g (mean: 33.22 g [SD 1.36]), and the 10 males were 73–95 mm TL (mean: 84.7 mm TL [SD 2.50]) and 22.9–60.1 g (mean: 41.85 g [SD 5.00]).

After a specimen was thawed, the food items were collected from its stomach, separated under a MicroMed MC-2[1] stereomicroscope (CIT Nelian, Moscow, Russia), and weighed to the nearest milligram with analytical scales (R160P, Sartorius, Bohemia, New York). Fish specimens and food items were identified with the aid of Tuponogov and Kodolov (2014), Oku et al. (2017), and Voskoboinikova (2015).

Gonads of 14 females and 2 males (size: 64–92 mm TL and 30.1–38.5 g) were fixed in 10% formalin, dehydrated, cleared with xylol, embedded in paraffin, sliced into sections 5 µm thick, and stained with hematoxylin and Ehrlich's eosin. An Olympus BX45 microscope (Olympus Corp., Tokyo, Japan) equipped with a Leica DC 100 digital camera (Leica Microsystems, Buffalo Grove, IL) was used for imaging. Diameters of oocytes and intracellular structures were measured by using the software ImageJ, vers. 1.51 (Rasband, 2018).

The maturity phases of each ovary and testis were classified on the basis of the most advanced stage of germ cells observed in histological sections, according to the scale described by Guzmán et al. (2017). Ovaries were divided into 5 phases of development: onset of vitellogenesis, early vitellogenic, mid-vitellogenic, late vitellogenic, and periovulatory. Phase of testis maturity was determined on the basis of the presence or absence of male germ cells in a gonad: early recrudescence (spermatogonia and spermatocytes), mid-recrudescence (spermatogonia, spermatocytes, and spermatids), late recrudescence (spermatogonia, spermatocytes, spermatids, and spermatozoa), spermiating (spermatozoa prevail), and postspawning (spermatogonia and residual spermatozoa). Oocyte development was determinated by using the following stages and their associated indicators: primary growth (PG, absence of cortical alveoli and yolk granules), early developing (Vtg1, cortical alveoli and scattered yolk granules along the outer region of the cytoplasm), developing (Vtg2, yolk granules partly occupy the cytoplasm), fully vitellogenic (Vtg3, cytoplasm completely filled with yolk), and maturing (M, yolk globule fusion and nucleus migration).

Absolute and relative fecundity were estimated by using the gravimetric method (Murua and Saborido-Rey, 2003) for 5 frozen females (size: 74–95 mm TL and 25.4–60.1 g)

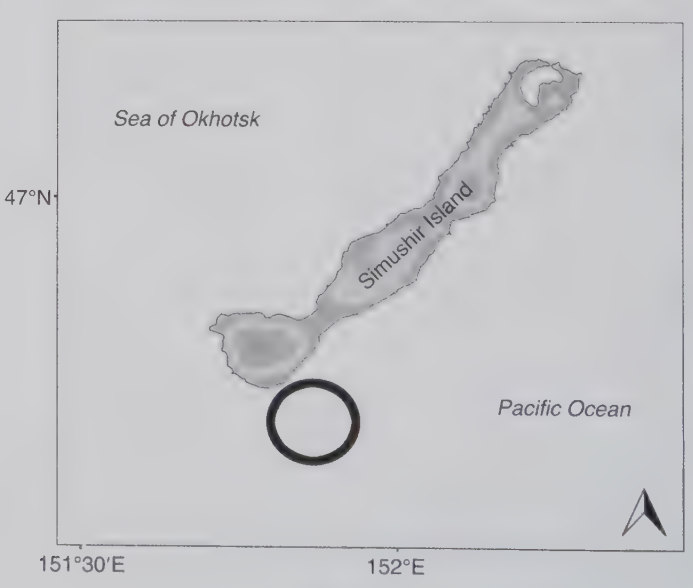

Figure 1

Map showing the location (outlined with a black circle) where 69 adult Fedorov's lumpsucker (*Eumicrotremus fedorovi*) were caught during 19–25 March 2017 off Simushir Island, located near the center of the Kuril Islands in the Sea of Okhotsk in the northwest Pacific Ocean.

[1] Mention of trade names or commercial companies is for identification purposes only and does not imply endorsement by the National Marine Fisheries Service, NOAA.

at the late vitellogenetic and periovulatory macroscopic phases of gonadal maturity. A piece of ovarian tissue was taken from the median portion of the gonad from each specimen. The subsample of each ovary, representing 5–10% of the gonad weight, was weighed, and all advanced oocytes (1.7–2.3 mm in diameter) in the subsample were counted. The gonadosomatic index (GSI) and absolute (F_{abs}) and relative (F_{rel}) fecundity were estimated as follows:

$$GSI = (GW \times 100) / BW, \quad (1)$$

$$F_{abs} = (n \times GW) / w, \text{ and} \quad (2)$$

$$F_{rel} = (n \times GW) / (w \times BW), \quad (3)$$

where n = the number of advanced oocytes in the subsample;
w = the weight of the subsample (in grams);
GW = the gonad weight (in grams); and
BW = the body weight (in grams) of the specimen.

Standard deviations, Pearson's correlation coefficients (r), Spearman rank correlation coefficients (ρ), and P-values were calculated by using Microsoft Excel 2010 (Microsoft Corp., Redmond, WA) and statistical software R, vers. 3.6.3 (R Core Team, 2020).

Results

Diet

The stomachs of most of the specimens examined were full. The level of digestion in most cases made it possible to determine the species or taxon of food items. The weight of the boluses ranged from 9 to 3727 mg. Young walleye pollock (*Gadus chalcogrammus*), 36–61 mm TL; northern lampfish (*Stenobrachius leucopsarus*), 18–25 mm TL; and northern smoothtongue (*Leuroglossus schmidti*), 19–23 mm TL, as a group accounted for the majority of fish food items (Table 1). Walleye pollock were found in almost 70% of stomachs and composed over 40% of the total weight of boluses collected from the specimens with food in their stomachs (65 of 69 specimens).

Table 1

Frequency of occurrence and proportion of the total mass of food items found in the stomach contents of Fedorov's lumpsucker (*Eumicrotremus fedorovi*) caught during 19–25 March 2017 off Simushir Island, located near the center of the Kuril Islands in the northwest Pacific Ocean.

Food item	Occurrence of food items (%)	Mass proportion (%)
Gadus chalcogrammus	69.57	40.55
Hyperiida	65.22	14.03
Mysida	62.32	26.44
Calanoida	52.17	3.98
Gammarida	44.93	3.86
Stenobrachius leucopsarus	40.58	9.93
Leuroglossus schmidti	2.90	0.65

After walleye pollock, crustacean species were the most frequent food items (Table 1). Hyperiids were represented by only 2 species—*Themisto pacifica* and *Primno macropa*. Copepods were represented by several species of Calanoida, including *Neocalanus cristatus*, *Gaetanus minutus*, *Paraeuchaeta elongata*, *Onchocalanus magnus*, *Pseudochirella obtusa*, *Cornucalanus indicus*, *Scaphocalanus* sp., and *Neocalanus* spp. All calanoids were adults in the final development stage. *Paraeuchaeta elongata* was the most common copepod found in stomachs. Unfortunately, representatives of Mysidae lost most of their identifying characteristics when they were eaten by Fedorov's lumpsucker, and we could not identify them to the lowest taxon. Gammarids were represented by *Cyphocaris challengeri* (most commonly), *Photis reinhardi*, and a few specimens from the families Phoxocephalidae and Lysianassidae. In addition to the taxa given in Table 1, there were several minor food items—2 specimens of Caprelloidea, both belonging to the family Caprellidae; a few small shrimp; the digested remains of fish from an unknown species; and a single squid, whose morphological features indicate that it is a specimen of either the *Taonius belone* or the *Gonatopsis borealis*.

Reproduction

Female Fedorov's lumpsucker have a pair of elongated ovaries attached to the dorsal wall of their body cavity. Ovaries at the phase of onset of vitellogenesis were small and flaccid, with no oocytes visible to the eye. Results of histological analysis indicate the presence of oocytes at the stage of PG, with some oocytes at the Vtg1 stage and oocytes sporadically at the Vtg2 stage (Fig. 2A). Oocytes at the PG stage had a mean diameter (Ø) of 128 µm (SD 43) (Fig. 3), were ovoid, with basophilic cytoplasm and a large round nucleus in central position, and were found in all gonads (Fig. 4, A and D). Oocytes at the stage of Vtg1 had a mean Ø of 325 µm (SD 103) and were characterized by secondary growth at the beginning of vitellogenesis. Compared with that of the PG oocytes, the cytoplasm of the Vtg1 oocytes was more acidophilic with cortical alveoli, scattered yolk granules, and oil droplets (Fig. 4, A, B, and D).

Oocytes at the stage of Vtg2 had a mean Ø of 533 µm (SD 102), were characterized by cytoplasm partially filled with yolk, and were found in gonads in the mid- and late vitellogenic phases (Fig. 4, A, B, and D). Early vitellogenic gonads were bigger and less flaccid than ovaries at the onset of vitellogenesis and had scattered, visible small eggs with Ø less than 1 mm. Most germ cells were at the stages of PG and Vtg1, and Vtg2 germ cells were also found (Fig. 2B). Mid-vitellogenic ovaries were light orange in color, and oocytes were visible to the eye with Ø of about 1 mm. In such gonads, Vtg2 was the prevailing stage of oocytes (Fig. 2C). Late vitellogenic ovaries were dense and bright orange in color, and oocytes were clearly visible with Ø from 1.0 to 1.6 mm (Fig. 2D). Most germ cells in

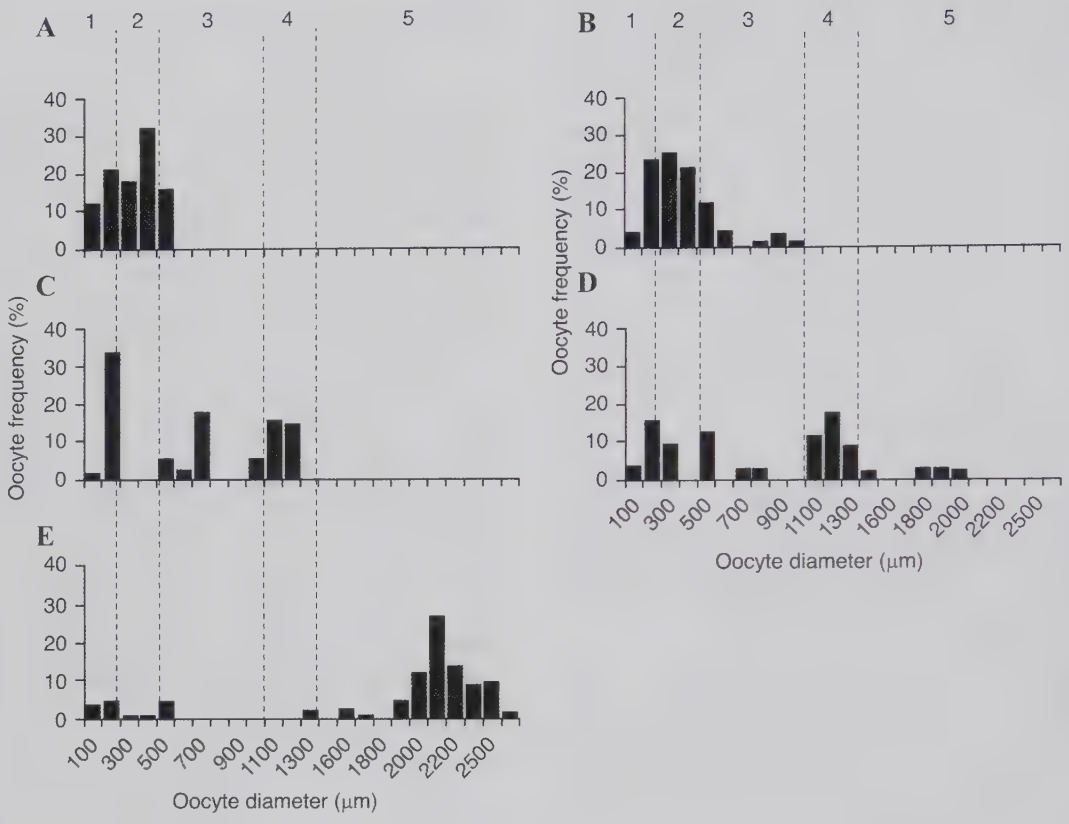

Figure 2

Frequency of occurrence of oocytes in Fedorov's lumpsucker (*Eumicrotremus fedorovi*) caught during 19–25 March 2017 off Simushir Island, by oocyte size and macroscopic phase of ovarian maturity: (**A**) onset of vitellogenesis, (**B**) early vitellogenesis, (**C**) mid-vitellogenesis, (**D**) late vitellogenesis, and (**E**) periovulatory. The vertical dashed lines indicate approximate boundaries between the sizes of oocytes at different histological stages of development: primary growth (1), early developing (2), developing (3), fully vitellogenic (4), and maturing (5).

such ovaries were at the Vtg3 stage. In Vtg3 oocytes, which had a mean Ø of 1106 μm (SD 83), the cytoplasm was completely filled with yolk globules (Fig. 4C). Periovulatory gonads were voluminous and contained oocytes with Ø of about 2 mm and clearly visible oil droplets in germ cell cytoplasm. Most of the oocytes were at the M and PG stages (Fig. 2E). In M oocytes, which had a mean Ø of 2036 μm (SD 321), there were elongated masses of yolk globules with large oil droplets. Cytoplasm was surrounded by a zona radiata and a large chorion that was 28–30 μm thick (Fig. 4, D and E).

Absolute fecundity ranged from 297 eggs in the smallest female (size: 74 mm TL and 25.4 g; GSI: 9%) to 494 eggs in the largest female (size: 95 mm TL and 60.0 g; GSI: 12%), and mean F_{abs} was 409 eggs (SD 87.9). Relative fecundity ranged from 7 to 12 eggs/gram of body weight, and mean F_{rel} was 9 eggs/gram of body weight (SD 1.9). The only reliable correlation between body characteristics and fecundity is the negative correlation between body length and F_{rel} (r=–0.92, P≤0.05; ρ=–0.97, P≤0.05; df=3). The correlations between body length and weight and F_{abs} are generally positive but with low support (P>0.05).

The testes of both males for which gonads were examined were classified as at the mid-recrudescence phase. The most advanced germ cells were spermatids; spermatogonia and spermatocytes were also present. Such composition of male germ cells indicates that active spermatogenesis was ongoing but that spermiogenesis had not yet begun. Germ cells were organized within cysts, surrounded by Sertoli cells and the interstitial compartment. The germinal compartment, consisting of male germ cells and Sertoli cells, was lobed, with spermatogonia distributed throughout the length of the lobes (Fig. 4F).

Discussion

The presence of benthic, benthopelagic, and pelagic species in guts of Fedorov's lumpsucker indicates that this species makes regular and significant vertical migrations; therefore, this species may be considered a

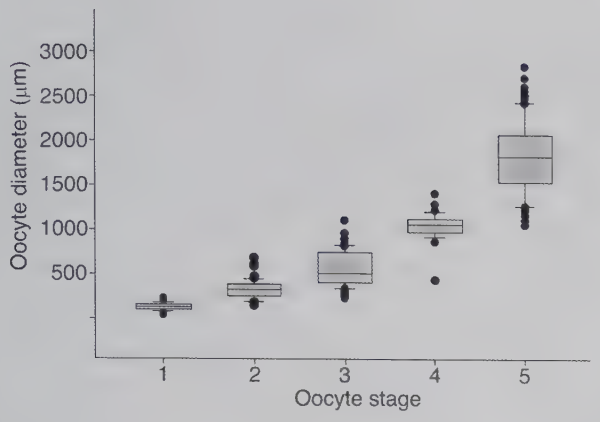

Figure 3

Box plot of the relationship between oocyte diameter and histological stages of maturity for Fedorov's lumpsucker (*Eumicrotremus fedorovi*) caught during 19–25 March 2017 around Simushir Island. The stages of oocyte development are primary growth (1), early developing (2), developing (3), fully vitellogenic (4), and maturing (5). The upper and lower parts of each box represent the first and third quartiles (the 25th and 75th percentiles), and the horizontal line is the median. The error bars indicate 1.5 times the interquartile range, and the black circles represent values outside this range.

eurybathic species, as has been reported previously for all lumpsucker species (Chuchukalo, 2006; Gordeev and Sokolov, 2020). All 3 fish species found in the stomach contents of Fedorov's lumpsucker—the walleye pollock, northern lampfish, and northern smoothtongue—are quite common in the area of and use the shelf of the Kuril Islands as breeding grounds. It is interesting that we did not find cumaceans or isopods in the stomach contents because they usually follow gammarids on the shelf (Neiman, 1988). Perhaps it is due to the feeding selectivity or the mosaic of bottom fauna.

A detailed analysis of food items allowed us to compare our results with the available data on the diet of congeners of the Fedorov's lumpsucker. According to Roshchin (2006), who studied the diet of Atlantic spiny lumpsucker in the Barents Sea, pelagic crustaceans of the family Hyperiidae, that is *Themisto abyssorum* and *T. libellula*, form the bulk of the food bolus of the Atlantic spiny lumpsucker. Benthic gammarids of the family Lysianassidae and a high Arctic species, *Gammarus wilkitzkii*, were also found. Northern shrimp (*Pandalus borealis*); a euphausiid, *Thysanoessa inermis*; and polychaetes of the genus *Nereis* were found in only a few of the examined lumpsucker. Berge and Nahrgang (2013) stated that there was a similar pattern of Atlantic spiny lumpsucker feeding on *Themisto libellula* in the environs of Spitzbergen, an island in the Svalbard archipelago in Norway. They also noted chaetognaths in boluses. The Pacific Ocean representative, Pacific spiny lumpsucker, studied in the Gulf of Patience off the eastern coast of Sakhalin Island in Russia, feeds mainly on hyperiids, euphausiids, and decapod larvae (Tabunkov and Chernysheva, 1985).

The most recent study on the diet of a lumpsucker species (Antonenko et al., 2009) stated that the Siberian lumpsucker (*E. asperrimus*) feeds almost entirely on the hyperiid *T. japonica* in the waters of the Primorsky Krai (Maritime Territory) of Russia. *Primno macropa* and euphausiids of the genus *Thysanoessa* were rarely found. According to Chuchukalo et al. (1999), *E. tartaricus* feeds equally on both planktonic hyperiids and on young boreopacific armhook squid (*Gonatopsis borealis*) in the northern part of the Sea of Okhotsk. Spinous lumpfish studied in the Sea of Okhotsk fed mostly on hyperiids, such as *Themisto japonica* and *T. libellula*, and on euphausiids, including *Thysanoessa raschii* and *Thysanoessa* sp.; juvenile squid, pteropods, mysids, polychaetes, gammarids, and juvenile fish were only occasionally found (Orlov, 1994; Melnikov, 1995; Kuznetsova, 1997). There is also a record that, in 1993, spinous lumpfish fed mainly on isopods and the ctenophore *Beroe* sp. (Kuznetsova, 1997). Northern smoothtongue and leatherfin lumpsucker have feeding habits quite similar to that of the Pacific spiny lumpsucker (Chuchukalo, 2006).

Therefore, Fedorov's lumpsucker, similarly to other studied species of *Eumicrotremus*, feeds on actively moving crustaceans. However, the diet of Fedorov's lumpsucker is differentiated from that of other studied congeneric species by the large proportions by mass of the diet that are fish and mysids (51.10% and 26.44%, respectively; Table 1). Chuchukalo (2006) wrote that the narrow food specialization (on hyperiids and euphausiids) of most lumpsucker species is not typical for plankton-eating species of fish and is probably attributable to the similarity of behavior, morphological features, and close ecology of these species. Our research revealed that the diet of the Fedorov's lumpsucker could include almost any benthopelagic animal; therefore, the genus *Eumicrotremus* could be labeled as euryphagous. Because the majority of the food items found in specimens stomachs in this study were in good condition, it can be presumed that food was sucked into the mouths of individuals with a stream of water that resulted from a sharp increase in the volume of the buccal cavity.

Size–frequency analyses of oocytes revealed discontinuous oogenesis (determinate fecundity), group-synchronous ovarian organization (release of eggs once in the spawning season), and total spawning, following the classification of Murua and Saborido-Rey (2003). Similar reproductive strategies have been recorded for other representatives of Cyclopteridae, such as the smooth lumpsucker (Zhukova et al., 2018).

Semelparous species have very low or exhausted reserves of PG oocytes in prespawning gonads (Mouchlianitis et al., 2019). The presence of quite a lot of PG oocytes in all examined ovaries and of primary spermatogonia in testes examined in our study confirms that the Fedorov's lumpsucker is an iteroparous species.

The chorion and thick zona radiata present in ovaries of Fedorov's lumpsucker correspond to the condition of eggs in

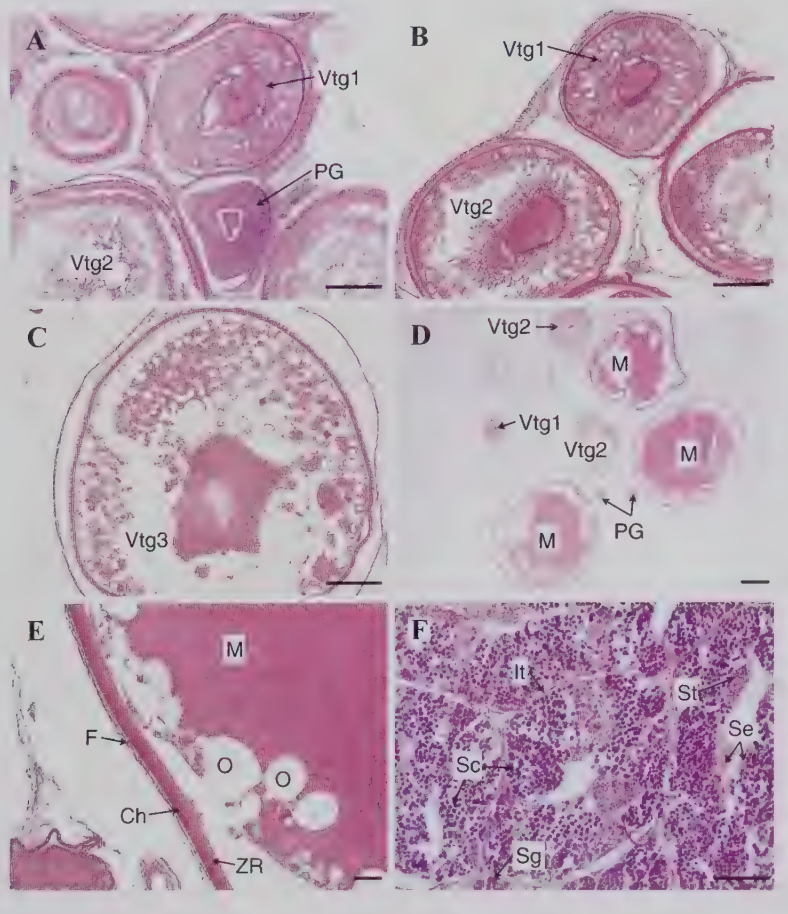

Figure 4

Images of gonads of Fedorov's lumpsucker (*Eumicrotremus fedorovi*), caught during 19–25 March 2017 around Simushir Island, at various macroscopic phases of development: (**A**) early vitellogenesis, (**B**) mid-vitellogenesis, (**C**) late vitellogenesis, and (**D**, **E**) periovulatory ovaries and (**F**) a mid-recrudescence testis. The histological stages, structures of germ cells, and gonadal elements are indicated in the images as follows: primary growth (PG), early developing (Vtg1), developing (Vtg2), fully vitellogenic (Vtg3), and maturing (M) oocytes, as well as oil droplets (O), zona radiata (ZR), chorion (Ch), follicular layer (F), spermatogonia (Sg), spermatocytes (Sc), spermatids (St), Sertoli cells (Se), and interstitial tissue (It). The lengths of the scale bars represent 100 µm (panels A, B, and E), 200 µm (panel C), 500 µm (panel D), and 50 µm (panel F).

specimens of other fish species that are releasing demersal eggs. Adhesive and demersal eggs have been reported for other species of Cyclopteridae (Washington et al., 1984) and for representatives of the families Liparidae, Osmeridae, Salmonidae, Pleuronectidae, and Clupeidae (Able and Musick, 1976; Stehr and Hawkes, 1979).

The sizes of germ cells at different stages of development found in our study were comparable to those reported for the smooth lumpsucker (Zhukova et al., 2018). The diameters of oocytes at the M stage were the same as those in lumpfish and a little smaller than those in Atlantic spiny lumpsucker and Siberian lumpsucker (Wienerroither et al., 2011; Panchenko and Balanov, 2020).

The F_{abs} of the Fedorov's lumpsucker in our study was significantly lower than that reported for other species of Cyclopteridae. For example, in another study, fecundity of lumpfish ranged from 50,000 to 159,000 eggs (Gregory and Daborn, 1982). The values of F_{abs} of Atlantic spiny lumpsucker and smooth lumpsucker have been reported to be more than 1000 eggs (Dolgov[2]; Hutchings[3]) and between 24,240 and 63,756 eggs (Zhukova et al., 2018), respectively. Such low values of F_{abs} and low GSI values are due to the smaller body size of Fedorov's lumpsucker (size: 74–95 mm TL; GSI: 9–12%) compared with the size of lumpfish (size: 370–450 mm TL; mean GSI: 18% [SD 5.8]) and of smooth lumpsucker (size: 170–350 mm TL; GSI: 31–56%) (Zhukova et al., 2018). Among close relatives of the Fedorov's lumpsucker, only the Atlantic spiny lumpsucker had lower GSI values in prespawning females with similar body length (77.30 mm [SD 15.80]), with GSI values of 4.5% according to Hutchings[3] or 1.4–4.8% according to Berge and Nahrgang (2013). This circumstance is in line with the very weak positive correlation (linear regression: coefficient of multiple determination=0.31) between total weight and the GSI, indicating equal gonadal development between each size class (Berge and Nahrgang, 2013). The F_{rel} was 2 times lower in Fedorov's lumpsucker than in smooth lumpsucker (Zhukova et al., 2018). In both species, F_{rel} is also associated with the size of females.

The structure of the testes and distribution of spermatogonia for the males examined in our study indicate that male gonads were of the unrestricted lobular testis type, as defined by Uribe et al. (2014). Similar testis types have been recorded for lumpfish (Guercini, 2019) and for other teleost species of Percidae, Centropomidae, Rachycentridae, Cichlidae, Gadidae, Synbranchidae, and Erythrinidae (Grier et al., 1980; Taylor et al., 1998; Brown-Peterson et al., 2002; Lo Nostro et al., 2003; Bizzotto and Godinho, 2007). Therefore, the results of our study provide the first data on the diet and reproductive features for the rarely caught Fedorov's lumpsucker.

[2] Dolgov, A. V. 1994. Some aspects of biology of non-target fish species in the Barents Sea. ICES CM 1994/O:12, 23 p. [Available from website.]

[3] Hutchings, J. A. 2002. Ecology and biodiversity of commercially unexploited marine fishes in the Northwest Atlantic, 14 p. Final report. Dalhousie Univ., Halifax, Canada.

Acknowledgments

We wish to thank the crew of the FV *Anatoly Torchinov* (Primorskaya Rybolovnaya Co. Ltd.) for help with sampling, O. Voskoboinikova (Zoological Institute, Russian Academy of Sciences [RAS], St. Petersburg) for help with fish identification, A. Basin (Shirshov Institute of Oceanology, RAS, Moscow) for the identification of gammarids, V. Napazakov (Pacific Branch of Russian Federal Research Institute of Fisheries and Oceanography, Vladivostok) for the identification of hyperiids, and F. Lishchenko (Severtsov Institute of Ecology and Evolution, RAS, Moscow) for the identification of the squid.

Literature cited

Able, K. W., and J. A. Musick.
1976. Life history, ecology, and behavior of *Liparis inquilinus* (Pisces: Cyclopteridae) associated with sea scallop, *Placopecten magellanicus*. Fish. Bull. 74:409–421.

Antonenko, D. V., O. I. Pushchina, and S. F. Solomatov.
2009. Seasonal distribution and some features of the biology of spiny lumpfish *Eumicrotremus asperrimus* (Cyclopteridae, Scorpaeniformes) in the northwestern part of the Sea of Japan. J. Ichthyol. 47:674.

Berge, J., and J. Nahrgang.
2013. The Atlantic spiny lumpsucker *Eumicrotremus spinosus*: life history traits and the seemingly unlikely interaction with the pelagic amphipod *Themisto libellula*. Pol. Polar Res. 34:279–287.

Bizzotto, P. M., and H. P. Godinho.
2007. Morphometric evaluation of the spermatogenesis in trahira *Hoplias malabaricus* (Bloch) (Characiformes, Erythrinidae). Rev. Bras. Zool. 24:541–544.

Brown-Peterson, N. J., H. J. Grier, and R. M. Overstreet.
2002. Annual changes in the germinal epithelium determine male reproductive classes of the cobia. J. Fish Biol. 60:178–202.

Chuchukalo, V. I.
2006. Feeding and feeding relations of nekton and nektobenthos in Far Eastern Seas, 484 p. Tikhookean. Nauchno-Issled. Rybokhoz. Tsentr (TINRO), Vladivostok, Russia. [In Russian.]

Chuchukalo, V. I., V. V. Lapko, N. A. Kuznetsova, A. M. Slabinsky, V. V. Napazakov, V. F. Nadtochiy, V. N. Koblikov, and O. I. Pushchina.
1999. Feeding of bottom fish on the shelf and the continental slope of the northern part of the Sea of Okhotsk in summer 1997. Izv. Tikhookean. Nauchno-Issled. Rybokhoz. Tsentra (TINRO) 126:24–57. [In Russian.]

Cox, P., and M. Anderson.
1922. No. 1: a study of the lumpfish (*Cyclopterus lumpus* L.). Contrib. Can. Biol. Fish. 1:1–20.

Davenport, J.
1985. Synopsis of biological data on the lumpsucker, *Cyclopterus lumpus* (Linnaeus, 1758). FAO Fish. Synop. 147, 31 p. FAO, Rome.

Froese, R., and D. Pauly (eds.).
2020. FishBase. World wide web electronic publication, vers. 12/2020. [Available from website, accessed February 2021].

Gordeev, I. I., and S. G. Sokolov.
2020. Macroparasites of epipelagic and eurybathic fishes in the north-western Pacific. Invertebr. Zool. 17:118–132.

Gregory, R. S., and G. R. Daborn.
1982. Notes on adult lumpfish *Cyclopterus lumpus* L. from the Bay of Fundy. Proc. N.S. Inst. Sci. 32:321–326.

Grier, H. J., J. R. Linton, J. F. Leatherland, and V. L. De Vlaming.
1980. Structural evidence for two difference testicular types in teleost fishes. Am. J. Anat. 159:331–345.

Guercini, E.
2019. Effects of light and temperature regimes on the sexual maturation of male lumpfish (*Cyclopterus lumpus*). M.S. thesis, 37 p. Nor. Univ. Sci. Technol., Trondheim, Norway. [Available from website.]

Guzmán, J. M., J. A. Luckenbach, M. A. Middleton, K. C. Massee, C. Jensen, F. W. Goetz, A. J. Jasonowicz, and P. Swanson.
2017. Reproductive life history of sablefish (*Anoplopoma fimbria*) from the U.S. Washington coast. PLoS ONE 12(9):e0184413.

Kennedy, J.
2018. Oocyte size distribution reveals ovary development strategy, number and relative size of egg batches in lumpfsh (*Cyclopterus lumpus*). Polar Biol. 41:1091–1103.

Kuznetsova, N. A.
1997. Feeding of some plankton-eating fish in the Sea of Okhotsk during the summer period. Izv. Tikhookean. Nauchno-Issled. Rybokhoz. Tsentr (TINRO) 122:255–275. [In Russian.]

Lo Nostro, F., H. Grier, L. Andreone, and G. A. Guerrero.
2003. Involvement of the gonadal germinal epithelium during sex reversal and seasonal testicular cycling in the protogynous swamp eel, *Synbranchus marmoratus* Bloch 1795 (Teleostei, Synbranchidae). J. Morphol. 257:107–126.

Mecklenburg, C. W., and B. A. Sheiko.
2003. Family Cyclopteridae Bonaparte 1831—lumpsuckers. Calif. Acad. Sci., Annotated Checkl. Fishes 6, 17 p. [Available from website.]

Melnikov, I. V.
1995. Distribution and some features of Soldatov's lumpsucker *Eumicrotremus soldatovi* biology in the Sea of Okhotsk. J. Ichthyol. 35:433–439. [In Russian.]

Mouchlianitis, F. A., A. F. Belo, A. R. Vieira, B. R. Quintella, P. R. Almeida, and K. Ganias.
2019. Primary and secondary oocyte growth dynamics in anadromous semelparous Allis shad *Alosa alosa*. J. Fish Biol. 95:1447–1456.

Murua, H., and F. Saborido-Rey.
2003. Female reproductive strategies of marine fish species of the North Atlantic. J. Northwest Atl. Fish. Sci. 33:23–31.

Neiman, A. A.
1988. Quantitative distribution and trophic structure of the benthic shelf of the World Ocean, 101 p. VNIRO Publ. House, Moscow, Russia. [In Russian.]

Oku, K., H. Imamura, and M. Yabe.
2017. Phylogenetic relationships and a new classification of the family Cyclopteridae (Perciformes: Cottoidei). Zootaxa 4221:1–59.

Orlov, A. M.
1994. Some characteristics of distribution and biological status of *Eumicrotremus soldatovi* (Cyclopteridae) in the northeastern part of the Sea of Okhotsk during the spring. J. Ichthyol. 34:122–127.

Panchenko, V. V., and A. A. Balanov.
2020. The distribution of adult males of the Siberian lumpsucker *Eumicrotremus asperrimus* (Tanaka, 1912) (Cyclopteridae) off the northern Primorsky Krai Coast, Sea of Japan, and remarks on the reproduction of this species. Russ. J. Mar. Biol. 46:81–87.

R Core Team.
2020. R: a language and environment for statistical computing. R Foundation for Statistical Computing, Vienna, Austria. [Available from website, accessed August 2020.]
Rasband, W. S.
2018. ImageJ. U.S. Natl. Inst. Health, Bethesda, MD. [Available from website.]
Roshchin, E. A.
2006. New data on morphometry, feeding, and parasitic fauna of Atlantic spiny lumpsucker *Eumicrotremus spinosus* (Cyclopteridae) from the Barents Sea. J. Ichthyol. 46:582–586.
Stehr, C. M., and J. W. Hawkes.
1979. The comparative ultrastructure of the egg membrane and associated pore structures in the starry flounder, *Platichthys stellatus* (Pallas), and pink salmon, *Oncorhynchus gorbuscha* (Walbaum). Cell Tissue Res. 202:347–356.
Tabunkov, V. D., and E. R. Chernysheva.
1985. Feeding non-target fish species in the Gulf of Patience. Izv. Tikhookean. Nauchno-Issled. Rybokhoz. Tsentr (TINRO) 110:98–104. [In Russian.]
Taylor, R. G., H. J. Grier, and J. A. Whittington.
1998. Spawning rhythms of common snook in Florida. J. Fish Biol. 53:502–520.
Tuponogov, V. N., and L. S. Kodolov.
2014. Field guide for commercial and common species of fish of the Far Eastern Seas of Russia, 336 p. Russkiy Ostrov Publ., Vladivostok, Russia. [In Russian.]
Uribe, M. C., H. J. Grier, and V. Mejía-Roa.
2014. Comparative testicular structure and spermatogenesis in bony fishes. Spermatogenesis 4(3):e983400.
Voskoboinikova, O. S.
2015. New genus of the family Cyclopteridae—Microancathus gen. n. (Pisces: Cottoidei: Cyclopteridae) with description of a new species *Microancathus tokranovi* sp. n. Tr. Zool. Inst. RAN 319(2):215–228. [In Russian.]
Washington, B. B., H. G. Moser, W. A. Laroche, and W. J. Richards.
1984. Scorpaeniformes: development. *In* Ontogeny and systematics of fishes (H. G. Moser, J. Richards, D. M. Cohen, M. P. Fahay, A.W. Kendall, and S. L. Richards, eds.), p. 405–428. Am. Soc. Ichthyol. Herpetol., Spec. Publ. 1. Allen Press, Lawrence, KS.
Wienerroither, R., Johannesen, E., Dolgov, A., Byrkjedal, I., Bjelland, O, Drevetnyak, K., Eriksen, K. B., Høines, Å., Langhelle, G., Langøy, et al.
2011. Atlas of the Barents Sea fishes. IMR/PINRO Joint Rep. Ser. 1-2011, 272 p. [Available from website.]
Zhukova, K., O. A. Maznikova, and A. M. Orlov.
2018. Gonadal maturation of the female smooth lumpsucker (*Aptocyclus ventricosus*). Fish. Bull. 116:153–160.

National Marine Fisheries Service
NOAA

Fishery Bulletin
established in 1881

Spencer F. Baird
First U.S. Commissioner of Fisheries and founder of *Fishery Bulletin*

Validation of the use of vertebrae and dorsal-fin spines for age determination of spiny dogfish (*Squalus acanthias*) in the western North Atlantic Ocean

Kelsey C. James (contact author)[1]
Lisa J. Natanson[1]
Christopher Flight[2]
Cindy Tribuzio[3]
John Hoey[1]
Camilla McCandless[1]

Email address for contact author: kelsey.james@noaa.gov

[1] Northeast Fisheries Science Center
National Marine Fisheries Service, NOAA
28 Tarzwell Drive
Narragansett, Rhode Island 02882
Present address for contact author: Southwest Fisheries Science Center
National Marine Fisheries Service, NOAA
8901 La Jolla Shores Drive
La Jolla, California 92037

[2] Dauphin Island Sea Lab
101 Bienville Boulevard
Dauphin Island, Alabama 36528

[3] Alaska Fisheries Science Center
National Marine Fisheries Service, NOAA
17109 Point Lena Loop Road
Juneau, Alaska 99801

Abstract—Spiny dogfish (*Squalus acanthias*) are traditionally aged by counting band pairs on dorsal-fin spines; however, wear and tear of the spines make obtaining accurate age estimates of older spiny dogfish difficult. Vertebral centra are an alternate structure that can be used to estimate age, but success in their use has been varied. We conducted a tag-recapture study using oxytetracycline injections to validate annual deposition in both dorsal-fin spines and vertebral centra of spiny dogfish. When band pairs in vertebral centra were used, time at liberty was significantly underestimated. Additionally, band-pair counts were found to change along the vertebral column of an individual, further refuting the use of vertebral centra to generate age estimates. Band-pair deposition in dorsal-fin spines was confirmed to be annual in spiny dogfish at liberty for up to 2.6 years. Dorsal-fin spines should continue to be used to age spiny dogfish, and vertebral centra are not a viable alternative.

Manuscript submitted 14 July 2020.
Manuscript accepted 26 March 2021.
Fish. Bull. 119:41–49 (2021).
Online publication date: 8 April 2021.
doi: 10.7755/FB.119.1.6

The views and opinions expressed or implied in this article are those of the author (or authors) and do not necessarily reflect the position of the National Marine Fisheries Service, NOAA.

Spiny dogfish (*Squalus acanthias*) range from Labrador, Canada, to Florida in the western North Atlantic Ocean but are most common from Nova Scotia, Canada, to Cape Hatteras, North Carolina (Collette and Klein-MacPhee, 2002). In the western North Atlantic Ocean, spiny dogfish have been landed in commercial fisheries on a small scale since the 1930s (Rago and Sosebee, 2009). Landings of spiny dogfish soared in the 1970s until foreign fishing ceased in 1977, when the Fishery Conservation and Management Act of 1976 became effective (Fishery...2018), and spiny dogfish were declared "underutilized" by the late 1980s (Rago and Sosebee, 2009; DFO, 2020). In the United States, a large-scale directed fishery targeting mature females began in the 1990s, resulting in a significant reduction in female spawning stock biomass (NEFSC, 1998). In Canada, smaller scale directed fishing during 1998–2008 targeted mostly adult males with a mix of juvenile males and mature females (DFO, 2020). The population of spiny dogfish in the western North Atlantic Ocean was declared overfished in 1998 (NEFSC, 1998). Effective management practices led to population rebuilding, and as of the stock assessment completed in 2006, spiny dogfish in the western North Atlantic Ocean are no longer considered overfished and no overfishing has been occurring (NEFSC, 2006). These stock assessments rely on accurate life history characteristics, including validated age and growth.

Age determination for the spiny dogfish and its closely related congeneric species, the Pacific spiny dogfish (*S. suckleyi*) has been studied extensively. Note that, until 2010, *S. suckleyi* was considered the same species as *S. acanthias* (Ebert et al., 2010; Veríssimo et al., 2010), and many studies did not distinguish between the 2 species. For the purposes of this paper, however, *spiny dogfish* refers only to *S. acanthias*. Both species have been aged since at least the 1930s, through the use of a variety of methods (Kaganovskaia, 1933; Holden and Meadows, 1962; Jensen, 1965; Ketchen, 1975; Jones and Geen[1]; Nammack et al., 1985; McFarlane and Beamish, 1987; Saunders and McFarlane, 1993; Campana et al., 2006, 2009; McFarlane and King, 2009; Tribuzio et al., 2010; Bubley et al., 2012; Tribuzio et al., 2017). The use of dorsal-fin spines has long been considered the standard for age determination of spiny dogfish because early researchers were unable to elucidate band pairs in vertebrae (Kaganovskaia, 1933; Tribuzio et al., 2016). The use of fin spines, meanwhile, has the issue of wear that obscures or eliminates growth bands and requires the use of correction factors that may or may not be suitable (Ketchen, 1975; Taylor et al., 2013).

Over time, improvements in the ability to enhance band pairs led to attempts at age determination with vertebrae because the use of these structures did not require correction factors. This development has allowed comparisons between band-pair counts of dorsal-fin spines and vertebral centra (Bubley et al., 2012; Tribuzio et al., 2017). Bubley et al. (2012) concluded that use of vertebral counts resulted in more reliable and accurate age estimates that produced biologically appropriate growth parameters for spiny dogfish than the variable ages from the use of dorsal-fin spines that requires correction factors to account for lost annuli from wear. On the other hand, Tribuzio et al. (2017) found vertebral counts underestimated counts of unworn dorsal-fin spines of Pacific spiny dogfish over 10 years old.

Compounding the decision of what structure to use to age spiny dogfish are various age validation studies. In a reevaluation of data from early studies (McFarlane and Beamish, 1987) that used oxytetracycline (OTC) on dorsal-fins spines of Pacific spiny dogfish at liberty for up to 20 years, the band pairs on the dorsal-fin spines were considered annual. However, in 3 individuals at liberty for 20–21 years, 7–18 band pairs were missing (McFarlane and King, 2009). Campana et al. (2006) validated ages of spiny dogfish from the region of the western North Atlantic Ocean in Canada, using bomb radiocarbon techniques, and determined that band-pair formation in dorsal-fin spines was annual up to at least 25 years. Neither Bubley et al. (2012) nor Tribuzio et al. (2017) validated band-pair deposition in vertebral centra, but in both studies marginal increment analysis was used and results indicate annual periodicity in band-pair formation in vertebral centra. Given the importance of age estimates in stock assessment, it is vital to validate the age determination methods.

Appropriate stock assessment and management rely on accurate age determinations for spiny dogfish because these ages facilitate calculation of growth, mortality, age at maturity, and longevity estimates. In view of the history of the spiny dogfish fishery, and the need for accurate biological information for management, an intensive cooperative research program was initiated by NOAA to obtain detailed life history data. This paper reports on one portion of this program, specifically, the use of vertebrae and dorsal-fin spines to determine age and growth. The primary goal of this study was to attempt to validate the periodicity in formation of band pairs in vertebral centra of spiny dogfish by using individuals injected with OTC. Of secondary importance for this work was confirming validation of annual band-pair deposition in dorsal-fin spines of this species.

Materials and methods

Tagging and sample collection

Sampling cruises were conducted by 3 vessels in the Gulf of Maine, on Georges Bank, and off southern New England 5 times: in February 2011, in July 2011, in November and December 2011, in July and August 2012, and in November and December 2012. Spiny dogfish were collected during 20-min tows of otter trawls. During sampling in 2011, the first 5 spiny dogfish out of every 25 brought on board were selected for injection with OTC; however, in 2012, only the first 5 individuals from each tow were selected for injection with OTC. Straight-line fork length (FL), total length (TL), and stretch total length (STL) to the nearest millimeter, weight to the nearest 0.05 kg, and sex were recorded. Oxytetracycline was injected intramuscularly into each spiny dogfish at a dosage of 25 mg of OTC per kilogram of body weight (Holden and Vince, 1973). A rototag (Dalton ID Ltd.[2], Henley-on-Thames, UK) was then attached to the first dorsal fin before release (Kohler and Turner, 2001).

Recaptured sharks were returned whole to the Narragansett Laboratory of the NOAA Northeast Fisheries Science Center. All specimens were frozen prior to examination. Spiny dogfish were measured (FL, TL, and STL) and weighed. Whole vertebral columns and the second dorsal-fin spine were extracted for age validation.

Validation of ages from vertebrae and dorsal-fin spines

For consistency, vertebrae 19–23, which are among the largest vertebrae, were removed from each specimen of spiny dogfish. Only vertebrae from individuals with

[1] Jones, B. C., and G. H. Geen. 1977. Age and growth of spiny dogfish (*Squalus acanthias*) in the Strait of Georgia, British Columbia. Fish. Mar. Serv., Tech. Rep. 699, 16 p. [Available from website.]

[2] Mention of trade names or commercial companies is for identification purposes only and does not imply endorsement by the National Marine Fisheries Service, NOAA.

times at liberty (TAL) greater than 1 year were used for validation. From each specimen, 1 centrum was processed for band-pair count (hereafter referred to as the *histology section*) and 1 centrum was processed for OTC mark analysis (hereafter referred to as the *OTC section*). The histology section was processed by using thin sectioning methods to enhance the band pairs following Natanson et al. (2007). The OTC section was embedded in TAP Clear-Lite casting resin (TAP Plastics, San Leandro, CA) and sectioned through the frontal plane with an IsoMet Low Speed Saw (Buehler, Lake Bluff, IL) by using paired diamond-edged blades separated by a 0.6-mm spacer. Sections were stored individually in capsules in 70% ethanol and kept in the dark to preserve the OTC mark. Two photographs of the OTC section were taken under reflected light by using 1) white light and 2) long-wave ultraviolet light (366 nm) with a Nikon DSRi2 digital camera (Nikon Corp., Tokyo, Japan) attached to a Nikon SMZ1500 stereomicroscope (Nikon Instruments Inc., Melville, NY). The number of band pairs (consisting of 1 opaque and 1 translucent band) distal to the OTC mark was counted.

The distance from OTC mark to the centrum edge was measured in Adobe Photoshop CC 2017 (Adobe Inc., San Jose, CA) on the OTC section and transferred to the histology section to determine the location of the OTC mark relative to the band pairs. Because of the slight differences in sizes of adjacent vertebra, a ratio was used to calculate the position of the OTC mark on the histology section (Natanson, 1993). Band pairs past the OTC mark were then counted on the histology section; a half of a band pair indicated that the OTC mark was in the ultimate band (either translucent or opaque).

Dorsal-fin spines were removed, scraped clean of excess tissue, and thoroughly dried. Digital images of the dried second dorsal-fin spines with OTC marks regardless of TAL were photographed by using an MTI CCD-72 video camera (Dage-MTI Inc., Michigan City, IN) attached to an SZX9 Olympus stereomicroscope (Olympus Corp., Tokyo, Japan) with long-wave ultraviolet light (366 nm). The OTC image was then superimposed over an identical image taken under reflected white light by using Adobe Photoshop CC 2017. Band pairs past the OTC mark were then counted.

Linear regressions were performed on the data from each structure to determine if band-pair deposition was annual. Annual deposition is supported if the slope of the regression of the number of band pairs past the OTC mark against the TAL is not significantly different from 1 (i.e., the 95% confidence interval [CI] overlaps 1). Linear regressions were calculated for data from the vertebral centra and the dorsal-fin spines in R, vers. 3.4.4 (R Core Team, 2018).

Vertebral column analysis

For preliminary analysis of the whole vertebral column, one adult female spiny dogfish (87.0 cm FL) was collected separately in 2019 to compare the number of band pairs among centra along the vertebral column. This individual was not one of the recaptured individuals because a fresh, large individual was desired, and it was needed to avoid any potential shrinkage of the vertebrae during prolonged frozen storage. Fork length, TL, STL, weight, sex, and maturity status were recorded. Vertebra numbers 1–80 from the head to the tail were measured to the nearest 0.1 mm in 3 dimensions: dorsoventral diameter (hereafter referred to as *dorsal*), lateral diameter (hereafter referred to as *lateral*), and rostrocaudal length (hereafter referred to as *length*). Each measurement was plotted against centrum number to observe changes in vertebral shape along the vertebral column. To determine if the number of band pairs varied along the vertebral column, every fifth vertebra was processed histologically and band pairs were counted as outlined above. No assumptions were made about the birth date of spiny dogfish; therefore, only whole band pairs are reported for this analysis. The band-pair count also was plotted by centrum number. The mean band-pair count and 95% CI of the mean were calculated among centra for the vertebral column. If the band-pair counts of more than 5% of the centra examined were outside of the calculated 95% CI, the band-pair counts differed significantly along the vertebral column (James and Natanson, 2020).

Results

Tagging and sample collection

A total of 4306 spiny dogfish were injected with OTC, tagged, and released. Between July 2011 and September 2016, 148 spiny dogfish were recaptured and returned whole to the Narragansett Laboratory. No OTC-injected spiny dogfish were returned after 2016. Time at liberty ranged from 1 d to 4.8 years. Eighty-seven individuals had TALs greater than 1 year; an OTC mark was observed in the vertebrae of 41 of these individuals (47.1%; 33 females and 9 males). Out of the 148 dorsal-fin spines examined, 45 spines had an OTC mark (30.4%; 40 females and 5 males). All 45 dorsal-fin spines with an OTC mark were included in analysis regardless of TAL to increase the sample size. Twenty-one individuals had an OTC mark in both the vertebrae and the dorsal-fin spine (Fig. 1). The size range of all examined individuals was 51.5–87.5 cm FL at tagging and 52.8–87.3 cm FL at recapture (Tables 1 and 2). Some individuals shrank in FL over time, and this reduction in size is an artifact of the combination of small inaccuracies from measuring live spiny dogfish at capture and from measuring the recaptured spiny dogfish after being frozen.

Validation of ages from vertebrae and dorsal-fin spines

The number of band pairs past the OTC mark in vertebral centra does not support annual periodicity of band-pair formation. Vertebral centra had 0.5–2.5 band pairs past

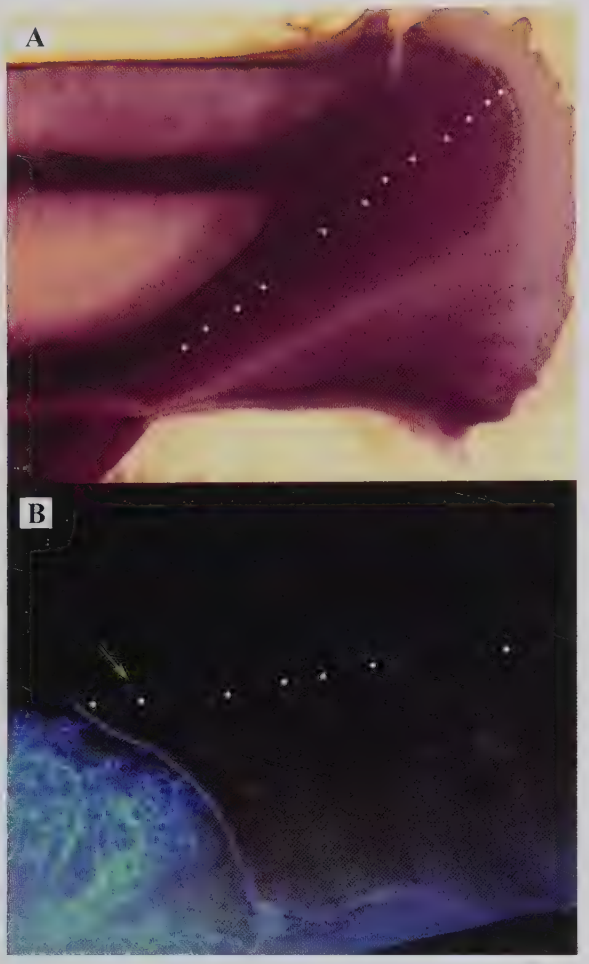

Figure 1

Overlay of an oxytetracycline mark (**A**) onto a histology section of vertebral centra (dotted green line) and (**B**) onto a dorsal-fin spine (green arrow) of a spiny dogfish (*Squalus acanthias*) (specimen ID code: SPD21) tagged off the coast of New England in 2011. White dots indicate all band pairs in panel A and the last 7 band pairs in panel B. This individual was at liberty for 1.2 years. Only half of a band pair formed on the vertebrae (panel A), and one and a half band pairs formed on the dorsal-fin spine (panel B).

the OTC mark for spiny dogfish at liberty for 1.1–4.8 years (Table 1). Fewer band pairs were consistently seen than would be expected if band pairs were annual (Fig. 2). The slope of the line at 0.126 (95% CI: −0.078–0.330) is significantly different from the 1:1 reference line, confirming that, when vertebral band pairs were used, TAL was consistently underestimated.

Dorsal-fin spines had 0.5–3.5 band pairs past the OTC mark for spiny dogfish at liberty for 0.1–2.6 years (Table 2). In contrast to that for vertebrae, the number of band pairs past the OTC mark in dorsal-fin spines did confirm annual periodicity of band-pair formation (Table 2, Fig. 2). Annual periodicity is supported, and the regression slope of 0.786 (95% CI: 0.558–1.013) is not significantly different from the 1:1 reference line.

Vertebral column analysis

For the vertebral column analysis of one adult female, both centrum measurements and band-pair counts varied along the vertebral column. Vertebral band-pair counts roughly followed vertebral centra morphology (Fig. 3). The lowest band-pair count was observed in the vertebra directly behind the neurocranium (vertebra 1), and the highest count was found at vertebra 40. Six of the 17 centra examined (35.3%) had band-pair counts that fell outside of the 95% CI (11.566–13.022) of the average band-pair count (12.294) along the entire vertebral column; therefore, the band-pair counts differed significantly along the vertebral column (Fig. 3).

Discussion

In this study, the results of OTC validation indicate that band pairs in vertebrae are not deposited annually in spiny dogfish. Use of counts of band pairs past the OTC mark consistently underestimated TAL for this species. Additionally, our results support previously published results indicating that band-pair deposition in fin spines is annual (Campana et al., 2006). On the basis of our results, we conclude that vertebrae are not an appropriate structure to use to estimate age for spiny dogfish.

Using a more detailed method, we were able to also obtain distinct band pairs in the vertebral centra of spiny dogfish. However, because of the prevalent underestimation of age observed from the location of the OTC mark within vertebral centra, we cannot recommend this structure for age determination of this species. These results are consistent with a growing number of studies with findings that indicate that vertebral band pairs do not accurately reflect age in sharks throughout their lives (see Harry, 2018; Natanson et al., 2018). In an attempt to understand the deposition of band pairs, Natanson et al. (2018) investigated the morphology and band-pair counts along the vertebral columns of several shark species and found that, in each species, band-pair counts varied along the vertebral column in relationship to vertebral size, not time, indicating a structural component to the band pairs. In our study, we found the same variation in band-pair counts along the vertebral column of a spiny dogfish. As per the species in the Natanson et al. (2018) study, lower band-pair counts were associated with smaller centra, indicating that band pairs are also related to the structure of the vertebra rather than to time in this species. Additionally, if band pairs were deposited annually, the same band-pair counts would be expected for every vertebra within an individual (Natanson et al., 2018). Although this finding for spiny dogfish is interesting, it is based on one specimen, and further work on more specimens of this species

Table 1

Tag-recapture data and band-pair counts for the 41 recaptured spiny dogfish (*Squalus acanthias*) that had a time at liberty (TAL) greater than 1 year and an oxytetracycline (OTC) mark in a vertebra. Specimens were tagged in the Gulf of Maine, on Georges Bank, and off southern New England during 2011 and 2012. Fork length at tagging (TFL), fork length at recapture (RFL), TAL, and other data are arranged by increasing TAL.

Specimen ID code	Sex	TFL (cm)	RFL (cm)	Date tagged	TAL (years)	No. of band pairs past OTC mark
SPD411	F	67.0	69.9	3-Aug-2012	1.05	2.5
SPD73	F	73.0	73.2	16-Jul-2011	1.10	1.0
SPD40	F	76.0	76.6	12-Jul-2011	1.11	1.5
SPD50	F	61.0	68.1	14-Jul-2011	1.11	1.0
SPD36	F	71.0	73.8	17-Jul-2011	1.12	1.5
SPD12	F	87.5	87.3	13-Jul-2011	1.13	0.5
SPD54	M	72.0	70.0	16-Jul-2011	1.16	0.5
SPD46	F	77.0	77.2	13-Jul-2011	1.16	0.5
SPD90	F	80.0	79.6	16-Jul-2011	1.17	1.0
SPD21	F	73.0	74.7	17-Jul-2011	1.19	0.5
SPD81	F	72.4	73.0	27-Nov-2011	1.20	0.5
SPD72	F	77.5	77.6	17-Jul-2011	1.23	1.0
SPD88	F	79.8	77.9	12-Jul-2011	1.28	0.5
SPD75	F	78.0	76.9	13-Jul-2011	1.32	0.5
SPD80	F	74.0	74.7	16-Jul-2011	1.32	1.0
SPD76	F	70.0	74.3	17-Jul-2011	1.33	1.5
SPD31	M	66.0	67.5	14-Feb-2011	1.49	1.0
SPD45	M	58.7	57.0	10-Feb-2011	1.56	0.5
SPD14	M	67.5	65.8	11-Feb-2011	1.58	0.5
SPD116	F	77.4	77.1	27-Nov-2011	1.58	0.5
SPD414	F	82.1	83.2	2-Dec-2011	1.60	0.5
SPD437	F	75.0	76.7	12-Jul-2011	1.60	0.5
SPD409	F	75.0	75.5	1-Dec-2011	1.62	1.0
SPD418	F	79.0	79.4	2-Dec-2011	1.62	1.5
SPD435	F	73.0	75.4	15-Jul-2011	1.63	1.0
SPD408	M	64.9	63.7	26-Nov-2011	1.70	0.5
SPD788	F	72.0	70.0	4-Dec-2012	1.71	1.0
SPD443	F	70.0	71.8	5-Dec-2011	1.74	0.5
SPD428	M	65.2	64.4	2-Dec-2011	1.81	0.5
SPD427	F	77.0	76.9	27-Nov-2011	1.94	1.5
SPD410	F	75.0	76.9	13-Jul-2011	2.02	0.5
SPD426	F	75.0	75.7	2-Dec-2011	2.12	0.5
SPD430	M	68.0	67.5	16-Feb-2011	2.47	0.5
SPD252	M	51.5	52.8	16-Feb-2011	2.54	0.5
SPD415	F	80.0	79.8	16-Jul-2011	2.58	1.0
SPD253	M	65.2	63.5	17-Feb-2011	2.61	1.5
SPD422	F	73.0	74.2	16-Jul-2011	2.61	0.5
SPD439	F	76.0	76.9	16-Jul-2011	2.63	0.5
SPD787	F	76.0	75.5	16-Jul-2011	3.10	1.0
SPD789	F	76.0	73.3	16-Jul-2011	3.41	1.5
SPD792	F	79.0	80.9	1-Dec-2011	4.80	2.0

and on specimens of Pacific spiny dogfish would lead to more robust conclusions.

The absence of an OTC mark in wild specimens in mark-recapture studies is well-documented (e.g., Smith, 1984; McFarlane and Beamish, 1987). In our study, an OTC mark was not found in many recaptured individuals in either vertebral centra or dorsal-fin spines, with OTC marking success rates of 47.1% and 30.4%, respectively. Other studies have had success rates for OTC marking in vertebrae ranging from 37.5% (Harry et al., 2013) to 100%

Table 2

Tag-recapture data and counts of band pairs past the oxytetracycline (OTC) mark for the 45 recaptured spiny dogfish (*Squalus acanthias*) that had an OTC mark on a dorsal-fin spine. Specimens were tagged in the Gulf of Maine, on Georges Bank, and off southern New England during 2011 and 2012. Fork length at tagging (TFL), fork length at recapture (RFL), time at liberty (TAL), and other data are arranged by increasing TAL.

Specimen ID code	Sex	TFL (cm)	RFL (cm)	Date tagged	TAL (years)	No. of band pairs past OTC mark
SPD68	F	65.0	65.4	3-Dec-2012	0.08	0.5
SPD34	F	78.2	78.6	31-Jul-2012	0.08	0.5
SPD66	F	77.0	77.6	4-Dec-2012	0.09	0.5
SPD69	F	77.0	77.4	30-Nov-2012	0.10	0.5
SPD52	F	74.6	73.3	5-Aug-2012	0.12	0.5
SPD29	F	77.5	76.5	1-Dec-2011	0.28	0.5
SPD71	F	67.8	67.1	6-Aug-2012	0.28	0.5
SPD429	F	74.0	72.3	1-Dec-2012	0.41	0.5
SPD26	F	83.0	83.5	1-Dec-2011	0.42	0.5
SPD56	F	72.0	71.5	15-Jul-2011	0.48	0.5
SPD30	F	76.0	74.1	28-Nov-2011	0.59	0.5
SPD41	F	77.0	79.3	28-Nov-2011	0.65	0.5
SPD438	F	82.4	83.5	1-Aug-2012	0.74	0.5
SPD48	M	65.0	65.1	26-Nov-2011	0.75	0.5
SPD17	F	76.2	78.2	25-Nov-2011	0.75	0.5
SPD43	F	72.0	73.0	27-Nov-2011	0.78	1.5
SPD15	M	65.0	65.5	25-Nov-2011	0.82	0.5
SPD24	F	76.7	77.3	16-Jul-2011	0.90	1.5
SPD23	F	80.0	79.4	13-Jul-2011	1.00	1.0
SPD411	F	67.0	69.9	3-Aug-2012	1.05	1.0
SPD44	F	71.0	74.3	12-Jul-2011	1.09	1.5
SPD40	F	76.0	76.6	12-Jul-2011	1.11	1.5
SPD50	F	61.0	68.1	14-Jul-2011	1.11	2.0
SPD36	F	71.0	73.8	17-Jul-2011	1.12	1.5
SPD12	F	87.5	87.3	13-Jul-2011	1.13	1.0
SPD417	F	76.0	76.1	16-Jul-2011	1.15	2.0
SPD46	F	77.0	77.2	13-Jul-2011	1.16	1.0
SPD21	F	73.0	74.7	17-Jul-2011	1.19	1.5
SPD75	F	78.0	76.9	13-Jul-2011	1.32	1.0
SPD76	F	70.0	74.3	17-Jul-2011	1.33	2.0
SPD14	M	67.5	65.8	11-Feb-2011	1.58	1.0
SPD116	F	77.4	77.1	27-Nov-2011	1.58	2.5
SPD414	F	82.1	83.2	2-Dec-2011	1.60	2.0
SPD437	F	75.0	76.7	12-Jul-2011	1.60	1.0
SPD409	F	75.0	75.5	1-Dec-2011	1.62	1.0
SPD436	F	73.0	75.1	12-Jul-2011	1.62	2.5
SPD418	F	79.0	79.4	2-Dec-2011	1.62	1.0
SPD408	M	64.9	63.7	26-Nov-2011	1.70	1.0
SPD788	F	72.0	70.0	4-Dec-2012	1.71	1.0
SPD420	F	78.0	76.6	2-Dec-2011	1.93	1.0
SPD427	F	77.0	76.9	27-Nov-2011	1.94	2.0
SPD413	F	77.0	79.9	16-Jul-2011	1.97	1.5
SPD426	F	75.0	75.7	2-Dec-2011	2.12	2.0
SPD252	M	51.5	52.8	16-Feb-2011	2.54	3.5
SPD422	F	73.0	74.2	16-Jul-2011	2.61	2.0

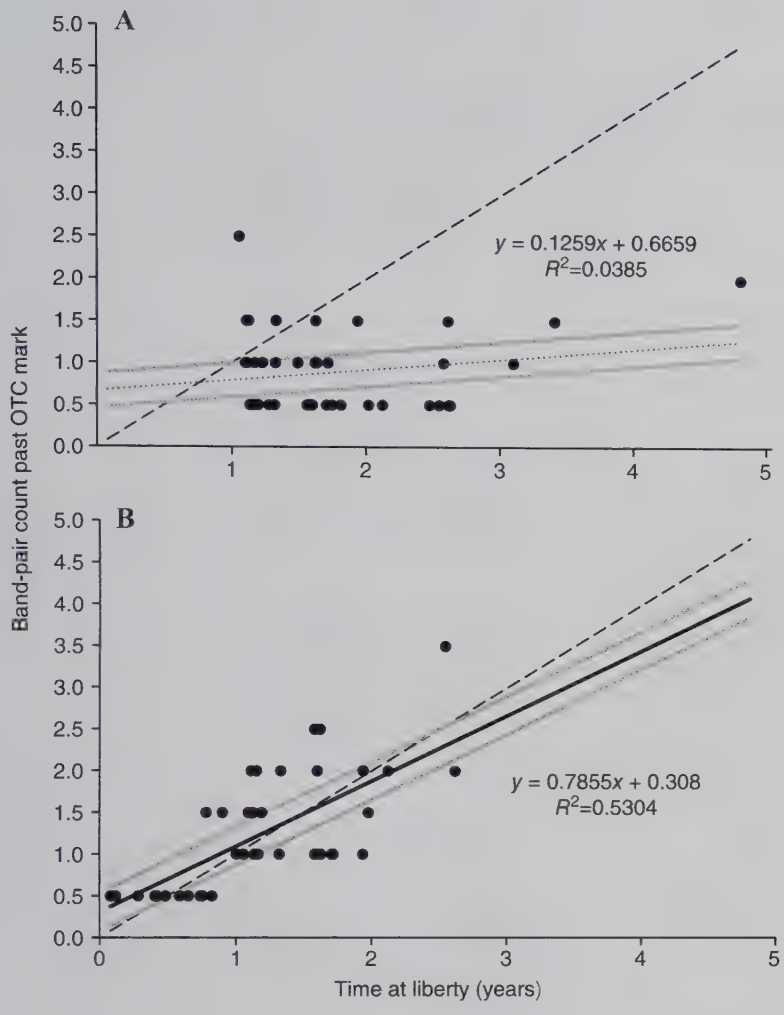

Figure 2

Relationship of time at liberty and the number of band pairs past the oxytetracycline (OTC) mark in the (**A**) vertebrae and (**B**) dorsal-fin spines of spiny dogfish (*Squalus acanthias*) tagged in the Gulf of Maine, on Georges Bank, and off southern New England during 2011 and 2012. The dotted line in panel A and the solid line in panel B indicate linear regressions. The 95% confidence intervals (CIs) of the slope of the linear regressions (gray lines) do not include a 1:1 relationship (dashed line) in panel A (95% CI: −0.078–0.330) and do include a 1:1 relationship (dashed line) in panel B (95% CI: 0.558–1.013). R^2=coefficient of multiple determination.

(e.g., McAuley et al., 2006). Fewer studies have examined OTC deposition in dorsal-fin spines, but McFarlane and Beamish (1987) reported an OTC marking success rate of 34%. There has not been a direct comparison of OTC marking success rates between vertebral centra and dorsal-fin spines; therefore, it cannot be known if rates differ between structures. However, the success rate for OTC marking was lower in dorsal-fin spines than in vertebrae in our study and was similar to that reported by McFarlane and Beamish (1987). This result indicates that dorsal-fin spines may incorporate OTC less readily than vertebral centra.

One explanation for the absence of an OTC mark is insufficient mineralization directly after injection (Smith, 1984). Mineralization may slow seasonally (Jones and Geen, 1977) and with ontogeny (Francis et al., 2007; Natanson et al., 2018). In our study, spiny dogfish were injected with OTC in several seasons, but there were few recaptured individuals with OTC marks that had been injected in February (Tables 1 and 2). Similar results were reported by McFarlane and Beamish (1987), who found that OTC marks were visible at a higher rate in the dorsal-fin spines of spiny dogfish injected in the fall than in the spines of those injected in the spring. The low growth rates observed in our study and the generally large sizes of specimens (Tables 1 and 2) support the idea of slowed body growth and subsequently slowed mineralization, particularly for vertebrae (Francis et al., 2007, Natanson et al., 2018). Such small changes in growth compounded with inaccuracies from measuring live then frozen spiny dogfish could have resulted in the negative growth observed in our study. With the environmental and ontogenetic effects on mineralization and growth, low OTC marking success rates are not unexpected.

Age information is important for stock assessments intended to inform fisheries management. We investigated validation of annual deposition of band pairs in vertebral centra from spiny dogfish because of concerns over the effect on age estimates of wear and tear on dorsal-fin spines. Although band pairs on vertebral centra are distinct, the results of our study from the use of chemical marking indicate that band pairs are not deposited annually and, therefore, that use of band pairs on this structure underestimates age in spiny dogfish. In contrast, validation of the use of dorsal-fin spines is supported by our findings. Therefore, despite their limitations, fin spines are more representative of age than vertebrae in spiny dogfish.

Acknowledgments

We thank the Northeast Cooperative Research Program of the NOAA Northeast Fisheries Science Center, B. Gervelis, D. McElroy, and the fishermen that helped tag and recapture the spiny dogfish used in this study. We thank K. Wooley for helping process samples in the lab.

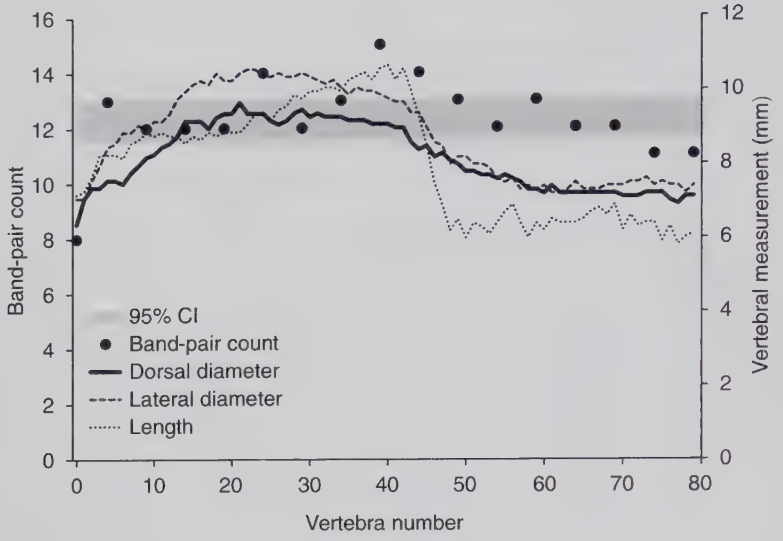

Figure 3

Band-pair counts (black circles) for each fifth vertebra within one adult female spiny dogfish (*Squalus acanthias*) collected off the coast of New England in 2019 compared with vertebra number and dorsal (solid line), lateral (dashed line), and length (dotted line) measurements of every vertebra. The gray area represents the 95% confidence interval (95% CI: 11.566–13.022) of the average band-pair count (12.294) of the vertebrae examined from this individual.

Literature cited

Bubley, W. J., J. Kneebone, J. A. Sulikowski, and P. C. W. Tsang.
2012. Reassessment of spiny dogfish *Squalus acanthias* age and growth using vertebrae and dorsal-fin spines. J. Fish Biol. 80:1300–1319.

Campana, S. E., C. Jones, G. A. McFarlane, and S. Myklevoll.
2006. Bomb dating and age validation using the spines of spiny dogfish (*Squalus acanthias*). Environ. Biol. Fishes 77:327–336.

Campana, S. E., W. Joyce, and D. W. Kulka.
2009. Growth and reproduction of spiny dogfish off the eastern coast of Canada, including inferences on stock structure. *In* Biology and management of dogfish sharks (V. F. Gallucci, G. A. McFarlane, and G. G. Bargmann, eds.), p. 195–208. Am. Fish. Soc., Bethesda, MD.

Collette, B. B., and G. Klein-MacPhee (eds.).
2002. Bigelow and Schroeder's fishes of the Gulf of Maine, 3rd ed., 748 p. Smithsonian Inst. Press, Washington, DC.

DFO (Fisheries and Oceans Canada).
2020. Assessment of Spiny Dogfish in the Northwest Atlantic. DFO Can. Sci. Advis. Sec. Sci. Advis. Rep. 2020/001. [Available from website.]

Ebert, D. A., W. T. White, K. J. Goldman, L. J. V. Compagno, T. S. Daly-Engel, and R. D. Ward.
2010. Resurrection and redescription of *Squalus suckleyi* (Girard, 1854) from the North Pacific, with comments on the *Squalus acanthias* subgroup (Squaliformes: Squalidae). Zootaxa 2612:22–40.

Fishery Conservation and Management Act of 1976. 16 U.S. Code 1801–1882 (2018). [Available from website.]

Francis, M. P., S. E. Campana, and C. M. Jones.
2007. Age under-estimation in New Zealand porbeagle sharks (*Lamna nasus*): is there an upper limit to ages that can be determined from shark vertebrae? Mar. Freshw. Res. 58:10–23.

Harry, A. V.
2018. Evidence for systemic age underestimation in shark and ray ageing studies. Fish Fish. 19:185–200.

Harry, A. V., A. J. Tobin, and C. A. Simpfendorfer.
2013. Age, growth and reproductive biology of the spot-tail shark, *Carcharhinus sorrah*, and the Australian blacktip shark, *C. tilstoni*, from the Great Barrier Reef World Heritage Area, north-eastern Australia. Mar. Freshw. Res. 64:277–293.

Holden, M. J., and P. S. Meadows.
1962. The structure of the spine of the spur dogfish (*Squalus acanthias* L.) and its use for age determination. J. Mar. Biol. Assoc. U.K. 42:179–197.

Holden, M. J., and M. R. Vince.
1973. Age validation studies on the centra of *Raja clavata* using tetracycline. ICES J. Mar. Sci. 35:13–17.

James, K. C., and L. J. Natanson.
2020. Positional and ontogenetic variation in the vertebral centra morphology in five batoid species. Mar. Freshw. Res.

Jensen, A. C.
1965. Life history of the spiny dogfish. Fish. Bull. 65:527–554.

Jones, B. C., and G. H. Geen.
1977. Age determination of an elasmobranch (*Squalus acanthias*) by X-ray spectrometry. J. Fish. Res. Board Can. 34:44–48.

Kaganovskaia, S.
1933. A method of determining the age and the compositions of the catches of the spiny dogfish (*Squalus acanthias* L.). Vestn. Dalnevost. Fil. Akad. Nauk SSSR 1–3:139–141.

Ketchen, K. S.
1975. Age and growth of dogfish *Squalus acanthias* in British Columbia waters. J. Fish. Res. Board Can. 32:43–59.

Kohler, N. E., and P. A. Turner.
2001. Shark tagging: a review of conventional methods and studies. Environ. Biol. Fishes 60:191–224.

McAuley, R. B., C. A. Simpfendorfer, G. A. Hyndes, R. R. Allison, J. A. Chidlow, S. J. Newman, and R. C. J. Lenanton.
2006. Validated age and growth of the sandbar shark, *Carcharhinus plumbeus* (Nardo 1827) in the waters off Western Australia. Environ. Biol. Fishes 77:385–400.

McFarlane, G. A., and R. J. Beamish.
1987. Validation of the dorsal spine method of age determination for spiny dogfish. *In* Age and growth of fish (R. C. Summerfelt and G. E. Hall, eds.), p. 287–300. Iowa State Univ. Press, Ames, IA.

McFarlane, G. A., and J. R. King.
2009. Re-evaluating the age determination of spiny dogfish using oxytetracycline and fish at liberty up to 20 years. *In* Biology and management of dogfish sharks (V. F. Gallucci, G. A. McFarlane, and G. G. Bargmann, eds.), p. 153–160. Am. Fish. Soc., Bethesda, MD.

Nammack, M. F., J. A. Musick, and J. A. Colvocoresses.
1985. Life history of spiny dogfish off the northeastern United States. Trans. Am. Fish. Soc. 114:367–376.

Natanson, L. J.
1993. Effect of temperature on band deposition in the little skate, *Raja erinacea*. Copeia 1993:199–206.

Natanson, L. J., J. A. Sulikowski, J. R. Kneebone, and P. C. Tsang.
2007. Age and growth estimates for the smooth skate, *Malacoraja senta*, in the Gulf of Maine. Environ. Biol. Fishes 80:293–308.

Natanson, L. J., G. B. Skomal, S. L. Hoffmann, M. E. Porter, K. J. Goldman, and D. Serra.
2018. Age and growth of sharks: do vertebral band pairs record age? Mar. Freshw. Res. 69:1440–1452.

NEFSC (Northeast Fisheries Science Center).
1998. 26th Northeast regional stock assessment workshop (26th SAW): stock assessment review committee (SARC) consensus summary of assessments. Northeast Fish. Sci. Cent. Ref. Doc. 98-03, 283 p. [Available from website.]
2006. 43rd Northeast regional stock assessment workshop (43rd SAW): 43rd SAW assessment summary report. Northeast Fish. Sci. Cent. Ref. Doc. 06-14, 43 p. [Available from website.]

R Core Team.
2018. R: a language and environment for statistical computing. R Foundation for Statistical Computing, Vienna, Austria. [Available from website, accessed March 2018.]

Rago, P. J., and K. A. Sosebee.
2009. The agony of recovery: scientific challenges of spiny dogfish recovery programs. *In* Biology and management of dogfish sharks (V. F. Gallucci, G. A. McFarlane, and G. G. Bargmann, eds.), p. 343–372. Am. Fish. Soc., Bethesda, MD.

Saunders, M. W., and G. A. McFarlane.
1993. Age and length at maturity of the female spiny dogfish, *Squalus acanthias*, in the Strait of Georgia, British Columbia, Canada. Environ. Biol. Fishes 38:49–57.

Smith, S. E.
1984. Timing of vertebral-band deposition in tetracycline-injected leopard sharks. Trans. Am. Fish. Soc. 113:308–313.

Taylor, I. G., V. Gertseva, and S. E. Matson.
2013. Spine-based ageing methods in the spiny dogfish shark, *Squalus suckleyi*: how they measure up. Fish. Res. 147:83–92.

Tribuzio, C. A., G. H. Kruse, and J. T. Fujioka.
2010. Age and growth of spiny dogfish (*Squalus acanthias*) in the Gulf of Alaska: analysis of alternative growth models. Fish. Bull. 108:119–135.

Tribuzio C. A., M. E. Matta, C. Gburski, N. Atkins, and W. Bubley.
2016. Methods for the preparation of Pacific spiny dogfish (*Squalus suckleyi*), fin spines and vertebrae and an overview of age determinations. Mar. Fish. Rev. 78(1–2):1–13.

Tribuzio, C. A., M. E. Matta, C. Gburski, C. Blood, W. Bubley, and G. H. Kruse.
2017. Are Pacific spiny dogfish lying about their age? A comparison of ageing structures for *Squalus suckleyi*. Mar. Freshw. Res. 69:37–47.

Veríssimo, A., J. R. McDowell, and J. E. Graves.
2010. Global population structure of the spiny dogfish *Squalus acanthias*, a temperate shark with an antitropical distribution. Mol. Ecol. 19:1651–1662.

National Marine
Fisheries Service
NOAA

Fishery Bulletin
established in 1881

Spencer F. Baird
First U.S. Commissioner
of Fisheries and founder
of *Fishery Bulletin*

Ontogenetic shifts and feeding strategies of 7 key species of Gadiformes in the western Mediterranean Sea

Encarnación García-Rodríguez (contact author)[1]
Miguel Vivas[1]
José M. Bellido[1]
Antonio Esteban[1]
María Ángeles Torres[2]

Email address for contact author: encarnacion.garcia@ieo.es

[1] Centro Oceanográfico de Murcia
Instituto Español de Oceanografía
Calle el Varadero 1
San Pedro del Pinatar
30740 Murcia, Spain

[2] Centro Oceanográfico de Cádiz
Instituto Español de Oceanografía
Puerto Pesquero
Muelle de Levante s/n
11006 Cádiz, Spain

Abstract—The trophic ecology of 7 key species of Gadiformes, the silvery pout (*Gadiculus argenteus*), Mediterranean bigeye rockling (*Gaidropsarus biscayensis*), European hake (*Merluccius merluccius*), blue whiting (*Micromesistius poutassou*), Mediterranean ling (*Molva macrophthalma*), greater forkbeard (*Phycis blennoides*), and poor cod (*Trisopterus minutus*), in the western Mediterranean Sea was explored. A total of 3192 fish stomachs were examined during 2011–2017 to investigate ontogenetic shifts in diet, trophic interactions (both interspecific and intraspecific), and feeding strategies. The results from applying multivariate statistical techniques indicate that all investigated species, except the Mediterranean bigeye rockling and poor cod, underwent ontogenetic dietary shifts, increasing their trophic level with size. The studied species hold different trophic positions, from opportunistic (e.g., the Mediterranean bigeye rockling, with a trophic level of 3.51) to highly specialized piscivore behavior (e.g., the Mediterranean ling, with a trophic level of 4.47). These insights reveal 4 different feeding strategies among the co-occurring species and size classes in the study area, as well as the degree of dietary overlap. Such information on ecological patterns within a fish assemblage, including species interactions, is often requested by those who aim tc implement ecosystem management. Therefore, these findings can be used to improve management of sustainable fisheries in this region.

Manuscript submitted 25 May 2020.
Manuscript accepted 9 March 2021.
Fish. Bull. 119:50–65 (2021).
Online publication date: 13 April 2021.
doi: 10.7755/FB.119.1.7

The views and opinions expressed or implied in this article are those of the author (or authors) and do not necessarily reflect the position of the National Marine Fisheries Service, NOAA.

One of the most important aspects of analysis of trophic interactions is the study of trophic levels, understood as a hierarchical way of classifying organisms according to their feeding relationships within an ecosystem, contributing to knowledge about the ecological role of a species (Cochran et al., 2019). This knowledge is critical in investigating predator–prey interactions and is necessary for an ecosystem-based approach to fisheries management (Christensen, 1996; García et al., 2003). Additionally, feeding patterns offer useful insights about the long-term stability of marine ecosystems (Trites, 2003; McDonald-Madden et al., 2016).

In general, fish change their diets with size to optimize their energetic return (Scharf et al., 2000; Juanes et al., 2002). In addition, ontogenetic shifts can be considered a mechanism to avoid, or at least minimize, intraspecific competition by allowing exploitation of different food resources at each developmental stage (Marrin, 1983; Castro and Hernández-García, 1995). More broadly, fish species have a wide range of strategies, on both intraspecific and interspecific levels, that result in and maintain resource partitioning (Madurell et al., 2008; Fanelli et al., 2009, 2013). Such strategies include not only food selection but also habitat selection and temporal segregation (Schoener, 1974). Hence, resource partitioning occurs when fish species are segregated into at least 1 of 3 niche dimensions. As a result, niche overlap is avoided and resource competition is minimized among fish species. This hypothesis is known as niche complementarity (Ebeling and Hixon, 1991) and assumes that a particular species, which overlaps with others in a given niche dimension, would separate along another dimension, maintaining resource partitioning. Describing and comparing these relationships, by using indices that reflect niche overlap or niche breadth, can help to explain

feeding behaviors that range from generalist to specialist in nature (Silva et al., 2014).

This study aimed to investigate niche complementarity and co-occurrence of 7 fish species of Gadiformes in the western Mediterranean Sea off the coast of Spain. In particular, we analyzed ontogenetic shifts in diet, trophic interactions (both interspecific and intraspecific), feeding strategies, and the degree of dietary overlap among the studied species, to ascertain the ecological patterns of dietary interrelationships within the fish assemblage.

The selected gadiform species can inhabit depths greater than 1000 m (Fanelli et al., 2013) and play an important role in the middle of the food web (i.e., in both bottom-up and top-down controls) within marine ecosystems (Libralato et al., 2006), indicating that they feed on different trophic levels (Miller et al., 2010). They are prey for many other fish species (e.g., Preciado et al., 2008; Rodríguez-Cabello et al., 2014), and they occupy different substrates, ranging from sandy to rocky (Cohen et al., 1990).

In the Mediterranean Sea, the biology and behavior of many species of Gadiformes are well-documented (Morte et al., 2001, 2002), and they are important commercially and ecologically. For example, the European hake (*Merluccius merluccius*) is one of the most common representatives of this group, considering the amount of landings, and is currently experiencing overexploitation, with fishing mortality rates around 1.8–8.1 times higher than the assumed reference level of fishing mortality that would provide maximum sustainable yield (Colloca et al., 2013).

In the western Mediterranean Sea, studies of fish feeding habits usually focus on a few species and omit trophic interactions, information about which is essential for an effective implementation of an ecosystem approach to fisheries management (García et al., 2003). For instance, off the coast of Spain, Macpherson (1978a) studied age-related seasonal feeding habits of blue whiting (*Micromesistius poutassou*) in the Gulf of Valencia and of silvery pout (*Gadiculus argenteus*) in the Catalan Sea. He also investigated the diet of the Mediterranean bigeye rockling (*Gaidropsarus biscayensis*) and Mediterranean ling (*Molva macrophthalma*) (Macpherson, 1978b, 1981). Bozzano et al. (1997) reported seasonal feeding habits of European hake in the Gulf of Lion off the coast of France, and Morte et al. (2001, 2002) analyzed the diet of poor cod (*Trisopterus minutus*) and greater forkbeard (*Phycis blennoides*) in the Gulf of Valencia. Unfortunately, none of these studies have investigated further interactions between species and fish assemblage.

Studies that address a broader geographic area and include ontogenetic shifts in diets of gadiform species, therefore, are scarce for the Mediterranean Sea off the coast of Spain, and it is necessary to fill this gap in knowledge as well as update current information. Additionally, the fish assemblage in the western Mediterranean Sea is currently facing problems of not only overfishing and biodiversity loss but also environmental pressures, such as the massive urbanization of coastlines, with increases in water pollution and decreases in sediments from principal rivers (e.g., Coll et al., 2010). Catch quality is decreasing, resulting in landings with a higher proportion of low-value species and a higher ratio of small to large fish. Furthermore, in the case of some of the most damaging and commonly used gear, namely bottom trawls, discard rates of low-value species are high (Bellido et al.[1]; Paradinas et al., 2016). Under this scenario of overfishing and environmental pressures, a declining trend in the landed biomass of the commercial species of Gadiformes investigated in our study has been observed in the area (MAGRAMA[2]; MAPAMA[3]; MAPA[4]). Consequently, more local and updated data on intraspecific and interspecific interactions are needed to develop ecosystem models for an ecosystem-based approach to fisheries management (Christensen and Walters, 2004; Gascuel, 2005).

Material and methods

Study area and sampling procedure

We carried out our study in the Mediterranean Sea off the coast of Spain from Cape Palos to Cape Creus (Fig. 1). According to the General Fisheries Commission for the Mediterranean, this area is also known as geographical subarea 06 (GSA-06), and it extends along 808 km of coastline, with a total area of 30,119 km^2 and depths of 40–800 m. The study area is characterized by high biodiversity (García-Rodríguez et al., 2011) and oligotrophic conditions. Nevertheless, within the study area, certain zones (e.g., Ebro Delta) are exceptions because of their moderate levels of primary production (Estrada, 1996). The main fishery resources in this area are demersal and benthic organisms, such as fish species (Osteichthyes and Chondrichthyes) and invertebrates (mollusks and crustaceans). Some of the fish species, such as the bogue (*Boops boops*) or blotched picarel (*Spicara maena*), are heavily discarded, or they are used as bait, although they are an increasing component of landings, mainly in the bottom-trawl fishery (Bellido et al.[1]). Most of these species, including the European hake and blue whiting, both of the order Gadiformes, are fully exploited or overexploited (Coll et al., 2008; Cardinale, 2012, 2013; Coll et al., 2014; FAO, 2018).

[1] Bellido, J. M., A. Carbonell, M. T. García, and M. González. 2014. The obligation to land all catches—consequences for the Mediterranean: in-depth analysis, 46 p. Policy Dep. B: Struct. Cohes. Policies, Dir.-Gen. Intern. Policies, Eur. Parliam., Brussels, Belgium. [Available from website.]

[2] MAGRAMA (Ministerio de Agricultura, Alimentación y Medio Ambiente). 2013–2015. Estadísticas pesqueras: Noviembre [2013–2015]. Minist. Agric. Aliment. Medio Ambiente, Madrid, Spain. [Available from website.]

[3] MAPAMA (Ministerio de Agricultura y Pesca, Alimentación y Medio Ambiente). 2016–2017. Estadísticas pesqueras: Noviembre [2016–2017]. Minist. Agric. Pesca Aliment. Medio Ambiente, Madrid, Spain. [Available from website.]

[4] MAPA (Ministerio de Agricultura, Pesca y Alimentación). 2018–2020. Estadísticas pesqueras: Noviembre [2018–2020]. Minist. Agric. Pesca Aliment., Madrid, Spain. [Available from website.]

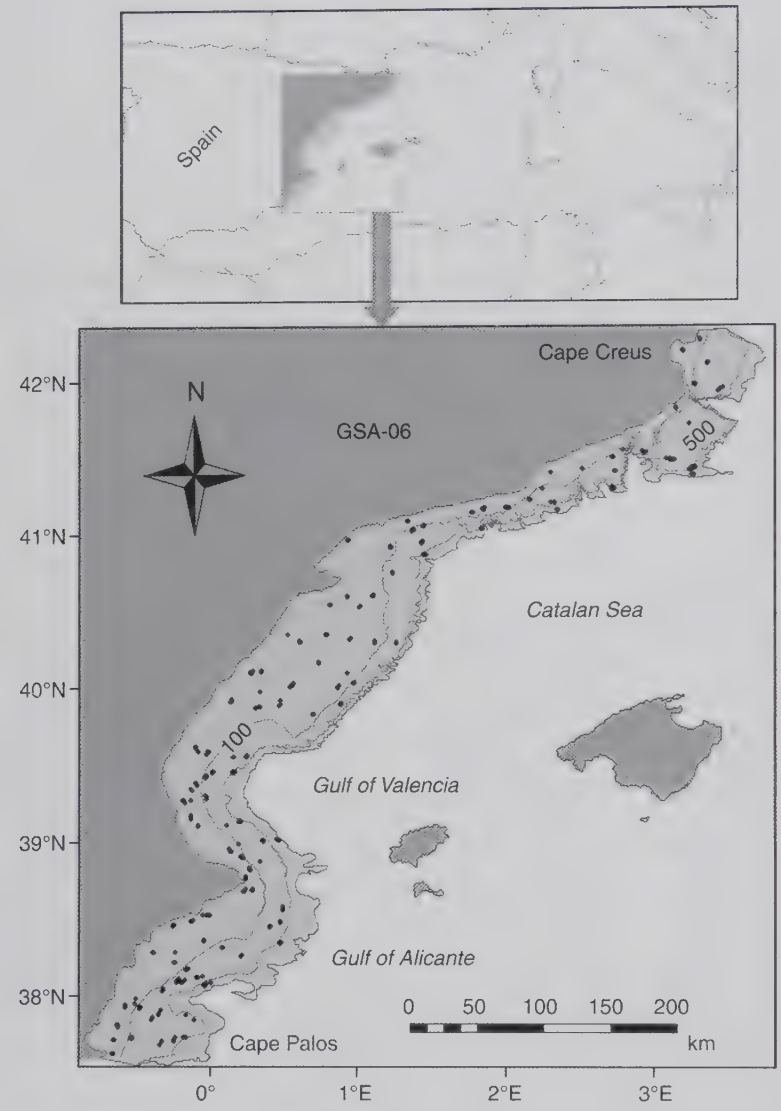

Figure 1

Map showing the locations where 7 species of Gadiformes were sampled between 2011 and 2017 in the Mediterranean Sea off the coast of Spain from Cape Palos to Cape Creus, in the geographical subarea 06 (GSA-06) defined by the General Fisheries Commission for the Mediterranean. Dots indicate the positions of the trawl tows conducted during surveys. The light gray shaded area indicates the area between isobaths of 40 and 800 m where specimens were caught.

Stomach samples were collected from fish caught during bottom-trawl surveys conducted as part of the Mediterranean International Trawl Survey (MEDITS) program in GSA-06 in 2011–2017 (Bertrand et al., 2002). The surveys of this program take place yearly from May through June for the purpose of evaluating the demersal resources throughout the study area. The standard MEDITS sampling gear is a bottom trawl called the GOC 73, which has a net with a mesh size of 40 mm and a codend with a mesh size of 20 mm. This gear is specifically designed for experimental fishing. A total of 604 trawl tows were carried out during daylight, from 0800 to 1800, at depths of 40–730 m.

For this investigation, we selected the species of the order Gadiformes that were most abundant in the study area: the silvery pout, Mediterranean bigeye rockling, Mediterranean ling, European hake, blue whiting, greater forkbeard, and poor cod. During the survey cruises in the study period, the contents of 3192 stomachs were analyzed on board vessels (for details for these 7 species, see Table 1). After each trawl tow, 10 individuals of each of the studied species were randomly sampled from the haul. For all specimens examined, total length (TL) in millimeters, sex, and maturity stage were recorded according to MEDITS guidelines (Bertrand et al., 2002). Later, diet was assessed quantitatively by measuring the volume of stomach contents with a trophometer, a calibrated device that consists of several semicylinders of different sizes (Olaso, 1990). The use of this instrument is helpful on board oceanographic vessels because it allows a large number of stomachs to be examined in a relatively short period.

Once a stomach was opened, its contents were analyzed under a binocular microscope (Leica MZ6[5], Leica Microsystems, Wetzlar, Germany). Prey found in stomachs (prey items) were identified to the lowest possible taxon by using published guides (Zariquiey, 1968; Lombarte et al., 2006) and our own reference collection. The degrees of digestion of all prey items identified were also noted, as fresh, partially digested, or fully digested. The stomachs that contained any items presumably consumed in the net during fishing operations (i.e., stomachs from individuals of anglerfish species) were excluded from the analyses. The presence of skeletal remains and other hard body parts was also recorded. Stomach samples from specimens that had regurgitated the contents of their stomachs were replaced with samples from individuals of a similar size class (García-Rodríguez et al., 2020). Following Robb (1992), the color and size of the gall bladder of European hake were used to determine if a specimen had an empty stomach or had regurgitated during the fishing operation.

[5] Mention of trade names or commercial companies is for identification purposes only and does not imply endorsement by the National Marine Fisheries Service, NOAA.

Table 1

Summary information related to the 7 most abundant species of Gadiformes sampled in the western Mediterranean Sea between 2011 and 2017. For each species, the scientific and common names, depth range (in meters), number of stomachs for which contents were examined, and size range (total lengths in millimeters) are provided.

Scientific name	Common name	Depth range	No. of stomachs	Size range
Gadiculus argenteus	Silvery pout	109–647	263	60–133
Gaidropsarus biscayensis	Mediterranean bigeye rockling	59–634	116	40–180
Molva macrophthalma	Mediterranean ling	86–634	164	83–740
Merluccius merluccius	European hake	34–722	1254	87–549
Micromesistius poutassou	Blue whiting	76–722	786	89–377
Phycis blennoides	Greater forkbeard	53–728	286	85–393
Trisopterus minutus	Poor cod	36–352	323	78–272

Dietary indices

Three conventional dietary indices were calculated to provide quantitative information on diet compositions of the gadiform species investigated. A raw data set including prey species for each predator species is included in Supplementary Table 1 (online only). The first index used was frequency of occurrence (%FO), defined as the number of stomachs containing a prey item compared with the total number of stomachs examined. The second index was the number index (%N), defined as the number of individuals of a prey item compared with the total number of individual prey ingested. The third index calculated was the volume index (%V), which represents the volume of a prey item compared with the total volume of ingested prey (Hyslop, 1980). Finally, the geometric index of importance (%GII), which incorporates both %FO and %V, was used to avoid redundancy in the combination of mathematically dependent measures instead of other traditional indices (Tirasin and Jørgensen, 1999). It was computed as follows (Assis, 1996):

$$\%GII_j = \left(\sum_{i=1}^{n} V_i\right)_j / n, \quad (1)$$

where V_i = the value of the ith relative measure of prey quantity for the prey group j (in this case, V_i=*%FO*+*%V*), and

n = the number of the relative measures of prey quantity used in the analysis (in this case, n=2, %FO and %V).

Therefore, in this study, the %GII was calculated as (*%V*+*%FO*)/2. Values for all indices are given as percentages.

Ontogenetic shifts in diet

Before identifying when ontogenetic shifts occur and establishing trophic groups based on different size classes, 10 major prey groups were identified according to taxonomic criteria and, in the case of fish species, habitat type criteria: small plankton; large plankton; Polychaeta; Cephalopoda; crab, lobster, and mantis shrimp species; shrimp species; Peracarida; demersal fish species; pelagic fish species; and benthopelagic fish species.

To investigate variation in a predator's diet according to size, trends in the volume index values of the most representative prey groups, mentioned in the previous paragraph, were plotted against fish length of predators to define the different categories that combine species and size class. We first compared both quantitative and qualitative methods. Results indicate similar outcomes for some species, such as the European hake or blue whiting, and outcomes were less realistic for those species with a small number of samples. Therefore, we decided to use a qualitative method based on a graphic technique that allows easy identification of the size at which the trend in the trophic strategy changed for each species studied. In the quantitative method, the number of size classes was estimated following the Sturges procedure (Scherrer, 1984), and in the qualitative method, the lengths were represented continuously at every millimeter along the x-axis of graphs.

This graphic technique allows qualitative identification of the size at which a trophic shift occurred. We used this size for each gadiform species studied to divide size classes into *large* and *small* categories (sizes varied depending on the species; Table 2). In addition, size at first maturity was plotted with the aim of linking it with the size at which a trophic shift occurred. Sizes at first maturity for all the studied species were based on previously published data from studies in nearby areas (Biagi et al., 1992; Benghali et al., 2014; European Parliament and Council, 2019; Ismen et al., 2019).

Trophic indices to describe feeding strategies

To describe the degree of dietary diversity of a given species, we used niche breadth in accordance with Levins's

Table 2

Dietary indices for each prey group identified in the stomach contents of specimens of 7 species of Gadiformes caught in the western Mediterranean Sea during 2011–2017. The number of trawl tows, sample size, range of total lengths (TLs), niche breadth, depth range, trophic level, and number of prey items also are provided for each of the 12 categories that combine species and size class (small [S] and large [L]). The dietary indices used in analyses include frequency of occurrence (%FO), the number of stomachs that contained a prey group compared with the total number of stomachs examined; the number index (%N), the number of individuals of a prey group compared with the total number of ingested prey; the volume index (%V), the volume of a prey group compared with the total volume of all prey ingested by a predator category; and the geometric index of importance (%GII), which incorporates both %FO and %V. A dash indicates that no consumption of that prey group was recorded for that species. The species studied include the silvery pout (*Gadiculus argenteus*) (GAD), Mediterranean bigeye rockling (*Gaidropsarus biscayensis*) (GAI), Mediterrenean ling (*Molva macrophtalma*) (MOL), European hake (*Merluccius merluccius*) (MER), blue whiting (*Micromesistius poutassou*) (MIC), greater forkbeard (*Phycis blennoides*) (PHY), and poor cod (*Trisopterus minutus*) (TRI).

Information type or prey group	Index	GAD_S	GAD_L	GAI	MOL_S	MOL_L	MER_S	MER_L	MIC_S	MIC_L	PHY_S	PHY_L	TRI
No. of trawl tows		16	29	45	26	20	90	154	25	36	13	56	45
Sample size		44	219	116	107	57	405	849	172	614	75	211	323
Length range (mm)		60–92	93–133	40–180	83–165	166–740	87–149	150–549	89–169	170–377	85–149	150–393	78–272
Niche breadth		0.51	0.39	0.34	0.14	0.30	0.60	0.45	0.24	0.28	0.64	0.17	0.14
Depth range (m)		109–647	131–647	59–634	122–327	86–634	34–342	34–722	76–611	137–722	53–728	176–728	36–352
Trophic level		3.47	3.57	3.93	4.36	4.49	3.95	4.24	3.98	4.21	3.99	3.99	3.94
No. of prey items		9	33	27	8	13	47	65	28	38	25	58	43
Small plankton	%FO	18.8	11.9	17.7	–	–	–	–	–	–	1.5	1.0	–
	%V	14.3	5.4	3.0	–	–	–	–	–	–	0.0	0.0	–
	%N	79.9	60.7	30.2	–	–	–	–	–	–	0.4	0.2	–
	%GII	16.5	8.7	10.3	–	–	–	–	–	–	0.7	0.5	–
Large plankton	%FO	46.9	51.5	7.8	2.6	4.6	40.6	19.4	87.28	46.8	13.0	13.6	9.9
	%V	48.8	47.2	1.6	0.1	1.5	29.0	8.1	59.9	26.5	11.6	4.4	2.7
	%N	10.8	29.6	4.0	2.2	5.5	83.1	69.0	98.1	58.3	13.2	8.4	11.9
	%GII	47.8	49.4	4.7	1.3	3.0	34.8	13.8	73.5	36.7	12.3	9.0	6.3
Polychaeta	%FO	–	0.5	1.0	–	–	–	–	–	0.2	8.7	1.9	1.2
	%V	–	0.3	1.8	–	–	–	–	–	2.8	2.6	0.1	0.4
	%N	–	0.0	0.4	–	–	–	–	–	0.0	2.1	0.6	0.5
	%GII	–	0.4	1.4	–	–	–	–	–	1.5	5.7	1.0	0.8
Cephalopoda	%FO	–	–	–	–	–	2.0	3.3	–	2.7	–	1.9	2.8
	%V	–	–	–	–	–	2.3	3.7	–	1.2	–	1.1	2.8
	%N	–	–	–	–	–	0.3	0.9	–	0.5	–	0.4	1.0
	%GII	–	–	–	–	–	2.1	3.5	–	2.0	–	1.5	2.8

(*Continued on next page*)

Table 2 (*Continued*)

Information type or prey group	Index	GAD_S	GAD_L	GAI	MOL_S	MOL_L	MER_S	MER_L	MIC_S	MIC_L	PHY_S	PHY_L	TRI
Crab, lobster, and mantis shrimp species	%FO	–	0.5	38.2	–	–	1.7	1.6	–	0.5	52.2	54.4	33.4
	%V	–	0.2	51.5	–	–	1.5	1.1	–	0.1	35.4	23.3	19.2
	%N	–	0.0	17.4	–	–	0.3	0.5	–	0.1	22.5	22.1	21.9
	%GII	–	0.3	44.9	–	–	1.6	1.4	–	0.3	43.8	38.9	26.3
Shrimp species	%FO	3.1	9.4	18.6	–	6.8	25.5	25.0	1.7	27.5	18.8	82.5	65.9
	%V	2.1	16.0	12.8	–	4.7	20.3	16.8	2.4	18.9	18.2	63.8	65.5
	%N	0.3	1.1	8.5	–	13.7	6.5	8.6	0.1	10.4	7.5	51.0	51.4
	%GII	2.6	12.7	15.7	–	5.7	22.9	20.9	2.0	23.2	18.5	73.2	65.7
Peracarida	%FO	21.9	18.8	37.3	3.9	4.5	12.4	3.1	1.7	1.8	55.1	22.8	14.2
	%V	24.6	12.0	17.5	0.1	0.4	3.4	1.1	0.3	1.2	32.1	1.4	3.8
	%N	5.0	4.0	36.4	3.3	17.8	4.0	1.2	0.2	0.5	54.3	12.4	9.1
	%GII	23.2	15.4	27.4	2.0	2.5	7.9	2.1	1.0	1.5	43.6	12.1	9.0
Demersal fish species	%FO	–	–	7.8	16.9	31.8	15.8	6.9	3.4	0.2	–	17.5	6.2
	%V	–	–	11.9	17.3	38.0	16.0	4.8	0.6	2.1	–	4.7	3.9
	%N	–	–	3.1	27.2	27.4	2.7	2.0	0.2	0.0	–	4.3	3.2
	%GII	–	–	9.9	17.1	34.9	15.9	5.8	2.0	1.2	–	11.1	5.1
Pelagic fish species	%FO	–	–	–	–	–	10.4	42.1	1.7	0.7	–	–	0.3
	%V	–	–	–	–	–	14.5	44.4	7.1	2.2	–	–	0.7
	%N	–	–	–	–	–	1.6	12.2	0.2	0.2	–	–	0.2
	%GII	–	–	–	–	–	12.5	43.2	4.4	1.5	–	–	0.5
Benthopelagic fish species	%FO	9.4	13.9	–	41.6	43.2	9.7	18.9	15.4	64.8	–	3.9	1.2
	%V	10.2	18.8	–	82.5	55.4	13.0	19.9	29.8	45.0	–	1.3	1.0
	%N	4.0	4.4	–	67.4	35.6	1.5	5.6	1.2	29.9	–	0.8	0.7
	%GII	9.8	16.3	–	62.0	49.3	11.4	19.4	22.6	54.9	–	2.6	1.1

standardized index (Levins, 1968). This index ranges from 0 to 1, with values close to 0 indicating a specialized diet and those close to 1 indicating more generalized feeding habits. This index was computed as follows:

$$B_i = \frac{1}{N-1} \times \frac{1}{\sum_j p_{ij}^2 - 1}, \quad (2)$$

where B_i = Levins's standardized index;
p_{ij} = the proportion of prey j in the diet of predator i; and
N = the total number of prey groups.

The trophic niche overlap among the different studied species was estimated by using the simplified Morisita index (Morisita, 1959), which compares pairs of species with values ranging between 0.00 (no prey overlap) to 1.00 (full prey overlap) as follows:

$$C_{jk} = \frac{2\sum p_{ij} p_{jk}}{\sum p_{ij}^2 + \sum p_{ik}^2}, \quad (3)$$

where C_{ik} = the simplified Morisita index for predators i and k, and
p_{ij} and p_{kj} = the proportions of predators i and k with prey j in their stomachs.

The trophic level (T) was calculated by using the following formula developed by Christensen and Pauly (1992):

$$T = 1 + (\Sigma\, DC_{ij})(NT_j), \quad (4)$$

where DC_{ij} = the proportion of prey j in the diet of the predator i, and
NT_j = the trophic level of prey j.

Trophic levels of prey were determined empirically by using local information or, when this information was not available, by using the modeled area (Cortés, 1999; Ebert and Bizzarro, 2007; Fanelli et al., 2011; Jacobsen and Bennett, 2013; Corrales et al., 2015; for details on the species of prey for which these cited references were sources of local information on trophic levels, see Supplementary Table 2 [online only]). In this study, the trophic level of each of the defined categories based on species and size class was first calculated by weighting its average biomass obtained during the surveys of the MEDITS program conducted in 2011–2017.

Co-occurrence measures

To analyze patterns of species associations related to food resource partitioning, we studied interspecific and intraspecific co-occurrence. Therefore, for the entire study period, we accounted for the abundance of all species and size classes estimated during surveys. The abundance of Mediterranean bigeye rockling was underestimated because of the low selectivity of the gear used to catch this small species. Therefore, this species was not included in the co-occurrence analysis. The Jaccard index (S_{ij}) was used to measure co-occurrence, as an expression of association between species (Jaccard, 1901):

$$S_{ij} = a / (a + b + c), \quad (5)$$

where a = the number of occasions in which both species or size classes are present;
b = the number of occasions in which only one of the species is present; and
c = the number of occasions in which only the other species is present.

This index was calculated as the percentage of occasions that both species or size classes appeared in the same haul. In this study, the only hauls that were considered were those in which at least one of the species or size classes of each pair was present.

Statistical analyses

All data were standardized by using square-root transformation, and a Bray–Curtis similarity matrix was calculated. One-way analyses of similarity were performed to identify significant differences ($P<0.05$) in trophic strategies between pairs of size classes (i.e., intraspecific competition). We used the software PRIMER 6 (PRIMER-e, Quest Research Ltd., Aukland, New Zealand) (Clarke and Gorley, 2006) to estimate global R as a scaled measure of the separation between groups of samples, with values ranging from 0 (no differences) to 1 (completely different) (Clarke, 1993).

Similarity percentage analysis was applied to determine which prey groups contributed most to the dissimilarity in diet composition between such pairs. According to these results, new species-and-size categories were considered for further analyses. Finally, clustering methods and multidimensional scaling were used to analyze prey affinities and to discern feeding strategies that possibly were different between the studied species among size classes. All calculations were done by using PRIMER 6.

Results

Diet composition and ontogenetic variation

Overall, for all studied species as a group, the most common prey groups in terms of %V were large plankton; crab, lobster, and mantis shrimp species; shrimp species; and benthopelagic fish species. Large plankton, represented mainly by euphausiids, was the most common prey (mostly for silvery pout and blue whiting). In the case of decapod species, the red snapping shrimp (*Alpheus glaber*), green shrimp (*Chlorotocus crassicornis*), and angular crab (*Goneplax rhomboides*), all members of Pleocyemata, were the most abundant prey (mostly for Mediterranean bigeye rockling, poor cod, and greater forkbeard). Finally, benthopelagic fish species were primarily represented by blue whiting and myctophids as prey for studied species (mostly for Mediterranean ling and blue whiting) (Table 3). The raw data set

Table 3

Volume index (%V) values for prey groups identified in the stomach contents of specimens of 7 key species of Gadiformes caught in the western Mediterranean Sea during 2011–2017. The %V value for a prey group represents the volume of that prey item compared with the total volume of all prey ingested by specimens of that species. The 7 species are the silvery pout (*Gadiculus argenteus*) (GAD), Mediterranean bigeye rockling (*Gaidropsarus biscayensis*) (GAI), Mediterrenean ling (*Molva macrophtalma*) (MOL), European hake (*Merluccius merluccius*) (MER), blue whiting (*Micromesistius poutassou*) (MIC), greater forkbeard (*Phycis blennoides*) (PHY), and poor cod (*Trisopterus minutus*) (TRI). A dash indicates that no consumption of that prey group was recorded for that species. An asterisk indicates the prey group with the highest %V value for each species. Information on niche breadth and the number of prey items is also reported.

	%V						
Information type	GAD	GAI	MOL	MER	MIC	PHY	TRI
Niche breadth	0.34	0.34	0.17	0.38	0.26	0.16	0.14
No. of prey items	33	27	15	74	49	60	43
Prey group							
Small plankton	6.2	3.0	–	0.0	–	0.0	–
Large plankton	51.6*	1.6	0.9	12.0	40.3*	4.9	2.7
Polychaeta	0.3	1.8	–	–	1.9	0.4	0.4
Cephalopoda	–	–	–	3.7	0.8	1.0	2.8
Crab, lobster, and mantis shrimp species	0.1	51.5*	–	0.8	0.1	24.4	19.2
Shrimp species	12.4	12.8	2.5	14.4	13.2	60.6*	65.5*
Peracarida	11.1	17.5	0.3	1.0	0.9	2.8	3.8
Demersal fish species	–	11.9	22.6	6.6	1.7	4.3	3.9
Pelagic fish species	–	–	–	40.8*	3.6	–	0.7
Benthopelagic fish species	18.3	–	73.8*	20.6	37.4	1.6	1.0

provided in Supplementary Table 1 (online only) documents in detail the different prey items found in stomachs and identified to the lowest taxonomic level in this study.

Regarding the ontogenetic variation in diet, for each of the studied species, the graph indicates trends in trophic strategies for 2 prey groups that were the opposite of the other, and this observation of different trends enabled us to establish a cutoff between the 2 size classes: the size at which a trophic shift occurred (Fig. 2). Only in the case of the silvery pout did the selected cutoff between size classes seem to be related to size at first maturity. For the Mediterranean bigeye rockling, no data are available on size at first maturity in the study area.

The results obtained for species and size classes indicate that silvery pout fed mainly on large plankton (%GII=51.2%, %V=51.6%, %FO=50.9%), with *Euphausia krohnii* as the most predominant prey species. The diet of Mediterranean bigeye rockling was based primarily on crab, lobster, and mantis shrimp species (%GII=44.9%, %V=51.5%, %FO=38.2%) and species of Peracarida (%GII=27.4%, %V=17.5%, %FO=37.3%), represented mainly by *Calocaris macandreae* and *Lophogaster typicus*, respectively. Benthopelagic fish species (%GII=57.0%, %V=73.8%, %FO=40.2%) composed the major prey group for Mediterranean ling, for which the most commonly consumed prey was another species of Gadiformes, the silvery pout. Pelagic fish species (%GII=29.0%, %V=40.8%, %FO=17.2%) and large plankton (%GII=15.1%, %V=12.0%, %FO=18.3%) were the main prey groups for European hake, with European anchovy (*Engraulis encrasicolus*) and euphausiids being the most important of the consumed prey, respectively. Blue whiting fed mainly on large plankton (%GII=39.3%, %V=40.3%, %FO=38.3%) and benthopelagic fish species (%GII=36.5%, %V=37.4%, %FO=35.6%), of which euphausiids and the myctophid horned lanternfish (*Ceratoscopelus maderensis*) were the main prey, respectively. Similar prey items were also found in the diet of both greater forkbeard and poor cod: prey species were primarily shrimp species (%GII=61.8%, %V=60.6%, and %FO=62.9% and %GII=65.7%, %V=65.5%, and %FO=65.6%, respectively), with red snapping shrimp as the most-represented prey.

Results of the one-way analyses of similarity indicate that there were significant differences in trophic composition between size classes ($P \leq 0.05$) for all species studied except for the Mediterranean bigeye rockling and poor cod (Suppl. Table 3) (online only). Moreover, results of the similarity percentage analysis for the 5 species that had ontogenetic shifts identify the contribution of each prey item to the mean Bray–Curtis dissimilarity for each species. The average dissimilarity between size classes ranged from 41% for Mediterranean ling to 75% for European hake. These differences were a result of the distinct contribution of major prey groups to the stomach contents in specimens examined for each species (Suppl. Table 4) (online only). The major prey groups contributing the most to the ontogenetic shifts in the diet of silvery pout were large plankton and Peracarida, and for Mediterranean ling, the major prey groups were teleosts, such as demersal and benthopelagic fish species. Pelagic fish, large plankton, and shrimp species

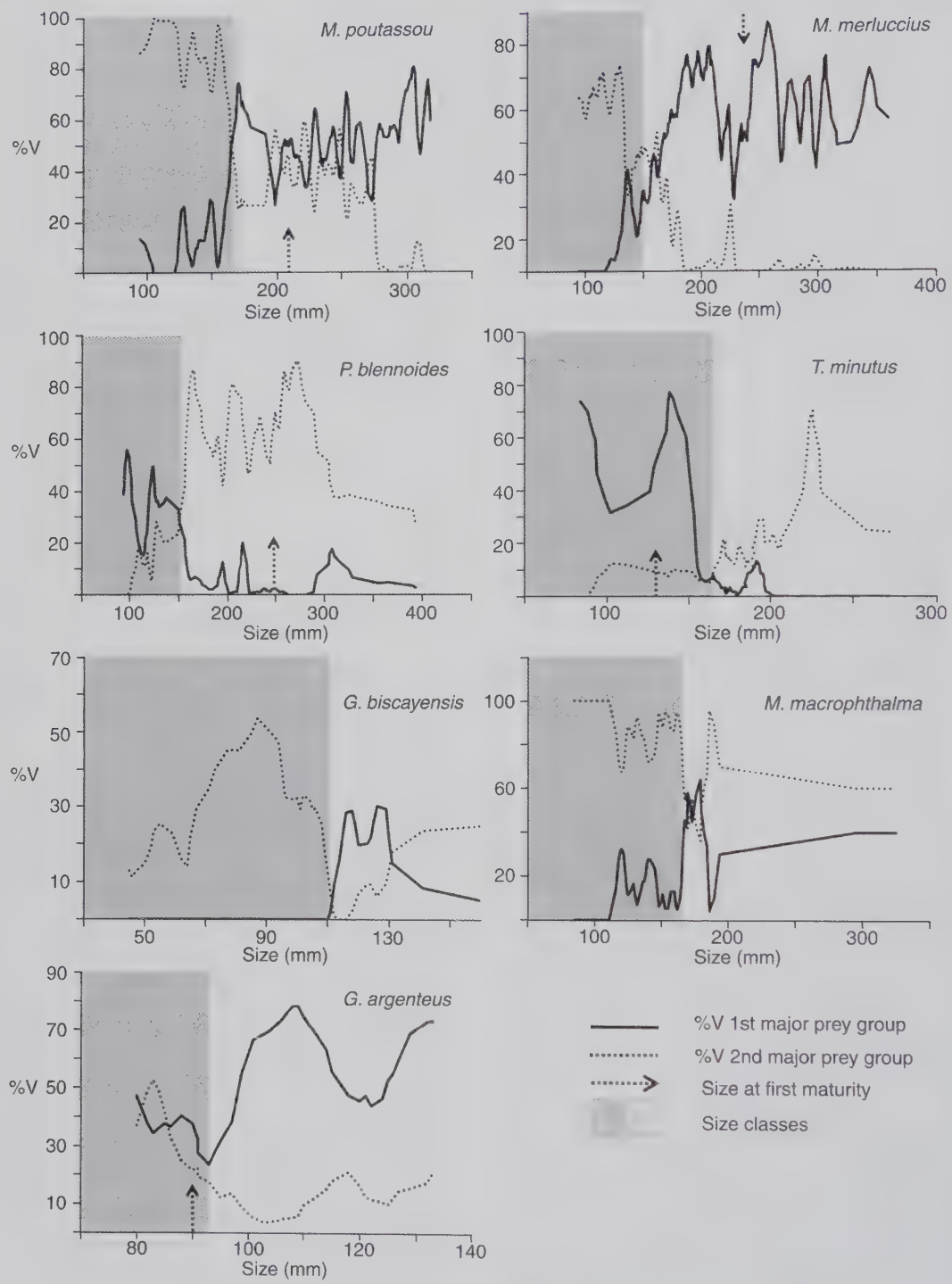

Figure 2

Trends in volume index (%V) values for the first and second major prey groups in relation to sizes of specimens of 7 species of Gadiformes caught in the western Mediterranean Sea during 2011–2017. These graphs were used in a qualitative method to identify the size at which the trophic strategy changed for each species studied. This size is considered the cutoff between small (gray shaded area) and large size classes for each species. Sizes are given as total lengths. Arrows indicate the size at first maturity for each species, except for the Mediterranean bigeye rockling (*Gaidropsarus biscayensis*) and Mediterrenean ling (*Molva macrophtalma*) because this information was not available for these species. The other species studied include the blue whiting (*Micromesistius poutassou*), European hake (*Merluccius merluccius*), greater forkbeard (*Phycis blennoides*), poor cod (*Trisopterus minutus*), and silvery pout (*Gadiculus argenteus*).

accounted for more than 60% of the diet of European hake. Species of large plankton and benthopelagic fish species contributed most to the diet of blue whiting (accounting for approximately 34% and 32% of the diet of this species, respectively); greater forkbeard fed mainly on shrimp species and species of Peracarida (Suppl. Table 4) (online only).

Trophic ecology

The trophic niche breadth index (B_i) was highest for European hake, Mediterrean bigeye rockling, and silvery pout (Table 3). Conversely, poor cod had the lowest B_i value, with a strong preference for red snapping shrimp (%V=44.1%), despite the high number of prey items (52) identified in its diet.

Niche breadth across the 12 categories that are based on species and size class was lowest (B_i=0.136) for the small size class of Mediterranean ling; whereas, the small size class of greater forkbeard ranked the highest (B_i=0.636).

Simplified Morisita index values ranged from 0.00 (pair of the small size class of Mediterranean ling and –the small size class of greater forkbeard) to 1.00 (pair of the large size class of greater forkbeard and poor cod) (Table 4). Overall, niche overlap was highest between the small size class of greater forkbeard and poor cod, whose diet had a high proportion of shrimp species, represented principally by red snapping shrimp. The lowest values were found between the small size class of Mediterranean ling and poor cod as well as greater forkbeard.

The lowest and highest trophic levels were inferred for silvery pout (trophic level=3.51) and the large size class of Mediterranean ling (trophic level=4.49), respectively. Within this range, only Mediterranean ling and the large size classes of European hake and blue whiting were determined to be at a trophic level ≥4, representative of top predators (Table 2). For all species, with the exception of the greater forkbeard, which had no changes in trophic level with size, the large size classes were at a higher trophic level. The greatest increases in trophic level linked to an ontogenetic shift occurred in European hake (from 3.95 to 4.24) and blue whiting (from 3.98 to 4.21).

Feeding strategies

Four groups of predators were identified on the basis of different feeding strategies (Fig. 3). The first group consisted of species with strong preferences for decapods, such as the Mediterranean bigeye rockling, poor cod, and greater forkbeard. The red snapping shrimp was the dominant prey species for the large size class of greater forkbeard (%V=35.3%) and for poor cod (%V=44.1%), and *Calocaris macandreae* (%V=32.0%) and angular crab (%V=15.6%) were the main prey species for Mediterranean bigeye rockling and the small size class of greater forkbeard. The second group was composed of both size classes of Mediterranean ling, with silvery pout as the dominant prey (with %V values of 52.4% and 24.3% for the small and large size classes, respectively).

The third group identified was composed of both size classes of silvery pout, which had a high preference for large plankton, although in the case of small silvery pout, species of Peracarida were also consumed. In both size classes, euphausiids were the most common prey item (with %V values of 46.8% and 36.8% for the small and large size classes, respectively).

Table 4

Simplified Morisita index values, which indicate trophic niche overlap between pairs of 12 categories of gadiform species for which stomach contents from specimens caught in the western Mediterranean Sea from 2011 through 2017 were examined. Categories combine species and size class (small [S] and large [L]; length ranges for size classes are provided in Table 2). Asterisks indicate extreme index values, defined as those ≥0.9 and <0.1. The species studied were the silvery pout (*Gadiculus argenteus*) (GAD), Mediterranean bigeye rockling (*Gaidropsarus biscayensis*) (GAI), Mediterrenean ling (*Molva macrophtalma*) (MOL), European hake (*Merluccius merluccius*) (MER), blue whiting (*Micromesistius poutassou*) (MIC), greater forkbeard (*Phycis blennoides*) (PHY), and poor cod (*Trisopterus minutus*) (TRI).

Category	GAD_S	GAD_L	GAI	MOL_S	MOL_L	MER_S	MER_L	MIC_S	MIC_L	PHY_S	PHY_L	TRI
GAD_S	1.00											
GAD_L	0.92*	1.00										
GAI	0.18	0.17	1.00									
MOL_S	0.16	0.31	0.04*	1.00								
MOL_L	0.17	0.31	0.13	0.90*	1.00							
MER_S	0.64	0.80	0.24	0.30	0.46	1.00						
MER_L	0.22	0.36	0.12	0.35	0.38	0.67	1.00					
MIC_S	0.83	0.91*	0.04*	0.42	0.39	0.71	0.39	1.00				
MIC_L	0.57	0.79	0.11	0.73	0.71	0.72	0.53	0.78	1.00			
PHY_S	0.46	0.43	0.88	0.00*	0.03*	0.37	0.17	0.21	0.24	1.00		
PHY_L	0.10	0.33	0.53	0.03*	0.12	0.47	0.32	0.10	0.36	0.56	1.00	
TRI	0.09*	0.32	0.49	0.03*	0.11	0.47	0.33	0.08*	0.35	0.54	1.00*	1.00

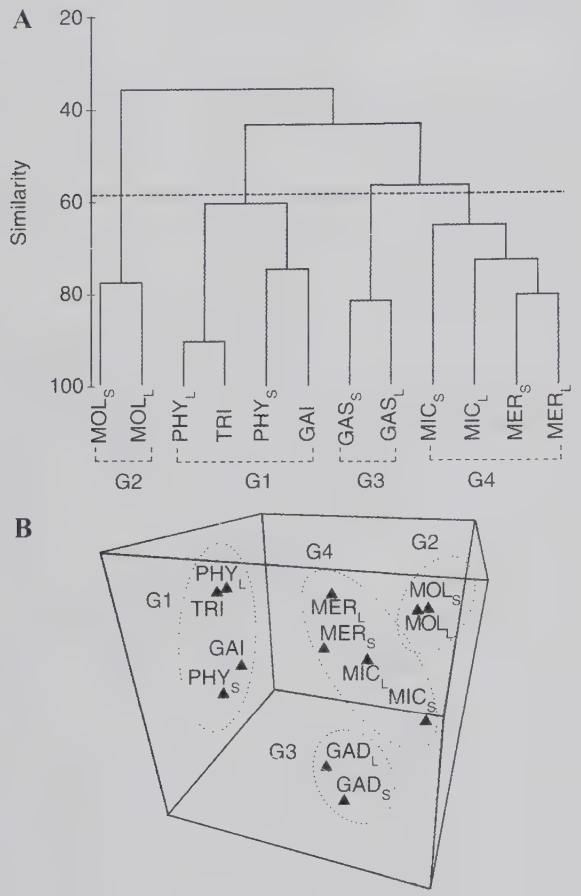

Figure 3

Multidimensional scaling ordination of stomach contents of specimens of 7 species of Gadiformes caught in the western Mediterranean Sea from 2011 through 2017. In the (**A**) 2-dimensional and (**B**) 3-dimensional plots, dashed lines indicate or dotted lines surround predator groups (G1, G2, G3, and G4) identified by using cluster analysis based on feeding strategies. Results are given for 12 categories that combine species and size class (small [S] and large [L]; length ranges for size classes are provided in Table 2). The horizontal dashed line in panel A indicates the threshold similarity for group selection. The species studied include the Mediterrenean ling (*Molva macrophtalma*) (MOL), greater forkbeard (*Phycis blennoides*) (PHY), poor cod (*Trisopterus minutus*) (TRI), Mediterranean bigeye rockling (*Gaidropsarus biscayensis*) (GAI), silvery pout (*Gadiculus argenteus*) (GAD), blue whiting (*Micromesistius poutassou*) (MIC), and European hake (*Merluccius merluccius*) (MER).

The last group was represented by both size classes of blue whiting and European hake. The small size classes of both of these species preyed mostly on large plankton, with euphausiids as the most prevalent prey (with %V values of 51.3% and 24.3%, respectively). Benthopelagic fish species, namely the horned lanternfish (%V=19.3%) and the jewel lanternfish (*Lampanyctus crocodilus*) (%V=17.9%), were the main prey for the large size class of blue whiting. Pelagic fish species, such as the European anchovy (*Engraulis encrasicolus*) (%V=30.3%) and European pilchard (*Sardina pilchardus*) (%V=9.9%), were the species most widely consumed by the large size class of European hake.

Co-occurrence and trophic overlap

The highest percentages of co-occurrence were found for the associations of European hake with poor cod (75.8%) and blue whiting with greater forkbeard (64.1%) (Fig. 4). Conversely, the lowest values of co-occurrence were observed for Mediterranean ling with poor cod (11.3%) and European hake with Mediterranean ling (14.1%). These results, together with analysis of trophic levels, indicate a high niche overlap between silvery pout and blue whiting and a low degree of overlap between Mediterranean ling and poor cod.

All species had an intraspecific trophic overlap greater than 0.50. Greater forkbeard had the lowest value (0.56), and silvery pout had the highest value (0.92). On the other hand, low co-occurrence was found for both blue whiting and Mediterranean ling (0.16 and 0.20, respectively), and high values of co-occurrence were found for European hake, greater forkbeard, and silvery pout (0.77, 0.69, and 0.68, respectively).

Discussion

Our comprehensive study of feeding habits and trophic relationships among 7 fish species of the order Gadiformes that are important to fisheries in the western Mediterranean Sea explored ecological patterns such as those of ontogenetic variation in diet or trophic and spatial segregation of species. The results of this work can inform efforts to improve management of resource partitioning within and among these species in a broad geographic area (i.e., the entire GSA-06).

Our data indicate that the species studied are structured into 4 major guilds based on their feeding habits. The first group comprises the Mediterranean bigeye rockling, poor cod, and greater forkbeard. These species occupy medium-high positions within the food web. Their diets have previously been reported to consist of decapods and other small crustaceans, for example, for poor cod or greater forkbeard in the Catalan Sea (Macpherson, 1978b), in the Gulf of Valencia (Morte et al., 2001, 2002), and in the Adriatic Sea (Dulčić and Dulčić, 2004). However, for Mediterranean bigeye rockling, our results differ from those of Macpherson (1978b), who identified *Eusergestes arcticus* and northern krill (*Meganyctiphanes norvegica*) as the predominant prey. Our results indicate that *Calocaris macandrae* was the primary prey species of Mediterranean bigeye rockling, and it is worth noting that this species was also found to be cannibalistic. These differences may be related to the 38-year gap between the 2 studies or are possibly a result of the fact that our sampling did not explore seasonal dietary

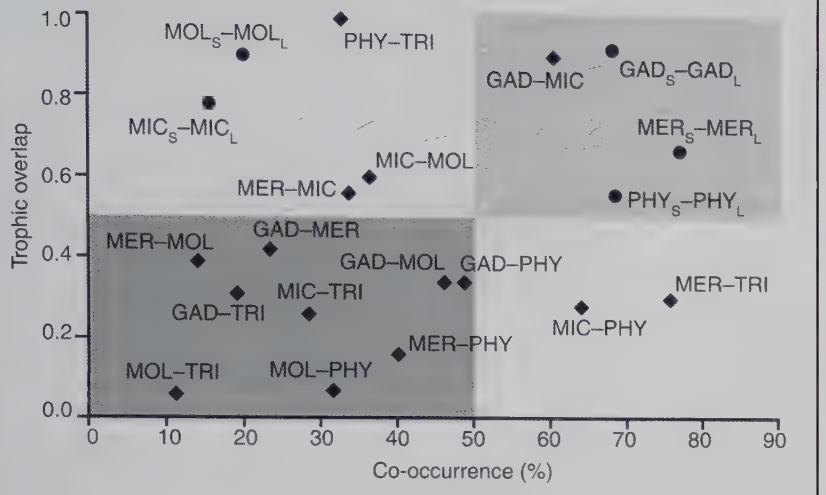

Figure 4

Level of trophic overlap and percentage of co-occurrence for pairs of 12 categories of 7 gadiform species for which stomach contents from specimens caught in the western Mediterranean Sea during 2011–2017 were examined. The 12 categories combine species and size class (small [S] and large [L]; length ranges for size classes are provided in Table 2). Diamonds and circles indicate interspecific and intraspecific interactions, respectively. Pairs in the dark gray area had low niche overlap, and pairs in the light gray area had high niche overlap. The species studied include the silvery pout (*Gadiculus argenteus*) (GAD), Mediterranean bigeye rockling (*Gaidropsarus biscayensis*) (GAI), European hake (*Merluccius merluccius*) (MER), blue whiting (*Micromesistius poutassou*) (MIC), Mediterrenean ling (*Molva macrophtalma*) (MOL), greater forkbeard (*Phycis blennoides*) (PHY), and poor cod (*Trisopterus minutus*) (TRI).

changes; we restricted our study to the spring, when the MEDITS is carried out. This high degree of predation on decapod crustaceans by greater forkbeard and poor cod is indicative of a narrow trophic niche breadth compared with that of the Mediterranean bigeye rockling, which was found to have more generalist feeding habits. Moreover, and in agreement with results reported by Morte et al. (2002), an ontogenetic shift occurred in the diet of greater forkbeard in our study, but our findings differ from those of Morte et al. (2001) for poor cod in that no ontogenetic dietary shift was found.

The second group consists of both size classes of Mediterranean ling, and this species had the highest trophic levels among the 7 species studied. The diet of this species is primarily composed of benthopelagic and demersal fishes, such as the silvery pout and poor cod. This evidence indicates that the Mediterranean ling occupies a narrow trophic niche, a finding that is in agreement with the results previously reported by Macpherson (1981) for the same study area.

A third trophically distinct group is composed of both size classes of silvery pout, which is the only species primarily exploiting resources at the base of the food web, playing an important role in the energy flow from the lowest levels to the top of the food web. The majority of the diet of the silvery pout consists of a variety of small crustaceans, such as euphausiids and shrimp species, confirming the feeding habit observations previously reported by Macpherson (1978a) for silvery pout in the western Mediterranean. Therefore, these results indicate that the silvery pout consumes a broad range of prey items, a diet characteristic of a generalist feeder. We also found ontogenetic variation for this species, with it becoming a more specialized predator as its trophic level increased. This result contrasts with the findings reported by Macpherson (1978a), who observed no clear link between diet and size for the silvery pout.

The last of the 4 feeding guilds we identified is represented by both size classes of European hake and blue whiting, which occupy a position high in the food web. As has been observed for Mediterranean ling, both the European hake and blue whiting seem to be primarily piscivorous, although their diets in addition include shrimp species (*Pasiphaea* spp.) and large plankton, particularly euphausiids (e.g., northern krill). For European hake, our findings are consistent with those of other studies from the western Mediterranean Sea (Bozzano et al., 1997; Cartes et al., 2009). However, slight differences were found when comparing the diets of fish sampled in waters of the North Atlantic Ocean and the eastern Mediterranean Sea, where crustaceans were relatively less important and mackerels play the role reserved for sardines in our study area (Guichet, 1995; Velasco and Olaso, 1998; Philips, 2012). Regarding blue whiting, our results agree with those reported by Olaso and Rodríguez-Marín[6], Velasco et al.[7], and Gutiérrez-Zabala et al.[8] for this species in the Cantabrian Sea off the northern coast of Spain, but they contrast with the findings of Preciado et al. (2002) for blue whiting in the south of Galicia in the northwest of Spain and of Torres et al. (2013) for this species in the Gulf of Cadiz off the southern coasts of Portugal and

[6] Olaso, I., and E. Rodríguez-Marín. 1995. Alimentación de veinte especies de peces demersales pertenecientes a la división VIIIc del ICES. Otoño 1991. Inst. Esp. Oceanogr., Inf. Téc. 157, 56 p. [In Spanish.] [Available from Inst. Esp. Oceanogr., Calle Corazón María 8, 28002 Madrid, Spain.]

[7] Velasco, F., I. Olaso, and F. de la Gándara. 1996. Alimentación de veintidós especies de peces demersales de la división VIIIc del ICES. Otoños de 1992 y 1993. Inst. Esp. Oceanogr., Inf. Téc. 164, 62 p. [In Spanish.] [Available from Inst. Esp. Oceanogr., Calle Corazón María 8, 28002 Madrid, Spain.]

[8] Gutiérrez-Zabala, J. L., F. Velasco, and I. Olaso. 2001. Alimentación de veintiuna especies de peces demersales de la división VIIIc del CIEM. Otoños de 1994 y 1995. Inst. Esp. Oceanogr., Datos Resúm. 16, 61 p. [In Spanish.] [Available from Inst. Esp. Oceanogr., Calle Corazón María 8, 28002 Madrid, Spain.]

Spain. In these latter 2 papers, a higher dependency on crustaceans, particularly euphausiids, was reported.

As far as differences in diet compositions between the European hake and blue whiting in our study are concerned, the European hake was found to prey mainly on pelagic fish species (i.e., sardines and European anchovy), as well as on benthopelagic (e.g., blue whiting) and demersal (e.g., poor cod) fish species, and the blue whiting was found to feed mainly on benthopelagic fish species (e.g., the horned lanternfish and jewel lanternfish). This ability of European hake to prey on different groups resulted in the European hake occupying the broadest trophic niche of all the species studied. Hence, in relation to ontogenetic shifts in diet, both species are characterized by a decreasing consumption of euphausiids and an increasing proportion of fish species with size. All of these results agree with those reported by Bozzano et al. (1997) for work in the Gulf of Lion and by Cartes et al. (2009) for a study in the Balearic Islands, a small archipelago off the northeastern coast of Spain.

Results for examination of niche breadth indicate a pattern that relates size class to niche breadth. The small size classes had a broader trophic niche than that of the large size classes, for all species studied except the Mediterranean ling, with ontogenetic growth leading to greater specialization in these species. In contrast, the Mediterranean ling is a specialist piscivorous species, the larger size of the specimens of which, in comparison to the size of individuals of other species studied, allowed it to have access to a greater number of potential prey in its diet. Therefore, its trophic niche increased with the ontogenetic development of specimens. Our findings for the Mediterranean ling indicate a relationship between size class and trophic level, with the trophic level being lower in the small size classes and increasing after the ontogenetic shift. This difference in the trophic level between size classes was greater for those species located higher in the trophic web (e.g., the European hake, blue whiting, and Mediterranean ling).

We found that the studied species of Gadiformes exploit food resources at different trophic levels of the food web, indicating ontogenetic shifts in diet and resource partitioning. The silvery pout, for example, plays a role closer to that of a primary consumer, with the specimens that composed the small size class being those with the lowest trophic level. Fish species that play a similar role within the food web include species of *Gobius*, *Mullus*, *Symphodus*, and *Diplodus*, according to Karachle and Stergiou (2017). An intermediate trophic position is occupied by the poor cod, greater forkbeard, Mediterranean bigeye rockling, and the small size classes of blue whiting and European hake, as well as of the blackmouth catshark (*Galeus melastomus*) and species of *Serranus*, *Pagellus*, and *Chelidonichthys* (Karachle and Stergiou, 2017). Large specimens of European hake and blue whiting have a position in the upper part of the food web, along with species of *Raja* and *Scorpaena* (Karachle and Stergiou, 2017). Finally, the Mediterranean ling, primarily a piscivorous species, is in the highest trophic level, similar to other piscivorous species such as the common dentex (*Dentex dentex*), greater amberjack (*Seriola dumerili*), bluefin tuna (*Thunnus thynnus*), and John dory (*Zeus faber*) (Karachle and Stergiou, 2017).

If an ecosystem is structured in accordance with the hypothesis of niche complementarity (Ebeling and Hixon, 1991), on the basis of the distribution and diet of the species involved, the structure should have consistently low niche overlap such that the coexistence of similar species occurs because of differences in resource use (Pianka, 1973; Schoener, 1974). We investigated the dietary overlap of coexisting species for which a partitioning of trophic resources was found among species and size classes. This finding indicates that the 7 species studied occupy different trophic positions, ranging from a generalized feeding behavior to specialized piscivorous habits. These results might complement those reported by Macpherson (1978a) and Morte et al. (2001, 2002), who investigated changes with season and depth, respectively, in the diets of blue whiting, silvery pout, poor cod, and greater forkbeard. They related availability of prey to diet depending on the season. Moreover, differences in the patterns of species distribution reduce niche overlap even further.

Only 3 pairs of species had a co-occurrence greater than 50%, with the pairs of blue whiting and greater forkbeard and of European hake and poor cod having by far the highest values of spatial overlap but correspondingly low values of trophic overlap. This distributional and trophic strategy minimizes interspecific competition. Cases in point are the Mediterranean ling and blue whiting, which may avoid intraspecific competition through this mechanism. Only the species pair of silvery pout and blue whiting had high values for both indices, indicating strong competition for resources between these 2 species.

For 5 of the 7 species, excluding the Mediterranean bigeye rockling and poor cod, ontogenetic shifts in diet were found, shifts that allowed them to occupy several niches or subniches simultaneously (Deselle et al., 1978; Keast, 1978). These ontogenetic shifts were associated with an increase in inferred trophic levels for all the species, contributing to increasing segregation between size classes (Pauly et al., 2001). Although the size classes described in this study are related to shifts in trophic strategies, intraspecific trophic overlap was observed for those 5 species that had ontogenetic shifts in their diets, and the intraspecific overlap was generally higher than the interspecific overlap. This result is in line with that of Bergstad (1991), who found that the effects of competitive interactions are more likely to occur between size classes of the same species than between different species.

Of those 5 species, the greater forkbeard, European hake, and silvery pout had high co-occurrence that involved strong competition for food resources, resulting in high intraspecific trophic overlap. An important aspect of this kind of competition is cannibalism, which was found in European hake, and this result is in agreement with findings reported by Macpherson (1979), Bozzano (1997),

and Cartes et al. (2009) for studies in the western Mediterranean Sea, as well as in nearby regions of the Atlantic Ocean (Torres et al., 2013; López-López et al., 2015).

Acknowledgments

The authors express their gratitude to all the people who worked on surveys of the MEDITS program. Data collection was co-funded by the European Union (EU) through the European Maritime and Fisheries Fund within the national program for the collection, management, and use of data in the fisheries sector and support for scientific advice regarding the EU Common Fisheries Policy.

Literature cited

Assis, C. A.
1996. A generalized index for stomach contents analysis in fish. Sci. Mar. 60:385–389.

Benghali, S. M., S. Mouffok, A. Kherraz, and Z. Boutiba.
2014. Reproductive biology and growth of greater forkbeard *Phycis blennoides* (Brünnich, 1768) in Western Algerian coasts (Osteichthyes, Gadidae). J. Biol. Environ. Sci. 4(6):389–398.

Bergstad, O. A.
1991. Distribution and trophic ecology of some gadoid fish of the Norwegian deep. Sarsia 75:315–325.

Bertrand, J. A., L. Gil de Sola, C. Papaconstantinou, G. Relini, and A. Souplet.
2002. The general specifications of the MEDITS surveys. Sci. Mar. 66(S2):9–17.

Biagi, F., S. de Ranieri, and C. Viva.
1992. Recruitment, length at first maturity and feeding of poor-cod, *Trisopterus minutus capelanus*, in the northern Tyrrhenian Sea. Boll. Zool. 59(1):87–93.

Bozzano, A., L. Recasens, and P. Sartor.
1997. Diet of the European hake *Merluccius merluccius* (Pisces: Merluciidae) in the Western Mediterranean (Gulf of Lions). Sci. Mar. 61:1–8.

Cardinale, M., G.-C. Osio, and A. Charef (eds.).
2012. Report of the scientific, technical and economic committee for fisheries on assessment of Mediterranean Sea stocks—part 1 (STECF 12–19), 494 p. JRC Sci. Policy Rep. JRC 76735. Publ. Off. Eur. Union, Luxembourg, Luxembourg. [Available from website.]
2013. Report of the scientific, technical and economic committee for fisheries (STECF) 2012 assessment of Mediterranean Sea stocks—part 2 (STECF 13–05), 618 p. JRC Sci. Policy Rep. JRC 81592. Publ. Off. Eur. Union, Luxembourg, Luxembourg. [Available from website.]

Cartes, J. E., M. Hidalgo, V. Papiol, E. Massutí, and J. Moranta.
2009. Changes in the diet and feeding of the hake *Merluccius merluccius* in the shelf-break of Balearic Islands: influence of the mesopelagic-boundary community. Deep-Sea Res., I 56:344–365.

Castro, J. J., and V. Hernández-García.
1995. Ontogenetic changes in mouth structures, foraging behaviour and habitat use of *Scomber japonicus* and *Illex coindetii*. Sci. Mar. 59:347–355.

Christensen, V.
1996. Managing fisheries involving predator and prey species. Rev. Fish Biol. Fish. 6:417–442.

Christensen, V., and D. Pauly.
1992. ECOPATH II—a software for balancing steady-state ecosystem models and calculating network characteristics. Ecol. Model. 61:169–185.

Christensen, V., and C. J. Walters.
2004. Ecopath with Ecosim: methods, capabilities and limitations. Ecol. Model. 172:109–139.

Clarke, K. R.
1993. Non-parametric multivariate analyses of changes in community structure. Aust. J. Ecol. 18:117–143.

Clarke, K. R., and R. N. Gorley.
2006. PRIMER v6: user manual/tutorial, 190 p. PRIMER-E, Plymouth, UK.

Cochran, J. K., H. J. Bokuniewicz, and P. L. Yager (eds.).
2019. Encyclopedia of ocean sciences, 3rd ed., 4306 p. Academic Press, London.

Cohen, D. M., T. Inada, T. Iwamoto, and N. Scialabba.
1990. FAO species catalogue. Vol. 10. Gadiform fishes of the world (Order Gadiformes). An annotated and illustrated catalogue of cods, hakes, grenadiers and other gadiform fishes known to date. FAO Fish. Synop. 125, 442 p. FAO, Rome.

Coll, M., I. Palomera, S. Tudela, and M. Dowd.
2008. Food-web dynamics in the South Catalan Sea ecosystem (NW Mediterranean) for 1978–2003. Ecol. Model. 217:95–116.

Coll, M., C. Piroddi, J. Steenbeek, K. Kaschner, F. B. R. Lasram, J. Aguzzi, E. Ballesteros, C. N. Bianchi, J. Corbera, T. Dailianis, et al.
2010. The biodiversity of the Mediterranean Sea: estimates, patterns, and threats. PLoS ONE 5(8):e11842.

Coll, M., M. Carreras, M. J. Cornax, E. Massutí, E. Morote, X. Pastor, A. Quetglas, R. Sáez, L. Silva, I. Sobrino, et al.
2014. Closer to reality: reconstructing total removals in mixed fisheries from Southern Europe. Fish. Res. 154:179–194.

Colloca, F., M. Cardinale, F. Maynou, M. Giannoulaki, G. Scarcella, K. Jenko, J. M. Bellido, and F. Fiorentino.
2013. Rebuilding Mediterranean fisheries: a new paradigm for ecological sustainability. Fish Fish. 14:89–109.

Corrales, X., M. Coll, S. Tecchio, J. M. Bellido, A. M. Fernández, and I. Palomera.
2015. Ecosystem structure and fishing impacts in the northwestern Mediterranean Sea using a food web model within a comparative approach. J. Mar. Syst. 148:183–199.

Cortés, E.
1999. Standardized diet compositions and trophic levels of sharks. ICES J. Mar. Sci. 56:707–717.

Deselle, W. J., M. A. Poirrier, J. S. Rogers, and R. C. Cashner.
1978. A discriminant functions analysis of sunfish (*Lepomis*) food habits and feeding niche segregation in the Lake Pontchartrain, Louisiana estuary. Trans. Am. Fish. Soc. 107:713–719.

Dulčić, J., and Z. Dulčić.
2004. Feeding habits of the Mediterranean poor cod *Trisopterus minutus capelanus* (Lacépède) (Pisces: Gadidae) from the eastern central Adriatic. Ann. Ser. Hist. Nat. 14:189–196.

Ebeling, A. W., and M. A. Hixon.
1991. Tropical and temperate reef fishes comparison of community structures. *In* The ecology of fishes on coral reefs (P. F. Sale, ed.), p. 509–563. Academic Press, San Diego, CA.

Ebert, D. A., and J. J. Bizzarro.
2007. Standardized diet compositions and trophic levels of skates (Chondrichthyes: Rajiformes: Rajoidei). Environ. Biol. Fishes 80:221–237.

Estrada, M.
1996. Primary production in the northwestern Mediterranean. Sci. Mar. 60(Suppl. 2):55–64.
European Parliament and Council.
2019. Consolidated text: Regulation (EU) No. 1380/2013 of the European Parliament and of the Council of 11 December 2013 on the Common Fisheries Policy, amending Council Regulations (EC) No. 1954/2003 and (EC) No. 1224/2009 and repealing Council Regulations (EC) No. 2371/2002 and (EC) No. 639/2004 and Council Decision 2004/585/EC, 52 p. Publ. Off. Eur. Union, Luxembourg, Luxembourg. [Available from website.]
Fanelli, E., J. E. Cartes, F. Badalamenti, P. Rumolo, and M. Sprovieri.
2009. Trophodynamics of suprabenthic fauna on coastal muddy bottoms of the southern Tyrrhenian Sea (Western Mediterranean). J. Sea Res. 61:174–187.
Fanelli, E., J. E. Cartes, and V. Papiol.
2011. Food web structure of deep-sea macrozooplankton and micronekton off the Catalan slope: insight from stable isotopes. J. Mar. Syst. 87:79–89.
Fanelli, E., J. E. Cartes, V. Papiol, and C. López-Pérez.
2013. Environmental drivers of megafaunal assemblage composition and biomass distribution over mainland and insular slopes of the Balearic Basin (Western Mediterranean). Deep-Sea Res., I 78:79–94.
FAO.
2018. The state of Mediterranean and Black Sea fisheries 2018, 172 p. Gen. Fish. Comm. Mediterr., Rome. [Available from website.]
García, S. M., A. Zerbi, C. Aliaume, T. Do Chi, and G. Lasserre.
2003. The ecosystem approach to fisheries: issues, terminology, principles, institutional foundations, implementation and outlook. FAO Fish. Tech. Pap. 443, 71 p. FAO, Rome. [Available from website.]
García-Rodríguez, M., P. Abelló, A. Fernández, and A. Esteban.
2011. Demersal assemblages on the soft bottoms off the Catalan-Levante coast of the Spanish Mediterranean. J. Mar. Sci. 2011:16.
García-Rodríguez, E., M. Vivas, M. A. Torres, A. Esteban, J. M. Bellido.
2020. Revealing environmental forcing in the different trophic guilds of fish communities off the Western Mediterranean Sea. J. Sea Res. 166, 101958.
Gascuel, D.
2005. The trophic-level based model: a theoretical approach of fishing effects on marine ecosystems. Ecol. Model. 189:315–332.
Guichet, R.
1995. The diet of European hake (*Merluccius merluccius*) in the northern part of the Bay of Biscay. ICES J. Mar. Sci. 52:21–31.
Hyslop, E. J.
1980. Stomach contents analysis—a review of methods and their application. J. Fish Biol. 17:411–429.
Ismen, A., C. C. Yigin, M. A. Ihsanoglu, and M. I. Oz.
2019. Age, growth and reproduction of silvery pout (*Gadiculus argenteus* Guichenot, 1850) in the Saros Bay (Northeastern Aegean Sea). Thalassas 35:599–605.
Jaccard, P.
1901. Distribution de la flore alpine dans le Bassin des Drouces et dans quelques régions voisines. Bull. Soc. Vaud. Sci. Nat. 37:241–272. [In French.]
Jacobsen, I. P., and M. B. Bennett.
2013. A comparative analysis of feeding and trophic level ecology in stingrays (Rajiformes; Myliobatoidei) and electric rays (Rajiformes: Torpedinoidei). PLoS ONE 8(8):e71348.
Juanes, F., J. A. Buckel, and F. S. Scharf.
2002. Feeding ecology of piscivorous fishes. *In* Handbook of fish biology and fisheries, vol. 1 (P. J.B. Hart and J. D. Reynolds, eds.), p. 267–283. Blackwell Science, Malden, MA.
Karachle, P. K., and K. I. Stergiou.
2017. An update on the feeding habits of fish in the Mediterranean Sea (2002–2015). Mediterr. Mar. Sci. 18:43–52.
Keast, A.
1978. Trophic and spatial interrelationships in the fish species of an Ontario temperate lake. Environ. Biol. Fishes 3:7–31.
Levins, R.
1968. Evolution in changing environments: some theoretical explorations, 121 p. Princeton Univ. Press, Princeton, NJ.
Libralato, S., V. Christensen, and D. Pauly.
2006. A method for identifying keystone species in food web models. Ecol. Model. 195:153–171.
Lombarte, A., Ò. Chic, V. Parisi-Baradad, R. Olivella, J. Riera, E. García-Ladona.
2006. A web-based environment from shape analysis of fish otoliths. The AFORO database. Sci. Mar. 70:147–152.
López-López, L., V. Bartolino, and I. Preciado.
2015. Role of prey abundance and geographical variables in a demersal top predator's feeding habits (*Merluccius merluccius*). Mar. Ecol. Prog. Ser. 541:165–177.
Macpherson, E.
1978a. Régimen alimentario de *Micromesistius poutassou* (Risso, 1810) y *Gadiculus argenteus argenteus* Guichenot, 1850 (Pisces, Gadidae) en el Mediterráneo occidental. Invest. Pesq. 42:305–316.
1978b. Régimen alimentario de *Phycis blennoides* (Brünich) y *Antonogadus megalokynodon* (Kolombatovic) (Pisces: Gadidae) en el Mediterráneo occidental. Invest. Pesq. 42:455–466.
1979. Estudio sobre las relaciones tróficas en peces bentónicos de la costa catalana. Ph.D. diss., 220 p. [In Spanish.] Univ. Barcelona, Barcelona, Spain. [Available from website.]
1981. Resource partitioning in a Mediterranean demersal fish community. Mar. Ecol. Prog. Ser. 4:183–193.
Madurell, T., E. Fanelli, and J. E. Cartes.
2008. Isotopic composition of carbon and nitrogen of suprabenthic fauna in the NW Balearic Islands (western Mediterranean). J. Mar. Syst. 71:336–345.
Marrin, D. L.
1983. Ontogenetic changes and intraspecific resource partitioning in the tahoe sucker, *Catostomus tahoensis*. Environ. Biol. Fishes 8:39–47.
McDonald-Madden, E., R. Sabbadin, E. T. Game, P. W. J. Baxter, I. Chadès, and H. P. Possingham.
2016. Using food-web theory to conserve ecosystems. Nat. Commun. 7:10245.
Miller, T. W., R. D. Brodeur, G. Rau, and K. Omori.
2010. Prey dominance shapes trophic structure of the northern California Current pelagic food web: evidence from stable isotopes and diet analysis. Mar. Ecol. Prog. Ser. 420:15–26.
Morisita, M.
1959. Measuring of the dispersion and analysis of distribution patterns. Mem. Fac. Sci., Kyushu Univ., Ser. E, Biol. 2:215–235.
Morte, M. S., M. J. Redón, and A. Sanz-Brau.
2001. Feeding habits of *Trisopterus minutus capelanus* (Gadidae) off the eastern coast of Spain (western Mediterranean). Mar. Ecol. 22:215–229.
2002. Diet of *Phycis blennoides* (Gadidae) in relation to fish size and season in the western Mediterranean (Spain). Mar. Ecol. 23:141–155.

Olaso, I.
1990. Distribución y abundancia del megabentos invertebrado en fondos de la plataforma cantábrica. Inst. Esp. Oceanogr., Publ. Esp. 5, 128 p. [In Spanish.] [Available from Inst. Esp. Oceanogr., Calle Corazón María 8, 28002 Madrid, Spain.]

Paradinas, I., M. Marín, M. G. Pennino, A. López-Quílez, D. Conesa, D. Barreda, M. Gonzalez, and J. M. Bellido.
2016. Identifying the best fishing-suitable areas under the new European discard ban. ICES J. Mar. Sci. 73:2479–2487.

Pauly, D., M. L. Palomares, R. Froese, P. Sa-a, M. Vakily, D. Preikshot, and S. Wallace.
2001. Fishing down Canadian aquatic food webs. Can. J. Fish. Aquat. Sci. 58:51–62.

Philips, A. E.
2012. Feeding behavior of the European hake *Merluccius merluccius* Linnaeus, 1758 (Family: Gadidae) from Egyptian Mediterranean waters off Alexandria. Egypt. J. Aquat. Res. 38:39–44.

Pianka, E. R.
1973. The structure of lizard communities. Annu. Rev. Ecol. Syst. 4:53–74.

Pinnegar, J. K., S. Jennings, C. M. O'Brien, and N. V. C. Polunin.
2002. Long-term changes in the trophic level of the Celtic Sea fish community and fish market price distribution. J. Appl. Ecol. 39:377–390.

Preciado, I., J. L. Gutiérrez-Zabala, F. Velasco, and I. Olaso.
2002. Dieta de otoño de once especies de peces demersales en la plataforma Atlántica del sur de Galicia. Nova Acta Cient. Compostel., Biol. 12:125–141.

Preciado, I., F. Velasco, and I. Olaso.
2008. The role of pelagic fish as forage for the demersal fish community in the southern Bay of Biscay. J. Mar. Syst. 72:407–417.

Robb, A. P.
1992. Changes in the gall bladder of whiting (*Merlangius merlangus*) in relation to recent feeding history. ICES J. Mar. Sci. 49:431–436.

Rodríguez-Cabello, C., L. Modica, F. Velasco, F. Sánchez, and I. Olaso.
2014. The role of silvery pout (*Gadiculus argenteus*) as forage prey in the Galician and Cantabrian Sea ecosystem (NE Atlantic) in the last two decades. J. Exp. Mar. Biol. Ecol. 461:193–200.

Rosas-Luis, R., R. Villanueva, and P. Sánchez.
2014. Trophic habits of the Ommastrephid squid *Illex coindetii* and *Todarodes sagittatus* in the northwestern Mediterranean Sea. Fish. Res. 152:21–28.

Scharf, F. S., F. Juanes, and R. A. Rountree.
2000. Predator size-prey size relationships of marine fish predators: interspecific variation and effects of ontogeny and body size on trophic-niche breadth. Mar. Ecol. Prog. Ser. 208:229–248.

Scherrer, B.
1984. Biostatistique, 850 p. Gaëtan Morin, Montreal, Canada.

Schoener, T. W.
1974. Resource partitioning in ecological communities. Science 185:27–39.

Silva, M. V., R. H. Morales, and M. M. Nava.
2014. Métodos clásicos para el análisis del contenido estomacal en peces. Biológicas 16(2):13–16.

Tirasin, E. M., and T. Jørgensen.
1999. An evaluation of the precision of diet description. Mar. Ecol. Prog. Ser. 182:243–252.

Torres, M. A., M. Coll, J. J. Heymans, V. Christensen, and I. Sobrino.
2013. Food-web structure of and fishing impacts on the Gulf of Cadiz ecosystem (South-western Spain). Ecol. Model. 265:26–44.

Trites, A. W.
2003. Food webs in the ocean: who eats whom and how much? *In* Responsible fisheries in the marine ecosystem (M. Sinclair and G. Valdimarsson, eds.), p. 125–141. FAO, Rome.

Velasco, F., and I. Olaso.
1998. European hake *Merluccius merluccius* (L., 1758) feeding in the Cantabrian Sea: seasonal, bathymetric and length variations. Fish. Res. 38:33–44.

Zariquiey Alvarez, R.
1968. Crustáceos decápodos ibéricos. Investig. Pesq., vol. 32, 510 p. Inst. Inv. Pesq., Barcelona, Spain.

National Marine
Fisheries Service
NOAA

Fishery Bulletin
established in 1881

Spencer F. Baird
First U.S. Commissioner
of Fisheries and founder
of *Fishery Bulletin*

Effects of ocean acidification on larval Atlantic surfclam (*Spisula solidissima*) from Long Island Sound in Connecticut

Shannon L. Meseck (contact author)
Renee Mercaldo-Allen
Paul Clark
Catherine Kuropat
Dylan Redman
David Veilleux
Lisa Milke

Email address for contact author: shannon.meseck@noaa.gov

Milford Laboratory
Northeast Fisheries Science Center
National Marine Fisheries Service, NOAA
212 Rogers Avenue
Milford, Connecticut 06460

Abstract—The Atlantic surfclam (*Spisula solidissima*) supports a $29.2-million fishery on the northeastern coast of the United States. Increasing global carbon dioxide (CO_2) in the atmosphere has resulted in a decrease in ocean pH, known as ocean acidification (OA), in Atlantic surfclam habitat. The effects of OA on larval Atlantic surfclam were investigated for 28 d by using 3 different levels of partial pressure of CO_2 (pCO_2): low (344 µatm), medium (821 µatm), and high (1243 µatm). Samples were taken to examine growth, shell height, time to metamorphosis, survival, and lipid concentration. Larvae exposed to a medium pCO_2 level had a hormetic response with significantly greater shell height and growth rates and a higher percentage that metamorphosed by day 28 than larvae exposed to the high- and low-level treatments. No significant difference in survival was observed between treatments. Although no significant difference was found in lipid concentration, Atlantic surfclam did have a similar hormetic response for concentrations of phospholipids, sterols, and triacylglycerols and for the ratio of sterols to phospholipids, indicating that larvae may have a homeoviscous adaptation to OA at medium pCO_2 levels. Our results indicate that larval Atlantic surfclam have some tolerance to slightly elevated pCO_2 concentrations but that, at high pCO_2 levels, they may be susceptible to OA.

Manuscript submitted 28 July 2020.
Manuscript accepted 10 May 2020.
Fish. Bull. 119:66–76 (2021).
Online publication date: 25 May 2021.
doi: 10.7755/FB.119.1.8

The views and opinions expressed or implied in this article are those of the author (or authors) and do not necessarily reflect the position of the National Marine Fisheries Service, NOAA.

The process of ocean acidification (OA) occurs when increased atmospheric carbon dioxide (CO_2) from anthropogenic activities (i.e., burning of fossil fuels and deforestation) is absorbed by ocean waters (Caldeira and Wickett, 2003; Raven et al.[1]; Doney et al., 2009). Consequently, concentrations of dissolved CO_2 and bicarbonate ions (HCO_3^-) rise, while concentration of carbonate ions (CO_3^{2-}), pH, and calcium carbonate saturation level (Ω) decline (Feely et al., 2004, 2010; Hönisch et al., 2012; Duarte et al., 2013). In recent years, the ocean's natural capacity for buffering, a process that normally occurs over a geologic timescale of 10,000–100,000 years, has been unable to keep pace with the rate of acidification (Hönisch et al., 2012; Zeebe, 2012; Zeebe et al., 2016), resulting in a global ocean pH drop of 0.1. This ongoing shift in the carbonate system and corresponding decline in pH and Ω may affect the growth and survival of marine organisms.

Representative concentration pathways (RCPs) are used to predict future CO_2 concentrations. By the year 2100, under the RCP 8.5 scenario (high emissions) used in climate modeling, CO_2 levels will be >1000 µatm, and under the RCP 6.0 scenario, CO_2 levels will be in the range of 720–1000 µatm (IPCC, 2014). Projected increases in CO_2 by 2100 are expected to result in a reduction of 0.2–0.4 in pH and in a 50% decline in aragonite saturation level ($\Omega_{aragonite}$), a measure often used in relation to Ω because aragonite is a common form of calcium carbonate in ocean waters (Feely et al., 2004, 2010; Hartin et al., 2016). It has been predicted that, by the year 2300, CO_2 levels will be >2000 µatm and will correspond to an additional drop of 0.4 in pH (Feely et al., 2004, 2010; Hartin et al., 2016).

In a recent climate vulnerability assessment of fish and invertebrates on the continental shelf of the northeastern

[1] Raven, J., K. Caldeira, H. Elderfield, O. Hoegh-Guldberg, P. Liss, U. Riebesell, J. Shepherd, C. Turley, and A. Watson. 2005. Ocean acidification due to increasing atmospheric carbon dioxide. R. Soc. Policy Doc. 12/05, 57 p. [Available from website.]

United States, shellfish species were categorized as highly susceptible to changing climate conditions (Hare et al., 2016). A conclusion of most of the research on effects of OA on marine mollusks has been that larval shellfish are more sensitive to OA than those in juvenile and adult stages (Gledhill et al., 2015; Siedlecki et al., 2021). In larval experiments with bay scallop (*Argopecten irradians*) (Talmage and Gobler, 2009; White et al., 2013), eastern oyster (*Crassostrea virginica*) (Miller et al., 2009; Talmage and Gobler, 2009; Gobler and Talmage, 2014), and northern quahog (*Mercenaria mercenaria*) (Green et al., 2004, 2009; Talmage and Gobler, 2009), reduced rates of survival and growth have been observed when larvae were exposed to acidification levels predicted to occur by 2100. The findings of these studies indicate that an $\Omega_{aragonite}$ of ~1.5 results in physiological responses in marine bivalve species. These studies focused on bivalve species that reside in estuarine water, where changes in temperature, salinity, and partial pressure of CO_2 (ρCO_2) can occur at daily rates (Feely et al., 2010; Dickinson et al., 2013; Duarte et al., 2013), and their results may not be applicable to coastal bivalve species.

A synthesis of available reports on ecological consequences of ocean and coastal acidification for species in the Northeast U.S. continental shelf large marine ecosystem has identified that to date little is known on how coastal bivalve species will respond to OA (Hare et al., 2016). Recently, juvenile Atlantic surfclam (*Spisula solidissima*) were found to have modified physiological processes at CO_2 levels of RCP 8.5 scenario during a 12-week exposure, with them being more sensitive than previously studied estuarine bivalves (i.e., oyster species and the blue mussel, *Mytilus edulis*) to increasing ρCO_2 levels (Pousse et al., 2020). The results of that study highlight the need to understand how larval Atlantic surfclam will respond to OA conditions.

Atlantic surfclam are planktonic larvae, transitioning to the pediveliger stage with a foot and "swimming-crawling" behavior (Fay et al., 1983; Cargnelli et al., 1999). Larval Atlantic surfclam are concentrated near the thermocline and are transported horizontally by currents (Zhang et al., 2015, 2016; Chen et al., 2019). Along the coast of the northeastern United States, surface waters of the Atlantic Ocean and Gulf of Maine are characterized by high variability, both spatially (with increased acidification northward) and seasonally (with the lowest values during winter and the highest values in summer) (Biao et al., 2004; Wang et al., 2013; Xu et al., 2017; Goldsmith et al., 2019; Friedland et al., 2020). Records of carbonate chemistry of the subsurface water column in the Gulf of Maine have included $\Omega_{aragonite}$ levels that were lowest in the spring, ranging from 0.9 at the seafloor to 2.2 at the surface, and highest during the summer, ranging from 1.4 at the bottom to 2.6 at the surface, with a seasonal range of 1.0–2.0 (Wanninkhof et al., 2015; Wang, 2016). Wang et al. (2017) observed a decrease of 0.01 in $\Omega_{aragonite}$ for every 1 µmol/kg increase in dissolved inorganic carbon (DIC), similar to what has been observed in the open ocean (Bates et al., 2014). Recently, an oceanographic glider, an autonomous underwater vehicle, was used off the coast of New Jersey to measure subsurface pH levels, which ranged from 7.91 to 8.20, and to measure $\Omega_{aragonite}$, which ranged from 1.5 to 2.2 with higher readings at the surface (Saba et al., 2019).

Although there is evidence of increasing ρCO_2 concentrations in waters where larval Atlantic surfclam are concentrated during development, data are sparse at the thermocline, and the processes and drivers of these changes are not understood fully (Boehme et al., 1998; Wang et al., 2017). The limited data that is available, combined with model projections for the entire region, indicate that some areas in the region where Atlantic surfclam concentrate will reach global levels of ρCO_2 predicted for 2100 as early as 2030–2050 (Ekstrom et al., 2015; Siedlecki et al., 2021).

Characterizing the effects of OA on Atlantic surfclam is complex in part because of the presence of 2 subspecies along the coast of the northeastern United States (Hare and Weinberg, 2005). Both subspecies are referred to as Atlantic surfclam; however, there are physiological differences between the 2 subspecies. The more northern subspecies, *S. s. solidissima*, is larger in size (length: 150–200 mm) and lives longer (25–30 years) than the more southern subspecies, *S. s. similis*, which ranges in length from 76 to 122 mm and lives for 4.0–5.5 years (Walker and O'Beirn, 1996; Weinberg and Helser, 1996). The subspecies differ in geographic range, with the northern subspecies of Atlantic surfclam found from the Gulf of Saint Lawrence in Canada south to Cape Hatteras in North Carolina and with the southern subspecies thought to be distributed primarily in shallow nearshore environments along the coast of Cape Hatteras and in waters of the Gulf of Mexico off the coast of the southeastern United States.

The Connecticut Bureau of Aquaculture identifies Atlantic surfclam in Long Island Sound (LIS) as *S. solidissima*, but results of DNA analysis indicate that *S. s. similis*, although it is considered the more southern subspecies, is located primarily off the coast of Massachusetts; there also is a confirmed population of the southern subspecies in waters of New York in LIS (Hare et al., 2010). Results of a recent survey conducted by the NOAA Northeast Fisheries Science Center indicate that the southern subspecies of Atlantic surfclam may be shifting northward because of increased water temperatures (NEFSC, 2017). The Mid-Atlantic Fishery Management Council in fiscal year 2019 solicited studies to examine whether there has been an expansion of the distribution of the southern subspecies of Atlantic surfclam into the habitat of the northern subspecies, recognizing there are potential implications for stock assessments if multiple species that are genetically different are managed together.

Until the geographical distribution of both subspecies is better understood, we will make no assumption of which subspecies was used in our experiment and will refer to the brood stock and larvae of Atlantic surfclam in our study as *S. solidissima*. This choice is consistent with current management of the commercial industry for Atlantic surfclam as a single fishery, with harvesting concentrated

in estuarine waters of LIS, nearshore coastal waters (0–5 km [0–3 mi]) of New Jersey and New York, and offshore waters along the Atlantic coast from New Jersey to Virginia. Highly valued, the Atlantic surfclam fishery generated more than $29.2 million in revenue during 2019 (National Marine Fisheries Service, commercial fisheries landings database, available from website).

Changes in environmental conditions of the habitat of Atlantic surfclam are comparable to changes in the open ocean, with seasonal variability in $\Omega_{aragonite}$ near or below the physiological threshold of 1.5 identified for other bivalves, yet there have been no studies examining how larval Atlantic surfclam respond to increasing pCO_2 levels. On the basis of the RCP 6.0 and RCP 8.5 scenarios (IPCC, 2014) and current conditions of the habitat of Atlantic surfclam, our study investigated the effect of low, medium, and high levels of pCO_2 (344, 821, and 1243 µatm) on growth, mortality, and metamorphosis of larval Atlantic surfclam. We hypothesized that larvae of Atlantic surfclam might have reduced rates of survival and growth and experience longer times to metamorphosis with increased pCO_2 concentrations. We also hypothesized that allocation of energetic resources in larval Atlantic surfclam, measured by using lipid concentrations, might change in response to variations in carbonate chemistry.

Materials and methods

Spawning

Adult brood stock of Atlantic surfclam were collected from 2 locations in LIS. In 2014, 32 clam were caught on 4 November from Stratford, Connecticut, and 75 individuals were collected on 6 November from Norwalk, Connecticut, from on board a commercial shellfish boat. The brood stock acclimated for 169 d at the Milford Laboratory (41°12′43.82″N, 73°3′12.96″W) of the Northeast Fisheries Science Center in a flow-through seawater system (16°C [standard deviation 3]) delivering natural seston that was supplemented with a drip of cultured *Tetraselmis chui* (strain PLY429). Brood stock were conditioned for spawning following the protocol outlined in Goldberg (1989). On 22 April 2015, 30 scrubbed Atlantic surfclam from both collection sites were placed in a spawning table filled with 10-µm-filtered seawater. To induce spawning, seawater temperature was increased by 2°C every 30 min, to a maximum of 26°C. Upon release of gametes, male and female Atlantic surfclam were placed into separate glass dishes. Gametes were collected from 7 females and 5 males, and then pooled eggs were fertilized with pooled sperm in ambient seawater, yielding a total fertilized egg count of 81.6 million.

After fertilization, 30 embryos/mL were added to each of 9 clean 15-L buckets containing 10 L of 0.35-µm-filtered seawater that had been pumped directly from Milford Harbor and bubbled with CO_2 to reach target conditions (described in the "Experimental design" section). Larvae were fed after 24 h with cultured *Tisochrysis lutea* (isolator number: T-ISO) at an algal density of 50,000 cells/mL (Goldberg, 1989). Every Monday, Wednesday, and Friday, the larvae in buckets were screened, buckets were cleaned, and water in the buckets was replaced with preconditioned water for each pCO_2 treatment level. Cleaning helped reduce ciliate levels that were present in all treatments. Larval experiments were conducted from 22 April through 20 May 2015.

Experimental design

Nine buckets were placed in a temperature-controlled water table (Table 1). The target pCO_2 levels (~400, ~800, and ~1200 µatm) were chosen on the basis of RCP scenarios for future CO_2 concentrations in the region and the 3 levels identified in the guide to best practices for OA research and data reporting (Riebesell et al., 2011). Compressed air was passed through a PureGas[2] CO_2 absorber (Altec Air, Broomfield, CO) before being delivered to GFC mass flow controllers for air and carbon dioxide (Aalborg Instruments and Controls, Orangeburg, NY). The CO_2-stripped air was mixed with research-grade CO_2 to create and maintain 3 target pCO_2 treatment levels and was distributed to 3 replicate buckets per treatment at a moderate aeration rate (12 L/min) that is routinely used in bivalve culture (Loosanoff and Davis, 1963; Bayne, 1965).

Biological sampling

Larvae samples for examining size, survival, metamorphosis, and lipids were taken on a volume basis weekly when buckets were cleaned. Briefly, larvae were screened on a nylon mesh sieve (40–150 µm) and concentrated in a 100-mL graduated cylinder. A subsample of 1 mL was removed from the graduated cylinder and preserved in a 1% solution of buffered formalin for measurement of shell heights (maximum length, from anterior to posterior, parallel to the hinge; number of samples [n]=50 larvae). When the experiment began on 22 April 2015, 4 samples were taken for initial measurements of size, and triplicate samples from each bucket were obtained and preserved weekly for size measurements and for determination of the percentages of all larvae in the sample that had died (percent mortality) and that had undergone metamorphosis by using an Olympus inverted microscope (Olumpus IX51, Olympus Corp., Tokyo, Japan) and the software ImageJ, vers. 1.49 (Rasband, 2015).

Lipid samples were obtained at the end of the experiment on day 28. Known volumes (0.3–0.5 mL) of concentrated Atlantic surfclam were collected and placed in glass tubes that had been prerinsed with methanol and chloroform. Samples were stored in 2 mL of chloroform, purged of air with nitrogen gas, and held at –80°C until analysis

[2] Mention of trade names or commercial companies is for identification purposes only and does not imply endorsement by the National Marine Fisheries Service, NOAA.

Table 1

Carbonate chemistry and environmental characteristics measured at low, medium, and high levels of partial pressure of carbon dioxide (ρCO_2) and used to investigate the effect of ρCO_2 levels on laboratory-reared larval Atlantic surfclam (*Spisula solidissima*) in 2015. The variables include mean measured pH (seawater scale, pH measured at 20°C), pH in situ (seawater scale, pH at the temperature of the experiment), temperature (°C), salinity, ρCO_2 (µatm), total dissolved inorganic carbon (DIC) (µmol/kg), and saturation levels of calcite ($\Omega_{calcite}$) and aragonite ($\Omega_{aragonite}$) for the duration of the experiment. Values are means with standard errors of the mean in parentheses. Asterisks (*) indicate values that were measured directly and not calculated by using the program CO2SYS. The adult brood stock used to rear individuals for this study were collected in 2014 from Long Island Sound near Stratford and Norwalk, Connecticut.

	Treatment level of ρCO_2		
Characteristic	Low	Medium	High
pH measured*	7.972 (0.003)	7.629 (0.003)	7.462 (0.003)
pH in situ	8.073 (0.003)	7.734 (0.003)	7.568 (0.003)
Temperature*	18.8 (0.1)	18.9 (0.1)	18.9 (0.1)
Salinity*	25.72 (0.08)	25.73 (0.08)	25.73 (0.08)
ρCO_2	343.9 (5.9)	820.8 (6.0)	1242.9 (5.9)
DIC*	1800.66 (2.35)	1903.74 (2.39)	1953.32 (2.37)
$\Omega_{calcite}$	3.46 (0.01)	1.74 (0.02)	1.22 (0.02)
$\Omega_{aragonite}$	2.18 (0.01)	1.09 (0.01)	0.77 (0.01)

was to begin. Samples were shipped overnight to the Memorial University of Newfoundland for lipid analysis, where they were extracted by following a modified Folch procedure (Parrish, 1999), and lipid classes were identified by using a Chromarod-Iatroscan system for thin-layer chromatography and flame ionization detection (Mark V, Iatron Laboratories, Tokyo, Japan).

Carbonate chemistry measurements

Seawater samples were collected from each bucket for carbonate chemistry measurements immediately before and after water changes (n=63). One sample per bucket was obtained by placing a tube fit with an airstone into the bottom of each bucket and filling 500-mL polypropylene collection bottles to overflow (1.5 times) by using a peristaltic pump. The airstone ensured that larvae and phytoplankton were not collected with the seawater samples. Samples were analyzed immediately for pH and DIC.

Total pH was determined colorimetrically by using m-Cresol purple indicator dye (Sigma-Aldrich, St. Louis, MO) (Dickson and Goyet[3]) with an Ocean Optics 2000+ UV spectrometer (Ocean Insight, Orlando, FL). All samples were analyzed for DIC without the addition of preservatives on a DIC analyzer (AS-C3, Apollo SciTech, LLC, Newark, DE). To ensure precision, replicate samples (n=5) of certified reference material also were analyzed, resulting in 1 standard deviation of 2.7 µmol/kg for total DIC replicates and of 0.0014 for total pH. The DIC instrument was part of a previous international, interlaboratory exercise for comparison of DIC in test seawater samples with low and high CO_2 levels; DIC during our study measured within 0.5% of assigned values (Bockmon and Dickson, 2015). Seawater temperature and salinity were measured daily by using a YSI Model 85 handheld oxygen, conductivity, salinity, and temperature system (YSI, Inc., Yellow Springs, OH). Dissolved inorganic carbon and pH values were entered into the program CO2SYS (Pierrot et al., 2006) to calculate ρCO_2 (in microatmospheres), calcite saturation level ($\Omega_{calcite}$), and $\Omega_{aragonite}$ by using the following constants: K'_1, K'_2 from Mehrbach et al. (1973) and refit by Dickson and Millero (1987), K hydrogen sulfate from Dickson (1990), and total boron from Uppström (1974).

Statistical analyses

The software Statgraphics Plus (vers 17.1.12, Statgraphics Technologies, The Plains, VA) was used for all statistical analyses. All data were checked for normality by using the Shapiro–Wilk test, with a significance level of 0.05, and for equal variance prior to statistical analysis.

[3] Dickson, A. G., and C. Goyet (eds.). 1994. Handbook of methods for the analysis of the various parameters of the carbon dioxide system in sea water, version 2. U.S. Dep. Energy, Oak Ridge Natl. Lab., Carbon Dioxide Inf. Anal. Cent. ORNL/CDIAC-74, 180 p. [Available from website.]

Linear growth during the larval stage (Powell et al., 2002; Pace et al., 2006) was estimated with this equation:

$$y = mx + b,$$

where y = length (in micrometers);
m = slope (in micrometers per day);
x = time (in days); and
b = intercept (initial length in micrometers).

For each bucket, mean rates of shell growth (in micrometers per day, with standard errors of the mean [SE]) were determined by the slope of shell length versus age. An analysis of covariance was used to compare the regression lines and to discern if they were statistically significant ($P<0.05$). If a significant difference was detected between slopes, further examination was done by using analysis of variance. Data for lipid concentration (in micrograms per gram of wet weight), for percent lipid (lipid concentration divided by total lipid concentration multiplied by100) and for percentages of all larvae in the sample that survived and that had successfully completed metamorphosis were collected at the end of the experiment. All data collected as percentages were transformed with arcsine (square root) prior to statistical analysis and prior to analysis of variance. Least square difference was used to determine different homogeneous groups. For all statistical analyses, degrees of freedom equaled 6.

Results

Seawater physicochemical variables

Carbonate chemistry and environmental variables in the 3 pCO_2 treatments are shown in Table 1. Values for measured pH were 7.972 (SE 0.003), 7.629 (SE 0.003), and 7.462 (SE 0.003) for the treatments with low, medium, and high levels of pCO_2, respectively. Values of DIC were 1800.66 µmol/kg (SE 2.35) for the low-pCO_2 treatment, 1903.74 µmol/kg (SE 2.39) for the medium-pCO_2 treatment, and 1953.32 µmol/kg (SE 2.37) for the high-pCO_2 treatment. Other carbonate system characteristics (pCO_2, $\Omega_{calcite}$, $\Omega_{aragonite}$, and pH in situ) were calculated at the in situ temperature and are reported in Table 1. The calculated levels of pCO_2 were 343.9 µatm (SE 5.9), 820.8 µatm (SE 6.0), and 1242.9 µatm (SE 5.9) for the 3 treatments with different experimental conditions. There was a significant difference in pCO_2 (F ratio=2945, $P<0.01$) between the low-, medium-, and high-pCO_2 treatments. Mean seawater temperature (18.9°C [SE 0.1]) and salinity (25.73 [SE 0.08]) remained stable throughout the study period (Table 1).

Larval growth, survival, metamorphosis, and lipids

Significant differences were observed in the final shell height of Atlantic surfclam from fertilization to metamorphosis at the conclusion of the experiment, with greater shell height (in micrometers) for individuals in the medium-pCO_2 treatment than for those in the treatments with low and high pCO_2 levels (F ratio=6.986, P=0.03; Fig. 1). The specimens in the medium-pCO_2 treatment had a final shell height that measured 13% larger than those in the the high- and low-pCO_2 treatments, but there was no difference in final shell height between the individuals exposed to low and high pCO_2 levels. Larvae in the treatment with a medium pCO_2 level had a mean growth rate of 7.16 µm/d (SE 0.25) that was significantly greater (F ratio=5.84, P=0.04), 15% higher, than the mean rate observed for larvae in the low-pCO_2 treatment, 8.26 µm/d (SE 0.25). Growth rates of larvae under the high-pCO_2 treatment, with a mean rate of 7.25 µm/d (SE 0.25), were similar to those of larvae in the low-pCO_2 treatment.

Although larval survival did not differ significantly (F ratio=3.23, P=0.17) between treatments, survival rates in the medium-pCO_2 treatment (29% [SE 5]) were twice those observed in the treatments with high (17% [SE 5]) and low (11% [SE 5]) pCO_2 levels. After 28 d, significantly more larvae (F ratio=12.89, $P<0.01$) in the medium-pCO_2 treatment successfully completed metamorphosis (88% [SE 1]) than in the low- and high-pCO_2 treatments, at 65% (SE 6) and 61% (SE 5), respectively. There was no

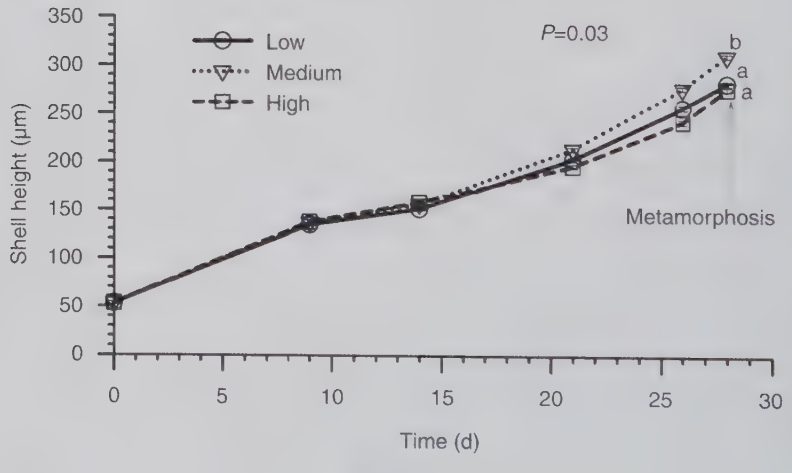

Figure 1

Mean shell height of laboratory-reared larval Atlantic surfclam (*Spisula solidissima*) over the 28 d of the experiment conducted in 2015 with 3 treatments that exposed larvae to low (circles, 344 µatm), medium (triangles, 821 µatm), and high (squares, 1243 µatm) levels of partial pressure of carbon dioxide (pCO_2). Differences in the letters at the end of regression lines indicate significant differences in final shell height between treatments (P=0.03). The adult brood stock used to rear individuals for this study were collected in 2014 from Long Island Sound near Stratford and Norwalk, Connecticut.

Table 1

Carbonate chemistry and environmental characteristics measured at low, medium, and high levels of partial pressure of carbon dioxide (pCO_2) and used to investigate the effect of pCO_2 levels on laboratory-reared larval Atlantic surfclam (*Spisula solidissima*) in 2015. The variables include mean measured pH (seawater scale, pH measured at 20°C), pH in situ (seawater scale, pH at the temperature of the experiment), temperature (°C), salinity, pCO_2 (µatm), total dissolved inorganic carbon (DIC) (µmol/kg), and saturation levels of calcite ($\Omega_{calcite}$) and aragonite ($\Omega_{aragonite}$) for the duration of the experiment. Values are means with standard errors of the mean in parentheses. Asterisks (*) indicate values that were measured directly and not calculated by using the program CO2SYS. The adult brood stock used to rear individuals for this study were collected in 2014 from Long Island Sound near Stratford and Norwalk, Connecticut.

	Treatment level of pCO_2		
Characteristic	Low	Medium	High
pH measured*	7.972 (0.003)	7.629 (0.003)	7.462 (0.003)
pH in situ	8.073 (0.003)	7.734 (0.003)	7.568 (0.003)
Temperature*	18.8 (0.1)	18.9 (0.1)	18.9 (0.1)
Salinity*	25.72 (0.08)	25.73 (0.08)	25.73 (0.08)
pCO_2	343.9 (5.9)	820.8 (6.0)	1242.9 (5.9)
DIC*	1800.66 (2.35)	1903.74 (2.39)	1953.32 (2.37)
$\Omega_{calcite}$	3.46 (0.01)	1.74 (0.02)	1.22 (0.02)
$\Omega_{aragonite}$	2.18 (0.01)	1.09 (0.01)	0.77 (0.01)

was to begin. Samples were shipped overnight to the Memorial University of Newfoundland for lipid analysis, where they were extracted by following a modified Folch procedure (Parrish, 1999), and lipid classes were identified by using a Chromarod-Iatroscan system for thin-layer chromatography and flame ionization detection (Mark V, Iatron Laboratories, Tokyo, Japan).

Carbonate chemistry measurements

Seawater samples were collected from each bucket for carbonate chemistry measurements immediately before and after water changes (n=63). One sample per bucket was obtained by placing a tube fit with an airstone into the bottom of each bucket and filling 500-mL polypropylene collection bottles to overflow (1.5 times) by using a peristaltic pump. The airstone ensured that larvae and phytoplankton were not collected with the seawater samples. Samples were analyzed immediately for pH and DIC.

Total pH was determined colorimetrically by using m-Cresol purple indicator dye (Sigma-Aldrich, St. Louis, MO) (Dickson and Goyet[3]) with an Ocean Optics 2000+ UV spectrometer (Ocean Insight, Orlando, FL). All samples were analyzed for DIC without the addition of preservatives on a DIC analyzer (AS-C3, Apollo SciTech, LLC, Newark, DE). To ensure precision, replicate samples (n=5) of certified reference material also were analyzed, resulting in 1 standard deviation of 2.7 µmol/kg for total DIC replicates and of 0.0014 for total pH. The DIC instrument was part of a previous international, interlaboratory exercise for comparison of DIC in test seawater samples with low and high CO_2 levels; DIC during our study measured within 0.5% of assigned values (Bockmon and Dickson, 2015). Seawater temperature and salinity were measured daily by using a YSI Model 85 handheld oxygen, conductivity, salinity, and temperature system (YSI, Inc., Yellow Springs, OH). Dissolved inorganic carbon and pH values were entered into the program CO2SYS (Pierrot et al., 2006) to calculate pCO_2 (in microatmospheres), calcite saturation level ($\Omega_{calcite}$), and $\Omega_{aragonite}$ by using the following constants: K'_1, K'_2 from Mehrbach et al. (1973) and refit by Dickson and Millero (1987), K hydrogen sulfate from Dickson (1990), and total boron from Uppström (1974).

Statistical analyses

The software Statgraphics Plus (vers 17.1.12, Statgraphics Technologies, The Plains, VA) was used for all statistical analyses. All data were checked for normality by using the Shapiro–Wilk test, with a significance level of 0.05, and for equal variance prior to statistical analysis.

[3] Dickson, A. G., and C. Goyet (eds.). 1994. Handbook of methods for the analysis of the various parameters of the carbon dioxide system in sea water, version 2. U.S. Dep. Energy, Oak Ridge Natl. Lab., Carbon Dioxide Inf. Anal. Cent. ORNL/CDIAC-74, 180 p. [Available from website.]

scenarios (Miller et al., 2009; Talmage and Gobler, 2009; White et al., 2013; Waldbusser et al., 2015). In studies of other clam species, increasing ρCO_2 above current levels resulted in linear decreases in growth and shell size of softshell clam (*Mya arenaria*) (Green et al., 2009, 2013; Clements and Hunt, 2014), northern quahog (Talmage and Gobler, 2009; Gobler and Talmage, 2014), eastern oyster (Talmage and Gobler, 2009), and Pacific oyster (*C. gigas*) (Waldbusser and Salisbury, 2014; Waldbusser et al., 2015). However, no effects at ρCO_2 concentrations of the RCP 8.5 scenario have been reported for the Olympia oyster (*Ostrea lurida*) (Waldbusser et al., 2016), Antarctic bivalve (*Laternula elliptica*) (Bylenga et al., 2015), or blue mussel (Gazeau et al., 2013). A hormetic response to OA exposure in bivalves, although not often reported, was recently reported for juvenile Atlantic surfclam (Pousse et al. 2020) and has been noted in other marine species, including copepod (Li and Gao, 2012; Thor and Oliva, 2015) and finfish (Miller et al., 2013, 2016) species.

Other bivalve species may experience a hormetic response, but it may be masked by the ρCO_2 levels chosen for other experiments, choices that can result in only a decrease being observed. For example, in a repeat study conducted in 2014 with eastern oyster by using a finer exposure resolution than that in our study, a maximal hormetic response at a ρCO_2 of 380 µatm was found for growth and percentage of larvae that completed metamorphosis (Gobler and Talmage, 2014). Unlike larvae of estuarine bivalve species, the larval Atlantic surfclam in our experiment were able to tolerate moderate OA levels. Future research should include a finer exposure resolution to determine the width of hormetic response in larvae of Atlantic surfclam.

In previous studies conducted with estuarine bivalves, larvae of most species were more sensitive to increased ρCO_2 than juveniles or adults. For example, for eastern oyster exposed to conditions of the RCP 6.0 scenario, larvae had reduced rates of growth rates and survival and a lower percentage of larvae completed metamorphosis (Talmage and Gobler, 2009), and for juveniles no significant difference was observed in growth at the ρCO_2 level of the RCP 6.0 scenario (Dickinson et al., 2012) or levels greater than that of the RCP 8.5 scenario (1700 µatm; Young and Gobler, 2018). For adult eastern oyster in other studies, no effects on growth or gaping were observed at ρCO_2 levels as high as 8000 µatm (Clements et al., 2017, 2018). A similar trend has been observed for blue mussel with larvae being more sensitive than adults (Thomsen et al., 2017).

Even though the results of this study were surprising, with increased growth at ρCO_2 levels predicted for the RCP 6.0 scenario, growth decreased at levels predicted for the RCP 8.5 scenario. Results of an experiment with juveniles of this subspecies indicate a similar hormetic response to that of larvae in our study (Pousse et al., 2020). Pousse et al. (2020) found metabolic depression in juvenile Atlantic surfclam exposed to ρCO_2 levels of 1350 µatm, making them more susceptible than Pacific oyster (Lannig et al., 2010) and blue mussel (Thomsen and Melzner, 2010). The larval Atlantic surfclam in our study were not exposed to the higher levels of ρCO_2 used on juveniles in the Pousse et al. (2020) study, but it would be interesting to determine when metabolic depression occurred in larvae considering the similar trends observed between these 2 studies. We cannot explain why larval and juvenile Atlantic surfclam may behave similarly or why larval Atlantic surfclam appear to tolerate higher levels of ρCO_2 than larvae of some other estuarine species like the eastern oyster; however, a possible reason may relate to how Atlantic surfclam allocate energy for growth and development. Bioenergetic studies, including those that include dynamic energy budget modeling, would provide insight into whether the small changes in growth observed in our study and in the study of Pousse et al. (2020) would have a long-term effect over the time period required for Atlantic surfclam to reach harvest size and would help to clarify variation in responses between bivalve species.

Parsons (2001) suggests that a hormetic response may reflect evolutionary adaptation of metabolic systems to environmental variables and may link to Darwinian fitness; however, there is little quantitative evidence currently available to confirm this hypothesis. Recent research on the response of bivalve larvae to OA has focused on population-level responses and the potential for evolutionary adaptation. Increased growth of larval Atlantic surfclam at elevated ρCO_2 concentrations during our study may reflect adaptation of adults in the source population. The wild adults used in this study were exposed to conditions during the summer in LIS, where in situ sediment levels of ρCO_2 can periodically range from 689 to 1828 µatm (Perry et al., 2015; Meseck et al., 2018; Snyder et al., 2019). Researchers have found that survival of larvae varied significantly between populations of the Sydney rock oyster (*Saccostrea glomerata*) (Parker et al., 2011) and Chilean mussel (*M. chilensis*), on the basis of the history of adult exposure to OA (Duarte et al., 2015). These findings indicate potential physiological and metabolic adaptations of shellfish populations to OA conditions.

It was beyond the scope of this study to determine the ability of Atlantic surfclam to adapt and evolve to shifting environmental conditions; however, future evolutionary adaptation studies should include both subspecies of Atlantic surfclam. There is an evolutionary divergence of 13.9% between the northern and southern subspecies, indicating long-term reproductive isolation of these subspecies (Hare and Weinberg, 2005; Hare et al., 2010) that may have allowed each to develop differential tolerances to OA conditions. A comparison between specimens of the 2 subspecies from the same location, exposed to increasing ρCO_2, might resolve whether there is an evolutionary divergence in OA tolerance between the subspecies, and the results of such an investigation could support more refined management of populations of Atlantic surfclam in New England.

Slower growth rates and smaller shell height in larvae from the high- and low-ρCO_2 treatments indicate that suboptimal conditions for larval Atlantic surfclam may stimulate a shift in allocation of energetic resources

away from allometric growth toward maintenance of metabolic or physiological homeostasis. Ocean acidification in marine environments can cause invertebrates to slow metabolism and may result in reduced growth and smaller body size (Pörtner et al., 2005; Gobler and Talmage, 2014). The hormetic response we observed in growth and time to metamorphosis of Atlantic surfclam may result from energetic changes reflected in lipid metabolism. Although there was no significant difference between the lipid levels in specimens among treatments, there was a consistent trend in the concentrations of phospholipids, sterols, and triacylglycerols and in the ratio of sterols to phospholipids, with the same hormetic response as that observed for growth. The trend we observed in these lipid levels among treatments may indicate an adaptive response of membranes to different environmental conditions, including temperatures and pressures (Crockett, 1998; Pernet et al., 2006, 2007), a process known as homeoviscous adaptation (HVA).

Homeoviscous adaptation in other marine organisms has been reported previously as an adaptive response to OA (Turk et al., 2007; Bennett et al., 2018). Slight decreases in phospholipid, sterol, and triacylglycerol levels and in the sterol-to-phospholipid ratio at low and high ρCO_2 levels, like those observed in our study, may provide a metabolically less expensive and energy-conserving mechanism to reduce expenditure of adenosine triphosphate (Crockett, 1998) that facilitates use of different ion exchange pathways (Kusumi et al., 1986). Pousse et al. (2020) found an HVA response in respiration rates and food selection efficiency of juvenile Atlantic surfclam. Further research on how HVA pathways are used in larvae under OA conditions should be pursued with the additional measurements of respiration rate, feeding rate, and scope for growth to help determine if OA can facilitate different metabolic pathways.

Movement of populations of Atlantic surfclam northward and into deeper water can be attributed to warming temperatures (Weinberg, 2005; Munroe et al., 2016). Limited ρCO_2 data, combined with modeling results, indicate that decreases in pH and $\Omega_{aragonite}$ occur in the areas to which Atlantic surfclam are moving (Wang, 2016; Saba et al., 2019; Friedland et al., 2020; Siedlecki et al., 2021). This study focused on only the ρCO_2 levels predicted for the RCP 6.0 and RCP 8.5 scenarios; we did not look at the role of increasing temperature. Under the RCP 6.0 and RCP 8.5 scenarios, increases in temperature are expected to occur concurrently with increased ρCO_2 levels. Future research should include examination of the response of Atlantic surfclam to OA under different temperatures to determine if the combined effects of temperature and OA changes their tolerance to ρCO_2 concentrations.

Atlantic surfclam can live up to 35 years and become harvestable within 5–7 years, and this study focused on a short portion of their lifespan. More information about the ρCO_2 levels experienced by larval, juvenile, and adult Atlantic surfclam during their lifetime is needed to better define the range of ρCO_2 concentrations on which future studies should focus. Further research should emphasize the bioenergetic pathways governing larval response to OA and address adaption and evolution by including genetic analysis. Finally, incorporating increased ρCO_2 levels into future research would provide information beneficial to fisheries management efforts.

Acknowledgments

The authors thank R. Goldberg, D. Perry, and J. Rose for technical assistance, J. Bloom from Copps Island Oysters and D. Carey of the Connecticut Department of Agriculture, Bureau of Aquaculture, for collection of brood stock of Atlantic surfclam, and the Northeast Fisheries Science Center for funding.

Literature cited

Bates, N. R., Y. M. Astor, M. J. Church, K. Currie, J. E. Dore, M. González-Dávila, L. Lorenzoni, F. Muller-Karger, J. Olafsson, and J. M. Santana-Casiano.
2014. A time-series view of changing ocean chemistry due to ocean uptake of anthropogenic CO_2 and ocean acidification. Oceanography 27(1):126–141.

Bayne, B. L.
1965. Growth and the delay of metamorphosis of the larvae of *Mytilus edulis* (L.). Ophelia 2:1–47.

Bennett, H., J. J. Bell, S. K. Davy, N. S. Webster, and D. S. Francis.
2018. Elucidating the sponge stress response; lipids and fatty acids can facilitate survival under future climate scenarios. Global Chang. Biol. 24:3130–3144.

Biao, X., D. Zhuhong, and W. Xiaorong.
2004. Impact of the intensive shrimp farming on the water quality of the adjacent coastal creeks from Eastern China. Mar. Pollut. Bull. 48:543–553.

Bockmon, E. E., and A. G. Dickson.
2015. An inter-laboratory comparison assessing the quality of seawater carbon dioxide measurements. Mar. Chem. 171:36–43.

Boehme, S. E., C. L. Sabine, and C. E. Reimers.
1998. CO_2 fluxes from a coastal transect: a time-series approach. Mar. Chem. 63:49–67.

Bylenga, C. H., V. J. Cummings, and K. G. Ryan.
2015. Fertilisation and larval development in an Antarctic bivalve, *Laternula elliptica*, under reduced pH and elevated temperatures. Mar. Ecol. Prog. Ser. 536:187–201.

Caldeira, K., and M. E. Wickett.
2003. Anthropogenic carbon and ocean pH. Nature 425:365.

Cargnelli, L. M., S. J. Griesbach, D. B. Packer, and E. Weissberger.
1999. Essential fish habitat source document: Atlantic surfclam, *Spisula solidissima*, life history and habitat characteristics. NOAA Tech. Memo. NMFS-NE-142, 13 p.

Chen, B., L. Lin, Z. Ma, T. Zhang, W. Chen, and D. Zou.
2019. Carbon and nitrogen accumulation and interspecific competition in two algae species, *Pyropia haitanensis* and *Ulva lactuca*, under ocean acidification conditions. Aquac. Int. 27:721–733.

Clements, J. C., and H. L. Hunt.
2014. Influence of sediment acidification and water flow on sediment acceptance and dispersal of juvenile soft-shell clams (*Mya arenaria* L.). J. Exp. Mar. Biol. Ecol. 453:62–69.

Clements, J. C., D. Bourque, J. McLaughlin, M. Stephenson, and L. A. Comeau.
2017. Extreme ocean acidification reduces the susceptibility of eastern oyster shells to a polydorid parasite. J. Fish Dis. 40:1573–1585.

Clements, J. C., L. A. Comeau, C. E. Carver, É. Mayrand, S. Plante, and A. L. Mallet.
2018. Short-term exposure to elevated pCO_2 does not affect the valve gaping response of adult eastern oysters, *Crassostrea virginica*, to acute heat shock under an *ad libitum* feeding regime. J. Exp. Mar. Biol. Ecol. 506:9–17.

Crockett, E. L.
1998. Cholesterol function in plasma membranes from ectotherms: membrane-specific roles in adaptation to temperature. Am. Zool. 38:291–304.

Dickinson, G. H., A. V. Ivanina, O. B. Matoo, H. O. Pörtner, G. Lannig, C. Bock, E. Beniash, and I. M. Sokolova.
2012. Interactive effects of salinity and elevated CO_2 levels on juvenile eastern oysters, *Crassostrea virginica*. J. Exp. Biol. 215:29–43.

Dickinson, G. H., O. B. Matoo, R. T. Tourek, I. M. Sokolova, and E. Beniash.
2013. Environmental salinity modulates the effects of elevated CO_2 levels on juvenile hard-shell clams, *Mercenaria mercenaria*. J. Exp. Biol. 216:2607–2618.

Dickson, A. G.
1990. Standard potential of the reaction: $AgCl\ (s) + 12H_2(g) = Ag(s) + HCl(aq)$, and and the standard acidity constant of the ion HSO_4^- in synthetic sea water from 273.15 to 318.15 K. J. Chem. Thermodyn. 22:113–127.

Dickson, A. G., and F. J. Millero.
1987. A comparison of the equilibrium constants for the dissociation of carbonic acid in seawater media. Deep Sea Res. Oceanogr., A 34:1733–1743.

Doney, S. C., V. J. Fabry, R. A. Feely, and J. A. Kleypas.
2009. Ocean acidification: the other CO_2 problem. Annu. Rev. Mar. Sci. 1:169–192.

Duarte, C. M., I. E. Hendriks, T. S. Moore, Y. S. Olsen, A. Steckbauer, L. Ramajo, J. Carstensen, J. A. Trotter, and M. McCulloch.
2013. Is ocean acidification an open-ocean syndrome? Understanding anthropogenic impacts on seawater pH. Estuar. Coast. 36:221–236.

Duarte, C., J. M. Navarro, K. Acuña, R. Torres, P. H. Manríquez, M. A. Lardies, C. A. Vargas, N. A. Lagos, and V. Aguilera.
2015. Intraspecific variability in the response of the edible mussel *Mytilus chilensis* (Hupe) to ocean acidification. Estuar. Coast. 38:590–598.

Ekstrom, J. A., L. Suatoni, S. R. Cooley, L. H. Pendleton, G. G. Waldbusser, J. E. Cinner, J. Ritter, C. Langdon, R. van Hooidonk, D. Gledhill, et al.
2015. Vulnerability and adaptation of US shellfisheries to ocean acidification. Nat. Clim. Chang. 5:207–214.

Fay, C. W., R. J. Neves, and G. B. Pardue.
1983. Species profiles: life histories and environmental requirements of coastal fishes and invertebrates (mid Atlantic): surf clam. U.S. Fish Wildl. Serv. FWS/OBS-82/11.13, 23 p.

Feely, R. A., C. L. Sabine, K. Lee, W. Berelson, J. Kleypas, V. J. Fabry, and F. J. Millero.
2004. Impact of anthropogenic CO_2 on the $CaCO_3$ system in the oceans. Science 305:362–366.

Feely, R. A., S. R. Alin, J. Newton, C. L. Sabine, M. Warner, A. Devol, C. Krembs, and C. Maloy.
2010. The combined effects of ocean acidification, mixing, and respiration on pH and carbonate saturation in an urbanized estuary. Estuar. Coast. Shelf Sci. 88:442–449.

Friedland, K. D., R. E. Morse, J. P. Manning, D. C. Melrose, T. Miles, A. G. Goode, D. C. Brady, J. T. Kohut, and E. N. Powell.
2020. Trends and change points in surface and bottom thermal environments of the US Northeast Continental Shelf Ecosystem. Fish. Oceanogr. 29:396–414.

Gazeau, F., L. M. Parker, S. Comeau, J.-P. Gattuso, W. A. O'Connor, S. Martin, H.-O. Pörtner, and P. M. Ross.
2013. Impacts of ocean acidification on marine shelled molluscs. Mar. Biol. 160:2207–2245.

Gledhill, D. K., M. M. White, J. Salisbury, H. Thomas, I. Mlsna, M. Liebman, B. Mook, J. Grear, A. C. Candelmo, R. C. Chambers, et al.
2015. Ocean and coastal acidification off New England and Nova Scotia. Oceanography 28(2):182–197.

Gobler, C. J., and S. C. Talmage.
2014. Physiological response and resilience of early life-stage Eastern oysters (*Crassostrea virginica*) to past, present and future ocean acidification. Conserv. Physiol. 2:cou004.

Goldberg, R.
1989. Biology and culture of the surf clam. *In* Clam mariculture in North America (J. Manzi and M. Castagna, eds.), p. 263–276. Elsevier Sci. Publ., Amsterdam, Netherlands.

Goldsmith, K. A., S. Lau, M. E. Poach, G. P. Sakowicz, T. M. Trice, C. R. Ono, J. Nye, E. H. Shadwick, K. A. StLaurent, and G. K. Saba.
2019. Scientific considerations for acidification monitoring in the U.S. Mid-Atlantic region. Estuar. Coast. Shelf Sci. 225:106189.

Green, M. A., M. E. Jones, C. L. Boudreau, R. L. Moore, and B. A. Westman.
2004. Dissolution mortality of juvenile bivalves in coastal marine deposits. Limnol. Oceanogr. 49:727–734.

Green, M. A., G. G. Waldbusser, S. L. Reilly, K. Emerson, and S. O'Donnell.
2009. Death by dissolution: sediment saturation state as a mortality factor for juvenile bivalves. Limnol. Oceanogr. 54:1037–1047.

Green, M. A., G. G. Waldbusser, L. Hubazc, E. Cathcart, and J. Hall.
2013. Carbonate mineral saturation state as the recruitment cue for settling bivalves in marine muds. Estuar. Coast. 36:18–27.

Hare, M. P., and J. R. Weinberg.
2005. Phylogeography of surfclams, *Spisula solidissima*, in the western North Atlantic based on mitochondrial and nuclear DNA sequences. Mar. Biol. 146:707–716.

Hare, M. P., J. Weinberg, O. Peterfalvy, and M. Davidson.
2010. The "southern" surfclam (*Spisula solidissima similis*) found north of its reported range: a commercially harvested population in Long Island Sound, New York. J. Shellfish Res. 29:799–807.

Hare, J. A., W. E. Morrison, M. W. Nelson, M. M. Stachura, E. J. Teeters, R. B. Griffis, M. A. Alexander, J. D. Scott, L. Alade, R. J. Bell, et al.
2016. A vulnerability assessment of fish and invertebrates to climate change on the Northeast U.S. continental shelf. PLoS ONE 11(2):e0146756.

Hartin, C. A., B. Bond-Lamberty, P. Patel, and A. Mundra.
2016. Ocean acidification over the next three centuries using a simple global climate carbon-cycle model: projections and sensitivities. Biogeosciences 13:4329–4342.

Hönisch, B., A. Ridgwell, D. N. Schmidt, E. Thomas, S. J. Gibbs, A. Sluijs, R. Zeebe, L. Kump, R. C. Martindale, S. E. Greene, et al.
2012. The geological record of ocean acidification. Science 335:1058–1063.

IPCC (Intergovernmental Panel on Climate Change).
2014. Climate change 2014: synthesis report. Contribution of working groups I, II and III to the fifth assessment report of the Intergovernmental Panel on Climate Change (Core writing team, R. K. Pachauri and L. A. Meyer, eds.), 151 p. ICPP, Geneva, Switzerland. [Available from website.]

Kusumi, A., W. K. Subczynski, M. Pasenkiewicz-Gierula, J. S. Hyde, and H. Merkle.
1986. Spin-label studies on phosphatidylcholine-cholesterol membranes: effects of alkyl chain length and unsaturation in the fluid phase. Biochim. Biophys. Acta 854:307–317.

Lannig, G., S. Eilers, H. O. Pörtner, I. M. Sokolova, and C. Bock.
2010. Impact of ocean acidification on energy metabolism of oyster, *Crassostrea gigas*—changes in metabolic pathways and thermal response. Mar. Drugs 8:2318–2339.

Li, W., and K. Gao.
2012. A marine secondary producer respires and feeds more in a high CO_2 ocean. Mar. Pollut. Bull. 64:699–703.

Loosanoff, V. L., and H. C. Davis.
1963. Rearing of bivalve mollusks. Adv. Mar. Biol. 1:1–136.

Mehrbach, C., C. H. Culberson, J. E. Hawley, and R. M. Pytkowicx.
1973. Measurement of the apparent dissociation constants of carbonic acid in seawater at atmospheric pressure. Limnol. Oceanogr. 18:897–907.

Meseck, S. L., R. Mercaldo-Allen, C. Kuropat, P. Clark, and R. Goldberg.
2018. Variability in sediment-water carbonate chemistry and bivalve abundance after bivalve settlement in Long Island Sound, Milford, Connecticut. Mar. Pollut. Bull. 135:165–175.

Miller, A. W., A. C. Reynolds, C. Sobrino, and G. F. Riedel.
2009. Shellfish face uncertain future in high CO_2 world: influence of acidification on oyster larvae calcification and growth in estuaries. PLoS ONE 4(5):e5661.

Miller, G. M., S.-A. Watson, M. I. McCormick, and P. L. Munday.
2013. Increased CO_2 stimulates reproduction in a coral reef fish. Global Chang. Biol. 19:3037–3045.

Miller, S. H., D. L. Breitburg, R. B. Burrell, and A. G. Keppel.
2016. Acidification increases sensitivity to hypoxia in important forage fishes. Mar. Ecol. Prog. Ser. 549:1–8.

Munroe, D. M., D. A. Narváez, D. Hennen, L. Jacobson, R. Mann, E. E. Hofmann, E. N. Powell, and J. M. Klinck.
2016. Fishing and bottom water temperature as drivers of change in maximum shell length in Atlantic surfclams (*Spisula solidissima*). Estuar. Coast. Shelf Sci. 170:112–122.

NEFSC (Northeast Fisheries Science Center).
2017. 61st northeast regional stock assessment workshop (61st SAW) assessment report. Northeast Fish. Sci. Cent. Ref. Doc. 17-05, 466 p. [Available from website.]

Pace, D. A., A. G. Marsh, P. K. Leong, A. J. Green, D. Hedgecock, and D. T. Manahan.
2006. Physiological bases of genetically determined variation in growth of marine invertebrate larvae: a study of growth heterosis in the bivalve *Crassostrea gigas*. J. Exp. Mar. Biol. Ecol. 335:188–209.

Parker, L. M., P. M. Ross, and W. A. O'Connor.
2011. Populations of the Sydney rock oyster, *Saccostrea glomerata*, vary in response to ocean acidification. Mar. Biol. 158:689–697.

Parrish, C. C.
1999. Determination of total lipid, lipid classes, and fatty acids in aquatic samples. *In* Lipids in freshwater ecosystems (M. T. Arts and B. C. Wainman, eds.), p. 4–20. Springer, New York.

Parsons, P. A.
2001. The hormetic zone: an ecological and evolutionary perspective based upon habitat characteristics and fitness selection. Q. Rev. Biol. 76:459–467.

Pernet, F., R. Tremblay, C. Gionet, and T. Landry.
2006. Lipid remodeling in wild and selectively bred hard clams at low temperatures in relation to genetic and physiological parameters. J. Exp. Biol. 209:4663–4675.

Pernet, F., R. Tremblay, L. Comeau, and H. Guderley.
2007. Temperature adaptation in two bivalve species from different thermal habitats: energetics and remodelling of membrane lipids. J. Exp. Biol. 210:2999–3014.

Perry, D. M., D. H. Redman, J. C. Widman Jr., S. Meseck, A. King, and J. J. Pereira.
2015. Effect of ocean acidification on growth and otolith condition of juvenile scup, *Stenotomus chrysops*. Ecol. Evol. 5:4187–4196.

Pierrot, D., E. Lewis, and D. W. R. Wallace.
2006. MS Excel program developed for CO2 system calculations. U.S. Dep. Energy, Oak Ridge Natl. Lab., Carbon Dioxide Inf. Anal. Cent. ORNL/CDIAC-105a. [Available from website.]

Pörtner, H. O., M. Langenbuch, and B. Michaelidis.
2005. Synergistic effects of temperature extremes, hypoxia, and increases in CO_2 on marine animals: from earth history to global change. J. Geophys. Res. Oceans 110:C09S10.

Pousse, E., M. E. Poach, D. H. Redman, G. Sennefelder, L. E. White, J. M. Lindsay, D. Munroe, D. Hart, D. Hennen, M. S. Dixon, et al.
2020. Energetic response of Atlantic surfclam *Spisula solidissima* to ocean acidification. Mar. Pollut. Bull. 161:111740.

Powell, E. N., E. A. Bochenek, J. M. Klinck, and E. E. Hofmann.
2002. Influence of food quality and quantity on the growth and development of *Crassostrea gigas* larvae: a modeling approach. Aquaculture 210:89–117.

Rasband, W. S.
2015. ImageJ. U.S. Natl. Inst. Health, Bethesda, MD. [Available from website, accessed June 2015.]

Riebesell, U., V. J. Fabry, L. Hansson, and J.-P. Gattuso (eds.).
2011. Guide to best practices for ocean acidification research and data reporting, 260 p. Publ. Off. Eur. Union, Luxembourg, Luxemburg. [Available from website.]

Saba, G. K., K. A. Goldsmith, S. R. Cooley, D. Grosse, S. L. Meseck, A. W. Miller, B. Phelan, M. Poach, R. Rheault, K. St.Laurent, et al.
2019. Recommended priorities for research on ecological impacts of ocean and coastal acidification in the U.S. Mid-Atlantic. Estuar. Coast. Shelf Sci. 225:106188.

Siedlecki, S. A., J. Salisbury, D. K. Gledhill, C. Bastidas, S. Meseck, K. McGarry, C. W. Hunt, M. Alexander, D. Lavoie, Z. A. Wang, et al.
2021. Projecting ocean acidification impacts for the Gulf of Maine to 2050: new tools and expectations. Elem. Sci. Anth. 9(1):0006.

Snyder, J. T., M. M. Whitney, H. G. Dam, M. W. Jacobs, and H. Baumann.
2019. Citizen science observations reveal rapid, multidecadal ecosystem changes in eastern Long Island Sound. Mar. Environ. Res. 146:80–88.

Talmage, S. C., and C. J. Gobler.
2009. The effects of elevated carbon dioxide concentrations on the metamorphosis, size, and survival of larval hard clams (*Mercenaria mercenaria*), bay scallops (*Argopecten irradians*), and Eastern oysters (*Crassostrea virginica*). Limnol. Oceanogr. 54:2072–2080.

Thomsen, J., and F. Melzner.
2010. Moderate seawater acidification does not elicit long-term metabolic depression in the blue mussel *Mytilus edulis*. Mar. Biol. 157:2667–2676.

Thomsen, J., L. S. Stapp, K. Haynert, H. Schade, M. Danelli, G. Lannig, K. M. Wegner, and F. Melzner.
2017. Naturally acidified habitat selects for ocean acidification–tolerant mussels. Sci. Adv. 3:e1602411.

Thor, P., and E. O. Oliva.
2015. Ocean acidification elicits different energetic responses in an Arctic and a boreal population of the copepod *Pseudocalanus acuspes*. Mar. Biol. 162:799–807.

Turk, M., V. Montiel, D. Žigon, A. Plemenitaš, and J. Ramos.
2007. Plasma membrane composition of *Debaryomyces hansenii* adapts to changes in pH and external salinity. Microbiology 153:3586–3592.

Uppström, L. R.
1974. The boron/chlorinity ratio of deep-sea water from the Pacific Ocean. Deep-Sea Res. Oceanogr. Abstr. 12:161–162.

Waldbusser, G. G., and J. E. Salisbury.
2014. Ocean acidification in the coastal zone from an organism's perspective: multiple system parameters, frequency domains, and habitats. Annu. Rev. Mar. Sci. 6:221–247.

Waldbusser, G. G., B. Hales, C. J. Langdon, B. A. Haley, P. Schrader, E. L. Brunner, M. W. Gray, C. A. Miller, I. Gimenez, and G. Hutchinson.
2015. Ocean acidification has multiple modes of action on bivalve larvae. PLoS ONE 10(6):e0128376.

Waldbusser, G. G., M. W. Gray, B. Hales, C. J. Langdon, B. A. Haley, I. Gimenez, S. R. Smith, E. L. Brunner, and G. Hutchinson.
2016. Slow shell building, a possible trait for resistance to the effects of acute ocean acidification. Limnol. Oceanogr. 61:1969–1983.

Walker, R. L., and F. X. O'Beirn.
1996. Embryonic and larval development of *Spisula solidissima similis* (Say, 1822) (Bivalvia: Mactridae). Veliger 39:60–64.

Wang, H.
2016. On shelf-slope water mass exchanges near Washington Canyon and Norfolk Canyon in the Mid-Atlantic Bight. M.S. thesis, 176 p. Coll. William Mary, Williamsburg, VA. [Available from website.]

Wang, H., X. Hu, W.-J. Cai, and B. Sterba-Boatwright.
2017. Decadal fCO_2 trends in global ocean margins and adjacent boundary current-influenced areas. Geophys. Res. Lett. 44:8962–8970.

Wang, Z. A., R. Wanninkhof, W.-J. Cai, R. H. Byrne, X. Hu, T.-H. Peng, and W.-J. Huang.
2013. The marine inorganic carbon system along the Gulf of Mexico and Atlantic coasts of the United States: insights from a transregional coastal carbon study. Limnol. Oceanogr. 58:325–342.

Wanninkhof, R., L. Barbero, R. Byrne, W.-J. Cai, W.-J. Huang, J.-Z. Zhang, M. Baringer, and C. Langdon.
2015. Ocean acidification along the Gulf Coast and East Coast of the USA. Cont. Shelf Res. 98:54–71.

Weinberg, J. R.
2005. Bathymetric shift in the distribution of Atlantic surfclams: response to warmer ocean temperature. ICES J. Mar. Sci. 62:1444–1453.

Weinberg, J. R., and T. E. Helser.
1996. Growth of the Atlantic surfclam, *Spisula solidissima*, from Georges Bank to the Delmarva Peninsula, USA. Mar. Biol. 126:663–674.

White, M. M., D. C. McCorkle, L. S. Mullineaux, and A. L. Cohen.
2013. Early exposure of bay scallops (*Argopecten irradians*) to high CO_2 causes a decrease in larval shell growth. PLoS ONE 8(4):e61065.

Xu, Y.-Y., W.-J. Cai, Y. Gao, R. Wanninkhof, J. Salisbury, B. Chen, J. J. Reimer, S. Gonski, and N. Hussain.
2017. Short-term variability of aragonite saturation state in the central Mid-Atlantic Bight. J. Geophys. Res. Oceans 122:4274–4290.

Young, C. S., and C. J. Gobler.
2018. The ability of macroalgae to mitigate the negative effects of ocean acidification on four species of North Atlantic bivalve. Biogeosciences 15:6167–6183.

Zeebe, R. E.
2012. History of seawater carbonate chemistry, atmospheric CO_2, and ocean acidification. Annu. Rev. Earth Planet. Sci. 40:141–165.

Zeebe, R. E., A. Ridgwell, and J. C. Zachos.
2016. Anthropogenic carbon release rate unprecedented during the past 66 million years. Nat. Geosci. 9:325–329.

Zhang, X., D. Haidvogel, D. Munroe, E. N. Powell, J. Klinck, R. Mann, and F. S. Castruccio.
2015. Modeling larval connectivity of the Atlantic surfclams within the Middle Atlantic Bight: model development, larval dispersal and metapopulation connectivity. Estuar. Coast. Shelf Sci. 153:38–53.

Zhang, X., D. Munroe, D. Haidvogel, and E. N. Powell.
2016. Atlantic surfclam connectivity within the Middle Atlantic Bight: mechanisms underlying variation in larval transport and settlement. Estuar. Coast. Shelf Sci. 173:65–78.

National Marine Fisheries Service
NOAA

Fishery Bulletin
established in 1881

Spencer F. Baird
First U.S. Commissioner of Fisheries and founder of *Fishery Bulletin*

An extension of the stepwise stochastic simulation approach for estimating distributions of missing life history parameter values for sharks, groupers, and other taxa

Kenneth A. Erickson (contact author)[1,3]
Marc O. Nadon[2,3]

Email address for contact author: kerick6@lsu.edu

[1] Department of Oceanography and Coastal Sciences
Louisiana State University
Energy Coast and Environment Building
93 South Quad Drive, Room 2263
Baton Rouge, Louisiana 70803

[2] Joint Institute for Marine and Atmospheric Research
School of Ocean and Earth Science and Technology
University of Hawaii at Manoa
1000 Pope Road
Honolulu, Hawaii 96822

[3] Pacific Islands Fisheries Science Center
National Marine Fisheries Service, NOAA
1845 Wasp Boulevard, Building 176
Honolulu, Hawaii 96818

Abstract—The limited resources and high species diversity associated with coastal fisheries present challenges to their effective management. Data-limited approaches to assessment of stocks are often used in these situations, but most assessments require basic life history information that is often unavailable. We expanded a stepwise meta-analytical approach in which statistical relationships between key life history traits are used to estimate parameters related to growth, maturity, and longevity. This approach was originally devised for 6 fish families and has been successfully implemented in the assessments of data-poor reef fish species in Hawaii and Guam. We expanded this approach to groupers, wrasses, grunts, and sharks and, here, present an R package that greatly simplifies its implementation. Further, we tested this expansion by selecting a species from each of these taxa and compared results from use of the stepwise approach to results from life history studies. Our results indicate agreement between the probability distributions from our stepwise approach and those from previous studies. Distributions from the stepwise simulation had higher variability but reasonable accuracy in estimating missing values of life history parameters. We also tested our approach against another meta-analytical life history approach that was recently published (and made available as the R package FishLife) and found our stepwise approach to be generally more precise and accurate.

Manuscript submitted 5 June 2020.
Manuscript accepted 30 April 2021.
Fish. Bull. 119:77–92 (2021).
Online publication date: 4 June 2021.
doi: 10.7755/FB.119.1.9

The views and opinions expressed or implied in this article are those of the author (or authors) and do not necessarily reflect the position of the National Marine Fisheries Service, NOAA.

Coastal fisheries provide sustenance and a source of income for millions of people across the globe (Kronen et al., 2010; Symes et al., 2015; FAO, 2016). These fisheries typically target hundreds of species from different taxa, and this high species diversity makes the management of these fisheries challenging (Ault et al., 2014). In addition, resources for fisheries research and management are often lacking, resulting in a paucity of data that limits the development of well-informed management plans (Fenner, 2012; Gilman et al., 2014; Hilborn and Ovando, 2014; Berkson and Thorson, 2015). Assessing these fisheries is further limited by a lack of long-term catch and fishing effort records needed to implement certain stock assessment models.

To compensate for shortcomings, recent stock assessment methods have been focused on the use of cost-efficient length data (Ault et al., 1998, 2008; Gedamke and Hoenig, 2006; Nadon et al., 2015; Hordyk et al., 2016; Rudd and Thorson, 2018; Nadon, 2019). These length-based methods require life history information related to growth: parameters of the von Bertalanffy growth function (von Bertalanffy, 1938), the asymptotic length (L_∞) and growth coefficient (K); natural mortality (M); and length at maturity (L_{mat}, the length at which 50% of individuals are mature). However, species-specific information on life history traits is missing for as many as 83% of exploited stocks globally (Froese and Binohlan, 2000). To address this issue, Nadon and Ault (2016) developed a stepwise stochastic simulation approach in which a local estimate of maximum length (L_{max}) and statistical relationships between life history parameters are used to estimate this missing information.

Fundamental relationships between life history traits in fish species were first observed by Beverton and Holt (1959). They pointed out that M and K are typically related by a ratio close to 1.5, that the ratio of L_{mat} to L_{∞} is typically around 0.66, and that L_{∞} and K have a negative power relationship that has a general form of $L_{\infty} \sim K^{-h}$, with a shape parameter (h), which is typically around 0.5. These relationships are referred to as *Beverton–Holt invariants* in the literature (Charnov, 1993) and are likely conserved through natural selection because of their link with the maximization of offspring (Beverton and Holt, 1959; Jensen, 1996, 1997; Charnov, 2008). Results of recent meta-analytical studies indicate that ratios differ significantly between taxa and are therefore better studied within taxa (Hordyk et al., 2015; Nadon and Ault, 2016; Thorson et al., 2017).

Relationships of life history traits are useful for the estimation of missing life history parameter values by relating ones, such as M, for which information is elusive to ones, such as L_{∞} and K, for which values are more easily obtained (Pauly, 1980), or by relating L_{max} to other length parameters (e.g., L_{mat}) (Froese and Binohlan, 2000, 2003; Jarić and Gačić, 2012). The aim of these studies was mainly to generate missing estimates for single parameters, and these studies were not taxon-specific, limiting their utility by ignoring the complex multivariate distribution between key life history parameters. As a solution, Nadon and Ault (2016) presented an approach that involves the use of Monte Carlo simulation draws and several regression model steps between life history parameters for 6 fish families. Their approach allows for complex relationships between parameters, while maintaining a multivariate error structure. This approach is analogous to the method in which a sequence of regressions is used for multiple imputation of missing data (Raghunathan et al., 2001; van Buuren, 2007; Ellington et al., 2015).

Nadon and Ault (2016) determined family-specific relationships between key life history traits after an extensive literature review for 6 families of coastal fish species: surgeonfishes, jacks, snappers, emperors, goatfishes, and parrotfishes. Peer-reviewed data-limited assessments of stocks in Hawaii (Nadon, 2017) and Guam (Nadon, 2019) have already been implemented by using this approach. The goal of our study was to extend the approach from Nadon and Ault (2016) to 3 additional families of tropical coastal fish species, groupers (Serranidae), wrasses (Labridae), and grunts (Haemulidae), as well as to sharks from the orders Carcharhiniformes and Lamniformes. We acknowledge that taxonomy is an evolving field and with new information can come new evidence for reclassification. Recently, this evolution has touched groupers with proposals to move the subfamily Epinephelinae, including the genus *Epinephelus*, under the family Epinephelidae instead of under the family Serranidae (Craig and Hastings, 2007; Smith and Craig, 2007; Ma and Craig, 2018). Although some classifications put grouper taxa under Epinephelidae instead of Serranidae, for the purposes of this study, we used Serranidae as the family name for species of Epinephelinae and other grouper species.

Additionally, we tested this approach against those of life history studies and against the approach of Thorson et al. (2017) as applied in their R package FishLife. We also developed, and present here, a new R package, StepwiseLH, that simplifies the implementation of the stepwise approach for all 10 included taxonomic groups. Our results will improve the capability to conduct stock assessments for these taxonomic groups in data-limited situations.

Materials and methods

Details of the stepwise approach

The approach presented in Nadon and Ault (2016) involves a series of regression models in which relationships between life history parameters are used to sequentially estimate missing values for life history parameters from the previously estimated parameters (Fig. 1, Table 1). Note that the regression models that relate these parameters

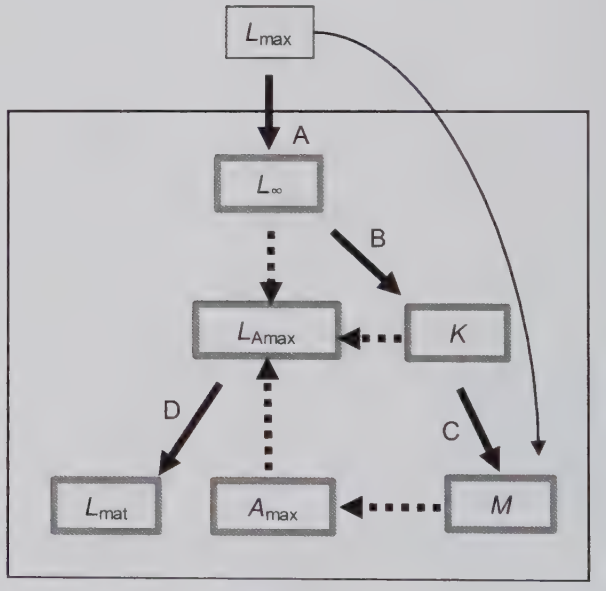

Figure 1

Depiction of one iteration of the stepwise stochastic simulation approach in which statistical relationships between key life history traits are used to estimate parameters related to growth, maturity, and longevity. The simulation starts with a local estimate of maximum length (L_{max}), and regression models A–D (solid arrows) are used successively to estimate a parameter from the one estimated in the previous model. The dashed arrows represent direct parameter calculations made by using deterministic equations (e.g., the oldest recorded age [A_{max}] is calculated by using natural mortality [M]). The rest of the parameters in this depiction include the asymptotic length (L_{∞}), expected length at the oldest recorded age (L_{Amax}), growth coefficient (K), and length at which 50% of individuals are mature (L_{mat}).

Table 1

List of life history parameters, with their definitions, used in the stepwise stochastic simulation to produce missing estimates of life history parameters for groupers (Serranidae), wrasses (Labridae), grunts (Haemulidae), and sharks from the orders Carcharhiniformes and Lamniformes. All lengths used for these parameters are total lengths.

Parameter	Definition
L_{Amax}	Expected length at the oldest recorded age (also known as L_λ)
L_{mat}	Length at which 50% of individuals reach maturity
L_{max}	Longest length in a growth study or 99th percentile of lengths in a population survey
L_∞	Asymptotic length (expected length at infinite age)
K	Brody growth coefficient of the von Bertalanffy growth function
A_0	Theoretical age at which length equals zero
A_{max}	Oldest recorded age (i.e., longevity)
M	Instantaneous natural mortality rate

are not universal but specific to taxonomic groups (e.g., snappers). The 4 models (A–D) of statistical relationships between life history parameters used in the stepwise approach (Fig. 1) are, sequentially, as follows:

$$\text{A) } L_\infty = b_0 + b_1 L_{max} + \varepsilon \text{ (linear function);} \quad (1)$$

$$\text{B) } \log(K) = \log(b_2) + b_3 \log(L_\infty) + \varepsilon \text{ (power function) or} \quad (2)$$

$$\log(K) = \log(b_2) + b_3 L_\infty + \varepsilon \text{ (exponential function);} \quad (3)$$

$$\text{C) } \log(M) = \log(b_4) + b_5 \log(K) + b_6 \log(L_{max}) + \varepsilon \text{ (power function) or} \quad (4)$$

$$\log(M) = \log(b_4) + b_5 K + b_6 L_{max} + \varepsilon \text{ (exponential function); and} \quad (5)$$

$$\text{D) } L_{mat} = b_7 + b_8 L_{Amax} + \varepsilon \text{ (linear function),} \quad (6)$$

where ε = a normally distributed error term (note: this error term can also be lognormally distributed for models A and D, if the residuals pattern indicates a lognormal distribution;
b = a model coefficient, either the slope or intercept; and
L_{Amax} = the expected length at the oldest recorded age (A_{max}).

These 4 models are used in the stepwise approach to generate probability distributions of the parameters L_∞, K, L_{mat}, and M as follows. First, a local estimate of L_{max} is obtained from a data set of representative lengths (note: we recommend using the 99th percentile of the length data set to avoid inclusion of an outlier L_{max} value and bootstrapping this data set to incorporate variability in L_{max}). Second, this L_{max} value is entered into model A (also referred to as L_{max}~L_∞) to obtain the expected L_∞ value at a given L_{max}. Third, a single random L_∞ value is sampled from the error distribution of L_∞ at that specific location on the linear regression model. Fourth, this random L_∞ value is used in model B to obtain the expected K value for this given L_∞ value. A random K value is then drawn from the error distribution at this location. Fifth, this random K value is entered into model C, which also includes the starting L_{max} value, to obtain the expected M value. A random M estimate is sampled at this location in the regression model.

Next, the previously estimated random L_∞, K, and M values are entered into the von Bertalanffy growth function to obtain L_{Amax}, also known as L_λ in Nadon and Ault (2016):

$$L_{Amax} = L_\infty (1 - e^{-K(A_{max} - A_0)}), \quad (7)$$

where A_0 = the age at length zero (a fitting parameter of the von Bertalanffy equation that is fixed at –0.6 in the stepwise approach, its overall mean value).

The parameter A_{max} is obtained by using the relationship of longevity to M presented in Hoenig (1983) and in Hewitt and Hoenig (2005), under the assumption that survivorship of a cohort at the oldest recorded age (S) was 5%, with this formula:

$$M = \frac{-\ln(0.05)}{A_{max}}. \quad (8)$$

Note that when implementing the stepwise approach, users can calculate an M estimate under a different equation or S value and are not bound to use an S of 0.05. The flexibility of natural mortality estimates is discussed further in the "Discussion" section.

Finally, the L_{Amax} value obtained by using Equation 7 is entered into model D to obtain the expected L_{mat} value, and a random L_{mat} is drawn from the error distribution at this location on the model D curve. This stepwise procedure is repeated several thousand times to obtain a multivariate probability distribution of all 4 life history parameters that can then be directly used in various stock assessment models. Uncertainty of regression model coefficients was included at every step by drawing a random set of regression coefficients from a normal multivariate distribution, defined by the variance–covariance matrix associated with these regression coefficients. Values of the variance–covariance matrix are presented in Table 2, along with model coefficients and residual error distributions.

Literature review and model fit for new taxa

The previous section describes how the stepwise procedure is implemented by using predictions from a series of 4 previously established regression models. Regression models used in each step are specific to individual taxonomic groups (e.g., parrotfishes, snappers, or jacks). To create 4 new family-specific models, we first reviewed the literature to generate new data sets of life history traits.

Table 2

Model functional form, error probability distribution, and variance–covariance matrix of regression coefficients for models A–D of statistical relationships between key life history parameters for 3 families of tropical coastal fish species and for sharks from the orders Carcharhiniformes and Lamniformes. For each taxon, the first line presents model functional forms and error distributions in brackets. Models are linear (L; $Y=b_0+b_1 \ldots X$) and power (P; $\log Y=b_0+b_1 \ldots \log X$) functions. Error distribution types are normal (N) and lognormal (LN). The first line also shows regression coefficients followed by the standard deviation for each distribution, given as the last value in the line. The second line presents the variance–covariance matrix of the regression parameters for 1-variable models (b_0 variance, b_1 variance, and b_0–b_1 covariance) and 2-variable models (b_0 variance, b_1 variance, b_2 variance, b_0–b_1 covariance, b_0–b_2 covariance, and b_1–b_2 covariance). The models relate the following parameters: the asymptotic length (L_∞), maximum length (L_{max}), growth coefficient (K), natural mortality (M), length at which 50% of individuals are mature (L_{mat}), and the expected length at the oldest recorded age (L_{Amax}). TL=total length.

	Model			
Taxon	(A) $L_\infty \sim L_{max}$	(B) $K \sim L_\infty$	(C) $M \sim K + L_{max}$	(D) $L_{mat} \sim L_{Amax}$
Haemulidae	[L,N] −29.3, 1.08, 53.5 2170, 0.0892, −4.15	[P,LN] 4.21, −0.87, 0.33 1.86, 0.05, −0.3	[P,LN] 6.11, 0.11, −1.28, 0.39 8.05, 0.11, 0.25, −0.47, −1.42, 0.0956	[L,N] 101, 0.5, 31.4 1420, 0.00787, −3.09
Labridae	[L,N] −61.3, 1.08, 53.8 976, 0.00377, −1.67	[P,LN] 4.15, −0.94, 0.5 1.54, 0.0453, −0.262	[P,LN] −2.61, 0.64, 0.27, 0.42 2.7, 0.0587, 0.1, −0.28, −0.515, 0.06	[L,LN] 70, 0.27, 0.28 1130, 0.0074, −2.54
Serranidae: small (≤100 cm TL)	[L,N] −19.7, 0.97, 60.9 552, 0.0017, −0.9	[P,LN] 3.69, −0.83, 0.49 0.42, 0.0104, −0.0653	[P,LN] 0.73, 0.23, −0.36, 0.35 0.404, 0.00774, 0.0125, −0.0296, −0.07, 0.0065	[L,LN] 53.6, 0.49, 0.13 193, 0.000709, −0.32
Serranidae: large (>100 cm TL)	[L,N] 5.11, 0.92, 95.4 15,179, 0.0081, −10.8	–	–	–
Sharks	[L,N] 95.9, 1.02, 217 10,100, 0.00165, −3.65	[P,LN] 6.77, −1.15, 0.47 1.91, 0.0327, −0.25	[P,LN] 3.65, 0.11, −0.69, 0.21 0.59, 0.00591, 0.013, −0.0336, −0.0862, 0.00603	[L,LN] −17.4, 0.79, 0.12 5080, 0.00265, −3.33

An extensive literature review was conducted by using several sources and collections (e.g., FishBase, Froese and Pauly, 2017; the libraries at the NOAA Pacific Islands Fisheries Science Center and North Carolina State University; and general Internet search tools) to find published studies related to growth (L_∞ and K), maturity (L_{mat}), and longevity (A_{max}, from which M is derived). Values of L_{max} were obtained from the same growth studies from which values of L_∞ and K were obtained, by taking the largest observed length in each study.

We originally included the following families in our literature review: Haemulidae (grunts), Holocentridae (squirrelfishes), Labridae (wrasses), Serranidae (groupers), and Siganidae (rabbitfishes), as well as sharks from various families. Groupers and wrasses include hundreds of small-bodied species (i.e., <10 cm total length), with nonexistent life history information, that we excluded from our search. We excluded species of groupers from the genus *Anthias* and species of wrasses from several genera, such as *Cirrhilabrus*, *Halichoeres*, *Labroides*, and *Pseudojuloides*. These species are characterized by extremely small body sizes, and their growth, maturity, and longevity traits are unlikely to have the same relationships as the traits of larger species in the same families. Researchers should not use the stepwise approach on species from these genera, even if life history studies for these species are available. In addition, the only family of sharks that had enough life history information to run an independent statistical analysis was Carcharhinidae, and almost all of the shark studies we found were on species from the orders Carcharhiniformes and Lamniformes. We therefore defined the shark group in our study described here as a group containing species from these 2 orders only.

We examined information available for 1134 species in these taxonomic groups, but we found published growth and maturity values for only 115 of those species (Table 3; for a list of these species and the literature used as sources of life history information, see Supplementary Table [online only]), highlighting the paucity of information available for assessment of these species. Because of a lack of published studies, we were unable to extend the approach of Nadon and Ault (2016) to squirrelfishes and rabbitfishes because only 2 and 6 species in these families had published life history data, respectively.

Raw data sets were generally unavailable from the studies in our literature review. We therefore had to rely on the fitted growth and maturity parameters from the von Bertalanffy growth function and on the logistic maturity model as fit in these studies. For growth parameters,

Table 3

Summary of estimates of life history parameters and other information in the data set for 6 taxonomic groups created through a literature review and used in this study. Data types include the asymptotic length (L_∞), growth coefficient (K), oldest recorded age (A_{max}), ratio of maximum length (L_{max}) to L_∞, ratio of natural mortality (M) to K, ratio of the length at which 50% of individuals are mature (L_{mat}) to the expected length at the oldest recorded age (L_{Amax}), and ratio of L_{mat} to L_∞. For the family Labridae, species from small-bodied genera were not included; for the family Serranidae, the *Anthias* genus was not included; and, for the shark group, only families from the orders Carcharhiniformes and Lamniformes were included. Standard deviations are provided in parentheses for ratios. All length values are total lengths.

Data type	Haemulidae (grunts)	Holocentridae (soldierfishes)	Labridae (wrasses)	Serranidae (groupers)	Sharks	Siganidae (rabbitfishes)
No. of species considered	134	86	334	264	287	29
No. of species with growth study	14	2	12	58	23	6
No. of species with maturity study	5	2	9	32	20	6
L_∞ (mm)	203–917	–	133–981	148–2006	733–4218	–
K (year^{-1})	0.19–1.00	–	0.07–0.89	0.06–1.39	0.04–1.01	–
A_{max} (years)	5–36	–	7–78	4–76	7–44	–
L_{max} to L_∞	1.02 (0.11)	–	1.12 (0.13)	1.10 (0.14)	0.95 (0.11)	–
M to K	0.55 (0.29)	–	0.68 (0.39)	0.81 (0.48)	1.53 (0.82)	–
L_{mat} to L_{Amax}	0.80 (0.14)	–	0.48 (0.16)	0.60 (0.10)	0.78 (0.10)	–
L_{mat} to L_∞	0.79 (0.15)	–	0.48 (0.17)	0.58 (0.12)	0.70 (0.12)	–

we selected only estimates for males and females combined. As a result, we were able to combine estimates from these studies more easily with data from others in which sex was undifferentiated. Further, sexes are not differentiated in most size-composition data sets in data-limited situations, and growth curves that are not sex specific are typically needed to run simple length-based assessment models with such data sets. For maturity, we obtained L_{mat} for females only, given that the reproductive potential of a stock is almost always tied to mature female biomass in population models. We converted all length values to total lengths in millimeters; total length was the length measurement used in this study and by Nadon and Ault (2016). Conversion factors obtained from FishBase were used to do so. In a limited number of cases in which multiple studies were available for a single species, we selected the most reliable source, on the basis of sample size and publication source.

For the parameter A_{max}, the age of the oldest reported fish in a study was selected. If multiple longevity values were available for a certain species, we selected the oldest recorded age as the A_{max} value. Values of M were obtained by using the approach presented in Hewitt and Hoenig (2005), under the assumption that 5% of a cohort is left at the oldest recorded age (S=0.05; see Equation 2). Note that this assumption was used to obtain M estimates to fit model C (i.e., M~K+L_{max}). In practice, when using the stepwise approach, we can convert the M estimates output from the model back to A_{max} values and calculate a new M estimate under a different set of assumptions (e.g., S=0.01; Pauly, 1980; Then et al., 2015). These options are available in the R package that implements the stepwise approach (see the "Discussion" section).

Quality control was performed on the studies found during the literature review by using the same guidelines outlined in Nadon and Ault (2016). Requirements included discarding any growth studies that involved length–frequency analysis or back-calculations. We kept only studies based on the aging of fish through the use of hard parts, primarily otoliths, vertebrae, and dorsal spines for sharks (Natanson et al., 2018; Natanson and Deacy, 2019). Finally, any studies that occurred in waters with mean sea-surface temperatures (SST) below 20°C were removed from consideration because of the well-established negative correlation between longevity and water temperature (Pauly, 1980; Jobling, 1994; Choat and Robertson, 2002). Exclusion of studies from regions with low temperatures was a sensible choice given that many of the families examined in our study are typically found in tropical waters where temperatures are usually well above the threshold of 20°C. Given that the ranges of our taxonomic groups center on tropical areas, only 3 species were excluded because of temperature criteria (1 wrasse and 2 groupers). The models also excluded genera that were clear outliers in certain families.

After obtaining the new data set of life history traits and putting it through quality control, we visually explored the shape of the functional relationships between paired parameters (L_{max}~L_∞, K~L_∞, M~K, and L_{mat}~L_{Amax}) by plotting data points in scatter plots for each new taxon (by *new*, we mean taxa added to those already included in the work of Nadon and Ault, 2016). We then tested the fit of linear, power, and exponential functions to these data points and obtained the maximum likelihood estimates for all parameters of models A–D by using the mle2 function of the package bbmle (vers. 1.0.19; Bolker, 2008; Fox, 2008) in the R statistical computing and programming environment (vers. 3.4.0; R Core Team, 2017).

Testing the expansion of the stepwise approach

To test our expansion of the approach of Nadon and Ault (2016), we compared the probability distributions of the values of life history parameters obtained through use of the stepwise approach with the probability distributions from published growth and maturity studies on a species in each of the new taxonomic groups. We selected these species on the basis of the availability of published values of life history parameters from in-depth studies and the availability of an independent estimate of L_{max} that we obtained from visual census data collected during NOAA diver surveys. We selected the blacktip reef shark (*Carcharhinus melanopterus*) (Chin et al., 2013), the camouflage grouper (*Epinephelus polyphekadion*) (Rhodes et al., 2011), the javelin grunter (*Pomadasys kaakan*) (Al-Husaini et al., 2002), and the redbreasted wrasse (*Cheilinus fasciatus*) (Hubble, 2003). The NOAA diver surveys are conducted every 3 years around approximately 50 islands and atolls in the central Pacific Ocean (the main and Northwestern Hawaiian Islands, American Samoa, and the Mariana Archipelago). For these surveys, a stratified random sampling design is used to select locations around the islands at which to count fish by using a stationary-point-count approach (Ayotte et al.[1]). During surveys, divers also record approximate total lengths of sighted fish to the nearest centimeter; divers are consistently trained in this exercise.

Next, we compared the precision and accuracy of the estimates of life history parameters from use of the stepwise procedure for the 4 new taxa included in this study. We used the same criteria as Nadon and Ault (2016) to evaluate the precision and accuracy of estimates made with the stepwise approach. We compared the widths of distributions of standard deviations (precision) and the distances between medians (accuracy) from the stepwise analysis with those from aging and maturity studies. We ran the stepwise simulation for these species, starting with local L_{max} values obtained from a data set of lengths of blacktip reef sharks, redbreasted wrasse, and camouflage grouper from NOAA diver surveys. We did not have an independent data set of lengths of javelin grunter; therefore, we used the 99th percentile of the lengths in the original growth study (Al-Husaini et al., 2002) as the L_{max} value for this species.

Finally, we evaluated the performance of the stepwise approach when determining a simple stock status metric, the spawning potential ratio (SPR) (Goodyear, 1990), by measuring its precision and accuracy as we did for the life history parameters. Spawning potential ratio is the ratio of spawning stock biomass (SSB) per recruit under a certain fishing mortality rate (F) divided by the same metric when fishing is absent:

$$SSB = \sum_{A_{mat}}^{A_{max}} \bar{N}_a \bar{W}_a, \quad (9)$$

where A_{mat} = the age at maturity (derived directly from L_{mat}), until A_{max};
$\bar{N}_a$ = the number of individuals; and
$\bar{W}_a$ = the expected individual weight (derived from a length–weight relationship; see Equation 10) in each age class a, beginning from A_{mat}.

The number of individuals in an age class is obtained by using the following exponential mortality equation:

$$\bar{N}_{a+\Delta a} = \bar{N}_a e^{-(S_a F + M)\Delta a}, \quad (10)$$

where S_a = the knife-edge selectivity at age a (set to age 2 for all species, to simplify comparisons).

Given that the SPR is a per-recruit metric, the number of fish at age 0 is simply set to 1 (i.e., $N_{a=0}=1$). Values for parameters of the dependent relationship of weight (W) to length (L) (α and β, where $W=\alpha \times L^{\beta}$), necessary for SPR calculations, were obtained from FishBase. Using the above equations, we calculated SPR values for all 4 test species at different fishing rates ranging from 0 to $F>4M$ from values of both the life history studies and stepwise approach. We then compared the SPR probability distributions of the test species in a fashion similar to that used for life history parameters. We calculated the SPR at different F values given the curvilinear relationship between the SPR and F.

Finally, we compared the stepwise parameter estimates to those from use of the alternative meta-analytical approach FishLife (Thorson et al., 2017). The FishLife approach fits a multivariate model with a taxonomic structure to generate probability distributions of life history parameters at different taxonomic levels (species, genus, family, order, and class). Using the R package FishLife (Thorson, 2017), we generated probability distributions for our 4 test species at the genus and family levels. We plotted these distributions with the results from use of the stepwise approach as well as with the published parameter estimates to evaluate their accuracy. All analyses were conducted in R.

Results

Life history parameter models for new taxa

The parameter L_{max} had a close relationship with L_{∞} for all 4 taxonomic groups (Fig. 2). All 4 relationships were best explained by a linear function with a relatively narrow normal error distribution. The standard deviation for sharks was much larger than for the other 3 groups (Table 2), an outcome that was expected given their larger size ranges. Larger (>1000 mm total length) grouper species had higher variability associated with L_{∞} estimates in comparison to smaller species; therefore, for analysis of the $L_{\infty} \sim L_{max}$

[1] Ayotte, P., K. McCoy, A. Heenan, I. Williams, and J. Zamzow. 2015. Coral reef ecosystem program standard operating procedures: data collection for rapid ecological assessment fish surveys. NOAA, Natl. Mar. Fish. Serv., Pac. Isl. Fish. Sci. Cent. Admin. Rep. H-15-07, 33 p. [Available from website.]

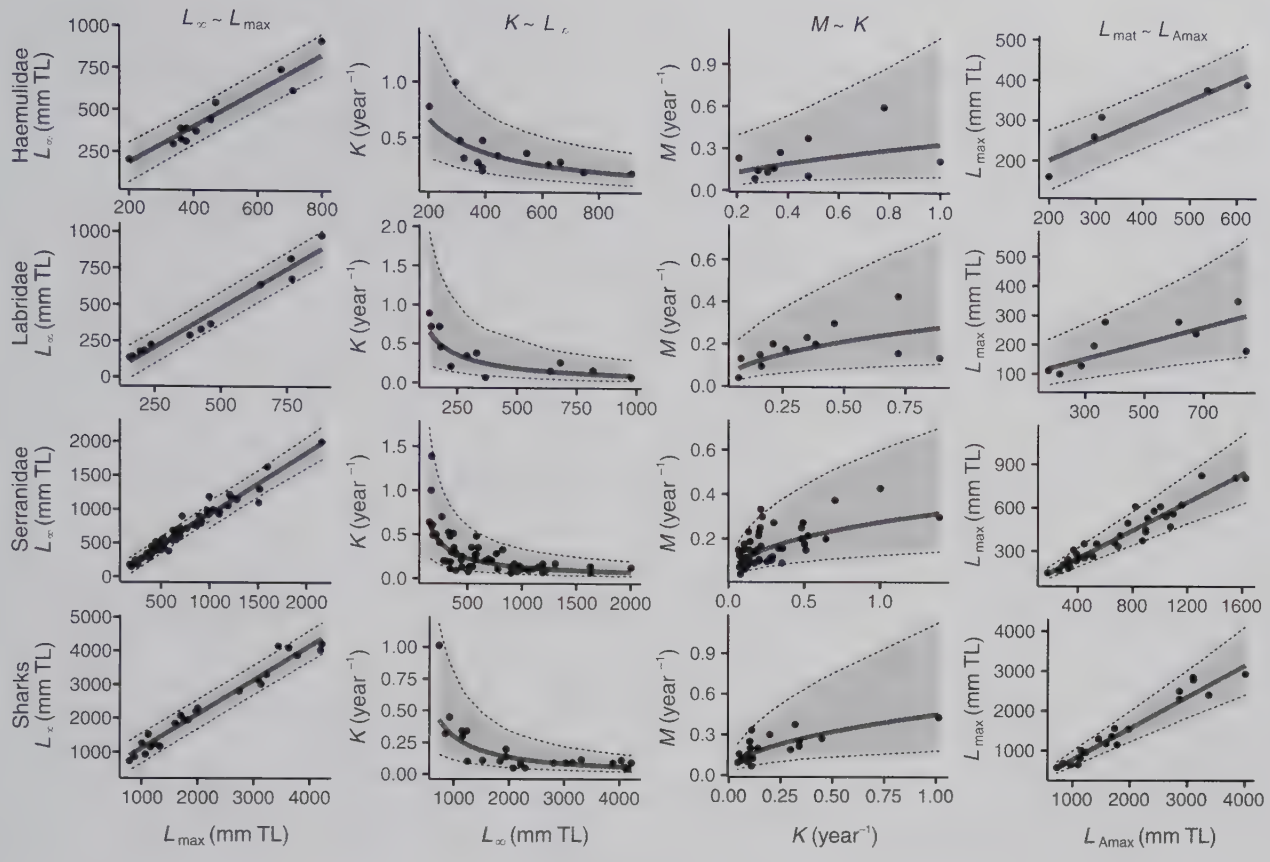

Figure 2

Modeled statistical relationships between life history parameters, the asymptotic length (L_∞), maximum length (L_{max}), growth coefficient (K), natural maturity (M), and expected length at the oldest recorded age (L_{Amax}), in 4 pairs for grunts (Haemulidae), wrasses (Labridae), groupers (Serranidae), and sharks from the orders Carcharhiniformes and Lamniformes. Black circles indicate the estimates of life history parameters obtained from studies. The solid dark gray lines are the lines of best fit, produced by using a linear or power model. Gray areas indicate the 95% confidence intervals of the lines of best fit. Note that model C (see Figure 1) also includes the L_{max} parameter for most families, but only the 1-variable M~K relationships are presented here. TL=total length.

relationship, we divided the grouper species into 2 size ranges by using an L_{max} break point of 1000 mm total length. The growth parameter K had a negative curvilinear relationship with the L_∞ parameter (Fig. 2). A power function best matched this relationship, and a lognormal error distribution was used to account for the decrease in variability that occurred as L_∞ values increased. A power function with a lognormal error distribution was also used to model M as a function of K and L_{max} (Fig. 2). Most of the available M and K data points were toward the lower end of the ranges of these parameters with only a few available data points at high values. It is likely that these limited data points had an outsized influence on the model fit. A positive, curvilinear relationship between M and K indicates slower growing fish have lower M, as was expected.

A linear model was used for all 4 relationships between L_{mat} and L_{Amax} (Fig. 2). Parameters for sharks, wrasses, and groupers were modeled with a lognormal error distribution because variability increased with larger L_{Amax} values, and parameters for grunts followed a normal error distribution. Maturity data were available for only 5 species of grunts, and the relationship would likely benefit from a larger sample size. As previously reported by Nadon and Ault (2016), L_{Amax} was a better predictor of L_{mat} than L_∞, as indicated by the higher coefficients of determination (r^2) for results from the L_{mat}~L_{Amax} models (Table 4).

Comparing distributions: stepwise approach, life history studies, and FishLife

For the 4 test species, we compared the probability distributions for key life history parameters generated by using the stepwise approach with those found in species-specific life history studies (Fig. 3). Like the results of the tests used by Nadon and Ault (2016), the estimates of life history parameters resulting from use of the stepwise approach had greater standard deviations than those from actual studies. The estimates from the stepwise simulation

Table 4

Overall coefficients of determination for the linear models of the relationships of the length at which 50% of individuals are mature (L_{mat}) as a dependent variable to either expected length at infinite age (L_∞) or to expected length at the oldest recorded age (L_{Amax}) for 3 families of tropical coastal fish species and for sharks from the orders Carcharhiniformes and Lamniformes.

Taxon	$L_{mat} \sim L_\infty$	$L_{mat} \sim L_{Amax}$
Haemulidae (grunts)	0.82	0.86
Labridae (wrasses)	0.36	0.46
Serranidae (groupers)	0.86	0.90
Sharks	0.91	0.95
All families	0.74	0.79

were reasonably accurate (i.e., useful for management purposes), generating median values within 25% of the estimates from life history studies for 14 of the 16 combinations of parameters and species (Table 5). Across all 4 test species, the stepwise predictions for M appear to be the most accurate. The blacktip reef shark was the test species with the most accurate results from the stepwise approach for all 4 parameters. The stepwise approach performed moderately well for the grunts on the basis of our test species javelin grunter. Despite high levels of variability, the stepwise approach appeared to be accurate for camouflage grouper, especially for L_∞, K, and M. The L_{mat} value was estimated at 352 mm in the test life history study and at 284 mm by using the stepwise approach, a result that can be explained by this species being an outlier with its L_{mat} close to 80% of its L_∞ (as opposed to 60% of the L_∞ for groupers, on average).

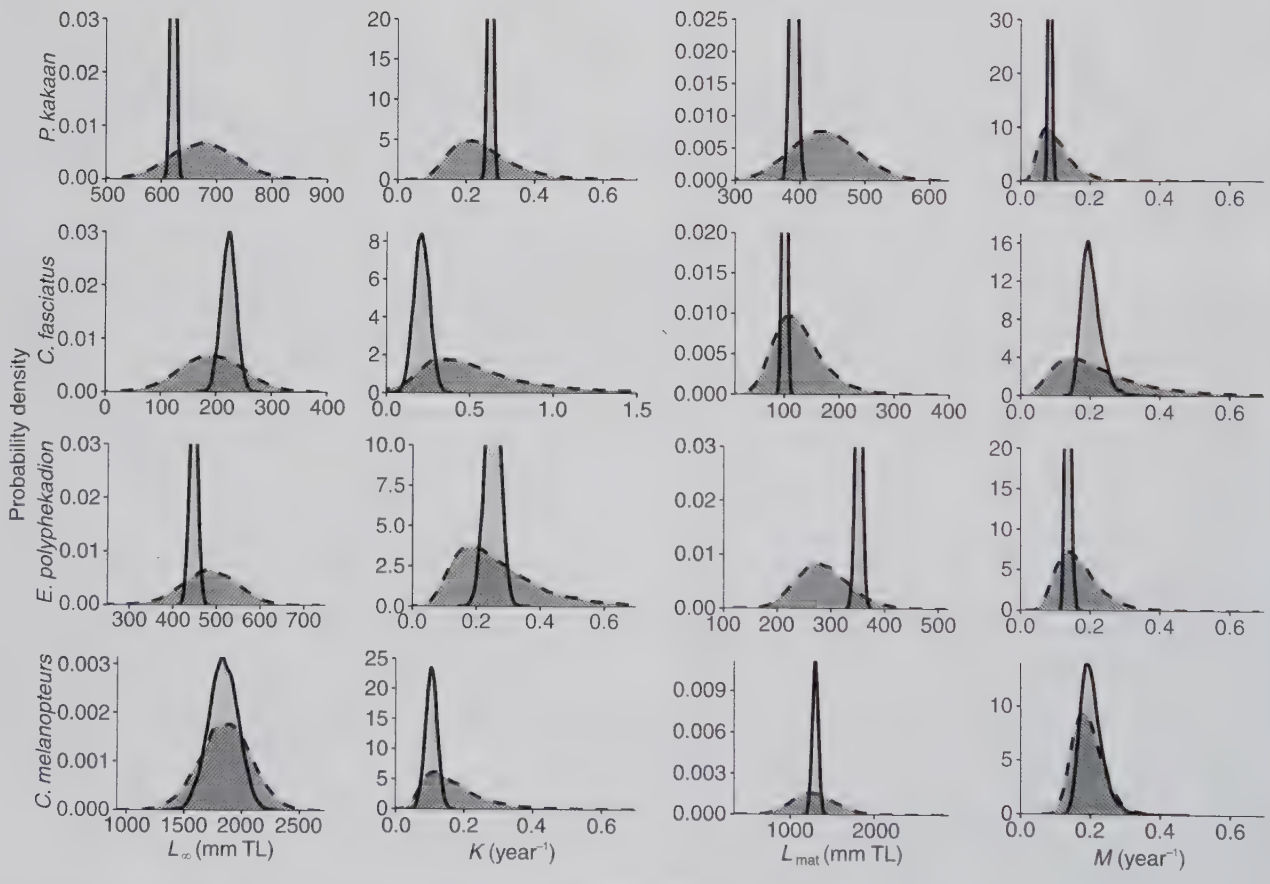

Figure 3

Probability distributions of estimates of life history parameters from life history studies (light gray areas and solid lines) and from use of the stepwise stochastic simulation approach (dark gray areas and dashed lines) for the 4 selected test species: javelin grunter (*Pomadasys kaakan*), redbreasted wrasse (*Cheilinus fasciatus*), camouflage grouper (*Epinephelus polyphekadion*), and blacktip reef shark (*Carcharhinidae melanopterus*). The parameters include the asymptotic length (L_∞), growth coefficient (K), length at which 50% of individuals are mature (L_{mat}), and natural mortality (M). TL=total length.

Table 5

Comparison of descriptive statistics of the probability distributions of life history parameters obtained from published life history studies to those from the use of the stepwise stochastic simulation approach for the 4 selected test species: javelin grunter (*Pomadasys kaakan*), redbreasted wrasse (*Cheilinus fasciatus*), camouflage grouper (*Epinephelus polyphekadion*), and blacktip reef shark (*Carcharhinidae melanopterus*). The life history and other model parameters include the maximum length (L_{max}), asymptotic length (L_{∞}), growth coefficient (K), length at which 50% of individuals are mature (L_{mat}), natural mortality (M), spawning potential ratio (SPR) at which fishing mortality (F) was equal to M, and SPR at which F was equal to 2 times M. The median, standard deviation (SD), ratio of the SD from stepwise simulation to the SD from life history studies (SD ratio), and the standardized distance between the stepwise medians and medians from life history studies (relative error [RE]) are presented for each parameter, except L_{max}, which was a measured value in the study. The median L_{max} values used to obtain probability distributions for the 4 test species are provided. TL=total length.

	P. kaakan		*C. fasciatus*		*E. polyphekadion*		*C. melanopterus*	
Parameter	Study	Stepwise	Study	Stepwise	Study	Stepwise	Study	Stepwise
L_{max} (mm TL)	–	655	–	236	–	520	–	1737
L_{∞} (mm TL)								
Median	621	675	223	192	447	487	1840	1862
SD	5	58	13	57	9	62	127	225
SD ratio	–	12	–	4	–	7	–	2
RE (%)	–	9	–	−14	–	9	–	1
K (year^{-1})								
Median	0.27	0.24	0.21	0.47	0.25	0.24	0.10	0.15
SD	0.01	0.09	0.05	0.35	0.02	0.14	0.02	0.09
SD ratio	–	13	–	7	–	8	–	5
RE (%)	–	−11	–	124	–	−4	–	50
L_{mat} (mm TL)								
Median	390	435	100	121	352	284	1300	1267
SD	5	52	4	45	6	50	35	260
SD ratio	–	10	–	11	–	8	–	7
RE (%)	–	12	–	21	–	−19	–	−3
M (year^{-1})								
Median	0.08	0.10	0.20	0.20	0.14	0.16	0.21	0.19
SD	0.004	0.05	0.02	0.16	0.01	0.07	0.03	0.05
SD ratio	–	13	–	8	–	7	–	2
RE (%)	–	25	–	0	–	14	–	−5
SPR F=M								
Median	0.38	0.39	0.22	0.29	0.27	0.35	0.09	0.12
SD	0.01	0.09	0.04	0.15	0.02	0.11	0.02	0.08
SD ratio	–	9	–	4	–	6	–	4
RE (%)	–	3	–	32	–	30	–	33
SPR F=2M								
Median	0.18	0.18	0.08	0.13	0.11	0.18	0.011	0.023
SD	0.01	0.07	0.02	0.11	0.01	0.08	0.005	0.033
SD ratio	–	7	–	6	–	8	–	7
RE (%)	–	0	–	63	–	64	–	109

To test the influence of the estimates of life history parameters from use of the stepwise approach on stock status, we used stepwise parameter predictions to calculate SPR distributions at F values ranging from 0 to more than 4 times M. The use of the stepwise approach and life history studies generated relatively similar median SPR values across the range of F, but the stepwise-derived SPR values were more variable, as expected, because of higher variability in life history parameters (Fig. 4). Higher variability was especially true for the redbreasted wrasse, given the low number of studies that were available for the wrasse family and the resulting higher uncertainty in parameter estimates from stepwise simulation. Averaged across all 4 test species, the absolute distance between the stepwise-derived SPR values and those from life history studies was 0.05 when F was equal to M and was 0.03 when F was equal to 2 times M. It is worth noting that, for 3 of the 4 test species, the SPR curve for estimates from use of the stepwise approach was higher than that for study values, but it is unclear if this bias is an implicit one, given the small number of species included in tests.

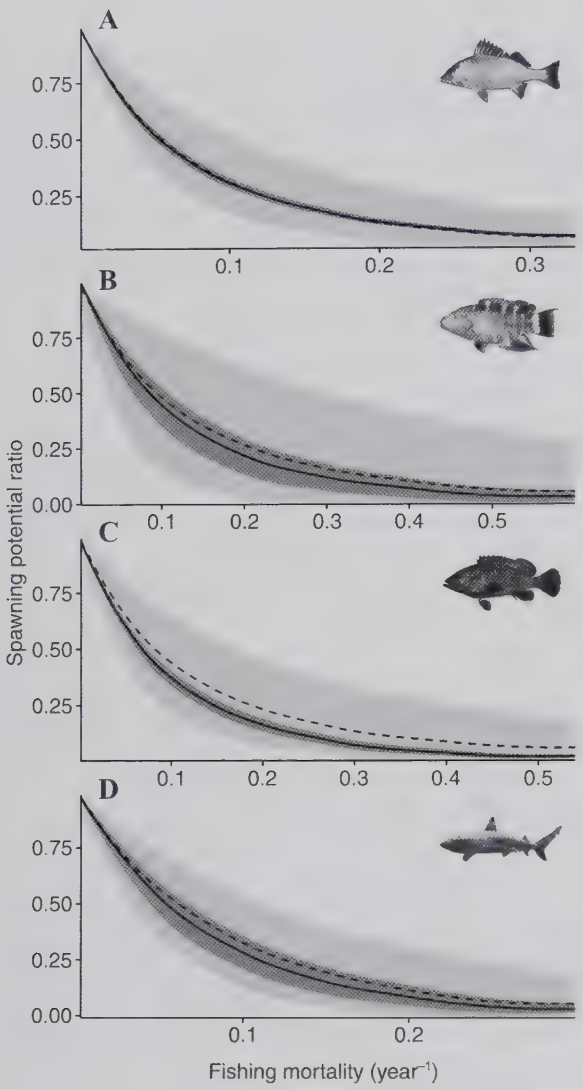

Figure 4

The spawning potential ratios at various fishing mortality rates derived by using parameter estimates from life history studies (dark gray areas and solid lines) and from use of the stepwise stochastic simulation approach (light gray areas and dashed lines) for the 4 selected test species: (**A**) javelin grunter (*Pomadasys kaakan*), (**B**) redbreasted wrasse (*Cheilinus fasciatus*), (**C**) camouflage grouper (*Epinephelus polyphekadion*), and (**D**) blacktip reef shark (*Carcharhinidae melanopterus*). Lines represent median values, and shaded areas represent 95% confidence intervals. Fishing mortality rates ranged from 0 to more than 4 times natural mortality.

Lastly, we compared the stepwise approach with the FishLife meta-analytical approach (Thorson et al., 2017). On average, the stepwise approach was more accurate than the FishLife approach implemented at both the genus and family levels for all parameters except K (Table 6, Figs. 5 and 6). The accuracy of the ratios of L_{mat} to L_{∞} was only slightly better for the stepwise approach. However, the accuracy of L_{∞}, M, L_{mat}, and the ratio of M to K was significantly higher for the stepwise approach. For example, the L_{mat} medians from stepwise simulation were on average 11% removed from the study values, and the L_{mat} average median values from the FishLife approach where more than 30% removed from those in published studies. In terms of precision, the stepwise approach was more precise for L_{∞}, M, and L_{mat}. The FishLife distributions were slightly more precise for the ratios of L_{mat} to L_{∞} and of M to K and more precise for the K parameter (standard deviations of 0.12 versus 0.17).

Discussion

Through this study, we have successfully extended the stepwise stochastic simulation approach to grouper, wrasse, grunt, and shark taxa. Our findings indicate that the stepwise approach could be further extended to fit specific management and scientific needs for additional families by replicating the effort in this study. The new models for these 4 taxa can now be used to calculate values for key life history parameters in data-poor situations and to implement stock assessment models (Nadon, 2017, 2019). The model in which the stepwise approach is applied now includes 10 taxonomic groups and is available as the R package StepwiseLH on the GitHub website.

Caveats

The stepwise approach, as well as other similar meta-analytical approaches, carries a lot of uncertainty into estimates of life history parameters and is not meant to replace proper life history studies. These approaches are meant to be temporary solutions to alleviate the pressing needs for assessment and management of data-poor fish populations. Although we tried to limit the sources of variability in our data set as much as possible, we had to make several compromises to retain a sufficient number of data points. For example, although most of the species-specific values of L_{max}, L_{∞}, K, and A_{max} used to create our data set are from single studies (and therefore single locations), maturity studies were often conducted separately and L_{mat} values can therefore be from a location different from the area where values of other parameters are from for many species. Specifically, 2 of the 5 maturity studies for grunts and 12 of the 32 maturity studies for groupers were not conducted at the same location as their corresponding growth studies (although only 2 of 20 shark maturity studies and none of the wrasse studies were conducted in different locations from those of their growth studies). This compromise may have added more variability to our L_{mat} estimates but likely did not introduce any specific biases.

Additionally, the lack of data points and different model fitting procedures for juveniles can have an effect on the L_{∞} and K parameter estimates. We tried controlling for

Table 6

Comparison of the accuracy and precision of estimates of life history parameters between use of the stepwise stochastic simulation approach and use of the FishLife approach. The reported values are the average results for all 4 of the selected test species. The FishLife model generated probability distributions at the genus and family levels. The parameters include the asymptotic length (L_∞), growth coefficient (K), natural mortality (M), length at which 50% of individuals are mature (L_{mat}), and the ratios of L_{mat} to L_∞ and of M to K. The accuracy metric is the standardized distance from the median values generated with the meta-analytical approaches to values from life history studies (in percentage units). Precision is reported as the standard deviation of each parameter (in millimeters for total lengths and on an annual basis for M and K). An asterisk (*) indicates that results are the most accurate or precise for that life history parameter among the approaches tested.

Modeling approach	L_∞	K	M	L_{mat}	L_{mat} to L_∞	M to K
Accuracy						
Stepwise	8*	45	11*	11*	17*	36*
FishLife (genus)	58	30*	99	50	19	87
FishLife (family)	17	45	86	30	18	78
Precision						
Stepwise	111*	0.17	0.08*	107*	0.13	0.46
FishLife (genus)	449	0.12*	0.14	248	0.08*	0.38*
FishLife (family)	611	0.21	0.22	340	0.10	0.42

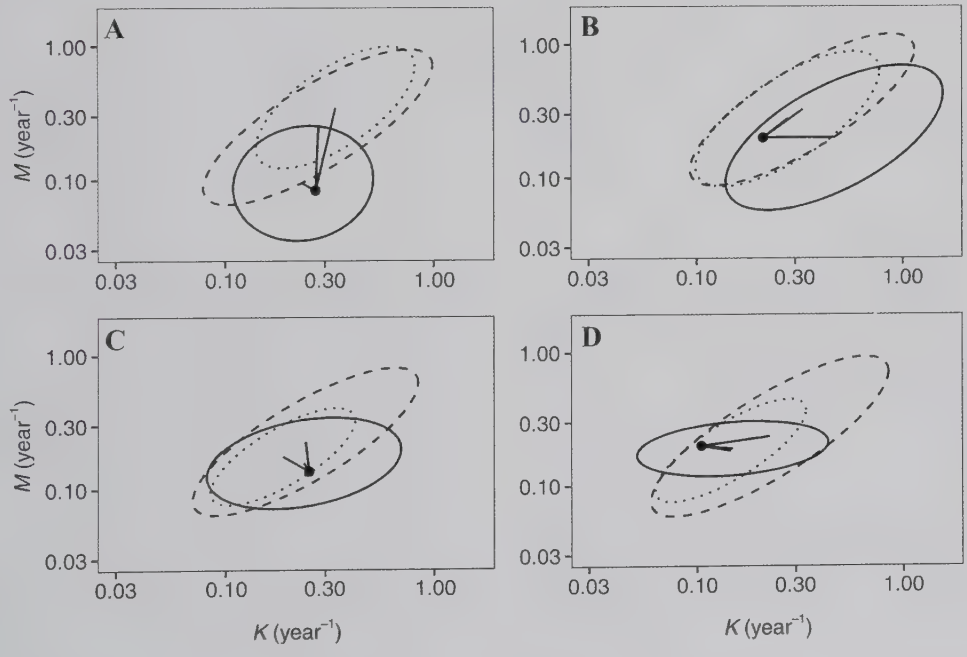

Figure 5

The 95% confidence intervals for probability distributions of natural mortality (M) and the growth coefficient (K) from use of the stepwise stochastic simulation approach (solid circular lines) and from use of the FishLife approach at both the genus (dotted circular lines) and family (dashed circular lines) levels for the 4 selected test species: (**A**) javelin grunter (*Pomadasys kaakan*), (**B**) red-breasted wrasse (*Cheilinus fasciatus*), (**C**) camouflage grouper (*Epinephelus polyphekadion*), and (**D**) blacktip reef shark (*Carcharhinidae melanopterus*). Published values from life history studies (black circles) are also presented for each species, with line segments connecting the median of the distributions to the study value.

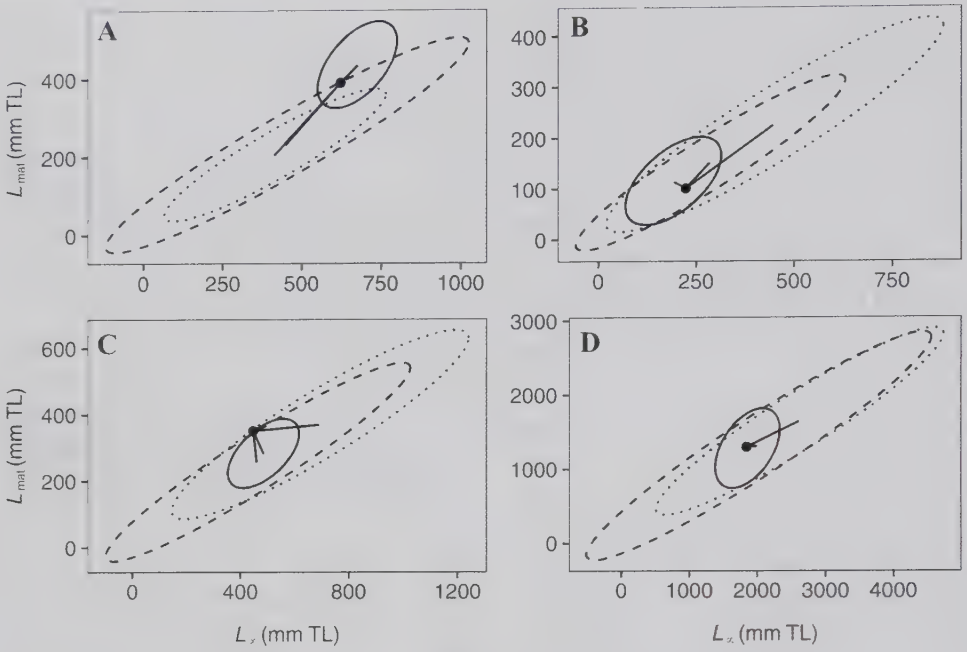

Figure 6

The 95% confidence intervals for probability distributions of the asymptotic length (L_∞) and length at which 50% of individuals are mature (L_{mat}) from use of the stepwise stochastic simulation approach (solid circular lines) and from use of the FishLife approach at both the genus (dotted circular lines) and family (dashed circular lines) levels for the 4 selected test species: (**A**) javelin grunter (*Pomadasys kaakan*), (**B**) redbreasted wrasse (*Cheilinus fasciatus*), (**C**) camouflage grouper (*Epinephelus polyphekadion*), and (**D**) blacktip reef shark (*Carcharhinidae melanopterus*). Published values from life history studies (black circles) are also presented for each species, with line segments connecting the median of the distributions to the study value. TL=total length.

this issue by removing growth studies with highly negative A_0 from the analysis (an indication of a lack of data points for juveniles needed to anchor the growth curve near the origin). Again, we believe removing studies with highly negative A_0 simply adds to the overall variability and does not introduce any specific bias.

Another caveat is that we used the SST at the locations of the life history studies, and those temperatures may not reflect the lifelong SST exposure of highly migratory species. In the study described here, the difference in temperatures is mainly a concern for certain shark species that may migrate between tropical and temperate waters. Therefore, our SST limit of 20°C may not exclude species that spend most of their time in SST <20°C if the study took place in a warmer climate. A difference in temperature may introduce a slight bias in M estimates, but it is unlikely that the tropical or temperate species that occur in SST above 20°C spend much time in very cold SST.

Further, we used the L_{max} value from NOAA diver surveys to distance our test from the L_{max} values in the original data set and to reduce the potential for confounding test results. The only input needed for the stepwise approach is L_{max}, and we wanted this value to come from an independent source. We could have used L_{max} from the original life history study, as we did for the javelin grunter, but we felt this was a more independent test.

Finally, it would have been more appropriate to test our stepwise approach on species not included in the regression models we used to build our approach. However, we did not want to exclude the data from our 4 test species in these regression models given our low sample sizes. It is important to note that parameter estimates for the 4 test species came from the same database (FishBase) as those used in the FishLife multivariate models; therefore, their inclusion does not bias our approach comparisons in favor of the stepwise approach.

Sources of variability in estimates of life history parameters

There are multiple sources of variability included in the distributions of life history parameters from the stepwise simulation. Some sources are directly modeled, others are likely indirectly included as part of the overall residual error of each model, and some minor sources of uncertainty were not included. The main source of

variability is interspecific genetic differences that are a result of natural selection. This source of variability was modeled explicitly by using parameter estimates for individual species as data points in our regression models. A certain amount of intraspecific geographical variability in both genetics and habitat conditions also contributes to variability in estimates of life history parameters. Consequently, there may be some concern that we pooled data from across the world and therefore ignored geographical differences within species. Unfortunately, given that published data for most species came from only one location, it was impossible for us to directly control for geographical heterogeneity in life history parameters. Geographical differences in values of life history parameters for species simply add to the overall variability of the stepwise parameter estimates and should not cause any specific bias.

Another source of variability that was directly modeled are regression model coefficients. Coefficient variability was included by randomly sampling the multivariate normal distribution, as defined by the variance–covariance matrix. Similarly, uncertainty in the starting L_{max} parameter was directly included by sampling from a distribution or by bootstrapping raw L_{max} observations. Furthermore, the lack of access to raw age-at-length and length-at-maturity data, coupled with the fact that most published reports from life history studies do not include a parameter variance–covariance matrix, prevented us from directly including uncertainty from fitted values (i.e., L_∞, K, and L_{mat}) in our models. This source of uncertainty, although not modeled explicitly, likely adds to the global residual error.

Finally, a few minor sources of uncertainty were not directly included because they are unlikely to have a major effect on output variability. Specifically, variability in A_0 is hard to measure given the sensitivity of this parameter to juvenile age-at-length data points. In our approach, we simply fixed this parameter to the overall mean of −0.6. Further, we did not include uncertainty in the relationships of fork or standard length to total length that we used to convert all parameter data to total lengths. Not including uncertainty from length conversions is unlikely to be a major source of error, and the studies that publish these conversion factors rarely provide their associated variability. Finally, we did not specifically include variability in the M estimates derived from A_{max} (Equation 8). The relationship between M and longevity depends on the assumption of S. We fixed S at 0.05 to convert our raw observations of A_{max} to M in order to model the M~K relationship. This assumption can be relaxed in the R package StepwiseLH by specifying an S value and generating M estimates under this new value. Uncertainty in the values of the S parameter could be included by researchers as a separate step by using Monte Carlo simulations on this parameter.

Despite the various sources of uncertainty described in this section, it is important to note that use of the stepwise approach still results in reasonably accurate parameter estimates, as demonstrated in our tests.

Parameter estimation

In addition to producing results from the 4 models that relate key life history traits, we calculated the following ratios: L_{max} to L_∞, L_{mat} to L_{Amax}, L_{mat} to L_∞, and M to K, all Beverton–Holt invariants. Results from comparison of these ratios from our study with those previously published indicate that the invariants differ among taxonomic groups in our study (groupers, grunts, wrasses, and lamniform and carcharhiniform sharks). Our findings are consistent with previous investigations of life history invariants that found similar variance in relationships of life history traits between taxonomic groups of fish (Charnov and Berrigan, 1991; Nadon and Ault, 2016; Thorson et al., 2017).

The ratio of M to K is of particular interest because the relationship between M and K determines the overall shape of a growth trajectory (Hordyk et al., 2015). In our study, we used the criteria from Prince et al. (2015) to define a ratio of M to K that was >1.0 as indeterminate growth and a ratio of M to K that was <1.0 as determinate growth. Species with determinate growth are limited to a maximum size after which growth mostly ceases (Lincoln et al., 1982), and species with indeterminate growth are not limited to a maximum size but typically see growth slow with size (Sebens, 1987). Sharks were the only group with a ratio of M to K that was >1.0 (1.53), indicating indeterminate growth. This observation for sharks is consistent with the findings of indeterminate growth in the literature (Pardo et al., 2013; Heupel et al., 2014). All other families in the study described here had determinate growth patterns with ratios of M to K <1.0.

On average, species with indeterminate growth will reach only a fraction of L_∞ at A_{max}, with an increasingly smaller proportion at higher ratios (Hordyk et al., 2015). Consequently, the ratio of M to K has a strong effect on the divergence between the parameters L_∞ and L_{Amax}. As this ratio increases, the curvilinearity of the growth trajectory decreases and L_∞ can increase drastically and become more of a fitting parameter than one related to L_{Amax}. An increase in the ratio of M to K ultimately reduces the ratio of L_{mat} to L_∞, while the ratio of L_{mat} to L_{Amax} stays similar. The described interactions between life history ratios can also lead to L_∞ being much higher than L_{max}, an outcome that may seem surprising but is to be expected for species with high ratios of M to K. This effect of the stepwise approach on the ratio of M to K was observed in our study: the groups with the highest ratios of M to K (groupers and sharks) had the greatest differences between the ratios of L_{mat} to L_∞ and of L_{mat} to L_{Amax}. Subsequently, as in the study of Nadon and Ault (2016), we used the L_{mat}~L_{Amax} relationship as the preferred model for obtaining L_{mat}. Our decision was further validated by r^2 values being higher when L_{Amax} was used as the predictor than when L_∞ was used.

To varying degrees, the relationships estimated with stepwise simulation in this study were similar to those established by Nadon and Ault (2016) with positive linear relationships between parameters in both the

L_∞~L_{max} and L_{mat}~L_{Amax} pairs, negative curvilinear relationships between parameters in the K~L_∞ pair, and a positive curvilinear relationship between parameters in the M~K pair. The apparent outlier to this trend is a less positive, almost linear relationship between parameters in the M~K pair for grunts that could be an effect of the small sample size (n=9) for this taxonomic group. In this situation, the K parameter contains limited information on M, but the relationship still defines the range of M values that is likely for grunts. A similar situation was found for surgeonfishes and goatfishes by Nadon and Ault (2016).

The shark group had a large standard deviation in the L_∞~L_{max} relationship. This difference was likely due to both the distribution of sizes for sharks and the decision to create the relationships for a taxonomic group broader than family. Our decision to group multiple families of sharks together was necessary because only one family of sharks, Carcharhinidae, had enough published life history information to generate family-specific relationships. We therefore extended the shark group in our study to comprise all families in the orders Carcharhiniformes and Lamniformes, which include most families of conservation concern, such as requiem (Carcharhinidae), hammerhead (Sphyrnidae), thresher (Alopiidae), mackerel (Lamnidae), and sand tiger (Odontaspididae) sharks. After comparing the relationships for only species of Carcharhinidae with the relationships for all species of Carcharhiniformes and Lamniformes, we determined that it was appropriate to use a model for all families in the orders Carcharhiniformes and Lamniformes, given the current lack of data for species not in Carcharhinidae. As more life history data become available, it would be appropriate to create more family-specific models for other shark families. Until then, we believe our approach provides a reasonable option to assess shark stocks in data-poor situations.

The average absolute percent difference in estimates of the SPR and of life history parameters from use of the stepwise approach and from life history studies for the 4 test species was only 19%. This level of difference is similar to the 22% average difference found by Nadon and Ault (2016). The differences between estimates from stepwise simulation compared favorably with average differences of 59% and 44% for genus- and family-level estimates from use of the FishLife approach, respectively. The model proved most successful in estimating L_∞, L_{mat}, and M, with an average absolute difference of only 8–11% between the stepwise estimates and those from life history studies. It is not entirely surprising that it was a struggle to estimate L_∞ and L_{mat} with the FishLife approach given that, in this approach, a local L_{max} estimate is not used within an L_{max}~L_∞ relationship to restrict L_∞ and L_{mat} estimates, as is done in the stepwise approach. The distributions of length parameter values estimated with the FishLife approach therefore effectively represent the range of values observed within a genus or family, a range that can be enormous (as evident in Figure 6). Wide distributions of length parameter values limit the utility of the FishLife approach to population assessment models, such as the length-based spawning potential ratio model (Hordyk et al., 2016), that can be parameterized with the ratios of M to K and of L_{mat} to L_∞. However, it is important to note that even these models will require a reasonable estimate of L_∞ to scale the length data used to fit model parameters.

In addition, note that the distribution of these ratios can also be output from the stepwise simulation. It was a struggle to use our model to predict K, for which there was an average percent difference of 47% between the stepwise simulation and FishLife model, including the 124% difference for redbreasted wrasse (K values were estimated with higher precision and accuracy when the FishLife approach was used; the K parameter was the only one for which FishLife outperformed the stepwise approach in both metrics). These large discrepancies in estimation of the K parameter did not have a strong effect on SPR estimation error because estimates of the SPR from use of the stepwise approach typically were within 0.05 of the value obtained from the relevant life history study.

The study described here has resulted in the extension of our capability to conduct stock assessments in data-poor situations to a greater number of species. Our stepwise approach is generally more precise and accurate than the FishLife approach, although more research comparing both approaches is certainly warranted. It is important to reiterate that these meta-analytical approaches are not meant to replace life history studies, which typically have well-designed spatial coverage, appropriate gear selection, large sample sizes, and peer-reviewed biological and statistical methods. We acknowledge that the stepwise approach presented here may introduce a large amount of uncertainty to any assessment relying on them, in comparison with a species- and location-specific life history study. The stepwise approach is meant to allow temporary assessments to be implemented. We highly recommend full integration of the uncertainty in estimates of life history parameters throughout any assessment. We also recommend that stock status and management metrics be viewed in a risk assessment context, in which greater uncertainty is directly related to more conservative management advice. Under these guidelines, predictions from the use of this approach have successfully been used to manage stocks in U.S. waters of the Pacific Ocean, passing independent expert reviews (Nadon and Ault, 2016; Nadon, 2019).

Acknowledgments

This study was part of the NOAA Ernest F. Hollings Undergraduate Scholarship Program, and we would like to thank the NOAA Office of Education and the NOAA Pacific Island Fisheries Science Center, Fisheries Research and Monitoring Division, for facilitating the research. A. Yau was integral in facilitating the visiting researcher. B. Taylor greatly improved the project with his expertise and professional advice. We thank J. O'Malley, B. Langseth, and 2 anonymous reviewers for their important feedback and comments on the manuscript.

Literature cited

Al-Husaini, M., A. Al-Baz, S. Al-Ayoub, S. Safar, Z. Al-Wazan, and S. Al-Jazzaf.
2002. Age, growth, mortality, and yield-per-recruit for nagroor, *Pomadasys kakaan*, in Kuwait's waters. Fish. Res. 59(1):101–115.

Ault, J. S., J. A. Bohnsack, and G. A. Meester.
1998. A retrospective (1979–1996) multispecies assessment of coral reef fish stocks in the Florida Keys. Fish. Bull. 96:395–414.

Ault, J. S., S. G. Smith, J. Luo, M. E. Monaco, and R. S. Appeldoorn.
2008. Length-based assessment of sustainability benchmarks for coral reef fishes in Puerto Rico. Environ. Conserv. 35:221–231.

Ault, J. S., S. G. Smith, J. A. Browder, W. Nuttle, E. C. Franklin, J. Luo, G. T. DiNardo, and J. A. Bohnsack.
2014. Indicators for assessing the ecological dynamics and sustainability of southern Florida's coral reef and coastal fisheries. Ecol. Indic. 44:164–172.

Berkson, J., and J. T. Thorson.
2015. The determination of data-poor catch limits in the United States: is there a better way? ICES J. Mar. Sci. 72:237–242.

Beverton, R. J. H., and S. J. Holt.
1959. A review of the lifespans and mortality rates of fish in nature, and their relation to growth and other physiological characteristics. *In* Ciba Foundation symposium—the lifespan of animals (colloquia on ageing), vol. 5 (G. E. W. Wolstenholme and M. O'Conner, eds.), p. 142–180. J. and A. Churchill Ltd., London.

Bolker, B. M.
2008. Ecological models and data in R, 408 p. Princeton Univ. Press, Princeton, NJ.

Charnov, E. L.
1993. Life history invariants: some explorations of symmetry in evolutionary ecology, 184 p. Oxford Univ. Press, Oxford, UK.
2008. Fish growth: Bertalanffy k is proportional to reproductive effort. Environ. Biol. Fishes 83:185–187.

Charnov, E. L., and D. Berrigan.
1991. Evolution of life history parameters in animals with indeterminate growth, particularly fish. Evol. Ecol. 5:63–68.

Chin, A., C. Simpfendorfer, A. Tobin, and M. Heupel.
2013. Validated age, growth and reproductive biology of *Carcharhinus melanopterus*, a widely distributed and exploited reef shark. Mar. Freshw. Res. 64:965–975.

Choat, J. H., and D. R. Robertson.
2002. Age-based studies. *In* Coral reef fishes: dynamics and diversity in a complex ecosystem (P. F. Sale, ed.), p. 57–80. Academic Press, San Diego, CA.

Craig, M. T., and P. A. Hastings.
2007. A molecular phylogeny of the groupers of the subfamily Epinephelinae (Serranidae) with a revised classification of the Epinephelini. Ichthyol. Res. 54:1–17.

Ellington, E. H., G. Bastille-Rousseau, C. Austin, K. N. Landolt, B. A. Pond, E. E. Rees, N. Robar, and D. L. Murray.
2015. Using multiple imputation to estimate missing data in meta-regression. Methods Ecol. Evol. 6:153–163.

FAO.
2016. The state of world fisheries and aquaculture 2016: contributing to food security and nutrition for all, 200 p. FAO, Rome. [Available from website.]

Fenner, D.
2012. Challenges for managing fisheries on diverse coral reefs. Diversity 4:105–160.

Fox, J.
2008. Applied regression analysis and generalized linear models, 2nd ed., 688 p. Sage Publ., Thousand Oaks, CA.

Froese, R., and C. Binohlan.
2000. Empirical relationships to estimate asymptotic length, length at first maturity and length at maximum yield per recruit in fishes, with a simple method to evaluate length frequency data. J. Fish Biol. 56:758–773.
2003. Simple methods to obtain preliminary growth estimates for fishes. J. Appl. Ichthyol. 19:376–379.

Froese, R., and D. Pauly (eds.).
2017. FishBase. World Wide Web electronic publication, vers. 05/2017. [Available from website.]

Gedamke, T., and J. M. Hoenig.
2006. Estimating mortality from mean length data in nonequilibrium situations, with application to the assessment of goosefish. Trans. Am. Fish. Soc. 135:476–487.

Gilman, E., K. Passfield, and K. Nakamura.
2014. Performance of regional fisheries management organizations: ecosystem-based governance of bycatch and discards. Fish Fish. 15:327–351.

Goodyear, C. P.
1990. Spawning stock biomass per recruit: the biological basis for a fisheries management tool. ICCAT Collect. Vol. Sci. Pap. 32:487–497. SCRS/89/082. [Available from website.]

Heupel, M. R., D. M. Knip, C. A. Simpfendorfer, and N. K. Dulvy.
2014. Sizing up the ecological role of sharks as predators. Mar. Ecol. Prog. Ser. 495:291–298.

Hewitt, D. A., and J. M. Hoenig.
2005. Comparison of two approaches for estimating natural mortality based on longevity. Fish. Bull. 103:433–437.

Hilborn, R., and D. Ovando.
2014. Reflections on the success of traditional fisheries management. ICES J. Mar. Sci. 71:1040–1046.

Hoenig, J.
1983. Empirical use of longevity data to estimate mortality rates. Fish. Bull. 82:898–903.

Hordyk, A., K. Ono, K. Sainsbury, N. Loneragan, and J. Prince.
2015. Some explorations of the life history ratios to describe length composition, spawning-per-recruit, and the spawning potential ratio. ICES J. Mar. Sci. 72:204–216.

Hordyk, A. R., K. Ono, J. D. Prince, and C. J. Walters.
2016. A simple length-structured model based on life history ratios and incorporating size-dependent selectivity: application to spawning potential ratios for data-poor stocks. Can. J. Fish. Aquat. Sci. 73:1787–1799.

Hubble, M.
2003. The ecological significance of body size in tropical wrasses (Pisces : Labridae). Ph.D. diss., 182 p. James Cook Univ., Douglas, Australia. [Available from website.]

Jarić, I., and Z. Gačić.
2012. Relationship between the longevity and the age at maturity in long-lived fish: Rikhter/Efanov's and Hoenig's methods. Fish. Res. 129–130:61–63.

Jensen, A. L.
1996. Beverton and Holt life history invariants result from optimal trade-off of reproduction and survival. Can. J. Fish. Aquat. Sci. 53:820–822.
1997. Origin of relation between K and L_{inf} and synthesis of relations among life history parameters. Can. J. Fish. Aquat. Sci. 54:987–989.

Jobling, M.
1994. Fish bioenergetics, 310 p. Chapman and Hall, London.

Kronen, M., A. Vunisea, F. Magron, and B. McArdle.
2010. Socio-economic drivers and indicators for artisanal coastal fisheries in Pacific island countries and territories

and their use for fisheries management strategies. Mar. Policy 34:1135–1143.

Lincoln, R., G. Boxhall, and P. Clark.
1982. A dictionary of ecology, evolution and systematics, 298 p. Cambridge Univ. Press, Cambridge, UK.

Ma, K. Y., and M. T. Craig.
2018. An inconvenient monophyly: an update on the taxonomy of the groupers (Epinephelidae). Copeia 106:443–456.

Nadon, M. O.
2017. Stock assessment of the coral reef fishes of Hawaii, 2016. NOAA Tech. Memo. NMFS-PIFSC-60, 212 p.
2019. Stock assessment of Guam coral reef fish, 2019. NOAA Tech. Memo. NMFS-PIFSC-82, 107 p.

Nadon, M. O., and J. S. Ault.
2016. A stepwise stochastic simulation approach to estimate life history parameters for data-poor fisheries. Can. J. Fish. Aquat. Sci. 73:1874–1884.

Nadon, M. O., J. S. Ault, I. D. Williams, S. G. Smith, and G. T. DiNardo.
2015. Length-based assessment of coral reef fish populations in the main and Northwestern Hawaiian Islands. PLoS ONE 10(8):e0133960.

Natanson, L. J., and B. M. Deacy.
2019. Using oxytetracycline validation for confirmation of changes in vertebral band-pair deposition rates with ontogeny in sandbar sharks (*Carcharhinus plumbeus*) in the western North Atlantic Ocean. Fish. Bull. 117:50–58.

Natanson, L. J., A. H. Andrews, M. S. Passerotti, and S. P. Wintner.
2018. History and mystery of age and growth studies in elasmobranchs. *In* Shark research: emerging technologies and applications for the field and laboratory (J. C. Carrier, M. R. Heithaus, and C. A. Simpfendorfer, eds.), p. 178–194. CRC Press, Boca Raton, FL.

Pardo, S. A., A. B. Cooper, and N. K. Dulvy.
2013. Avoiding fishy growth curves. Methods Ecol. Evol. 4:353–360.

Pauly, D.
1980. On the interrelationships between natural mortality, growth parameters, and mean environmental temperature in 175 fish stocks. ICES J. Mar. Sci. 39:175–192.

Prince, J., A. Hordyk, S. R. Valencia, N Loneragan, and K. Sainsbury.
2015. Revisiting the concept of Beverton–Holt life-history invariants with the aim of informing data-poor fisheries assessment. ICES J. Mar. Sci. 72:194–203.

R Core Team.
2017. R: a language and environment for statistical computing. R Foundation for Statistical Computing, Vienna, Austria. [Available from website, accessed May 2017.]

Raghunathan, T. E., J. M. Lepkowski, J. Van Hoewyk, and P. Solenberger.
2001. A multivariate technique for multiply imputing missing values using a sequence of regression models. Surv. Methodol. 27:85–95.

Rhodes, K. L., B. M. Taylor, and J. L. McIlwain.
2011. Detailed demographic analysis of an *Epinephelus polyphekadion* spawning aggregation and fishery. Mar. Ecol. Prog. Ser. 421:183–198.

Rudd, M. B., and J. T. Thorson.
2018. Accounting for variable recruitment and fishing mortality in length-based stock assessments for data-limited fisheries. Can. J. Fish. Aquat. Sci. 75:1019–1035.

Sebens, K. P.
1987. The ecology of indeterminate growth in animals. Annu. Rev. Ecol. Syst. 18:371–407.

Smith, W. L., and M. T. Craig.
2007. Casting the percomorph net widely: the importance of broad taxonomic sampling in the search for the placement of serranid and percid fishes. Copeia 1:35–55.

Symes, D., J. Phillipson, and P. Salmi.
2015. Europe's coastal fisheries: instability and the impacts of fisheries policy. Sociol. Rural. 55:245–257.

Then, A. Y., J. M. Hoenig, N. G. Hall, and D. A. Hewitt.
2015. Evaluating the predictive performance of empirical estimators of natural mortality rate using information on over 200 fish species. ICES J. Mar. Sci. 72:82–92.

Thorson, J. T.
2017. FishLife: predict life history traits for any fish. R package, vers. 1.0.2. [Available from website, accessed May 2020.]

Thorson, J. T., S. B. Munch, J. M. Cope, and J. Gao.
2017. Predicting life history parameters for all fishes worldwide. Ecol. Appl. 27:2262–2276.

van Buuren, S.
2007. Multiple imputation of discrete and continuous data by fully conditional specification. Stat. Methods Med. Res. 16:219–242.

von Bertalanffy, L.
1938. A quantitative theory of organic growth (Inquiries on growth laws. II). Hum. Biol. 10:181–213.

Fishery Bulletin

Guidelines for authors

Contributions published in *Fishery Bulletin* describe original research in marine fishery science, fishery engineering and economics, and marine environmental and ecological sciences (including modeling). Preference will be given to manuscripts that examine processes and underlying patterns. Descriptive reports, surveys, and observational papers may occasionally be published but should appeal to an audience outside the locale in which the study was conducted.

Although all contributions are subject to peer review, responsibility for the contents of papers rests upon the authors and not on the editor or publisher. *Submission of an article implies that the article is original and is not being considered for publication elsewhere.*

All submissions are subject to a double-blind review to remove the identity of author and reviewer during the review process.

Plagiarism and double publication are considered serious breaches of publication ethics. To verify the originality of the research in papers and to identify possible previous publication, manuscripts may be screened with plagiarism-detection software.

Manuscripts must be written in English; authors whose native language is not English are strongly advised to have their manuscripts checked by English-speaking colleagues before submission.

Once a paper has been accepted for publication, online publication takes approximately 2 weeks.

There is no cost for publication in *Fishery Bulletin*.

Types of manuscripts accepted by the journal

Articles generally range from 20 to 30 double-spaced typed pages (12-point font) and describe an original contribution to fisheries science, engineering, or economics. Tables and figures are not included in this page count, but the number of figures should not exceed 1 figure for every 4 pages of text. Articles contain the following divisions: abstract, introduction, methods, results, discussion, and conclusions.

Notes are generally less than 10 double-spaced typed pages (12-point font), including the Literature cited section. Like articles, notes describe an original contribution to fisheries science. They follow a format similar to that for articles: abstract, introduction, methods, results, and discussion, but the results and discussion sections may be combined and a conclusions section should not be included. They should include no more than 2 figures or tables (2 of each would be too many). They are distinguished from full articles in that they report a noteworthy new observation or discovery—such as the first report of a new species, a unique finding, condition, or event that expands our knowledge of fisheries science, engineering, or economics—and do not require a lengthy discussion. Manuscripts on range extensions will not be considered.

Companion articles should be submitted together and are published together as a scientific contribution. Both articles should address a closely related topic and may be articles that result from a workshop or conference.

Review articles of exceptional quality may be considered occasionally for publication on a case-by-case basis. They address a timely topic that is relevant to aspects of fisheries science. They should include an abstract, but the format of the article, per se, will be up to the author. Please contact the scientific editor to discuss your ideas regarding a potential review article before embarking on such a project.

Perspective essays generally are less than 5 double-spaced typed pages (12-point font) and provide clarification of misused terms or misunderstood topics in fisheries science. Essays are accepted at the discretion of the scientific editor. Opinion pieces on policy will not be considered. They should include an abstract and a list of the literature cited, but no other sections should divide the article. Please contact the scientific editor to discuss your idea before making a submission.

Preparation of manuscript

Title page should include authors' full names, affiliations, mailing addresses, and the senior author's email address.

Abstract should be limited to 200 words (one-half typed page), state the main scope of the research, and emphasize the authors' conclusions and relevant findings. Do not review the methods of the study or list the contents of the paper. Because abstracts are circulated by abstracting agencies, it is important that they represent the research clearly and concisely.

General text must be typed in 12-point Times New Roman font throughout. A brief introduction should convey the broad significance of the paper; the remainder of the paper should be divided into the following sections: Materials and methods, Results, Discussion, Conclusions, and Acknowledgments. Headings within each section must be short, reflect a logical sequence, and follow the rules of subdivision (i.e., there can be no subdivision without at least 2 subheadings). The entire text should be intelligible to interdisciplinary readers; therefore, all acronyms, abbreviations, and technical terms should be written out in full and defined the first time they are mentioned. Abbreviations should be used sparingly because they are not carried over to indexing databases and slow readability for those readers

outside a discipline. They should never be used for the main subject (e.g., species or method) of a paper.

For general style, follow the U.S. Government Publishing Office *Style Manual* (2016, available at website) and *Scientific Style and Format: the CSE Manual for Authors, Editors, and Publishers* (2014, 8th ed.) published by the Council of Science Editors. For scientific nomenclature, use the current edition of the American Fisheries Society's (AFS) *Common and Scientific Names of Fishes from the United States, Canada, and Mexico* and its companion volumes (*Crustaceans, Mollusks, Cnidaria and Ctenophora*, and *World Fishes Important to North Americans*). For species not found in the previously mentioned AFS publications and for more recent changes in nomenclature, use the Integrated Taxonomic Information System (ITIS, available at website), or, secondarily, the California Academy of Sciences *Catalog of Fishes* (available at website) for species names not included in ITIS. Common (vernacular) names of species should be lowercase. Citations must be given for the identification of specimens. For example, "Fish species were identified according to Collette and Klein-MacPhee (2002); sponges were identified according to Stone et al. (2011)."

Dates should be written as follows: 11 November 2018. Measurements should be expressed in metric units, for example, "58 metric tons (t);" if other units of measurement are used, please make this fact explicit to the reader. Use numerals, not words, to express whole and decimal numbers in the general text, tables, and figure captions (except at the beginning of a sentence). For example, "We considered 3 hypotheses. We collected 7 samples in this location." Use American spelling. Refrain from using the shorthand slash (/), an ambiguous symbol, in the general text.

Cite all software, special equipment, and chemical solutions used in the study within parentheses in the general text, including the version number, company name, and the city and state (or nation) of the company headquarters, for example, "SAS, vers. 9.4 (SAS Institute Inc., Cary, NC)."

Word usage and grammar that may be useful are the following:

- *Aging*
  For our journal, the word *aging* is used to mean both age determination and the aging process (senescence). Authors should make clear which meaning is intended where ambiguity may arise.

- *Fish and fishes*
  The plural of the word fish (a collective noun that implies individuals without regard to species) is *fish*.
  Example: The *fish* were collected by trawl net.
  Example: The numbers of *fish* collected that season were less than the numbers from previous years.

  The plural for *fish species* is *fishes* (a contrived plural used by taxonomists to mean several or more *fish species*) or one can use *fish species* (which is preferred in this journal for clarity across disciplines).
  Example: The *fishes* of Puget Sound [biodiversity is implied] or
  Example: The *fish species* of Puget Sound [preferred plural for clarity across disciplines].

- *Crab and crabs, squid and squids, etc.*
  The plural of the word *crab* (i.e., many individuals without regard to species) is *crab*.
  Example: The crab were sorted by weight.
  Example: Many red king *crab* were dying [Many individuals of one species of crab.]

  The plural of *crab species* is *crabs* (a word used by taxonomists) or *crab species* (the latter is preferred in this journal for clarity).
  Example: These *crabs* were selected for treatment. [Different crab species are implied.]
  Example: These *crab species* were selected for treatment. [Preferred word choice for clarity.]
  Example: Snow *crabs* are found throughout the North Pacific Ocean and Bering Sea. [There are 2 species of snow crab; therefore the word *crabs* can be used here.]
  Example: *Two species* of snow *crab* are found throughout the North Pacific Ocean and Bering Sea. [Preferred usage for clarity.]
  Example: Three crabs were selected for treatment. [3 species of crab are implied.]
  Example: Three crab species were selected for treatment. [Preferred word choice for clarity.]

- We use *fisherman* and *fishermen*, not *fisher* and *fishers*, in this journal. One can always use crew member, vessel operator, and angler (the latter for recreational fishing).

- *The definite article with common names of species*
  When the singular common name of a species represents the entire class or group to which it belongs, use the definite article.
  Example: Only one species of the genus *Salmo* is found in the Atlantic Ocean—*the* Atlantic salmon (*Salmo salar*).
  Example: The sonic emissions of *the* bottlenose dolphin are complex.

  For plural common names, this rule does not apply.
  Example: Chinook salmon are found throughout the Pacific Ocean.
  Example: Bottlenose dolphins are found in temperate and tropical waters.

- *Sex*
  For the meaning of male and female, use the word *sex*, not *gender*. Do not write, "fish were sexed." Write, "sex was determined."

- *Participles*
  As adjectives, participles must modify a specific noun or pronoun.
  Example: Using mark-recapture methods, these scientists determined the size of the population. [Correct. The participle *using* modifies the word *scientists*.]

Example: These scientists, based on the collected data, concluded that the mortality rate of these fish had increased. [Incorrect. The scientists were not based on the collected data.]

Example: These scientists concluded, on the basis of collected data, that the mortality rate of these fish had increased. [Correct. The offending participle has been eliminated and an adverbial phrase modifies the verb *concluded*.]

Equations and mathematical symbols should be set from a standard mathematical program (MathType or Equation Editor). Equations formatted in LaTex are not acceptable. For mathematical symbols in the general text (α, χ^2, π, $\pm$, etc.), use the symbols provided by the MS Word program and italicize all variables, except those variables represented by Greek letters and the superscript and subscript parts of variables and expressions. Do not use photo mode when creating these symbols in the general text, and do not cut and paste equations, letters, or symbols from a different software program.

Number equations (if there are more than one) for future reference by scientists; place the number within parentheses at the end of the first line of the equation.

Literature cited section comprises published works and those accepted for publication (in press) in peer-reviewed journals. Follow the name and year system for citation format in this section (i.e., citations should be listed alphabetically by the authors' last names, and then by year if there is more than one citation by the same author. A list of abbreviations for citing journal titles can be found on our website.

Authors are responsible for the accuracy and completeness of all citations. Avoid the use of multiple citations when a single citation sufficiently supports a statement; cite the work that first reported the information that supports a statement, not all of the subsequent works. Literature citation format: Authors (last name, followed by initials for first name and, if given, middle name of first author; then list names of additional authors with initials before last names). Year. Title of article. Abbreviated title of the journal in which it was published. Always include either the range of page numbers (for a journal article) or a total number of pages (for a book or other type of publication). List a sequence of citations in the general text chronologically, for example, "(Smith, 1932; Green, 1998; Smith and Jones, 2015)."

Acknowledgments should be no more than 6 lines of text. Only those who have contributed in an outstanding way should be acknowledged by name. For recognition of other persons or groups, use a general term, such as *crew*, *observers*, or *research coordinators*, and do not include names with these terms.

Digital object identifier (doi) code ensures that a publication has a permanent location online. A doi link (which may include a doi code) should be included at the end of citations of published literature. Authors are responsible for submitting accurate doi links. Faulty links will be deleted at the page-proof stage.

Footnotes are used for all documents that have not been formally peer reviewed and for observations and personal communications, but these types of references should be cited sparingly in manuscripts submitted to the journal.

All reference documents, administrative reports, internal reports, progress reports, project reports, contract reports, personal observations, personal communications, unpublished data, manuscripts in review, and council meeting notes are footnoted in 10-point font and placed at the bottom of the page on which they are first cited. Footnote format is the same as that for formal literature citations. A link to the online source (e.g., [Available from http://www... , accessed July 2017.]), or the mailing address of the agency or department holding the document, should be provided so that readers may obtain a copy of the document.

Tables are often overused in scientific papers; it is seldom necessary to present all the data associated with a study. Tables should not be excessive in size and must be cited in numerical order in the text. Headings should be short but ample enough to allow the table to be intelligible on its own.

All abbreviations and unusual symbols must be explained in the table legend. Other incidental comments may be footnoted with numeral footnote markers. Use asterisks only to indicate significance in statistical data. Do not put a table legend on a page separate from the table; place the legend above the table. *Do not submit tables in photo mode.*

- Note probability with a capital, italic *P*.
- Provide a zero before all decimal points for values less than one (e.g., 0.07).
- Round all values to 2 decimal points.
- Use a comma in numbers of 5 digits or more (e.g., 13,000 but 3000).

Figures must be cited in numerical order in the text. Graphics should aid in the comprehension of the text, but they should be limited to presenting patterns rather than raw data. The number of figures should not exceed 1 figure for every 4 pages of text.

Figure legends should explain all symbols and abbreviations seen in the figure and should be double spaced on a separate page at the end of the manuscript.

Line art and halftone figures should be saved at resolutions >600 dots per inch (dpi) and >300 dpi, respectively. Color is allowed in figures to show morphological differences among species (for species identification), to show stain reactions, to show gradations (such as those of temperature and salinity within maps), and to distinguish

between numerous lines and symbols in graphs. Figures approved for color should be saved in CMYK format.

All figures must be submitted as PDF, TIFF, or EPS files.

- Capitalize only the first letter of the first word and proper nouns in all labels within figures.
- Do not use overly large font sizes for labels in maps and for axis labels in graphs.
- Use the same point size for all labels, except for panel labels (e.g., **A**), which should be slightly larger than other labels (e.g., 11 point versus 8 point).
- Use a sans serif font for all labels. Panel labels (e.g., **A**), however, should be in Times New Roman font.
- Do not use bold fonts or bold lines in figures. Do not use italic fonts. Exceptions include use of italic fonts for labels of bodies of water in maps and a bold font for panel labels (e.g., **A**).
- Do not place outline rules around graphs.
- Do not include vertical and horizontal lines in the background of graphs. Ticks for values on the x-axis and y-axis will suffice.
- Place a north arrow and label degrees latitude and longitude (e.g., 170°E) in all maps. If scale of map requires more than degrees, use degrees minutes, not decimal degrees.
- Place panel labels (e.g., **A**, **B**, **C**) within the upper-left area of each graph or photo in a multi-panel figure, from left to right, then top to bottom. If the letter is not visible against a dark background, put a white box behind it. Do not use white labels.
- Avoid placing labels vertically or diagonally. Y-axis labels can be vertical. Words in horizontal labels can be stacked vertically to fit.
- Use symbols, shading, or patterns (not clip art) in maps and graphs.
- For scale bars in maps, use kilometers. Use the label *km* or *kilometers* (lowercased).

Supplementary materials that are considered essential, but are too large or impractical for inclusion in a paper (e.g., metadata, figures, tables, videos, and websites), may be provided at the end of an article. These materials are subject to the editorial standards of the journal. A URL to the supplementary material and a brief explanation for including such material should be sent at the time of initial submission of the paper to the journal.

- **Metadata, figures, and tables** should be submitted in standard digital format (MS Word or PDF file) and should be cited in the general text, for example, as ". . . was determined (Suppl. Table 3, Suppl. Fig. 1)."
- **Websites** should be cited with a URL in the general text.
- **Videos** must not be larger than 30 MB to allow a swift technical response for viewing the video. Authors should consider whether a short video uniquely captures what text alone cannot capture for the understanding of a process or behavior under examination in the article. Supply an online link to the location of the video.

Copyright law does not apply to *Fishery Bulletin*, which falls within the public domain. However, if an author reproduces any part of an article from *Fishery Bulletin*, reference to source is considered correct form (e.g., Source: Fish. Bull. 117:105).

Failure to follow these guidelines and failure to correspond with editors in a timely manner will delay publication of a manuscript.

Submission of manuscript

Submit a manuscript online at the ScholarOne Manuscripts website for *Fishery Bulletin*. Commerce Department authors must provide proof of internal clearance of their manuscripts with either a completed and signed NOAA Form 25-700 or a copy of the clearance email from the Research Publication Tracking System. For further details on electronic submission, please contact the associate editor, Cara Mayo, at

cara.mayo@noaa.gov.

When requested, the text and tables should be submitted in MS Word format. Each figure should be sent as a separate PDF, TIFF, or EPS file. Send a copy of a figure in the original software if conversion to any of these formats yields a degraded version of the figure.

Questions? If you have questions regarding these guidelines, please contact the managing editor, Kathryn Dennis, at

kathryn.dennis@noaa.gov.

Questions regarding manuscripts under review should be addressed to Associate Editor Cara Mayo.

Fishery Bulletin

Subscription form

Superintendent of Documents **Publications** Order Form

*5178

☐ YES, please send me the following publications:

____ Subscriptions to *Fishery Bulletin*
for $32.00 per year ($44.80 foreign)

The total cost of my order is $ _____ . Prices include regular domestic postage and handling and are subject to change.

_____
(Company or Personal Name) (Please type or print)

_____
(Additional address/attention line)

_____
(Street address)

_____
(City, State, ZIP Code)

_____
(Daytime phone including area code)

_____
(Purchase Order No.)

Charge your order. IT'S EASY!

VISA

MasterCard

Please Choose Method of Payment:

☐ Check payable to the Superintendent of Documents
☐ GPO Deposit Account ☐☐☐☐☐☐☐–☐
☐ VISA or MasterCard Account
☐☐☐☐☐☐☐☐☐☐☐☐☐☐☐☐
☐☐☐☐ (Credit card expiration date)

To fax your orders (202) 512-2104

_____
(Authorizing Signature)

Mail to: Superintendent of Documents
P.O. Box 979050, St. Louis, Missouri 63197
Tel. no. (U.S. callers): 866-512-1800
Tel. no. (International callers): 1-202-512-1800

Thank you for your order!

Also available online at
https://bookstore.gpo.gov/products/fishery-bulletin
email: ContactCenter@gpo.gov